UNIVERSIDAD COMPLUTENSE DE MADRID

FACULTAD DE CIENCIAS QUÍMICAS

DEPARTAMENTO DE BIOQUÍMICA Y BIOLOGÍA MOLECULAR

TESIS DOCTORAL

Estudio proteómico y metabolómico de la enfermedad cardiovascular en la búsqueda de nuevos biomarcadores

MEMORIA PARA OPTAR AL GRADO DE DOCTORA
PRESENTADA POR

Marta Martín Lorenzo

Directores

Gloria Álvarez Llamas
Fernando Vivanco Martínez

Madrid, 2015

© Marta Martín Lorenzo, 2015

UNIVERSIDAD COMPLUTENSE DE MADRID

Departamento de Bioquímica y Biología Molecular

ESTUDIO PROTEÓMICO Y METABOLÓMICO DE LA ENFERMEDAD CARDIOVASCULAR EN LA BÚSQUEDA DE NUEVOS BIOMARCADORES

Tesis Doctoral

Marta Martín Lorenzo

Madrid 2015

Directores: Dra. Gloria Álvarez Llamas

Dr. Fernando Vivanco Martínez

Resumen

Las enfermedades cardiovasculares son las responsables del mayor número de muertes en el mundo siendo la aterosclerosis la causante de la mayoría de ellas. Dado su desarrollo durante décadas de manera silente y asintomática, la comunidad clínica está de acuerdo en que se necesitan con urgencia nuevos paneles de marcadores de riesgo así como la identificación de nuevas dianas moleculares terapéuticas. El mejor entendimiento de los mecanismos operantes es también de extrema necesidad para un mejor conocimiento de la enfermedad. Estos dos aspectos constituyen el objetivo fundamental de esta tesis doctoral. Para ello, se han aplicado diferentes aproximaciones ómicas en diferentes fluidos y tejidos de un modelo animal de conejo de aterosclerosis temprana y en muestras humanas. El proteoma de la orina se estudió por electroforesis bidimensional y el metaboloma por resonancia magnética nuclear. Del estudio, uno de los pioneros en emplear la orina como fluido de interés en el campo de las enfermedades cardiovasculares, se desprenden dos paneles diferenciados: uno de progresión y otro de recuperación tras sufrir un evento cardiovascular agudo. Además el sistema de la calicreína-cinina y alteraciones en el metabolismo de la arginina-prolina paracen jugar un papel importante en el desarrollo de la enfermedad. En un estudio paralelo, se analizaron el proteoma y el metaboloma de aortas control y ateroscleróticas empleando la misma técnica proteómica y una variante de la resonancia conocida como resonancia de sólidos o de ángulo mágico, siendo la primera vez que se describe en la literatura su aplicación a arterias. Gracias a este estudio, se encontraron cambios en el metabolismo energético, el metabolismo de diferentes aminoácidos y el metabolismo de los glicerofosfolípidos, mientras se produce una remodelación arterial fundamentalmente en el citoesqueleto. De manera adicional, se hizo un estudio traslacional dirigido en el que se evaluó el reflejo en plasma de estas alteraciones. El resultado es un panel de riesgo que se compone de 3 enzimas y 3 metabolitos. En colaboración con el grupo del Dr. Liam McDonnell en LUMC, Holanda ("Leiden University Medical Center") se ha obtenido un mapa molecular arterial compuesto por proteínas y lípidos gracias a la técnica MALDI-Imaging. Primeramente se realizó una puesta a punto para alcanzar la resolución espacial adecuada para analizar las distintas capas arteriales (íntima y media) y así poder analizar *in situ* las moléculas presentes implicadas en la enfermedad manteniendo su localización original por comparación con el análisis histológico. Posteriormente, se aplicó la técnica MALDI-Imaging en un análisis comparativo entre aortas sanas y ateroscleróticas. Diferentes clases de lípidos se encontraron variados en las muestras patológicas localizados en la capa íntima y/o en

regiones calcificadas y, de entre las proteínas, destaca la Timosina β4, confinada en la capa íntima y que se propone como diana molecular y potencial marcador de riesgo cardiovascular.

Summary

Cardiovascular diseases remain the leading cause of death in the World. Significant progress has been achieved during the last years regarding the molecular basis of atherosclerosis, the usual underlying cause of a fatal event. The formation and development of the atheroma plaque have been revealed to be an enormously complicated network of correlated reactions occurring in the different layers of the artery. However, the mechanisms are not fully understood and due the silent and asymptomatic nature of the process, new markers are demanded. Indeed, it is mandatory, according to clinicians, to improve the current monitoring of plaque formation and, identify people at high cardiovascular risk in order to prevent a fatal event.

To approach molecular mechanisms underlying atherosclerosis development, a rabbit animal model of early atherosclerosis has been developed by special feeding: normal chow (control group) and cholesterol and Vitamin D rich diet (pathological group). Combined omics strategies were chosen for the investigation of those mechanisms in a blind approach of the molecules taking part in the complexity of the interactions happening in atherosclerosis development.

Urine is a valuable source of potential markers of disease. It is an easily accessible and an abundant fluid. However, it has not been widely studied in the context of cardiovascular diseases. Here, we have applied a combined strategy, after previous set up, by performing 2D-DIGE (2D- Differential In Gel Electrophoresis) analysis to study urine proteome and NMR (Nuclear Magnetic Resonance) to study urine metabolome. At proteome level, an extensive comparison between described desalting and purifying methods, and modified methods has been performed as published in *Electrophoresis* journal (Chapter 1). In total, eight different strategies were compared based on ultrafiltration, precipitation, dyalisis, size exclusion and solid phase extraction. Commercial PD10 columns (GE Healthcare) are recommended when interested in high molecular mass proteins and Oasis® cartridges for visualization of low molecular mass proteins. When studying atherosclerosis development in the search of markers with rabbit urine, Oasis® cartridges cleaning step was used. As a result, four proteins were found altered (Cathepsin D, Hemopexin, Kallikrein 1 and Zymogen granule protein 16B). At metabolome level, the comparison was performed based on a previous work carried in the laboratory [*Kidney International, 2014*] leading to nineteen metabolites altered at an early stage of atherosclerosis. Translational analysis was performed in a

target approach using SRM LC-MS/MS in human urine. Human urine samples were collected from healthy controls, and patients admitted with ACS (acute coronary syndrome) at two times points: admission and discharge. The combination of these studies, published at *Metabolomics* journal (Chapter 2) revealed common mechanisms operating during atherosclerosis development and its acute manifestation and some mechanisms particularly activated during the event. Interestingly, kallikrein-kinin system is implicated in atherosclerosis together with alterations in arginine and proline metabolism. Two molecular panels are proposed; progression marker panel, for those responding to both, early atherosclerosis and acute event: KLK1, ZG16B, 2-hydroxyphenylacetic acid, 3-hidroxybutyric acid, L-alanine, L-arabitol, N-acetylneuraminic acid and scyllo-inositol and recovery marker panel, for those that return to control levels at discharge: KLK1, ZG16B, 1-methyhydantoin, 3-hydroxybutyric acid and putrescine.

Similarly to the study of urine, a combined approach was performed using rabbit aortas. At proteomic level, 2D-DIGE analysis was performed using protein extracts. In total, twelve proteins related with actin myofilaments, typical plasma proteins, glucose metabolism, protein folding and enzymes were found altered at early atherosclerosis. At metabolome level, an alternative to classical NMR was applied. HRMAS (High resolution magic angle spinning) is also known as solid phase NMR. It offers the enormous advantage of allowing direct tissue measurement, no sample preparation is needed and the tissue can be recovered after analysis if necessary. It has been applied in other clinical studies successfully. However, as far as we know, this is the first time that atherosclerosis is studied using this approach. A total of 17 metabolites were found responders to atherosclerosis condition. These metabolites can be classified as choline and related metabolites, amino acids and others. In summary, these alterations point to a deregulation of the cytoskeleton, arterial remodeling, and impairment in energy metabolism, amino acids metabolisms and glycerophospholipids metabolism. In order to evaluate a potential translation of these observed changes into measurable alterations in an accessible fluid, plasma analysis was performed by SRM LC-MS/MS as target approach. Four enzymes responded in plasma: A1AT, PGK, PKM and ILK, and 8 metabolites: choline, acetylcholine, L-Glutamic acid, L-Valine, N-acetyl-L-alanine, Glucuronic acid, Glutathione and Pyruvic acid (as previously found in arterial tissue). ROC curves were obtained and, six molecules are finally proposed to compose marker

panel of cardiovascular risk. We postulate that the combination of PGK, PKM, ILK, glutamate, N-acetyl-L-alanine and valine in plasma can be used to monitor early stages of atherosclerosis. A manuscript compiling all these results is in preparation to be submitted to *BBA Molecular Basis of Disease* journal.

To gain further knowledge in the underlying biomolecular changes that accompany atherosclerosis development the original molecular location in arterial tissue should be maintained. In clinical investigation, a novel technique has emerged during the last two decades: MALDI-MSI (matrix-assisted laser desorption/ionization Mass Spectrometry Imaging). It is a novel *ex vivo* technique that offers the unique advantage to investigate the physiopathological changes taking place, directly in-tissue while retaining the localization of the analyzed molecules. In a simple way, it is like performing several inmunohistochemistry staining at a time. In atherosclerosis, only a few studies focused in lipids have been performed; however the two chapters presented in this thesis (chapter 4 and 5) are, as far as we know, show for the first time that spatially resolved mass spectrometry can be applied to atherosclerotic tissue looking for protein implications in the pathology. This part of the Thesis has been performed in collaboration with Dr. Liam McDonnell from LUMC (Leiden Univerity Medical Center), The Netherlands. Firstly, a set-up of the methodology was performed as the key for obtaining rich molecular profiles by MALDI-MSI from arteries. In order to remove salts and lipids from the tissue that could interfere in protein measurements, tissue samples were washed previous to the analysis. An in depth comparison between five different washes described in the literature was performed using carotid and mammary human arteries. They were compared in terms of number of peaks, mean intensity of spectra, signal to noise ratio, and number of excluded spectra, and visually inspected looking for no delocalization of the molecules due to tissue washing. Combining all these parameters, isopropanol wash is recommended in the study of arterial tissue. Not only because it was the best performing one, providing good molecular profiles with no delocalization, but also because it maintains tissue integrity allowing to perform histological staining protocols on the same tissue slice that was measured by MALDI-Imaging. Additionally and importantly, isopropanol wash allowed performing experiments at high spatial resolution, 30µm. This is mandatory to visualize changes taken place specifically located in a certain arterial layer. However, it is especially challenging due to the small dimension of the samples and because of the co-

occurrence of normal healthy tissue with fatty regions and calcified plaques. This high spatial resolution is required for look into specific arterial regions. This set-up has been published in *Journal of Proteomics* journal. A comparative study between healthy and early atherosclerosis rabbit aortas was performed by using this developed protocol for protein and lipid analysis. A total of 29 m/z values were detected as layer-defining molecular features, i.e., in media or intima layer or specifically localized in calcified plaque regions within the intima. Localized in the intima, increased expression of saturated fatty acids and lysolipids correlate with endothelial dysfunction. In relation to atherosclerosis progresion to plaque formation, up regulation of SM, PI and PG was found. Calcified regions within the intima were found to be rich in TG, PA, SM and PE-Cer. Protein Thymosin β4, with a fold change of 3.0 was found upregulated in intima layer by MSI and IHC and upregulated as well in atherosclerosic tissue compared with control. By performing IHC in human aortas we found that Thymosin β4 alteration and localization is confirmed in human arterial tissue. Because of that, we hypothesize that Thymosin β4 could be a good therapeutic target and potential marker of cardiovascular disease. This work is now under revision in *Journal of Proteomics*.

In conclusion, several omic approaches have been used in this thesis to elucidate atherosclerosis underlying mechanisms and looking for potential markers of cardiovascular risk, progression and recovery. Two novel approaches has been applied here for the first time in atherosclerosis basic research; HRMAS and MALDI Imaging for proteins. Together with the evaluation of a not very commonly used in cardiovascular research, although highly interesting fluid as urine. The combination of these complementary strategies represent a high effort in the better understanding of atherosclerosis. Different molecules, old known and new ones, have arosen to be involved in kallikerin-kinin system, cytoskeleton deregulation, impairment of energy metabolism, amino acids metabolism together with different lipids roles in early atherosclerosis context. What is more, three different panels has been postulated to monitor cardiovascular risk, prognosis and recovery after a fatal event.

Índice

Abreviaturas

2D-DIGE	Two dimension-Differential in gel electrophoresis
A1AT	Alpha-1 Antitrypsin
ACS	Acute coronary syndrome
AMI	Acute myocardial infraction
CVE	Cardiovascular Event
CXCL12	C-X-C motif chemokine 12
CXCR4	C-X-C chemokine receptor type 4
EC	Endothelial cells
EGF	Epidermal growth factor
FT-ICR	Fourier transform ion cyclotron resonance mass spectrometry
H&E	Hematoxylin & Eosin staining
HDL	High density lipoprotein
HRMAS	High resolution magic angle spinning
IHC	Inmunohistochemistry
ILK	Integrin linked kinase
KAP	kidney androgen-regualted protein
KLK1	Kallikrein 1
LC	Liquid cromatography
LC-MS/MS	Liquid cromatography coupled mass spectrometry
LDL	Low density lipoproteins
MALDI	Matrix Assistted Laser Desorption/Ionization
MALDI-MSI	Matrix Assistted Laser Desorption/Ionization- Mass Spectrometry Imaging
MMP	Matrix metalloproteinase
MS	Mass sepctrometry
MSI	Mass Spectrometry Imaging
NMR	Nuclear magnetic resonance

NO	Nitric oxid
ox-LDL	oxidized-Low density lipoptoteins
PA	Diacylglycerophosphates
PAF	Platelet activation factor
PE-Cer	Phosphoethanol-ceramides
PG	Diacylglycerophosphoglycerols
PGK	Phosphoglycerate kinase
PI	Glycerophosphoinositols
PKM	Pyruvate kinase muscle isozyme
ROS	Reactive oxygen species
SFA	Saturated Fatty Acids
SIMS-TOF	Secondary ion mass spectrometry-Time of flight
SM	Sphingomyelins
SRM	Selected reaction monitoring
TCFA	Thin-Cap fibroatheroma
TG	Triglycerides
TMAO	Trimethylamine N-oxide
TMB4SX	Thymosin β4 protein
VSMC	Vascular smooth muscle cells
ZG16B	Zymogen granule protein 16 rat homolog

INTRODUCCIÓN

ATEROSCLEROSIS: Desarrollo silente y asintomático

La etimología del término aterosclerosis proporciona ya información de en qué consiste esta enfermedad. En contra de lo que podría pensarse, no comparte raíz con la palabra arteria sino que se compone de dos palabras griegas *athéro:* pasta y *sklerós*: duro, que a grandes rasgos puede asociarse con lo que se conoce como placa de ateroma. La aterosclerosis es una enfermedad de etiología compleja que hoy en día se considera una situación de inflamación crónica (1) caracterizada por la acumulación de células inflamatorias, lipoproteínas y tejidos fibrosos en las paredes de las arterias grandes, preferencialmente en los sitios donde el torrente sanguíneo tiene un flujo turbulento (2). Comienza en la primera década de vida en la aorta y contínua durante las sucesivas décadas en la arteria coronaria (segunda década) y las arterias cerebrales (tercera y cuarta décadas) (1). De los estudios epidemiológicos se desprende que la aterosclerosis resulta de una compleja interacción entre la genética (edad, sexo, antecedentes familiares) y los factores de riesgo ambientales (3, 4). Dichos factores de riesgo son: hiperlipidemia, hipertensión, tabaquismo, obesidad, diabetes,… y funcionan de una manera no aditiva sino multiplicadora, es decir, la existencia de varios simultáneamente amplifica considerablemente el riesgo de padecer una enfermedad cardiovascular (5).

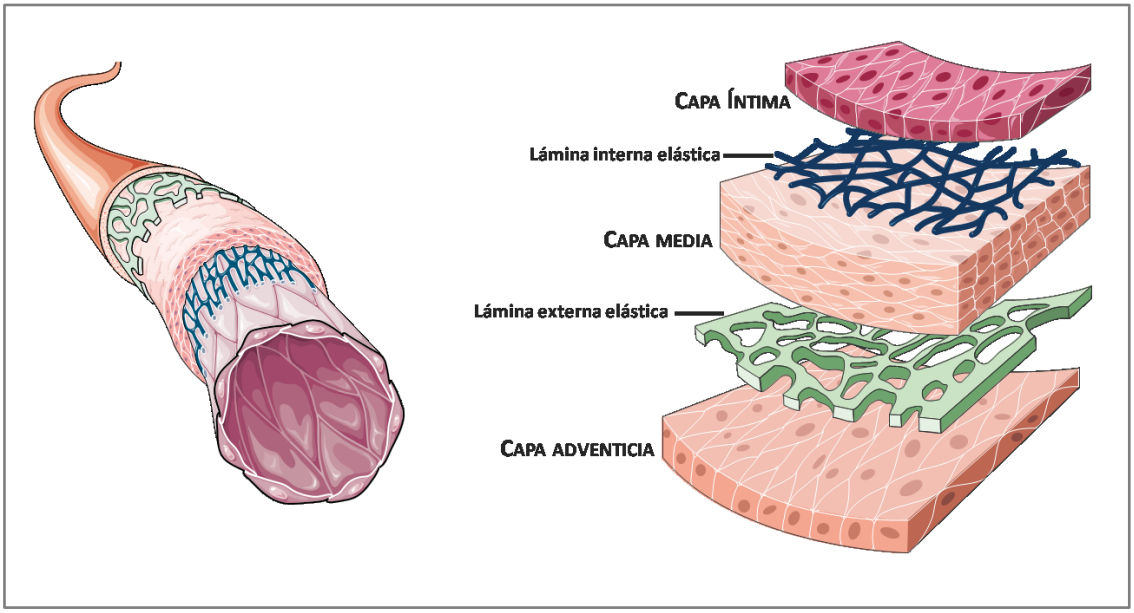

Figura 1. **Estructura de la pared vascular de un arteria sana**. Las arterias se componen de 3 capas concéntricas, del lumen hacia el exterior: capa íntima compuesta por células endoteliales, capa media formada por células vasculares de músculo liso y capa adventicia constituida por células epiteliales. Los límites de las tres capas están bien definidos por la lámina interna elástica que separa las túnicas íntima y media y la lámina externa elástica que separa la túnica media de la adventicia.

Las arterias se componen de tres capas fundamentalmente (Figura 1). De fuera hacia dentro; adventicia, formada fundamentalmente por células epiteliales; media, formada por células vasculares de músculo liso (VSMC: del inglés "vascular smooth muscle

cells") y la capa íntima que se encuentra en contacto con la sangre y que se constituye por una única capa células endoteliales (EC: del inglés "endotelial cells"). Las capas están perfectamente separadas por la lámina externa elástica (túnicas media y adventicia) y la lámina interna elástica (túnicas íntima y media). La aterosclerosis puede considerarse de modo simplificado como una respuesta a un daño (6, 7) por la cual se produce una remodelación en el vaso. Esa remodelación se va a producir fundamentalmente en las capas íntima y media. La formación de la placa de ateroma o aterogénesis se constituye de diferentes pasos progresivos tal y como se puede ver en la Figura 2.

- Disfunción endotelial: Las células endoteliales son una barrera selectiva de intercambio entre la sangre y los tejidos. Cuando hay una permeabilidad mayor de la adecuada y, por tanto, se permite una entrada a la capa íntima de macromoléculas como, por ejemplo, las LDL (del inglés "low density lipoproteins") la lesión está comenzando. Esto sucede, como ya se ha mencionado previamente, en las zonas de flujo turbulento y parece ser debido a una diferente forma de las células endoteliales en esa zona que hacen que sean zonas preferenciales del inicio de la lesión.

- Inflamación: Las LDL que han entrado se fijan en la zona subendotelial y van a ser modificadas hasta estar oxidadas: ox-LDL (del inglés "oxidized- low density lipoporteins"). El proceso de inflamación se desencadena con esas modificaciones unidas al reclutamiento desde el torrente sanguíneo de monocitos y linfocitos. Este reclutamiento se ve favorecido por cambios en la células endoteliales que ahora expresan moléculas de adhesión, por la estimulación de las células endoteliales para producir moléculas pro-inflamatorias y por la inhibición de la producción de óxido nitríco (NO).

- Formación de células espumosas: Los LDL subendoteliales cada vez se van oxidando más y eso permite una interacción con los macrófagos reclutados de forma que estos últimos engullen los ox-LDL hasta cambiar a células espumosas. Estas células espumosas contribuyen al desarrollo de la lesión por generación de citoquinas inflamatorias

- Formación de placas fibrosas, placa de ateroma: como consecuencia de la situación inflamatoria y la expresión de citoquinas y factores de crecimiento por parte de los macrófagos y los linfocitos T, las VSMCs características de la capa media ven favorecida su migración desde dicha capa a la capa íntima cambiando su fenotipo de estructural a sintetizador y produciendo proteínas de matriz extracelular, entre ellas colágeno. Al final se forma un núcleo lipídico rodeado por una capa fibrosa protectora constituyendo lo que se conoce como placa de ateroma.

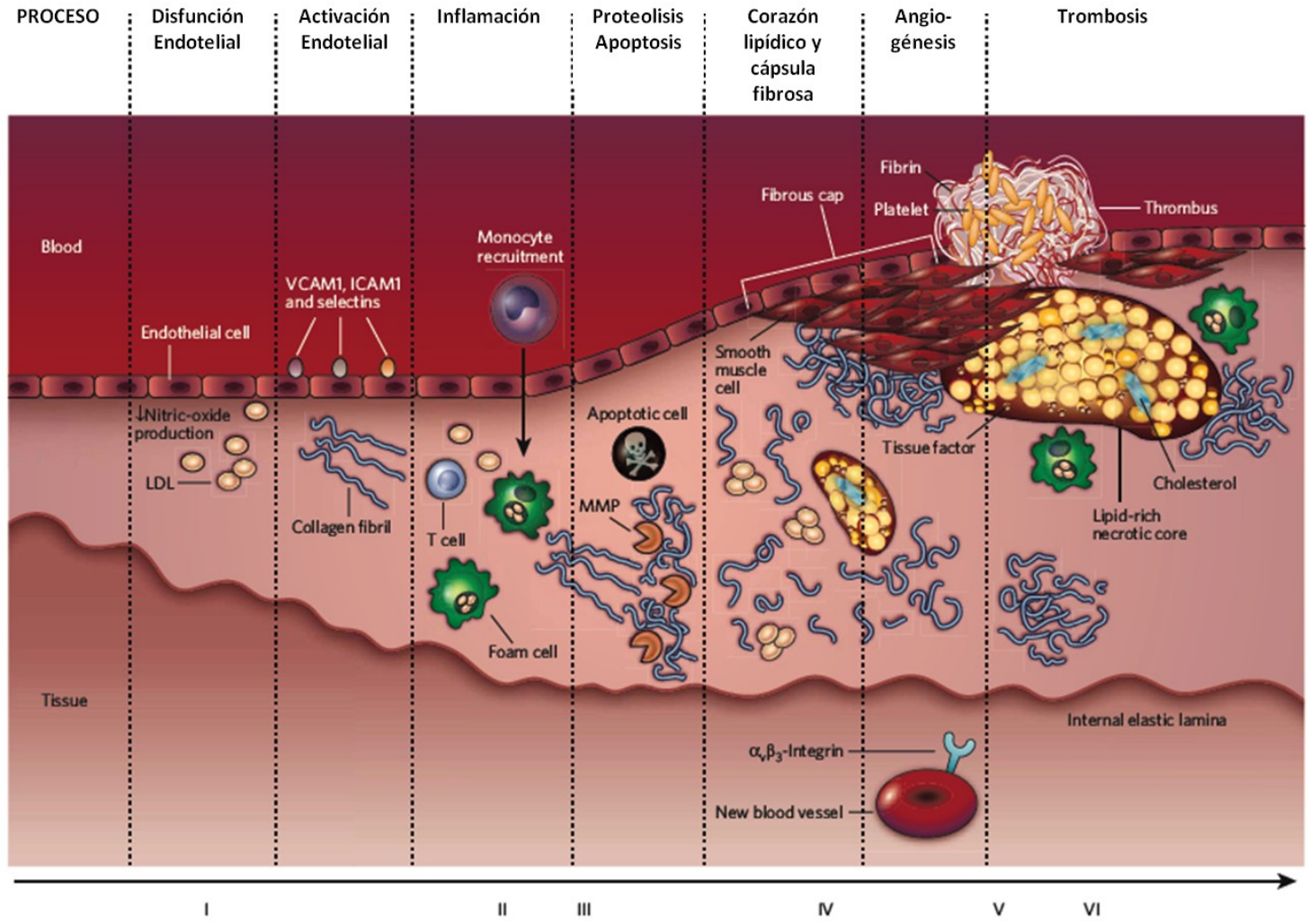

Figura 2. **Desarrollo de la placa de ateroma** representado espacialmente de izquierda a derecha, desde un vaso normal a una placa de ateroma con trombo. Adaptado de: *Sanz J., & Fayad Z.A. Imaging of atherosclerotic cardiovascular disease. Nature. 451, 953-957 (2008)*

- Evolución de las placas. Una vez formada, la placa puede evolucionar hacia una situación estable o ,por el contrario, inestable en función principalmente de su composición y del grosor de la capa fibrosa. Las placas estables pueden permanecer silentes sin provocar daño. Sin embargo, las inestables implican ruptura con las consecuencias que se detallan a continuación.

La complicación clínica más importante derivada de la aterosclerosis es una oclusión del flujo debido a la formación de un trombo o coágulo produciendo un infarto de miocardio (AMI, del inglés "Acute Myocardial Infraction") si la oclusión se produce en la arteria coronaria o un ictus en caso de producirse en la carótida(8). La capacidad del núcleo lipídico para formar trombos depende en gran medida del factor tisular que producen tanto las ECs como los macrofágos favorecido por las ox-LDL y que es un importante iniciador de la cascada de coagulación.

Las razones por las cuales se produce el trombo y se desencadenan los fatales hechos posteriores han sido y siguen siendo de gran interés tanto para clínicos como para investigadores (9) y se cree que las células y mediadores inflamatorios juegan un papel importante en la trombogenia de la placa (10). En el año 2000, *Virmani et al.* (11) establecieron las principales causas de la formación del trombo; ruptura de la placa, erosión de la placa y calcificación de los nódulos, señalando su prevalencia en los casos de evento (Figura 3). Para ello se basaron en un nuevo concepto postulado por *Peter Libby et al.* (12) que apuntaron que la capa fibrosa sufre un adelgazamiento antes de que se produzca una ruptura constituyéndose lo que se conoce como fibroateroma de capa fina (TCFA, del inglés "Thin-Cap Fibroatheroma") o placa vulnerable (13). Dicha ruptura de la placa se refiere a una lesión consistente en un corazón necrótico rodeado por una fina capa fibrosa, en general < 65µm, que al romperse libera sustancias altamente trombogénicas al torrente sanguíneo. Es el responsable de la mayor parte de los eventos, dos tercios del total de los casos clínicos. A continuación, por orden de incidencia en la población general y con mayor importancia en diabéticos, y primera causa en el caso de eventos en mujeres menores de 50 años, está la erosión de la placa. En este caso el trombo tiene una base rica en VSMCs y proteoglicanos. Por último, la razón más excepcional de la formación del trombo es debida a la erosión de nódulos calcificados. Las placas con calcificación se caracterizan por tener una capa fibrosa discontinúa, con una superficie luminar irregular con ausencia de ECs y con un trombo subyacente. En la actualidad se incluye una cuarta razón como causa de los síndromes agudos coronarios (ACS, del inglés " Acute Coronary Syndrom"), las hemorragias intra-placa (13). El porqué sucede la degradación de la capa parece estar relacionado con una degradación en la matriz extracelular (14) y un posterior estrés mecánico en la placa debilitada (15) pero en realidad los mecanismos en sí se desconocen.

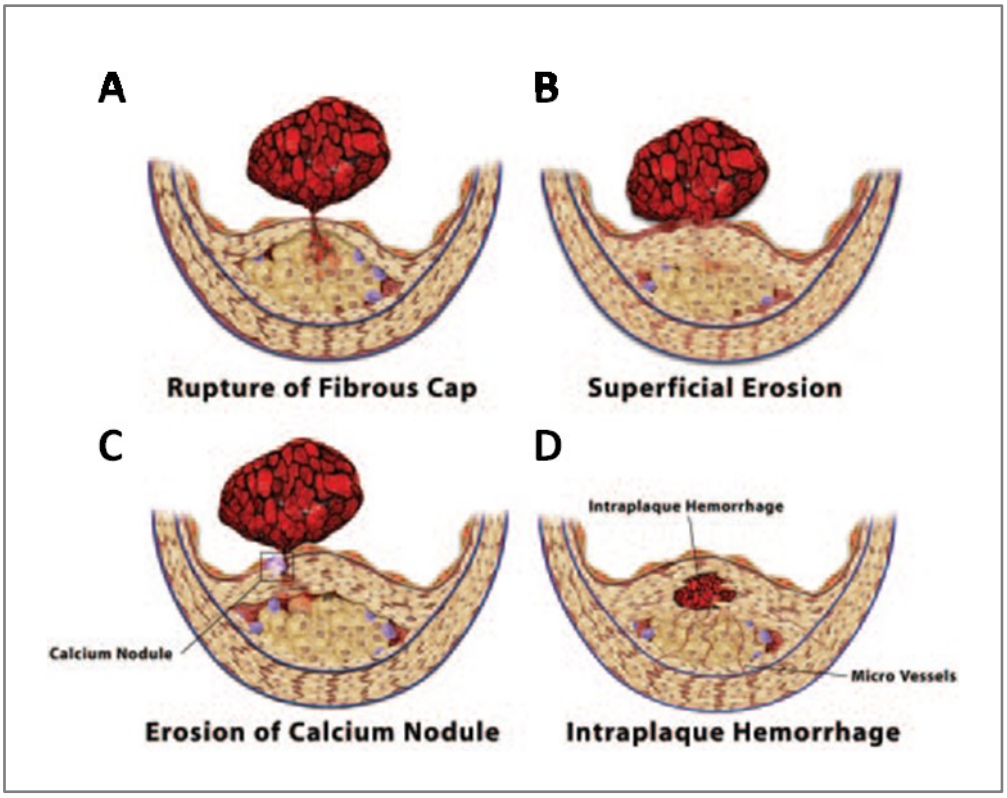

Figura 3. **Anatomía de las principales casusas de formación del trombo** por orden de incidencia (A>B>C>D). A: **Ruptura de la placa**. Al romperse la placa libera material altamente trombogénico al torrente sanguíneo. B: **Erosion Superficial**. Una erosión en las células endoteliales pone en contacto el material trombogénico con la sangre. C: **Calcificación de los nódulos**, Estas placas calcificadas son características por ser discontinuas lo que permiten la liberación del material trombogénico D: **Hemorragía intra-placa**. Responden a rupturas internas que van haciendo que la placa aumente de tamaño por su incorporación a las mismas y como consecuencia que el lumen vaya disminuyendo. Adaptado de: *Libby P., Theroux P.; Pathophysiology of Coronary Artery Disease. Circulation. 111:3481-3488 (2005)*

Cabe destacar también que a veces las rupturas se producen internamente. Clínicamente, éstas son rupturas sin relevancia pero el trombo producido se incorpora a la lesión provocando un crecimiento de la placa que a su vez produce un estrechamiento del lumen.

Es importante señalar también que las placas de ateroma no tienen porqué evolucionar siempre hacia un evento sino que existen situaciones intermedias en las que la placa es estable y lo que produce es un estrechamiento del vaso lo que produce una oclusión parcial y que corresponde a la situación clínica de angina.

ESTIMACIÓN DEL RIESGO CARDIOVASCULAR.

Las complicaciones cardiovasculares son la primera causa de muerte en el mundo. La razón subyacente de la mayoría es la aterosclerosis y el principal problema es que el engrosamiento de la pared arterial y el consecuente estrechamiento en el paso sanguíneo sucede lenta y silenciosamente durante décadas sin existir síntomas hasta el momento del evento. Esto es algo nefasto y además representa un elevado coste socio económico, por lo que supone una ventana de trabajo muy grande para el diagnóstico precoz y la evaluación del riesgo de los sujetos a desarrollar cualquiera de estas complicaciones. En las consultas primarias la evaluación de los riesgos de sufrir complicaciones cardiovasculares se basan en el uso de ecuaciones (Figura 4: composición interface de varios predictores) desarrolladas en base a estudios epidemiológicos. El estudio Framingham (16, 17) evalúa el riesgo de sufrir enfermedad cardiovascular en un plazo medio de diez años mediante ecuaciones que combinan datos de los factores de riesgos mencionados previamente: edad, sexo, niveles de colesterol, diabetes, hipertensión, tabaquismo, junto con la práctica de hábitos saludables de vida y sometimiento a tratamientos médicos para controlar alguno de esos factores de riesgo. Estas ecuaciones confieren gran importancia al sexo y a la edad dando menos valor a otros factores de riesgo especialmente en el caso de hombres menores de 45 años y mujeres menores de 65 años. Además se sospecha que pueden sobre o sub estimar el riesgo en función de las diferentes etnias o poblaciones. Todo esto hace que su valor individual sea limitado. En un paso más allá en Europa y bajo la guía de la Sociedad Europea de Cardiología (ESC, del inglés “European Society of Cardiovascular”) se recomienda el uso del estimador SCORE, que tiene en cuenta los datos estadísticos de cada país, generando así una ecuación idónea para cada país europeo (18). Sin embargo, hoy por hoy, va tomando fuerza la evaluación de estos riesgos a más largo plazo, en lo que se denomina “Lifetime Risk”. Consiste en la estimación del riesgo a lo largo de la vida. Las principales variaciones respecto a las anteriores estimaciones es que ahora tienen en consideración la duración a la exposición de los individuos al riesgo y se le confiere mayor importancia a los pequeños cambios durante la juventud que a los grandes cambios en personas de mayor edad (19). Con esto lo que se persigue es que se traten más jóvenes con riesgo real de sufrir un evento cardiovascular (ECV) y que menos personas mayores sean tratadas automáticamente.

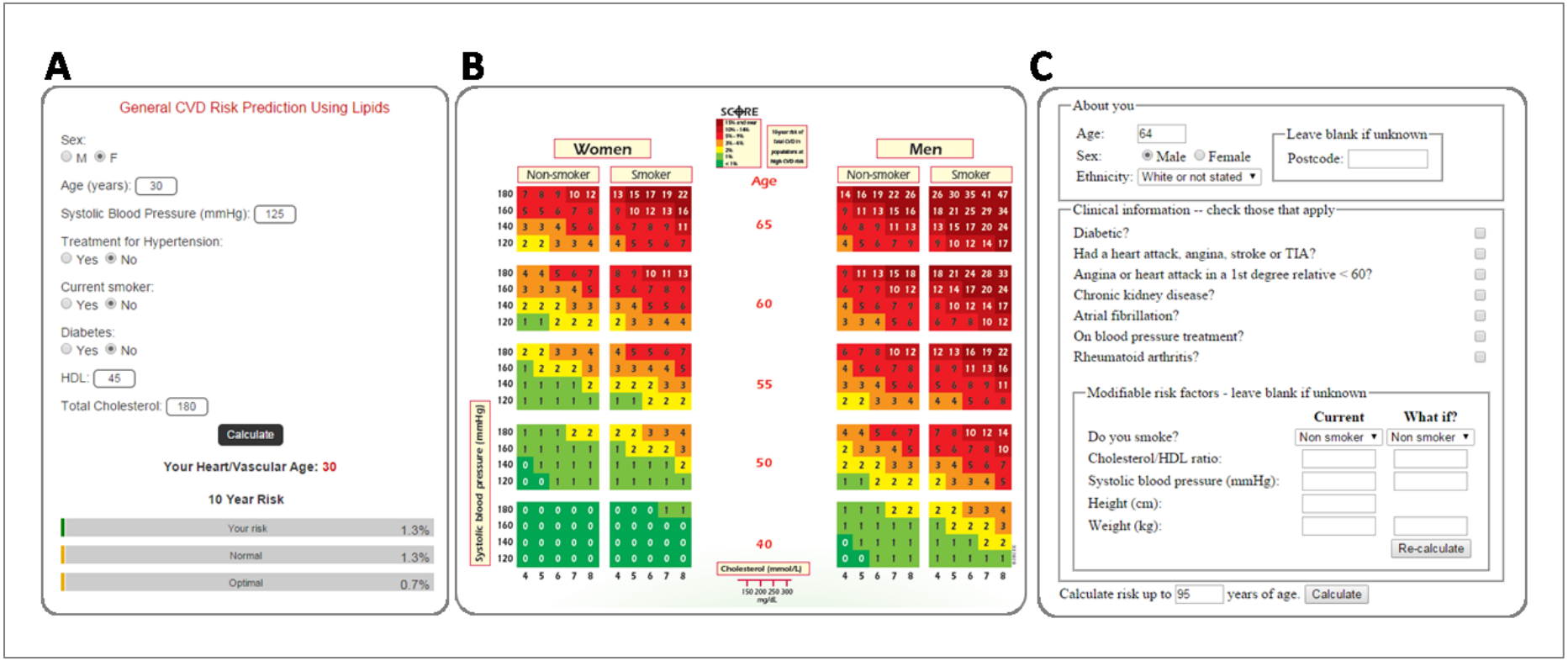

Figura 4. **Estimadores de riesgo cardiovascular**. A: **Estimador del estudio Framingham**. Está indicado para evaluar el riesgo de un individuo de sufrir un CVE en los próximos 10 años. Se indica para adultos a partir de 20 años que no hayn sufrido un ECV previo o Diabetes. B: **Estimador SCORE**. Calcula el riesgo de sufrir un CVE a 10 años basándose en la edad, el sexo, tabaquísmo, presión arterial y colesterol total, siendo la edad y el sexo los factores con mayor peso en la estimación. C: **Lifetime risk**. Estima el riesgo de sufrir un CVE a lo largo de la vida comparando con buenos controles por comparación de los siguientes factores de riesgo; tabaquísmo, índice de masa corporal, relación colesterol total/HDL y presión arterial.

IDENTIFICACIÓN DE NUEVOS MARCADORES MOLECULARES.

Actualmente los tratamientos farmacológicos aplicados a los individuos con alto riesgo ECV van enfocados a la reducción de lípidos, fijándose especialmente en los niveles en sangre de LDL-colesterol (20, 21). Diferentes estudios han demostrado que la reducción de esos niveles favorece placas más estables a la vez que se relacionada con diferentes efectos beneficiosos (10): reducción de la inflamación, tendencia a mayores niveles de colágeno, menor cantidad de ox-LDL, menos especies oxígeno reactivas (ROS, del inglés "reactive oxygen species"), mayor producción de NO endotelial y menor tendencia trombogénica.

Llegados a una situación de riesgo inminente, el protocolo señala realizar intervenciones quirúrgicas vasculares enfocadas al restablecimiento correcto del flujo sanguíneo. Debido a la ya mencionada ausencia de síntomas, en la mayoría de los casos los criterios de intervención se basan en la evaluación del grado de estenosis. Sin embargo, cada vez se tiene más creencia de que esto es un criterio pobre y más parámetros deben ser incluidos en la ecuación. Eso unido a la naturaleza reactiva y no preventiva de estas intervenciones ha hecho que muchos de los esfuerzos actuales estén puestos en tratar de estabilizar las lesiones y mejorar los factores sistémicos que aumentan la susceptibilidad a sufrir complicaciones trombóticas. En consonancia, se ha fomentado la investigación en la búsqueda de nuevos marcadores relacionados con los procesos conocidos de la formación de la placa (22). Es de especial interés la búsqueda de nuevos indicadores moleculares en fluidos biológicos, ya que permiten un diagnóstico no invasivo que puede servir para mejorar el criterio de intervenciones quirúrgicas recomendadas y permitir el desarrollo de tratamientos preventivos así como la monitorización de su efectividad. Sin olvidar potenciales marcadores asociados con genética o bien obtenidos, por ejemplo, mediante técnicas de imagen.

En términos generales, los biomarcadores se definen como "una característica que puede ser objetivamente medida y evaluada como un indicador de un proceso biológico normal, un proceso patológico o una respuesta farmacéutica a una intervención terapéutica" (23). Más particularmente, la "bondad" de un marcador se evalúa con respecto a tres caractarísticas principales: discriminación, calibración y reclasificación. La discriminación responde a la habilidad del marcador de distinguir entre aquellos sujetos que sufrirán de los que no una enfermedad. Calibración se refiere a la concordancia entre los riesgos predichos y los observados en subgrupos con diferentes niveles basales de riesgo. Por reclasificación se entiende la capacidad de un marcador de, considerando un nuevo riesgo, reclasificar correctamente el riesgo general del sujeto. Idealmente, todo nuevo marcador debe cumplir estas características. Resultantes de diferentes estudios hay moléculas asociadas a diferentes situaciones de la formación de la placa de ateroma que se han postulado como candidatos a marcadores en la patología aterosclerótica. De entre ellos, algunos de los más extendidos son los que se comentan brevemente a continuación. Relacionados con la acumulación de lípidos destaca Lp-PLA2 (del inglés "lipoprotein-associated phospholipase A2" que es una proteína que viaja con los LDL circulantes y se encarga de hidrolizar los fosfolípidos de

dichos LDL. Con respecto a la inflamación destacan la proteína C reactiva (CRP, del inglés: C-reactive protein) y la proteína C-reactiva de alta sensibilidad (hs-CRP, "high sensitivity, C-reactive protein). Relacionado con la situación de estrés latente en la aterosclerosis destaca el péptido tipo B natriurético (BNP: "B-type natriuretic peptide") que tiene propiedades vasodilatadoras, natriuréticas y antihipertroficas. Todos ellos se encuentran aumentados en la condición patológica (22, 24). Sin embargo todos estos marcadores circulantes en el plasma, no mejoran la predicción del riesgo de los individuos en demasía si no que únicamente parecen ser útiles en cuanto a reclasificar el riesgo individual de cada paciente en una categoría diferente a la que le confieren las estimaciones de riesgo generales pero no son capaces, o al menos hasta ahora no se ha demostrado, de discriminar o recalibrar. Estos hechos hacen pensar que quizá un único marcador no es suficiente por sí mismo y que, por el contrario, un grupo de marcadores es más posible que formen un panel suficientemente sensible y específico en la evaluación de la prognosis de la enfermedad estudiada.

LA ATEROSCLEROSIS DESDE UN ABORDAJE ÓMICO: Proteómica y Metabolómica.

En los últimos años las conocidas como técnicas ómicas han sufrido un desarrollo enorme, en gran parte gracias al desarrollo de nuevas tecnologías y se han posicionado como una importante estrategia en la búsqueda de nuevos marcadores. Estas técnicas no hacen pre-selección de candidatos por lo que proporcionan un abordaje sin sesgo en un momento fisiológico concreto. Debido a que la aterosclerosis es una enfermedad compleja y activa en la que se está produciendo la interacción de múltiples células (macrófagos, ECs, VSMCs) y organismos (corazón, riñones, hígado,...) (25, 26) el empleo de técnicas ómicas es más que adecuado ya que permite una evaluación conjunta de todos los sistemas y moléculas simultáneamente, entendido como un todo y enmarcado en lo que podemos llamar estudio de biología de sistemas. El abordaje de la aterosclerosis como patología mediante estrategias ómicas, no va a ser útil sólo en la búsqueda de marcadores sino que permite evaluar mecanismos subyacentes de la enfermedad conocidos así como aquellos que aún son desconocidos a la vez que es posible la identificación de nuevas moléculas implicadas en el desarrollo de los mismos.

La proteómica es la disciplina que estudia de manera dinámica todas las proteínas expresadas por un organismo, en un momento dado y bajo determinadas condiciones concretas de tiempo y ambiente, lo que se denomina proteoma (27). El flujo de trabajo y las técnicas más habitualmente empleadas se recogen en la Figura 5. Durante los últimos años muchos son los estudios que han aplicado la proteómica a la mejora del entendimiento de la aterosclerosis y la búsqueda de marcadores. Los proteomas y subproteomas más usados corresponden a tejido arterial y sangre/plasma y en menor instancia la orina como fluido alternativo.

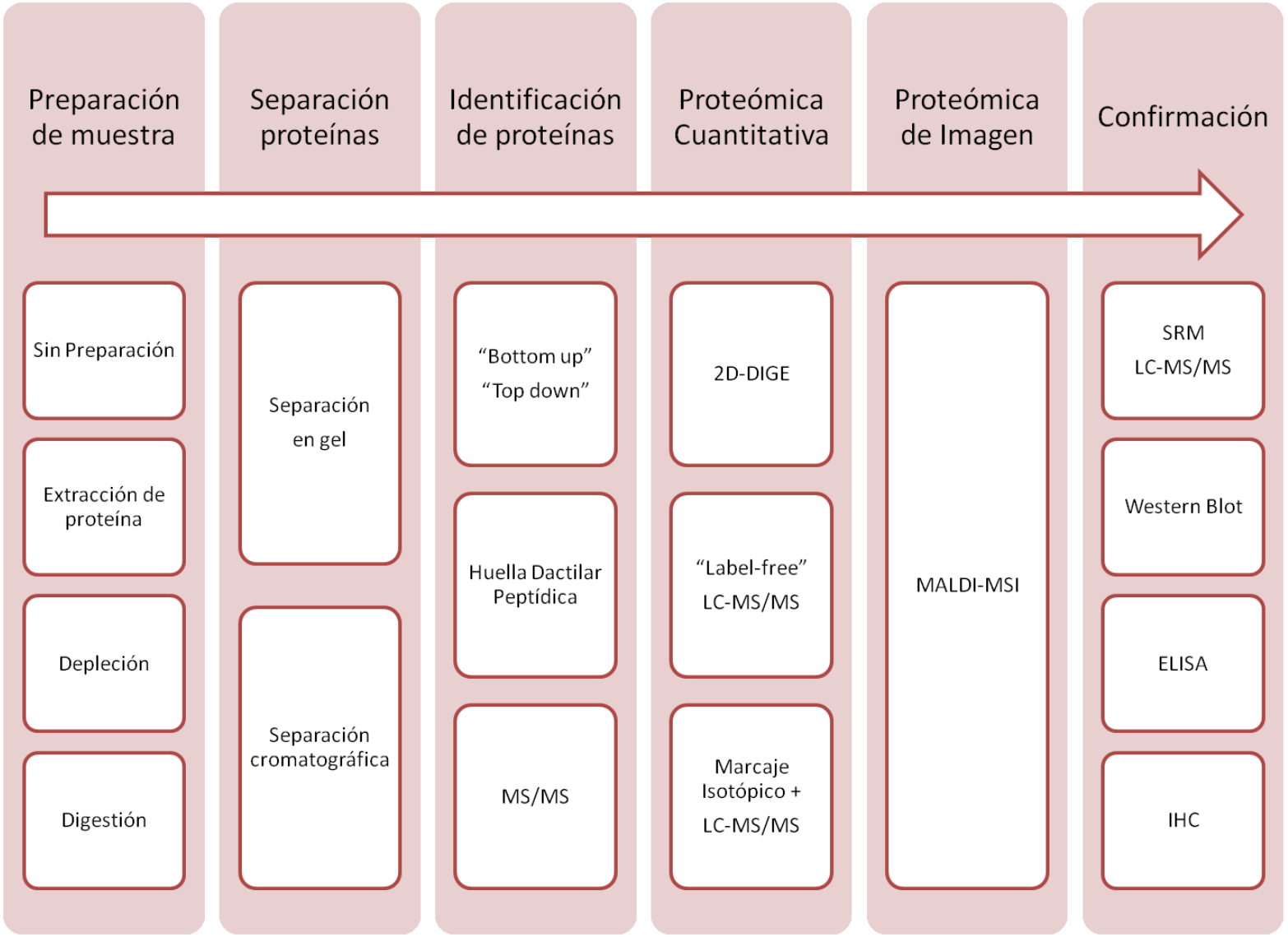
Preparación de muestra
Separación proteínas
Identificación de proteínas
Proteómica Cuantitativa
Proteómica de Imagen
Confirmación
Sin Preparación
Extracción de proteína
Depleción
Digestión
Separación en gel
Separación cromatográfica
"Bottom up"
"Top down"
Huella Dactilar Peptídica
MS/MS
2D-DIGE
"Label-free" LC-MS/MS
Marcaje Isotópico + LC-MS/MS
MALDI-MSI
SRM LC-MS/MS
Western Blot
ELISA
IHC

Figura 5.

Los estudios de tejido permiten la evaluación de los mecanismos subyacentes en la enfermedad y se han refinado enormemente en los últimos años. Los primeros estudios proteómicos de tejido se hicieron considerando el tejido arterial en conjunto en lo que se conoce como estudios de tejido completo. De esta forma se han estudiado los cambios proteómicos de los vasos durante la aterogénesis (28, 29) o las diferencias entre placas estables e inestables o con trombo (30-32). Posteriormente se analizaron subproteomas derivados del tejido como el análisis específico del proteoma de las VSMC (33) o, en nuestro caso, el secretoma (34). Un paso más allá fue la inclusión de la microdiseción por láser en la patología vascular. Gracias a ello nuestro grupo y otros se han acercado más a la composición característica de la capa íntima y media y a sus variaciones particulares en situaciones de enfermedad cardiovascular (35-37). La aparición en 1967 de la espectrometría de masas de imagen (38) y en especial los últimos avances en la última década en MALDI-MSI (del inglés "Matrix Assitted Laser Desorption/Ionization- Mass Spectrometry Imaging") abren una ventana al estudio de los mapas moleculares in situ de los tejidos arteriales y que están dando sus primeros pasos en la aterosclerosis tal y como se describe en capítulos posteriores de esta tesis doctoral (capítulos 4 y 5).

El plasma tiene una gran aplicabilidad en el diagnóstico clínico de rutina, por eso quizá es el fluido biológico donde mayor número de estudios proteómicos de aterosclerosis se han realizado. Sin embargo es importante señalar que tiene una limitación importante en el estudio de las proteínas ya que su composición proteica es en su mayoría albúmina y cadenas de IgG. Eso hace que sea difícil evaluar los cambios en el resto de proteínas presentes y que por ello sea imprescindible reducir el rango dinámico de concentración incluyendo un paso de depleción de dichos componentes mayoritarios. La mayor parte de los estudios se centra en marcadores de diagnóstico de riesgo de sufrir un evento cardiovascular, de esta forma se han estudiado variaciones en plasma en enfermedad coronaria (39), enfermedad arterial periférica (40) y en situaciones de evento (41-43).

La orina es una fuente alternativa de marcadores de obtención no invasiva que, sin embargo, no ha sido tan ampliamente estudiada en aterosclerosis. Representa un filtrado del plasma y proteínas del tracto urinario por lo que refleja no sólo una función renal normal sino también cualquier alteración fisiopatológica. Teniendo en cuenta que corazón y riñones constituyen un binomio de interacción bidireccional llamado síndrome cardio-renal [cita], la orina se presenta como una fuente rica de potenciales marcadores. Su uso está extendido en el diagnóstico clínico de rutina, con lo cual es una muestra biológica óptima para el estudio de la patología aterosclerótica. Hasta ahora pocos son los estudios que hay en la bibliografía en el campo de las ECV destacando dos, uno centrado en cardiopatía isquémica (44) y otro en un modelo de aterosclerosis en ratón apoE(-/-) (45). En los capítulos 1 y 2 de esta tesis doctoral, se describe la puesta a punto y el desarrollo de un estudio proteómico de aterosclerosis en orina.

La metabolómica es la disciplina que estudia los procesos biológicos en los que están involucrados los metabolitos, es decir, es el estudio sistemático de las huellas únicas que dejan los procesos celulares específicos a su paso en cuanto a moléculas pequeñas (metaboloma) (46). El flujo de trabajo y las técnicas más habitualmente empeladas se recogen en la Figura 6. De la misma forma que la proteómica, la metabolómica, aunque con menor expansión aún que el estudio de las proteínas, ha ayudado al mejor entendimiento de la aterosclerosis y a la búsqueda de marcadores [cita].

Los estudios de los metabolitos variados en respuesta al desarrollo de la aterosclerosis directamente en el tejido comenzaron siendo estudios de extractos del tejido, aunque en los últimos tiempos el avance de las técnicas de espectrometría de imagen y de la resonancia magnética nuclear (RMN) en su variante de HRMAS (del inglés "high resolution magic angle spinning"), ha permitido estudios directos (no desdructivos) en tejido e incluso con localización *in situ* gracias al SIMS-TOF y al MALDI-MSI. Trabajando con extractos de tejido se han encontrado metabolitos característicos de los estadios iniciales de la aterosclerosis (28), en comparación de estadios iniciales de engrosamiento y de placa formada (47) e incluso diferenciales de entre los diferentes tipos de placas (48) así como en otras patologías vasculares como la fibrilación auricular (49). La resonancia de protón de ángulo mágico (HRMAS) permite el estudio directo de tejido. Acorde a nuestro conocimiento no existe ningún estudio de los metabolitos implicados en el desarrollo de la ateroclerosis por HRMAS en la bibliografía. El presentado en el capítulo 3 de esta tesis doctoral sería por tanto el primero en el campo. Sin embargo, sí se han obtenido con éxito perfiles en estudios de corazón (50, 51). Gracias a las técnicas de imagen existen diferentes perfiles lipídicos correspondientes a las diferentes capas de la arteria (52) a la vez que se han caracterizado diferentes lípidos presentes en la placa de ateroma (53) o se ha hecho un seguimiento de los cambios de las moléculas pequeñas tras el uso de fármacos empleados en ECV (54). En el capítulo 4 de esta tesis doctoral, se describe un nuevo mapa lipídico de la lesión temprana aterosclerótica desde la capa media hasta zonas calcificadas.

Los estudios en fluidos biológicos, tanto en plasma como en orina suponen un abordaje menos directo, a priori, pero cuentan con la ventaja de ser accesibles en la práctica clínica. El descubrimiento de marcadores de desarrollo de aterosclerosis (55, 56), situaciones de riesgo (57, 58), así como en complicaciones cardiovasculares tales como ataque cardiaco (59-62), enfermedad cardiovascular periférica y auricular (49, 63) o en riesgo de desarrollar diabetes mellitus (64). El capítulo 2 de esta tesis doctoral describe un estudio por NMR de orina en aterosclerosis temprana a la vez que evalúa la recuperación de pacientes que han sufrido un evento cardiovascular. Por consiguiente, se emplea la NMR para abordar dos situaciones de vital importancia, el riesgo y la recuperación por un abordaje no aplicado hasta ahora, en cuanto a nuestro conocimiento se refiere.

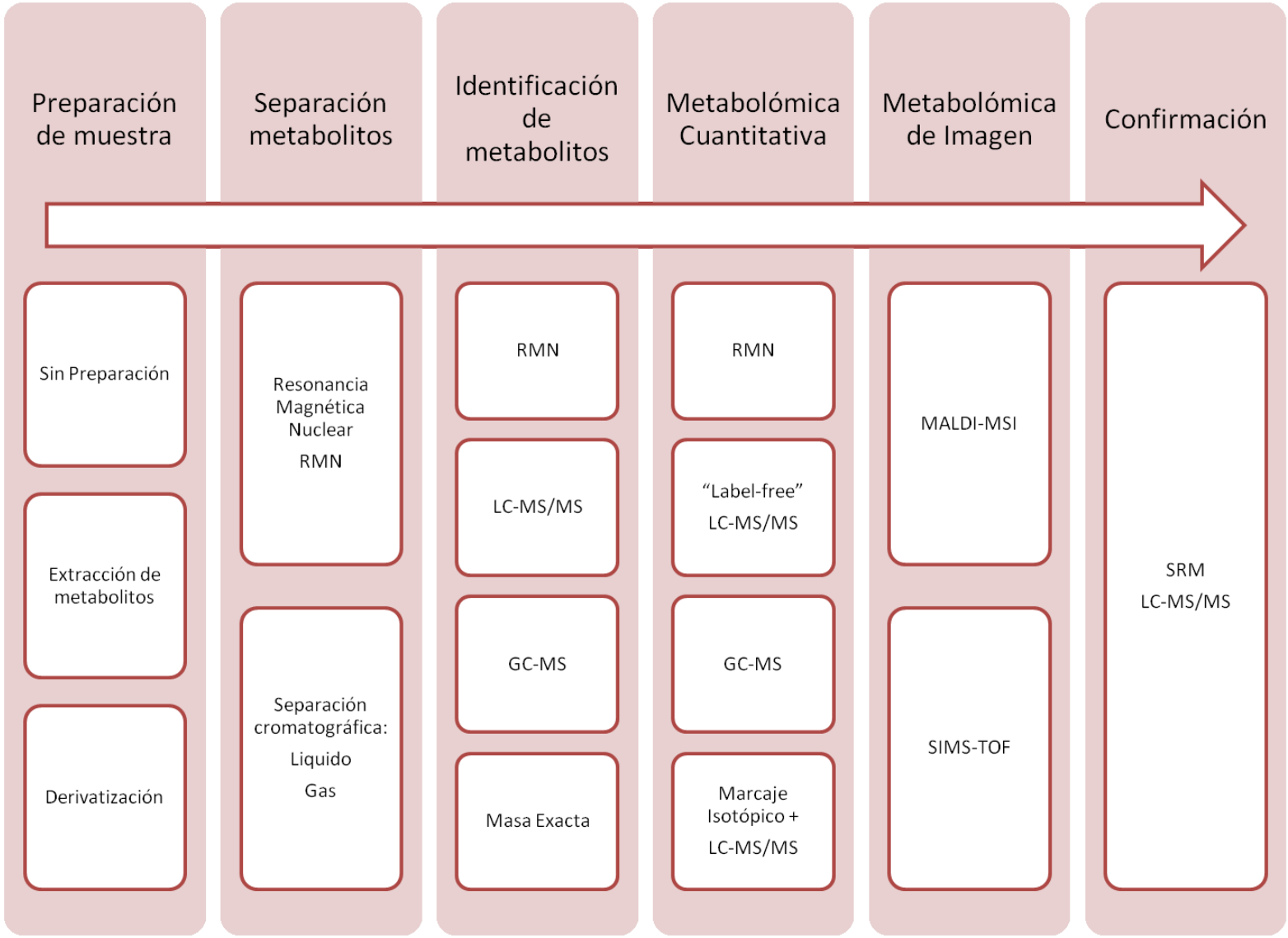
Preparación de muestra
Separación metabolitos
Identificación de metabolitos
Metabolómica Cuantitativa
Metabolómica de Imagen
Confirmación
Sin Preparación
Extracción de metabolitos
Derivatización
Resonancia Magnética Nuclear
RMN
Separación cromatográfica:
Liquido
Gas
RMN
LC-MS/MS
GC-MS
Masa Exacta
RMN
"Label-free"
LC-MS/MS
GC-MS
Marcaje Isotópico +
LC-MS/MS
MALDI-MSI
SIMS-TOF
SRM
LC-MS/MS

Figura 6.

A modo de conclusión cabe destacar que durante los últimos años se ha dado un incremento en el número de artículos publicados, algunos de ellos destacados citados previamente, que emplean técnicas ómicas en el estudio de la aterosclerosis en particular y de las enfermedades cardiovasculares en general demostrando la gran utilidad de estas técnicas en el campo. Considerando la gran complejidad de estas enfermedades junto con su carácter multifactorial y la búsqueda de una medicina más personalizada en cuanto a diagnóstico y tratamiento, parece lógico que la biología de sistemas forme parte de la clave para conseguir esos objetivos a los que aspira la comunidad clínica. En esta tesis doctoral de investigación básica se han combinado técnicas proteómicas y metabolómicas tanto de las consideradas como clásicas, como las de segunda generación con el ánimo de contribuir al mejor entendimiento y prevención de la aterosclerosis.

REFERENCIAS

1. Lusis AJ. Atherosclerosis. Nature 2000; 407:233-41.

2. Gimbrone MA, Jr. Vascular endothelium, hemodynamic forces, and atherogenesis. Am J Pathol 1999; 155:1-5.

3. Assmann G, Cullen P, Jossa F, Lewis B, Mancini M. Coronary heart disease: reducing the risk: the scientific background to primary and secondary prevention of coronary heart disease. A worldwide view. International Task force for the Prevention of Coronary Heart disease. Arterioscler Thromb Vasc Biol 1999; 19:1819-24.

4. Khot UN, Khot MB, Bajzer CT, et al. Prevalence of conventional risk factors in patients with coronary heart disease. JAMA 2003; 290:898-904.

5. Lusis AJ, Weinreb A, Drake TA. In: Textbook of Cardiovascular Medicine. 2389-2413. Topol EJ, editor. Lippincott-Raven; Philadelphia:1998.

6. Ross R. The pathogenesis of atherosclerosis: a perspective for the 1990s. Nature 1993; 362:801-9.

7. Libby P. Changing concepts of atherogenesis. J Intern Med 2000; 247:349-58.

8. Fuster V, Moreno PR, Fayad ZA, Corti R, Badimon JJ. Atherothrombosis and high-risk plaque: part I: evolving concepts. J Am Coll Cardiol 2005; 46:937-54.

9. Finn AV, Nakano M, Narula J, Kolodgie FD, Virmani R. Concept of vulnerable/unstable plaque. Arterioscler Thromb Vasc Biol 2010; 30:1282-92.

10. Libby P. Mechanisms of acute coronary syndromes and their implications for therapy. N Engl J Med 2013; 368:2004-13.

11. Virmani R, Kolodgie FD, Burke AP, Farb A, Schwartz SM. Lessons from sudden coronary death: a comprehensive morphological classification scheme for atherosclerotic lesions. Arterioscler Thromb Vasc Biol 2000; 20:1262-75.

12. Libby P, Schoenbeck U, Mach F, Selwyn AP, Ganz P. Current concepts in cardiovascular pathology: the role of LDL cholesterol in plaque rupture and stabilization. Am J Med 1998; 104:14S-8S.

13. Virmani R, Burke AP, Farb A, Kolodgie FD. Pathology of the unstable plaque. Prog Cardiovasc Dis 2002; 44:349-56.

14. Libby P. Molecular bases of the acute coronary syndromes. Circulation 1995; 91:2844-50.

15. Vengrenyuk Y, Carlier S, Xanthos S, et al. A hypothesis for vulnerable plaque rupture due to stress-induced debonding around cellular microcalcifications in thin fibrous caps. Proc Natl Acad Sci U S A 2006; 103:14678-83.

16. JBS 2: Joint British Societies' guidelines on prevention of cardiovascular disease in clinical practice. Heart 2005; 91 Suppl 5:v1-52.

17. Perk J, De BG, Gohlke H, et al. European Guidelines on cardiovascular disease

prevention in clinical practice (version 2012). The Fifth Joint Task Force of the European Society of Cardiology and Other Societies on Cardiovascular Disease Prevention in Clinical Practice (constituted by representatives of nine societies and by invited experts). Eur Heart J 2012; 33:1635-701.

18. Perk J, De BG, Gohlke H, et al. European Guidelines on cardiovascular disease prevention in clinical practice (version 2012). The Fifth Joint Task Force of the European Society of Cardiology and Other Societies on Cardiovascular Disease Prevention in Clinical Practice (constituted by representatives of nine societies and by invited experts). Eur Heart J 2012; 33:1635-701.

19. Marma AK, Berry JD, Ning H, Persell SD, Lloyd-Jones DM. Distribution of 10-year and lifetime predicted risks for cardiovascular disease in US adults: findings from the National Health and Nutrition Examination Survey 2003 to 2006. Circ Cardiovasc Qual Outcomes 2010; 3:8-14.

20. Goff DC, Jr., Lloyd-Jones DM, Bennett G, et al. 2013 ACC/AHA guideline on the assessment of cardiovascular risk: a report of the American College of Cardiology/American Heart Association Task Force on Practice Guidelines. J Am Coll Cardiol 2014; 63:2935-59.

21. Goff DC, Jr., Lloyd-Jones DM, Bennett G, et al. 2013 ACC/AHA guideline on the assessment of cardiovascular risk: a report of the American College of Cardiology/American Heart Association Task Force on Practice Guidelines. Circulation 2014; 129:S49-S73.

22. Hermus L, Lefrandt JD, Tio RA, Breek JC, Zeebregts CJ. Carotid plaque formation and serum biomarkers. Atherosclerosis 2010; 213:21-9.

23. Biomarkers and surrogate endpoints: preferred definitions and conceptual framework. Clin Pharmacol Ther 2001; 69:89-95.

24. Wang TJ. Assessing the role of circulating, genetic, and imaging biomarkers in cardiovascular risk prediction. Circulation 2011; 123:551-65.

25. Corti R, Hutter R, Badimon JJ, Fuster V. Evolving concepts in the triad of atherosclerosis, inflammation and thrombosis. J Thromb Thrombolysis 2004; 17:35-44.

26. Libby P, Theroux P. Pathophysiology of coronary artery disease. Circulation 2005; 111:3481-8.

27. Bjellqvist B, Ek K, Righetti PG, et al. Isoelectric focusing in immobilized pH gradients: principle, methodology and some applications. J Biochem Biophys Methods 1982; 6:317-39.

28. Mayr M, Chung YL, Mayr U, et al. Proteomic and metabolomic analyses of atherosclerotic vessels from apolipoprotein E-deficient mice reveal alterations in inflammation, oxidative stress, and energy metabolism. Arterioscler Thromb Vasc Biol 2005; 25:2135-42.

29. Sung HJ, Ryang YS, Jang SW, Lee CW, Han KH, Ko J. Proteomic analysis of differential protein expression in atherosclerosis. Biomarkers 2006; 11:279-90.

30. Donners MM, Verluyten MJ, Bouwman FG, et al. Proteomic analysis of differential protein expression in human atherosclerotic plaque progression. J Pathol 2005; 206:39-45.

31. Lepedda AJ, Cigliano A, Cherchi GM, et al. A proteomic approach to differentiate histologically classified stable and unstable plaques from human carotid arteries. Atherosclerosis 2009; 203:112-8.

32. Slevin M, Elasbali AB, Miguel TM, Krupinski J, Badimon L, Gaffney J. Identification of differential protein expression associated with development of unstable human carotid plaques. Am J Pathol 2006; 168:1004-21.

33. Mayr M, Zampetaki A, Sidibe A, et al. Proteomic and metabolomic analysis of smooth muscle cells derived from the arterial media and adventitial progenitors of apolipoprotein E-deficient mice. Circ Res 2008; 102:1046-56.

34. de la Cuesta F, Barderas MG, Calvo E, et al. Secretome analysis of atherosclerotic and non-atherosclerotic arteries reveals dynamic extracellular remodeling during pathogenesis. J Proteomics 2012; 75:2960-71.

35. Bagnato C, Thumar J, Mayya V, et al. Proteomics analysis of human coronary atherosclerotic plaque: a feasibility study of direct tissue proteomics by liquid chromatography and tandem mass spectrometry. Mol Cell Proteomics 2007; 6:1088-102.

36. de la Cuesta F, Alvarez-Llamas G, Maroto AS, et al. A proteomic focus on the alterations occurring at the human atherosclerotic coronary intima. Mol Cell Proteomics 2011; 10:M110.

37. de la Cuesta F, Zubiri I, Maroto AS, et al. Deregulation of smooth muscle cell cytoskeleton within the human atherosclerotic coronary media layer. J Proteomics 2013; 82:155-65.

38. Helmut Liebl. Ion Microprobe Mass Analyzer. Journal of Applied Physics 1967; 38:5277-83.

39. Donahue MP, Rose K, Hochstrasser D, et al. Discovery of proteins related to coronary artery disease using industrial-scale proteomics analysis of pooled plasma. Am Heart J 2006; 152:478-85.

40. Wilson AM, Kimura E, Harada RK, et al. Beta2-microglobulin as a biomarker in peripheral arterial disease: proteomic profiling and clinical studies. Circulation 2007; 116:1396-403.

41. Mateos-Caceres PJ, Garcia-Mendez A, Lopez FA, et al. Proteomic analysis of plasma from patients during an acute coronary syndrome. J Am Coll Cardiol 2004; 44:1578-83.

42. Darde VM, de la Cuesta F, Dones FG, Alvarez-Llamas G, Barderas MG, Vivanco F. Analysis of the plasma proteome associated with acute coronary syndrome: does a permanent protein signature exist in the plasma of ACS patients? J Proteome Res 2010; 9:4420-32.

43. Peronnet E, Becquart L, Poirier F, Cubizolles M, Choquet-Kastylevsky G, Jolivet-Reynaud C. SELDI-TOF MS analysis of the Cardiac Troponin I forms present in plasma from patients with myocardial infarction. Proteomics 2006; 6:6288-99.

44. Delles C, Schiffer E, von Zur MC, et al. Urinary proteomic diagnosis of coronary artery disease: identification and clinical validation in 623 individuals. J Hypertens 2010; 28:2316-22.

45. von Zur MC, Schiffer E, Sackmann C, et al. Urine proteome analysis reflects atherosclerotic disease in an ApoE-/- mouse model and allows the discovery of new candidate biomarkers in mouse and human atherosclerosis. Mol Cell Proteomics 2012; 11:M111.

46. Hunter P. Reading the metabolic fine print. The application of metabolomics to diagnostics, drug research and nutrition might be integral to improved health and personalized medicine. EMBO Rep 2009; 10:20-3.

47. Vorkas PA, Shalhoub J, Isaac G, et al. Metabolic Phenotyping of Atherosclerotic Plaques Reveals Latent Associations between Free Cholesterol and Ceramide Metabolism in Atherogenesis. J Proteome Res 2015; 14:1389-99.

48. Stegemann C, Drozdov I, Shalhoub J, et al. Comparative lipidomics profiling of human atherosclerotic plaques. Circ Cardiovasc Genet 2011; 4:232-42.

49. Mayr M, Yusuf S, Weir G, et al. Combined metabolomic and proteomic analysis of human atrial fibrillation. J Am Coll Cardiol 2008; 51:585-94.

50. Griffin JL, Williams HJ, Sang E, Nicholson JK. Abnormal lipid profile of dystrophic cardiac tissue as demonstrated by one- and two-dimensional magic-angle spinning (1)H NMR spectroscopy. Magn Reson Med 2001; 46:249-55.

51. Bollard ME, Murray AJ, Clarke K, Nicholson JK, Griffin JL. A study of metabolic compartmentation in the rat heart and cardiac mitochondria using high-resolution magic angle spinning 1H NMR spectroscopy. FEBS Lett 2003; 553:73-8.

52. Zaima N, Sasaki T, Tanaka H, et al. Imaging mass spectrometry-based histopathologic examination of atherosclerotic lesions. Atherosclerosis 2011; 217:427-32.

53. Mas S, Martinez-Pinna R, Martin-Ventura JL, et al. Local non-esterified fatty acids correlate with inflammation in atheroma plaques of patients with type 2 diabetes. Diabetes 2010; 59:1292-301.

54. Tanaka H, Zaima N, Ito H, et al. Cilostazol inhibits accumulation of triglycerides in a rat model of carotid artery ligation. J Vasc Surg 2013; 58:1366-74.

55. Teul J, Ruperez FJ, Garcia A, et al. Improving metabolite knowledge in stable atherosclerosis patients by association and correlation of GC-MS and 1H NMR fingerprints. J Proteome Res 2009; 8:5580-9.

56. Zhang F, Jia Z, Gao P, et al. Metabonomics study of atherosclerosis rats by ultra fast liquid chromatography coupled with ion trap-time of flight mass spectrometry. Talanta 2009; 79:836-44.

57. von Zur MC, Schiffer E, Zuerbig P, et al. Evaluation of urine proteome pattern analysis for its potential to reflect coronary artery atherosclerosis in symptomatic patients. J Proteome Res 2009; 8:335-45.

58. Yap IK, Brown IJ, Chan Q, et al. Metabolome-wide association study identifies multiple biomarkers that discriminate north and south Chinese populations at differing risks of cardiovascular disease: INTERMAP study. J Proteome Res 2010; 9:6647-54.

59. Laborde C, Mourino-Alvarez L, Posada-Ayala Ma, et al. Plasma metabolomics reveals a potential panel of biomarkers for early diagnosis in acute coronary syndrome. Metabolomics 2014; 10:414-24.

60. Jiang P, Dai W, Yan S, et al. Potential biomarkers in the urine of myocardial infarction rats: a metabolomic method and its application. Mol Biosyst 2011; 7:824-31.

61. Lewis GD, Wei R, Liu E, et al. Metabolite profiling of blood from individuals undergoing planned myocardial infarction reveals early markers of myocardial injury. J Clin Invest 2008; 118:3503-12.

62. Chan CX, Khan AA, Choi JH, et al. Technology platform development for targeted plasma metabolites in human heart failure. Clin Proteomics 2013; 10:7.

63. Shah SH, Hauser ER, Bain JR, et al. High heritability of metabolomic profiles in families burdened with premature cardiovascular disease. Mol Syst Biol 2009; 5:258.

64. Wang TJ, Larson MG, Vasan RS, et al. Metabolite profiles and the risk of developing diabetes. Nat Med 2011; 17:448-53.

OBJETIVOS

El objetivo general de esta tesis doctoral consiste en el estudio de los mecanismos subyacentes del desarrollo silente y asintomático de la aterosclerosis para un mejor entendimiento de la enfermedad, una identificación de potenciales dianas terapéuticas y una búsqueda de nuevos marcadores de riesgo cardiovascular, progresión y recuperación en caso de sufrir un evento cardiovascular agudo. Para ello se emplearán abordajes proteómicos y metabolómicos en orina, plasma y tejido, tanto conocidos como desarrollados a lo largo de esta Tesis Doctoral.

De este objetivo principal se derivan los siguientes objetivos particulares:

1. Identificación de nuevos marcadores moleculares (proteínas y metabolitos) en orina en respuesta al desarrollo temprano (silente) de aterosclerosis. Para ello se realizará un análisis combinado del proteoma y metaboloma de la orina de un modelo de conejo por electroforesis bidimensional de marcaje (DIGE) y resonancia magnética nuclear (NMR).

2. Confirmación de las proteínas y metabolitos alterados y posterior evaluación de su potencial en diagnóstico y monitorización de la recuperación en pacientes que han sufrido un evento cardiovascular agudo, empleando cromatografía de líquidos acoplada a espectrometría de masas (SRM-LC-MS/MS).

3. Estudio integral de tejido aórtico para identificación las principales moléculas (proteínas y metabolitos) alteradas en respuesta al desarrollo temprano de aterosclerosis, así como de los mecanismos subyacentes más relevantes. Se abordará mediante análisis por electroforesis bidimensional de marcaje (DIGE) y resonancia magnética nuclear de sólidos o resonancia magnética de ángulo mágico (HRMAS). Confirmación de las alteraciones y estudio de su reflejo en plasma por cromatografía de líquidos acoplada a espectrometría de masas (SRM-LC-MS/MS).

4. Obtención del mapa proteico y lipídico y análisis diferencial de arterias sanas y ateroscleróticas de un modelo animal de aterosclerosis temprana por aplicación de la espectrometría de masas de imagen, previo desarrollo de un método óptimo que permita por vez primera el análisis proteico de arterias por esta técnica. Identificación de moléculas diferencialmente expresadas en tejido humano aórtico.

Chapter 1

Urine 2-DE proteome analysis in healthy condition and kidney disease

Marta Martin-Lorenzo, *Laura Gonzalez-Calero, Irene Zubiri, Pedro J Diaz-Payno, Aroa Sanz-Maroto, Maria Posada-Ayala, Alberto Ortiz, Fernando Vivanco, Gloria Alvarez-Llamas*

Electrophoresis. 2014 Sep;35(18):2634-41. doi: 10.1002/elps.201300601

Las líneas prioritarias de investigación de nuestro laboratorio se centran en el estudio de la enfermedad cardiovascular (ECV) asociada al desarrollo de la aterosclerosis (tal y como se desarrolla en esta tesis doctoral) y en enfermedad renal crónica (ERC) en sus diferentes variantes. Uno de nuestros principales objetivos es la búsqueda de nuevos marcadores de diagnóstico temprano y pronóstico, así como la identificación de potenciales dianas terapéuticas.

La orina es un fluido de fácil obtención y ampliamente utilizado en el ámbito clínico. Además, constituye una fuente de potenciales marcadores de enfermedad lo que la convierte en un fluido de gran interés en este campo. La orina no representa únicamente el filtrado del plasma sino que también recoge proteínas procedentes del tracto urinario. Por ello resulta un fluido ideal para estudiar la fisiología y patología renales. Frecuentemente pacientes con función renal deteriorada presentan proteinuria, es decir, una concentración anormalmente elevada de la albúmina. Este hecho establece un sesgo en la comparación clínica y dificulta sobremanera la detección de moléculas alteradas que estén en baja concentración. En este contexto nuestro interés era encontrar el método más adecuado y de aplicabilidad general para cualquier muestra de orina.

La electroforesis bidimensional es una técnica proteómica clásica basada en una combinación de separación por punto isoeléctrico seguida de una separación por peso molecular de las proteínas. Se caracteriza por tener un alto rango lineal, buena reproducibilidad, permitir el estudio de las proteínas intactas y además es adecuada en el estudio de modificaciones post-traduccionales en un mismo gel. La aplicación de esta técnica a diferentes proteomas ha puesto de manifiesto que es una herramienta de gran valor en estudios de análisis porteómico diferencial y complementaria a las técnicas de más reciente desarrollo basadas en la espectrometría de masas. En la bibliografía existen numerosos estudios por electroforesis bidimensional que analizan el proteoma de la orina. Sin embargo, la orina tiene una matriz compleja que actúa o puede actuar como interferencia haciendo que se dé una disminución en la sensibilidad y la resolución. Numerosas metodologías están descritas en la literatura, pero en ningún caso existían, hasta la realización del trabajo presentado a continuación publicado en *Electrophoreis*, comparaciones homogéneas intra-grupo que permitiesen establecer un flujo de trabajo optimizado para el análisis de orina por electroforesis bidimensional. En el trabajo que se presenta a continuación se realiza una comparación exhaustiva de los métodos más frecuentemente utilizados y de variantes propuestas para desalinizar y purificar la orina previo al análisis por electroforesis bidimensional. Estos métodos están basados en ultrafiltración, precipitación, diálisis, exclusión por tamaño y extracción en fase sólida. Además se compararon dos de los métodos de depleción más descritos en la bibliografía.

El resultado final presenta una puesta a punto para el estudio del proteoma de muestras de orina de diferente origen que recomienda diferentes protocolos en función del tipo de proteínas a estudiar (bajo o alto peso molecular) y analiza cuándo es necesaria y conveniente una depleción de las proteínas mayoritarias como paso previo a cualquier análisis. Finalmente se establece un protocolo para los estudios de descubrimiento de

marcadores. Una aplicación del mismo en el campo de las enfermedades cardiovasculares está recogida en el siguiente capítulo de esta tesis doctoral.

Electrophoresis 2014, *35*, 2634–2641

Marta Martin-Lorenzo[1]*
Laura Gonzalez-Calero[1]*
Irene Zubiri[1]
Pedro J. Diaz-Payno[1]
Aroa Sanz-Maroto[1]
Maria Posada-Ayala[1]
Alberto Ortiz[2]
Fernando Vivanco[1,3]
Gloria Alvarez-Llamas[1]

[1]Department of Immunology, IIS-Fundacion Jimenez Diaz-UAM, Madrid, Spain
[2]Department of Nephrology, IIS-Fundacion Jimenez Diaz-UAM/IRSIN, Madrid, Spain
[3]Department of Biochemistry and Molecular Biology I, Universidad Complutense, Madrid, Spain

Received July 8, 2013
Revised May 14, 2014
Accepted May 27, 2014

Research Article

Urine 2DE proteome analysis in healthy condition and kidney disease

Urine is a source of potential markers of disease. In the context of renal disease, urine is particularly important as it may directly reflect kidney injury. Current markers of renal dysfunction lack both optimal specificity and sensitivity, and improved technologies and approaches are needed. There is no clear consensus about the best sample pretreatment procedure for 2DE analysis of the urine proteome. Sample pretreatment conditions spots resolution and detection sensitivity, critically. As a first goal, we exhaustively compared eight different sample cleaning and protein purification methodologies for 2DE analysis of urine from healthy individuals. Oasis® HLB cartridges allowed the detection of the highest number of low molecular weight proteins; while PD10 desalting columns resulted in the highest number of detected spots in the high molecular weight area. Sample pretreatment strategies were also explored in the context of proteinuria, a clinical condition often associated to renal damage. Testing of urine samples from 13 patients with hypertension or kidney disease and different levels of proteinuria identified Oasis® HLB cartridge purification in combination with albumin depletion by ProteoPrep kit as the best option for urine proteome profiling from patients with proteinuric (> 30 mg/L albumin in urine) renal disease.

Keywords:
Kidney disease / Proteinuria / Proteomics / Two-dimensional electrophoresis / Urine
DOI 10.1002/elps.201300601

Additional supporting information may be found in the online version of this article at the publisher's web-site

1 Introduction

There is consensus on the clinical interest of urine as an easily accessible biological fluid and rich source of potential markers of disease [1]. In fact, many studies have focused on urine in the search for novel molecular targets of potential use in the clinical setting from a diagnosis or prognosis point of view [2, 3]. Urine matrix may be a serious interference, negatively affecting sensitivity, and resolution, which ultimately conditions the number of detected proteins. Published studies focused on specific diseases usually detail the urine pretreatment procedure that was used preceding the discovery phase, but do not provide details on whether other pretreatment procedures were tested and what was their performance. 2DE is a very valuable tool in proteomics due to its high reproducibility and the ability to detect intact proteins, thus the first aim of this work is to perform an exhaustive comparison of the most frequently reported methodological approaches and additional strategies for urine desalting and proteome purification prior to 2DE analysis [4–6]. Eight different strategies were evaluated for control urine, including precipitation-based, solid-phase extraction-based, and dialysis/desalting-based strategies.

In a second aim, we approached the analysis of urine from renal disease patients with different levels of proteinuria. Urine has been investigated to study renal physiology and kidney diseases, as it represents a combination of both plasma ultrafiltrate and urinary tract proteins. Currently used markers of renal dysfunction lack both optimal specificity and sensitivity. Serum creatinine is the most widely used marker of renal dysfunction, but increased serum creatinine diagnostic is a late event and significant renal disease can occur with minimal or no change in creatinine [7]. Microalbuminuria is the best noninvasive marker available for diagnosis of kidney injury but limitations have been pointed out, i.e. it

Correspondence: Dr. Gloria Alvarez-Llamas, Department of Immunology, IIS-Fundacion Jimenez Diaz. Avenida Reyes Catolicos 2, 28040 Madrid, Spain
E-mail: galvarez@fjd.es
Fax: +34-915448246

*These authors contributed equally to this work.

© 2014 WILEY-VCH Verlag GmbH & Co. KGaA, Weinheim

ABSTRACT

Urine is a source of potential markers of disease. In the context of renal disease, urine is particularly important as it may directly reflect kidney injury. Current markers of renal dysfunction lack both optimal specificity and sensitivity, and improved technologies and approaches are needed. There is no clear consensus about the best sample pre-treatment procedure for 2-DE analysis of the urine proteome. Sample pre-treatment conditions spots resolution and detection sensitivity, critically. As a first goal, we exhaustively compared eight different sample cleaning and protein purification methodologies for 2-DE analysis of urine from healthy individuals. Oasis® HLB cartridges allowed the detection of the highest number of low molecular weight proteins; while PD10 desalting columns resulted in the highest number of detected spots in the high molecular weight area. Sample pre-treatment strategies were also explored in the context of proteinuria, a clinical condition often associated to renal damage. Testing of urine samples from 13 patients with hypertension or kidney disease and different levels of proteinuria identified Oasis® HLB cartridge purification in combination with albumin depletion by ProteoPrep kit as the best option for urine proteome profiling from patients with proteinuric (> 30 mg/L albumin in urine) renal disease.

INTRODUCTION

There is consensus on the clinical interest of urine as an easily accessible biological fluid and rich source of potential markers of disease (1). In fact, many studies have focused on urine in the search for novel molecular targets of potential use in the clinical setting from a diagnosis or prognosis point of view (2,3). Urine matrix may be a serious interference, negatively affecting sensitivity and resolution, which ultimately conditions the number of detected proteins. Published studies focused on specific diseases usually detail the urine pre-treatment procedure that was used preceding the discovery phase, but do not provide details on whether other pre-treatment procedures were tested and what was their performance. Two-dimensional electrophoresis (2-DE) is a very valuable tool in proteomics due to its high reproducibility and the ability to detect intact proteins, thus the first aim of this work is to perform an exhaustive comparison of the most frequently reported methodological approaches and additional strategies for urine desalting and proteome purification prior to 2-DE analysis (4-6). Eight different strategies were evaluated for control urine, including precipitation-based, solid-phase extraction-based and dialysis/desalting-based strategies.

In a second aim, we approached the analysis of urine from renal disease patients with different levels of proteinuria. Urine has been investigated to study renal physiology and kidney diseases, as it represents a combination of both plasma ultrafiltrate and urinary tract proteins. Currently used markers of renal dysfunction lack both optimal specificity and sensitivity. Serum creatinine (SCr) is the most widely used marker of renal dysfunction, but increased SCr diagnostic is a late event and significant renal disease can occur with minimal or no change in creatinine (7). Microalbuminuria is the best non-invasive marker available for diagnosis of kidney injury but limitations have been pointed out, i.e. it is considered a risk factor but some patients return to normal levels (normoalbuminuria); a significant decrement in glomerular filtration rate may occur in the presence of normal urinary albumin excretion; and histopathological changes in kidney structure may be already present in recently diagnosed microalbuminuric patients (8,9). Cystatin C has been more recently proposed to improve prediction accuracy, in combination with creatinine and urine albumin to creatinine ratio (ACR), although its clinical use is currently under investigation (10). Thus, given the limitations of current markers of renal disease, novel markers are needed (11). The –omics platforms provide a non-biased approach to identify novel potential markers (12,13).

In general terms, the probability to discover novel markers of disease increases as the depth of the protein coverage increases. To increase protein coverage a reduction of the dynamic range of protein concentrations is mandatory. This is of particular importance in the context of renal diseases when pathological proteinuria (excess amounts of serum proteins found in urine) is present (14). Pathological proteinuria usually occurs when an increased glomerular filtration of plasma proteins because of glomerular injury exceeds the capacity of the tubules to reabsorb the proteins.

We evaluate here the inclusion of a high-efficiency and controlled albumin depletion step in proteinuric samples. This additional step, applied when proteinuria exceeds a threshold, was investigated for 2-DE analysis of urine from renal disease patients.

MATERIALS AND METHODS

Urine sample collection and storage

Urine samples from 6 healthy donors who did not present history of diabetes mellitus, hypertension or renal or inflammatory disease were collected at IIS-Fundación Jiménez Díaz (Madrid, Spain). Urine samples from a total of 13 patients were collected at the Nephrology Division at Fundacion Jimenez Diaz and one patient at Cardiology Division at Hospital Tres Culturas (Toledo, Spain). Table 1 presents key clinical data. Sample collection procedures were in accordance with the Helsinki declaration and approved by local ethics committee. Signed informed consent was obtained from patients and healthy donors. A spot of morning random-catch urine sample was collected in a sterile container, transported to the laboratory and immediate frozen at -80ºC, unless urine pre-treatment and 2DE analysis directly followed. Frozen samples (20mL) were thawed in a water bath at 37ºC for a few minutes and centrifuged at 3000g for 10 minutes to eliminate cell debris. Supernatants were frozen at -80ºC until further processing, or directly used. They were filtered through Acrodisc® Syringe filters 0.2 μm (Pall) and ultrafiltrated for concentration in Amicon Ultra Centrifugal Filters (10kDa cut-off; Millipore), up to a final volume of 300-350μL, when required depending on the protocol. Samples undergoing this step will be referred as "concentrated". Samples were frozen at -80ºC until analysis.

Patient	Age	Sex	eGFR	Albuminuria (mg/L)[#]	DM	Disease	CKD stage
1	83	M	22	326	Yes	DN	4
2	49	F	118	13	No	LN	1
3	69	M	54	371	Yes	GN	3
4	55	M	52	862	No	LN	3
5	61	M	81	70	No	Vascular	2
6	69	F	52	5	No	UNK	3
7	53	M	42	5340	No	GN	3
8	31	F	124	157	No	GN	1
9	37	F	85	6160	No	LN	2
10	53	M	74	112	No	GN	2
11	40	M	65	1715	No	GN	2
12	29	F	70	1474	No	LN	2
13	51	M	126	10	No	Hypertension	No

Table 1. Clinical data of renal disease patients. eGFR: estimated glomerular filtration rate. LN: lupus nephritis. GN: glomerulonephritis. UNK: unknown etiology of chronic kidney disease (CKD). DM: diabetes mellitus. DN: diabetic nephropathy. [#]Measured in the same sample that was analyzed by 2-DE.

Urine sample pre-treatment: concentration and desalting

Urine samples from healthy individuals were used for the evaluation of the different methods to avoid disturbances caused by disease conditions. 1) *Ultrafiltration-based desalting*: 20mL urine were loaded in Amicon Ultra Centrifugal Filters, 10kDa cut-off (Millipore) and centrifuged at 3000g up to a final volume of 1mL; 4mL Milli-Q water was added to the retentate and centrifuged again, repeating the cycle a total of three times up to 300µL of final volume. The urine matrix was replaced by water. 2) *Acetone precipitation*: six volumes of chilled acetone (Diclisa) were added to one volume of concentrated urine and incubated at -20ºC at least 30 minutes, centrifuged at 14000g for 5 minutes and after removal of the supernatant , the pellet was resuspended in lysis buffer (7M urea (BioRad), 2M thiourea (BioRad), 4% CHAPS (BioRad)). 3) *TCA/Acetone precipitation*: the concentrated urine sample was resuspended in 1mL Milli-Q water and 200µL of 50% tricloroacetic acid (TCA, Sigma-Aldrich) solution were added. After brief vortexing, the mixture was placed at 4ºC for 30 minutes, centrifuged and the supernatant removed. The pellet was dissolved in 20µL Milli-Q water for 5 minutes at room temperature and 1mL of cold acetone was added, following incubation at -20ºC for at least 30 minutes. After centrifugation, the supernatant was removed and the pellet solved in lysis buffer. 4) *2D Clean-Up Kit* (GE Healthcare): concentrated urine samples were cleaned following manufacturer's instructions and the resulting protein pellet was resuspended in lysis buffer. 5) *PD10 Desalting columns (GE Healthcare)*: 300µl of concentrated urine samples were cleaned following the manufacturer's instructions using 0.01%NH_4OH (Sigma-Aldrich) as equilibration buffer; desalted urine samples were lyophilized and reconstituted in lysis buffer. 6) *Dialysis + lyophilization*: 300µl of concentrated urine samples were dyalyzed with Midi Pur-A-Lyzer (Sigma-Aldrich) in 300ml Milli-Q water for 1h at 4ºC followed by two water exchanges after overnight and 3h equilibration time; dialyzed samples were then lyophilized 7) *Dialysis + acetone precipitation: same as 6) but* precipitated in acetone as detailed in 2) instead of lyophilization. 8) *Oasis® HLB Cartridges (Waters, Milford, MA) after urine concentration*: the concentrated urine sample was diluted with Milli-Q water into a total volume of 500µL and loaded on top of the cartridges previously conditioned with 1mL acetonitrile (ACN, Merck) and 1mL 0.1% trifluoroacetic acid (TFA, Merck) solution; two washing steps followed by passing 1mL 0.1%TFA and 1mL Milli-Q water prior to sample elution in 0.5mL ACN twice. Clean urine samples (eluates 1 and 2) were collected in eppendorf tubes and solvent was removed in a Savant SpeedVac® concentrator up to dryness. Both eluates were solved in lysis buffer and combined in a total volume of 100µL. Total protein content was measured by the Bradford method prior to 2-DE analysis. Normalization for comparison was based on total amount of urinary protein loaded per gel.

High abundance proteins depletion

To evaluate the influence of high abundance proteins depletion in protein profiling by 2-DE in the context of renal disease, two different approaches were evaluated: ProteoPrep Immunoaffinity Albumin and IgG Depletion Kit (Sigma-Aldrich) and Agilent Human

14 Multiple Affinity Removal System (4.6x50mm column; Hu-14, Agilent Technologies). A spot urine sample (40mL) from a diabetic nephropathy patient (Patient 1 in Table 1) was concentrated by ultrafiltration as described and depleted following manufacturer's protocol. Albumin content was measured before, in order to avoid column overloading and uncompleted depletion. In both cases, depleted samples were eluted in the corresponding commercial elution buffer. Milli-Q water was added up to 0.5mL, and proteins purification was carried out in Oasis® HLB cartridges, as detailed before, prior to 2-DE analysis. Total protein content was measured by the Bradford method.

Two-dimensional electrophoresis (2-DE)

Protein samples resulting from the different protocols were solved in focusing solution (7 M urea, 2 M thiourea, 4% CHAPS, 65 mM DTT (Bio-Rad) and 1% (v/v) IPG Buffer (GE Healthcare)) and they were loaded onto Immobiline DryStrips, 18 cm long, pH 4-7 (GE Healthcare). Isoelectric focusing was carried out in a PROTEAN IEF CELL (BioRad) according to the following program: active rehydration at 50V for 12 h, 500V for 1h, up to 3500V for 3h (linear voltage ramping method), 3500V for 3h and up to 5000V until 45000V were accumulated. After IEF, strips were equilibrated in two 20 min steps in buffer containing 6M urea, 50mM Tris-HCl pH 8.8, 40% glycerol, 2% SDS and 1% DTT or 3.5% iodoacetamide (IAA). The second dimension was carried out on 14% running gels and that were then silver stained (GE Healthcare, Piscataway, NJ). Stained gels were digitized by using a GS-800 Calibrated Densitometer (Bio-Rad). Spot detection was carried out by means of DeCyder Differential Analysis Software version 6.5 (GE Healthcare).

RESULTS AND DISCUSSION

Comparison of urine desalting and proteins purification methods

The influence of sample desalting methods and protein purification strategies is not always visible on SDS-PAGE (15), thus we directly tested the performance of several urine pre-treatment methods in 2-DE profiling. In a first step, a total of 9 samples from 4 healthy donors were used for testing the performance of several urine pre-treatment methods in 2-DE profiling. A total of eight approaches for protein purification and urine desalting were tested as follows (2-DE representative images are shown in Figure 1): 1) ultrafiltration-based desalting (Fig. 1A), 2) proteins precipitation in acetone (Fig. 1B), 3) protein precipitation in TCA/acetone (Fig.1C), 4) 2D Clean-Up kit (Fig. 1D), 5) PD10 Desalting columns (Fig. 1E), 6) dialysis followed by lyophilization (Fig. 1F), 7) dialysis followed by acetone precipitation (Fig. 1G) and 8) Oasis® HLB cartridges (Fig. 1H). Total protein content loaded per gel was in the range of 60-70µg. Additionally, 130µg total protein were analyzed by 2-DE after sample cleaning-up by Oasis® HLB cartridges (Fig. 1I).

In all cases, protein spots were visualized with high resolution and good sensitivity improving previously published gel map (15-20). Mainly, two typical spots patterns

could be distinguished: one for ultrafiltration-, precipitation-, dialysis- and PD10 desalting-based methodologies (Fig. 1A-G), and another one for solid-phase extraction approaches (Fig. 1H, I), favoring the detection of high- or low-molecular weight proteins, respectively, in healthy donors' urine samples. By dividing the gel area in low or high molecular weight region (cut-off value 31kDa) differences can be appreciated depending on the approach used, in terms of number of spots detected (Table 2). Oasis® HLB cartridges allowed the detection of the highest number of low molecular weight proteins in control urine; while PD10 desalting columns resulted in the highest number of detected spots in the high molecular weight area. Depending on the region of interest and the specific proteins to be investigated, any of the two approaches may provide satisfactory data in terms of resolution.

Method	Spot number (High MW range)	Spot number (Low MW range)	Total Spot number
Ultracentrifugation	863	176	1039
Acetone precipitation	810	146	956
TCA/Acetone precipitation	624	176	800
2D Clean-up Kit	603	170	773
PD10 columns	**1040**	169	1209
Dialysis & Lyophilization	841	395	1236
Dialysis & Acetone precipitation	847	251	1098
Oasis® HLB cartridges	373	**665**	1038

Table 2. Number of spots detected in the high and low molecular weight (MW) area of the gel. The same amount of protein was loaded in all cases.

The reproducibility was evaluated by studying a spot urine sample from four different healthy donors obtained on the same or on different days (two donors were coincident with the ones recruited for the evaluation of pre-treatment methods, plus two additional donors). In particular, two aliquots of a same urine sample, from one donor, were analyzed on the same day (Figure 2A and 2B). Another urine sample from that same donor but collected on a different day was also analyzed on a different day (Figure 2C). Urine from 3 additional and different healthy donors was also analyzed for comparison (Figure 2D, 2E and 2F). Oasis® HLB cartridges were used. Comparable gel patterns were obtained supporting the reproducibility of the methodology. Additionally, Table 2 shows number of detected spots on images obtained with the different pre-treatment methods tested in urine from different individuals. Relative standard deviation calculated on spots number obtained with the different methods tested resulted in 17% RSD or 8% without considering precipitation-based protocols which are known for associated proteins loss. These values, even when corresponding to different methods and different individuals, confirmed the reproducibility of the urine analysis by 2-DE.

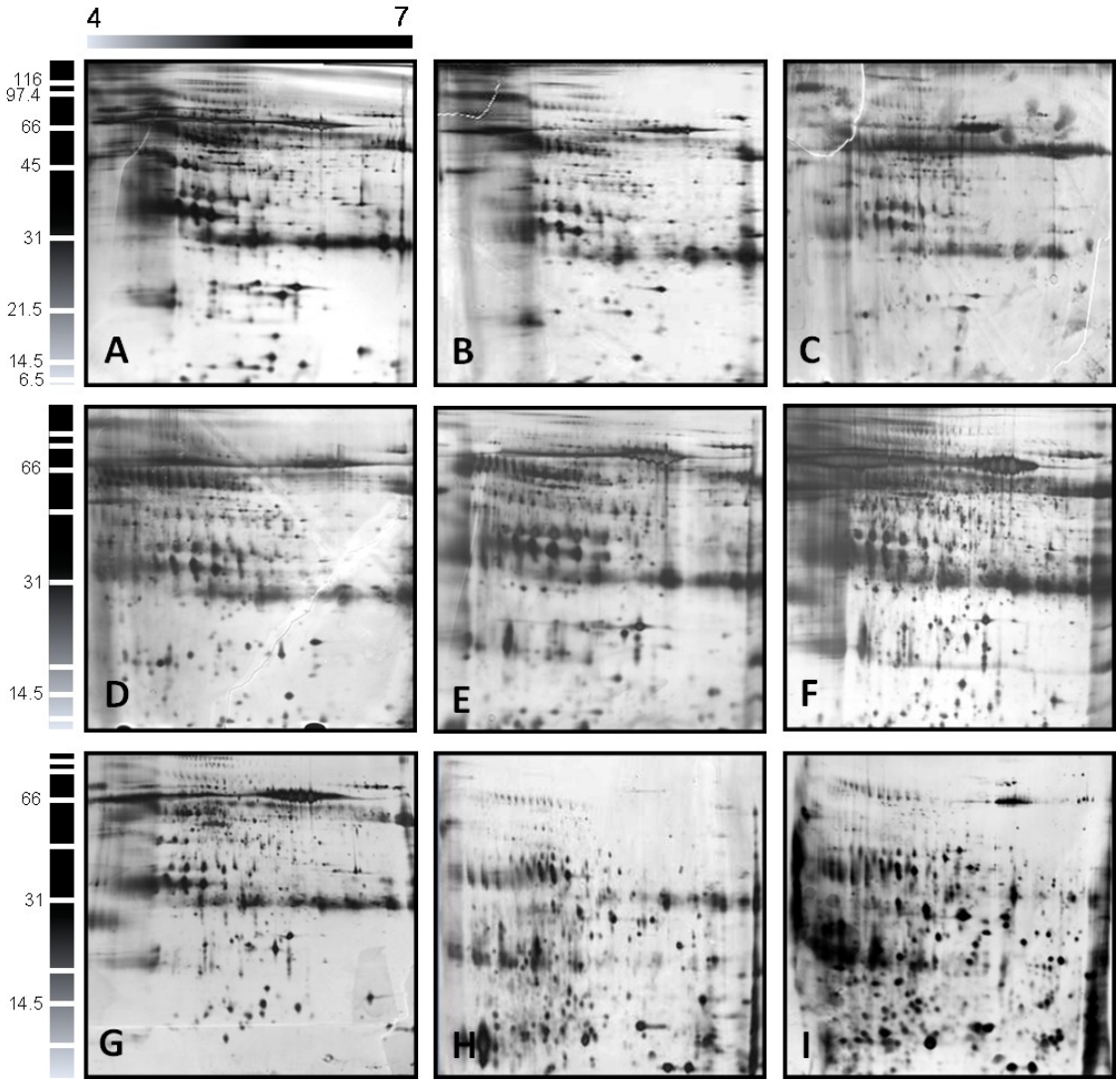

Figure 1. Two dimensional gel electrophoresis profiles of healthy urine samples previously treated as follows: A) Ultrafiltration-based desalting, B) Acetone precipitation, C) TCA/Acetone precipitation, D) 2D Clean-Up Kit, E) PD10 Desalting columns, F) Dialysis & lyophilization, G) Dialysis & acetone precipitation, H) Oasis® HLB cartridges, I) Oasis® HLB cartridges (same as H) but 130µg total protein loaded. If not specified, total protein loaded per gel was 60-70µg. Concentrated urine was used as starting point in all cases but A).

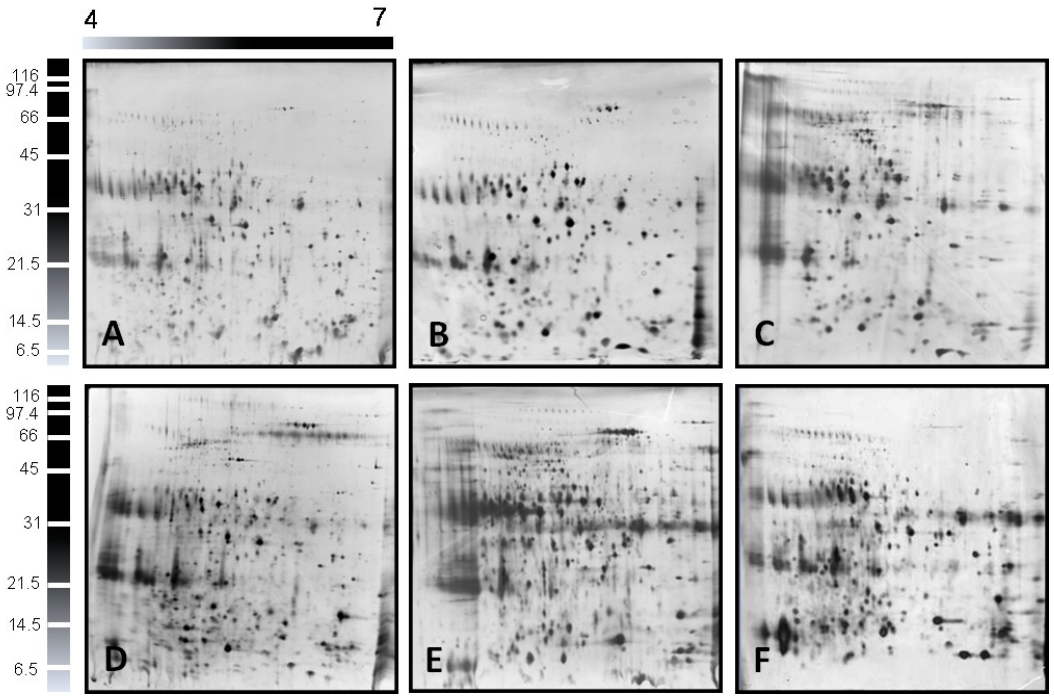

Figure 2. Two dimensional gel electrophoresis profiles of healthy urine samples concentrated and cleaned with Oasis® HLB cartridges (70µg total protein). A) and B) correspond to two aliquots of a spot urine sample from a healthy individual analyzed on the same day. C) Correspond to a spot urine sample from the same individual but collected on a different day. D), E) and F) correspond to spot urine samples from three additional different individuals also analyzed on different days.

Albumin depletion from urine in the context of proteinuria

Proteinuria is a clinical condition frequently present in patients with chronic kidney disease. This clinical situation is usually characterized by abnormally high presence of albumin (66kDa) in urine. As shown before, visualization of high-abundance protein chains at the upper and medium part of the gels seems to be attenuated when cleaning the urine samples from healthy donors by Oasis® HLB cartridge (Fig. 1H). Even after increasing the total amount of protein loaded (around 150µg total protein), the spots are well resolved without significant loss of resolution (Fig. 1I). Oasis® HLB cartridge is a highly reproducible, patented copolymer synthesized with a unique composition that is hydrophilic-lipophilic-balanced for both strong reversed-phase retention and water-wettability. It is used to adsorb both polar and non-polar compounds simultaneously from aqueous media and surface functionality is provided by m-Divinylbenzene & N-vinylpyrrolidone copolymer. Thus, we chose Oasis® HLB cartridges for further experiments in the search for the best methodology to accomplish 2-DE urine analysis in the renal disease context.

Albumin is the most abundant urine protein when glomerular injury is present. For proteomics analysis by 2-DE, albumin depletion may be a mandatory step when studying renal diseases in patients with different proteinuria levels. This will enrich the analyzed proteome in low-abundance proteins and additionally guarantee successful 2-

DE profiles, since albumin is a “disturbing interferent” which impedes high-resolution spot profiling (21).

In this context, and to extend the applicability of the methodology, we secondly aimed to evaluate the influence of albumin depletion in the analysis of proteinuric urine by 2-DE. The urine proteome from renal disease patients and healthy individuals has previously been compared by 2-DE. However, either albumin depletion was not performed, resulting in albumin as one of the differentially expressed proteins (22,23), or albumin depletion was not fully successful (21,24). Albumin depletion is as a mandatory step to 1) discover novel candidate markers which are present at low concentration and 2) to ensure proper comparison of clinical conditions at different proteinuria levels (25). For this purpose two depletion strategies were compared. The ProteoPrep Immunoaffinity Albumin and IgG Depletion Kit (Sigma-Aldrich) specifically removes albumin from human serum. Here, we tested this kit for urine, based on data from our laboratory when applied to depletion of human urine exosomal fraction (26). We compared this strategy with one of the most frequently applied to plasma proteomics studies (27): the Human 14 Multiple Affinity Removal System (4.6x50mm column; Hu-14, Agilent Technologies). This system has been specifically designed to deplete the 14 most- abundant proteins from human biological fluids such a plasma or serum. We had previously applied a similar approach to deplete the six most abundant proteins from plasma samples (28) and we now tested it for urine. This depletion step was additionally included in the protocol prior to sample treatment by Oasis® HLB cartridges. As a proof of concept, urine from a diabetic nephropathy patient (Patient 1 in Table 1) was analyzed. Figure 3 shows the 2-DE protein profiles corresponding to the same urine sample (Fig. 3A, non-depleted), and once depleted with both strategies (Fig. 3B, D). The high-abundance “contaminating” fraction obtained by both methodologies was also analyzed (Fig. 3C, E). The gel images evidenced a much better performance for the ProteoPrep Immunoaffinity Albumin and IgG Depletion Kit, as higher number of spots was clearly visualized in the depleted sample, and minor unspecific co-retention of proteins of interest bound to albumin fraction can be appreciated.

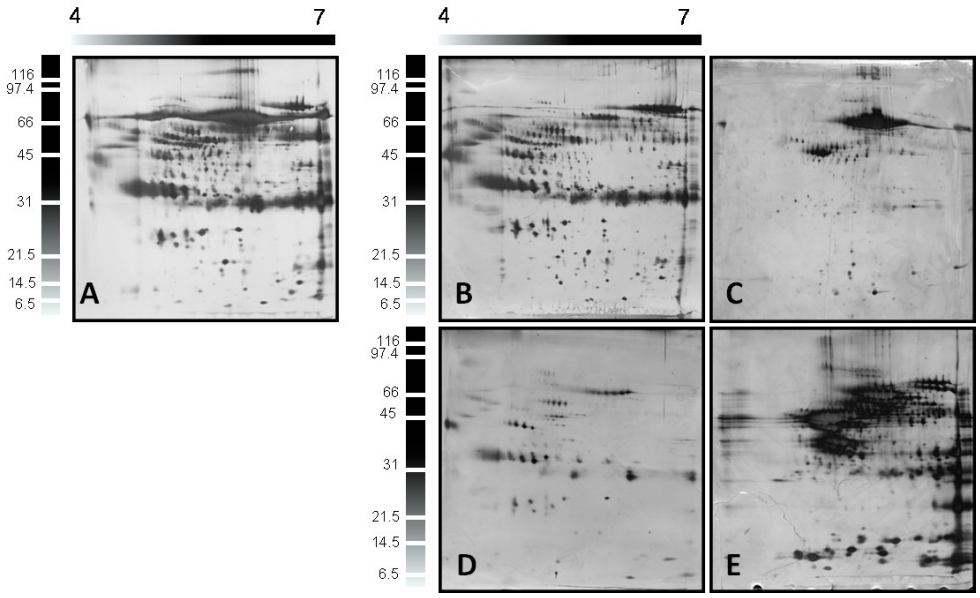

Figure 3. Two dimensional gel electrophoresis profiles of proteinuric urine with and without depletion. Urine from a diabetic nephropathy patient (Patient 1 in Table 1) was analyzed without depletion of major proteins A) and following depletion by two different methods: ProteoPrep Immunoaffinity Albumin and IgG Depletion Kit (depleted fraction shown in B) and Human 14 Multiple Affinity Removal System (depleted fraction shown in D). Retentates (high abundant proteins) from each method were also analyzed (C and E, respectively).

Urine analysis by 2-DE in human renal disease

Not all renal diseases are associated with proteinuria. Depending on the disease stage or severity, urinary albumin may completely impede co-detection of other proteins. The presence of serum proteins in urine is considered pathological when albuminuria values exceed 30mg/L: 30-300mg/L is referred to as microalbuminuria and >300mg/L as macroalbuminuria. Spot urine samples were collected from a total of 12 patients suffering from renal disease, including glomerulonephritis (GN), lupus nephritis (LN) or chronic kidney disease (CKD), and from one hypertensive patient with normal renal function (Table 1). Decision to perform albumin depletion by ProteoPrep Immunoaffinity Albumin and IgG Depletion Kit was evaluated in each case, and it was applied only when albuminuria was >30mg/L. It is recommended to measure albumin concentration specifically in the samples to be analyzed, in order to take into account variability in urinary albumin concentration dependent urine dilution as a consequence of fluid ingestion. This will ensure that the loading capacity of depletion columns is not exceeded. Urine samples were cleaned and proteins purified by Oasis® HLB cartridges as detailed in material and methods. In Figure 4, gel images obtained for each patient are shown. A comparable and reproducible spot pattern is observed in all patients, confirming an adequate performance of the pre-treatment method. It is worthwhile to note that decision to include or not an additional depletion step was performed based on the specific renal disease of the patients, resulting in a comparable spot pattern in all cases, thus supporting the applicability of the proposed methodology for quantitative differential analysis. In particular, albumin depletion when albumin content of urine sample is >30mg/L significantly improved 2-DE profiles, which otherwise would be

distorted by albumin as shown in Supplementary Figure. More than in terms of total number of detected spots, this can be better evaluated paying particular attention to the "albumin" area and below. As expected, this protein depletion allows improved patterns particularly appreciated in images shown in Figure 4J, K and L, which correspond to patients with the highest albuminuria levels in urine (>1500 mg/L). It is in this case where depletion step is strongly recommended.

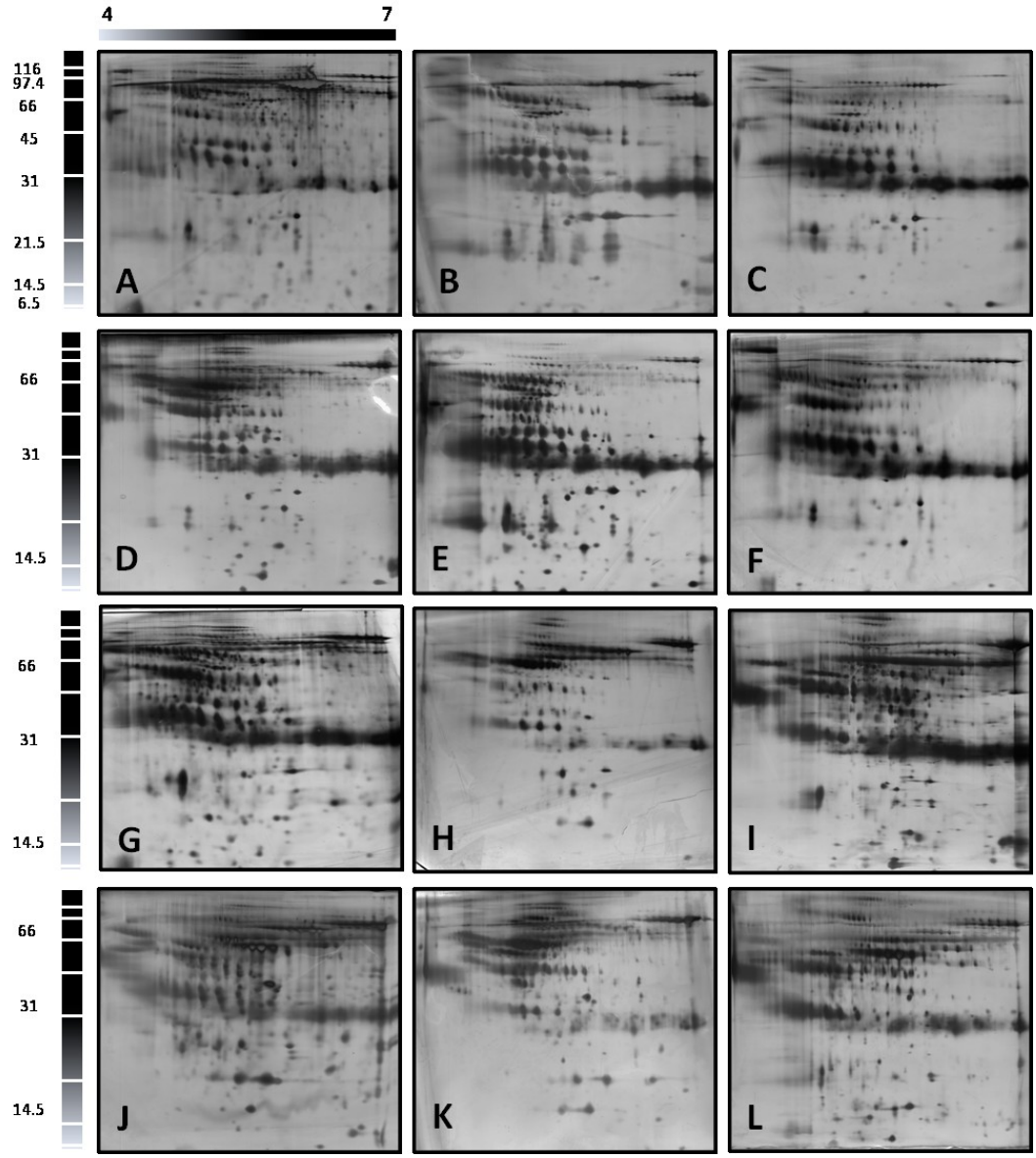

Figure 4. 2-DE gel images corresponding to the urine proteome pattern of twelve patients. Patients were classified according to albuminuria as follows. A,B,C: <30 mg/L; D,E,F: 30-300 mg/L; G,H,I: 300-1500 mg/L; J,K,L: >1500 mg/L. 2-DE images show urine profiles from 4 patients with lupus nephritis (LN) (A, H, I, K), 5 patients with glomerulonephritis (GN) (D, E, G, J, L), 2 patients with other chronic kidney diseases (CKD) (C, F) and one hypertensive patient with normal renal function (B). In all cases, urine proteins were purified by Oasis® HLB cartridges and 60 µg total protein was loaded per gel. A depletion step was included only when albumin exceeded 30 mg/L (from D to L).

CONCLUDING REMARKS

In conclusion, we performed an extensive comparison of urine sample pre-treatment methods for 2-DE proteomic analysis. Depending on protein/s or region/s of interest, an optimal protocol can be chosen among the eight evaluated here. In particular, Oasis® HLB or PD10 desalting performed the best for low or high molecular weight proteins analysis, respectively.

In the context of proteinuric renal disease, Oasis® HLB cartridge purification in combination with albumin depletion by ProteoPrep kit proved to be the best performing strategy for analysis of urine samples. However, the depletion step may be dispensable when albumin was lower than 30mg/L in the urine sample. In that case, urine samples can be analyzed by 2-DE applying, e.g. HLB Oasis pre-treatment, without depletion step. When albumin concentration is >30mg/L, the inclusion of the albumin-depletion step in the procedure guarantees clinical comparison of pathological conditions in the proteinuria context, increasing the detection of low-abundance proteins as marker candidates.

In conclusion, we show here an extensive compilation of different sample pre-treatment options for urine analysis by 2-DE. Additionally, we approached the urine analysis in the context of renal disease for individuals with different grades of proteinuria. Based on our data, future studies based on differential analysis between healthy and pathological groups, can be approached with improved 2-DE gel patterns where albumin negative influence can be minimized. Establishing a cut-off value above which additional albumin depletion step is recommended is here for the first time reported.

ACKNOWLEDGEMENTS

Funding from Instituto de Salud Carlos III: FIS PI11/01401, PIE13/00051, PI13/01873, FIS IF08/3667-1, RD07/006/0023, RD12/0021, CP09/00229, and Intensificación and Fundación Conchita Rábago de Jiménez Díaz, Cardiology Division in Hospital Tres Culturas in Toledo, and Montse Martínez from Proteomic Unit, Parque Científico de Madrid.

DISCLOSURE

Authors declare no financial/commercial conflicts of interest.

REFERENCES

[1] Court, M., Selevsek, N., Matondo, M., Allory, Y., Garin, J., Masselon, C. D., Domon, B., *Proteomics* 2011, *11*, 1160-1171.

[2] Casado-Vela, J., Gomez del Pulgar, T., Cebrian, A., Alvarez-Ayerza, N., Lacal, J. C., *Expert review of proteomics* 2011, *8*, 347-360.

[3] Zerefos, P. G., Aivaliotis, M., Baumann, M., Vlahou, A., *Proteomics* 2012, *12*, 391-400.

[4] Candiano, G., Santucci, L., Petretto, A., Bruschi, M., Dimuccio, V., Urbani, A., Bagnasco, S., Ghiggeri, G. M., *J.Proteomics* 2010, *73*, 829-844.

[5] Plews, M., Lamoureux, L., Simon, S. L., Graham, C., Ruddat, V., Czub, S., Knox, J. D., *Proteome.Sci.* 2011, *9*, 6.

[6] Zerefos, P. G., Vlahou, A., *Methods Mol.Biol* 2008, *428*, 141-157.

[7] Caramori, M. L., Fioretto, P., Mauer, M., *Diabetes* 2000, *49*, 1399-1408.

[8] Fioretto, P., Steffes, M. W., Mauer, M., *Diabetes* 1994, *43*, 1358-1364.

[9] Bangstad, H. J., Osterby, R., Dahl-Jorgensen, K., Berg, K. J., Hartmann, A., Nyberg, G., Frahm Bjorn, S., Hanssen, K. F., *Diabetologia* 1993, *36*, 523-529.

[10] Peralta, C. A., Shlipak, M. G., Judd, S., Cushman, M., McClellan, W., Zakai, N. A., Safford, M. M., Zhang, X., Muntner, P., Warnock, D., *JAMA : the journal of the American Medical Association* 2011, *305*, 1545-1552.

[11] Posada-Ayala, M., Zubiri, I., Martin-Lorenzo, M., Sanz-Maroto, A., Molero, D., Gonzalez-Calero, L., Fernandez-Fernandez, B., de la Cuesta, F., Laborde, C. M., Barderas, M. G., Ortiz, A., Vivanco, F., Alvarez-Llamas, G., *Kidney international* 2014, *85*, 103-111.

[12] Bonomini, M., Sirolli, V., Magni, F., Urbani, A., *Journal of nephrology* 2012, *25*, 865-871.

[13] Janech, M. G., Raymond, J. R., Arthur, J. M., *American journal of physiology. Renal physiology* 2007, *292*, F501-512.

[14] Julian, B. A., Suzuki, H., Suzuki, Y., Tomino, Y., Spasovski, G., Novak, J., *Proteomics. Clinical applications* 2009, *3*, 1029-1043.

[15] Tantipaiboonwong, P., Sinchaikul, S., Sriyam, S., Phutrakul, S., Chen, S. T., *Proteomics* 2005, *5*, 1140-1149.

[16] Gozal, D., Jortani, S., Snow, A. B., Kheirandish-Gozal, L., Bhattacharjee, R., Kim, J., Capdevila, O. S., *Am.J.Respir.Crit Care Med.* 2009, *180*, 1253-1261.

[17] Jiang, H., Guan, G., Zhang, R., Liu, G., Cheng, J., Hou, X., Cui, Y., *Diabetes/metabolism research and reviews* 2009, *25*, 232-241.

[18] Lafitte, D., Dussol, B., Andersen, S., Vazi, A., Dupuy, P., Jensen, O. N., Berland, Y., Verdier, J. M., *Clin.Biochem.* 2002, *35*, 581-589.

[19] Lamoureux, L., Simon, S. L., Plews, M., Ruddat, V., Brunet, S., Graham, C., Czub, S., Knox, J. D., *PloS one* 2013, *8*, e64044.

[20] Thongboonkerd, V., McLeish, K. R., Arthur, J. M., Klein, J. B., *Kidney Int.* 2002, *62*, 1461-1469.

[21] Magistroni, R., Ligabue, G., Lupo, V., Furci, L., Leonelli, M., Manganelli, L., Masellis, M., Gatti, V., Cavazzini, F., Tizzanini, W., Albertazzi, A., *Nephrology, dialysis, transplantation : official publication of the European Dialysis and Transplant Association - European Renal Association* 2009, *24*, 1672-1681.

[22] Candiano, G., Musante, L., Bruschi, M., Petretto, A., Santucci, L., Del, B. P., Pavone, B., Perfumo, F., Urbani, A., Scolari, F., Ghiggeri, G. M., *J.Am.Soc.Nephrol.* 2006, *17*, 3139-3148.

[23] Shui, H. A., Huang, T. H., Ka, S. M., Chen, P. H., Lin, Y. F., Chen, A., *Nephrol.Dial.Transplant.* 2008, *23*, 176-185.

[24] Soler-Garcia, A. A., Johnson, D., Hathout, Y., Ray, P. E., *Clinical journal of the American Society of Nephrology : CJASN* 2009, *4*, 763-771.

[25] Magagnotti, C., Fermo, I., Carletti, R. M., Ferrari, M., Bachi, A., *Clin.Chem.Lab Med.* 2010, *48*, 531-535.

[26] Zubiri, I., Vivanco, F., Alvarez-Llamas, G., *Methods in molecular biology (Clifton, N.J.)* 2013, *1000*, 209-220.

[27] Shuford, C. M., Hawkridge, A. M., Burnett, J. C., Jr., Muddiman, D. C., *Analytical chemistry* 2010, *82*, 10179-10185.

[28] Darde, V. M., de la Cuesta, F., Dones, F. G., Alvarez-Llamas, G., Barderas, M. G., Vivanco, F., *Journal of proteome research* 2010, *9*, 4420-4432.

SUPPLEMENTAL MATERIAL

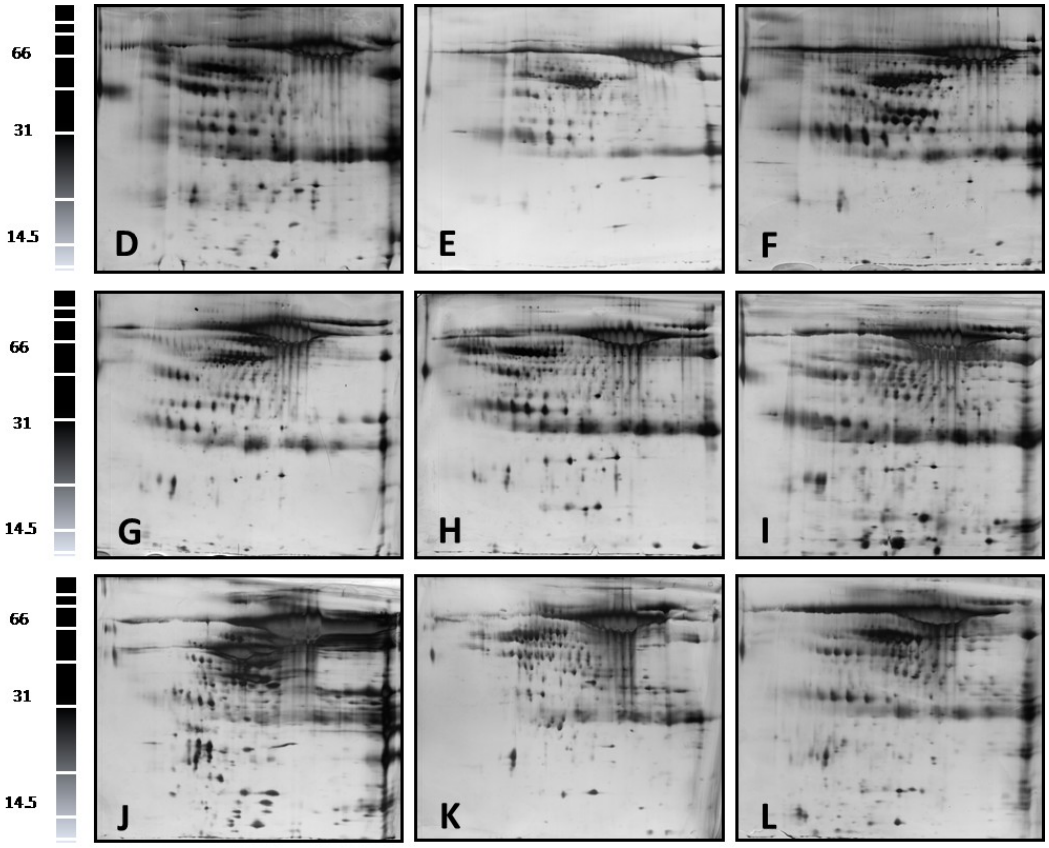

Supplementary Figure. 2-DE urine profiles when no albumin depletion was applied. D-L gels correspond to depleted urine samples labeled as such in Figure 4.

Chapter 2

KLK1 and ZG16B proteins and arginine-proline metabolism identified as novel targets to monitor atherosclerosis, acute coronary syndrome and recovery

Marta Martin-Lorenzo*, Irene Zubiri, Aroa S. Maroto, Laura Gonzalez-Calero, Maria Posada-Ayala, Fernando de la Cuesta, Laura Mourino-Alvarez, Luis F Lopez-Almodovar, Eva Calvo-Bonacho, Luis M. Ruilope, Luis R Padial, Maria G Barderas, Fernando Vivanco, Gloria Alvarez-Llamas*

Metabolomics 2014, doi: 10.1007/s11306-014-0761-8

La aterosclerosis tiene un desarrollo silente que demanda nuevos marcadores de riesgo cardiovascular para la monitorización del desarrollo de la placa que puede evolucionar hasta un evento fatal por ruptura de la misma o por oclusión del torrente sanguíneo. A día de hoy muchos de los mecanismos subyacentes en la aterosclerosis, que implican un elevado número de moléculas y sistemas interconectados entre sí se desconocen o no se comprenden en su totalidad. El abordaje de la enfermedad a través de herramientas ómicas permite una visión global, sin sesgo, y hace que simultáneamente se puedan estudiar dianas ya conocidas en la enfermedad así como nuevas moléculas que se erigirán como nuevos jugadores en los cambios fisiopatológicos de la aterosclerosis. Estas moléculas se podrán evaluar a posteriori para su confirmación como potencial biomarcador mediante experimentos dirigidos.

El trabajo presentado a continuación, publicado en *Metabolomics,* busca encontrar paneles marcadores en orina de aterosclerosis subyacente y silente. Como ya se ha comentado previamente en esta tesis doctoral, la orina es un fluido accesible y rico en información que, sin embargo, no ha sido muy estudiado en aterosclerosis donde estudios en plasma son más habituales. Las técnicas ómicas seleccionadas para este abordaje son la electroforesis diferencial de segunda dimensión (2D-DIGE) para el análisis porteómico y la resonancia magnética nuclear (NMR) para el análisis metabolómico. Ambas han sido puestas a punto previamente en nuestro laboratorio para el estudio de la orina: el análisis proteómico tal y como se describe en el capítulo anterior y el análisis metabolómico tal y como se recoge en *M Posada-Ayala et al*.

El estudio comprende un abordaje completo de la enfermedad cardiovascular desde los inicios de la formación de la placa, en un modelo de conejo de aterosclerosis temprana, hasta la situación extrema de sujetos que han sufrido un evento cardiovascular recogiendo muestras en el momento del ingreso y al alta. Este estudio ha puesto de manifiesto que hay mecanismos que actúan en la misma línea en ambas situaciones y que, sin embargo, hay otros que varían en función de si se está en la fase de desarrollo o por el contrario en una fase aguda. Esto hace que del estudio se desprendan diferentes paneles de marcadores; marcadores de progresión, marcadores de riesgo de evento cardiovascular y marcadores de recuperación. A su vez la identificación de estos marcadores refleja diferentes mecanismos que en este caso concreto parecen en todo momento ser mecanismos protectores de defensa del organismo. Destaca la implicación del sistema calicreína-cinina, del receptor tipo toll 2 y de cambios en los metabolismos de la arginina-prolina y glutatión.

En conclusión, el siguiente capítulo presenta la gran utilidad de técnicas ómicas puestas a punto para el caso concreto de la orina en la enfermedad aterosclerótica tanto en muestras de un modelo animal de conejo y de muestras humanas. Se proponen tres paneles de marcadores que responden a progresión, evento y recuperación, a la vez que se identifican los diferentes mecanismos subyacentes asociados a los mismos. La principal limitación del estudio es el reducido número de muestras humanas, que debería ser aumentado en futuros estudios. Este trabajo abre nuevas puertas en forma de

nuevas dianas terapéuticas y mecanismos subyacentes en el estudio de la aterosclerosis que de la misma manera deberán ser evaluados en detalle.

Metabolomics
DOI 10.1007/s11306-014-0761-8

ORIGINAL ARTICLE

KLK1 and ZG16B proteins and arginine–proline metabolism identified as novel targets to monitor atherosclerosis, acute coronary syndrome and recovery

Marta Martín-Lorenzo · Irene Zubiri · Aroa S. Maroto · Laura Gonzalez-Calero · Maria Posada-Ayala · Fernando de la Cuesta · Laura Mourino-Alvarez · Luis F. Lopez-Almodovar · Eva Calvo-Bonacho · Luis M. Ruilope · Luis R. Padial · Maria G. Barderas · Fernando Vivanco · Gloria Alvarez-Llamas

Received: 5 July 2014 / Accepted: 3 December 2014
© Springer Science+Business Media New York 2014

Abstract We pursued here the identification of specific signatures of proteins and metabolites in urine which respond to atherosclerosis development, acute event and/or recovery. An animal model (rabbit) of atherosclerosis was developed and molecules responding to atherosclerosis silent development were identified. Those molecules were investigated in human urine from patients suffering an acute coronary syndrome (ACS), at onset and discharge. Kallikrein1 (KLK1) and zymogen granule protein16B (ZG16B) proteins, and L-alanine, L-arabitol, scyllo-inositol, 2-hydroxyphenilacetic acid, 3-hydroxybutyric acid and *N*-acetylneuraminic acid metabolites were found altered in response to atherosclerosis progression and the acute event, composing a molecular panel related to cardiovascular risk. KLK1 and ZG16B together with 3-hydroxybutyric acid, putrescine and 1-methylhydantoin responded at onset but also showed normalized levels at discharge, constituting a molecular panel to monitor recovery. The observed decreased of KLK1 is in alignment with the protective mechanism of the kallikrein–kinin system. The connection between KLK1 and ZG16B shown by pathway analysis explains reduced levels of toll-like receptor 2 described in atherosclerosis. Metabolomic analysis revealed arginine and proline metabolism, glutathione metabolism and degradation of ketone bodies as the three main pathways altered. In conclusion, two novel urinary panels of proteins and metabolites are here for the first time shown related to atherosclerosis, ACS and patient's recovery.

Keywords Acute coronary syndrome · Urine · Kallikrein · Zymogen granule protein · Metabolites · Nuclear magnetic resonance · MRM · SRM

1 Introduction

Cardiovascular diseases (CVD) remain the leading cause of death in developed countries and are expected to become so in emerging countries (Roger 2011; Bassand and Hamm 2007). Due to the silent nature of the process, one of the

Electronic supplementary material The online version of this article (doi:10.1007/s11306-014-0761-8) contains supplementary material, which is available to authorized users.

M. Martín-Lorenzo · I. Zubiri · A. S. Maroto · L. Gonzalez-Calero · M. Posada-Ayala · F. Vivanco · G. Alvarez-Llamas (✉)
Department of Immunology, IIS-Fundacion Jimenez Diaz, UAM, REDinREN, Avenida Reyes Católicos 2, 28040 Madrid, Spain
e-mail: galvarez@fjd.es

F. de la Cuesta · L. Mourino-Alvarez · M. G. Barderas
Department of Vascular Physiopathology, Hospital Nacional de Parapléjicos, SESCAM, Toledo, Spain

L. F. Lopez-Almodovar
Department of Cardiac Surgery, Hospital Virgen de la Salud, SESCAM, Toledo, Spain

E. Calvo-Bonacho
Ibermutuamur, Madrid, Spain

L. M. Ruilope
Cardiovascular Risk and Hypertension, Instituto de Investigacion Hospital 12 de Octubre, Madrid, Spain

L. R. Padial
Department of Cardiology, Hospital Virgen de la Salud, SESCAM, Toledo, Spain

F. Vivanco
Department of Biochemistry and Molecular Biology I, UCM, Madrid, Spain

Published online: 14 December 2014

ABSTRACT

We pursued here the identification of specific signatures of proteins and metabolites in urine which respond to atherosclerosis development, acute event and/or recovery. An animal model (rabbit) of atherosclerosis was developed and molecules responding to atherosclerosis silent development were identified. Those molecules were investigated in human urine from patients suffering an acute coronary syndrome (ACS), at onset and discharge. Kallikrein1 (KLK1) and zymogen granule protein16B (ZG16B) proteins, and L-alanine, L-arabitol, scyllo-inositol, 2-hydroxyphenilacetic acid, 3-hydroxybutyric acid and N-acetylneuraminic acid metabolites were found altered in response to atherosclerosis progression and the acute event, composing a molecular panel related to cardiovascular risk. KLK1 and ZG16B together with 3-hydroxybutyric acid, putrescine and 1-methylhydantoin responded at onset but also showed normalized levels at discharge, constituting a molecular panel to monitor recovery. The observed decreased of KLK1 is in alignment with the protective mechanism of the kallikrein-kinin system. The connection between KLK1 and ZG16B shown by pathway analysis explains reduced levels of toll-like receptor 2 (TLR2) described in atherosclerosis. Metabolomic analysis revealed arginine and proline metabolism, glutathione metabolism and degradation of ketone bodies as the three main pathways altered.

In conclusion, two novel urinary panels of proteins and metabolites are here for the first time shown related to atherosclerosis, ACS and patient's recovery.

INTRODUCTION

Cardiovascular diseases (CVD) remain the leading cause of death in developed countries and are expected to become so in emerging countries (1) (2). Due to the silent nature of the process, one of the main questions is how to improve current monitoring of plaque formation, identify people at high cardiovascular risk and prevent a fatal event (3-5). To approach molecular mechanisms underlying atherosclerosis development, we chose here an omics strategy in view of the complexity of the interactions involved and cross-talk among the different organs, cells and molecules (6,7). At the discovery phase, no potential marker, no key target is pre-selected, but all the proteins and/or metabolites are investigated as a whole. Thus, those molecules whose relationship with the patho-physiological processes taking place is still unknown are also investigated. In the confirmation phase, a target approach is used to specifically measure the altered molecules discovered. Previous works in our laboratory have proved the potential of these omics approaches in cardiovascular research. Panels of proteins altered in plasma as a consequence of an acute coronary syndrome (ACS) (8) and proteins differentially secreted to the extracellular space from the human atherosclerotic tissue or healthy arteries (9), proving the potential of these omics approaches in cardiovascular research, in the search for markers of disease as well as in the understanding of molecular mechanisms directly occurring at tissue level (10,11). Similarly, different studies have pointed to panels of metabolites related to cardiovascular diseases (12-14).

We investigated the existence of a molecular panel of proteins and metabolites in urine which specifically respond to atherosclerosis in an animal model. Those proteins and metabolites identified as responders to atherosclerosis progression in animal samples were investigated, as a proof of concept, once atherosclerosis development has reached its maximum expression (an acute event) in human samples, to investigate a potential translation of main findings in animal model to human response. For such purpose, human urine was collected from patients at the onset of an ACS and at hospital discharge to specifically evaluate if those proteins and metabolites found altered in animal urine in response to atherosclerosis were also responders to the event condition itself and, if so, if they additionally normalize their levels once the patient has been discharged, i.e. return to control values.

METHODS

Animal model of atherosclerosis

Fourteen male New Zealand White rabbits (weight 2 to 2.5 kg) were divided in two study groups (7 animals per group): 1) animals fed with normal rabbit chow (control group); 2) animals fed with 1% cholesterol-enriched chow plus 50,000 IU/Kg vitamin D2 (Harlan, Indianapolis, Indiana) (pathological group). Vitamin D2 has been shown to accelerate the atherosclerotic process in this animal model by means of calcification (15). The high cholesterol diet rabbit model has been widely used for experimental atherosclerosis. The observed lesions resemble, at least partially, those seen in human plaques, mainly regarding the inflammatory component. Animals were housed in

individual cages in an air-conditioned room under a 12:12-h light-dark cycle. Principles of laboratory animal care were followed and all experimental procedures were approved by the Animal Care and Use Committee of the IIS-Fundación Jiménez Díaz, according to the guidelines for ethical care of the European Community. Blood samples were taken through the marginal vein of the ear at baseline, middle and end of the experimental model for the measurement of cholesterol and triglycerides by using Advia Chemistry systems (Siemens Healthcare Diagnostic Inc.). The sacrifice took place 13 weeks after. Animals were sedated with an injection of ketamine (100 mg/kg) and xylazine (20mg/kg) and then euthanized by injection of pentobarbital (50 mg/kg) directly in the heart. Ascending aortic section was dissected, rinsed in saline buffer and embedded in paraffin. Cross-sectional serial 5µm sections were subjected to Hematoxilin-Eosin (H&E), red alizarin staining (for visualization of calcium deposits) and immunohistochemistry (IHC) to localize macrophages and vascular smooth muscle cells (VSMCs) using antibodies against RAM11 and actin, respectively. Animals were sacrificed the same day early in the morning to minimize variation. Urine samples were taken directly from the urinary bladder at the time of sacrifice for proteins and metabolites analysis.

Human urine samples

Urine samples from patients were collected in sterile containers at the Cardiology Division in Hospital Virgen de la Salud (Toledo), and directly transported to the Immunology Department in IIS-Fundación Jiménez Díaz.

Subject	Sex	Age	HTN	Diabetes	Dyslipidemia	ACS
1	M	57	N	N	N	N
2	F	62	Y	N	Y	N
3	M	58	N	N	Y	N
4	F	58	N	N	Y	N
5	M	58	N	N	N	N
6	M	53	Y	N	N	N
7	M	52	Y	N	Y	N
8	M	80	Y	Y	Y	N
9	F	70	Y	N	N	N
10	M	52	N	N	N	NSTEACS
11	M	63	Y	N	Y	STEAMI
12	M	54	N	N	N	STEACS
13	M	73	Y	N	Y	STEACS
14	M	65	Y	N	Y	NSTEACS

Table 1. Clinical data. HTN: Hypertension; ACS: acute coronary syndrome; AMI: acute myocardial infarction. NSTEACS: non-ST segment elevation of ACS. STEACS: ST segment elevation of ACS. STEAMI: ST segment elevation of acute myocardial infarction. Control group: subjects 1-9; ACS group: subjects 10-14.

Fourteen individuals were admitted in the study and were classified as healthy (control group) or with ACS at two time points: at hospital admission (ACSt0) and at hospital discharge (ACSt1). Urine samples from patients were taken following admission after the acute coronary syndrome (t0) and at hospital discharge (t1), in any case following fasting specifically, as this condition is not feasible to be guaranteed particularly at t0. The same was applied for control samples which were randomly taken along the morning. Sample collection procedures were in accordance with the Helsinki declaration and were approved by the institution's ethics committee. All subjects received all appropriate information and signed a confidentiality agreement. The control group did not receive any medication known to interfere with the studied variables. Clinical data are shown in Table 1.

Proteomic analysis of animal urine samples by Differential Gel Electrophoresis (DIGE)

Animal urine samples were centrifuged at 3000g for 10 minutes to eliminate cell debris and supernatants were frozen at -80ºC until analysis. Frozen samples were thawed in a water bath at 37ºC, filtered through Acrodisc® Syringe filters 0.2 μm (Pall) and concentrated in Amicon Ultra Centrifugal Filters 10kDa cut-off (Millipore) up to a final volume of 300-350μL. Milli Q water was added to a total volume of 500μL and samples clean-up was carried out by solid phase extraction with Oasis HLB cartridges (Waters, Milford, MA), following manufacturer's instructions. Solvent was removed in a Savant SpeedVac® concentrator up to dryness and samples were dissolved in 100 μL lysis buffer (7M urea, 2M thiourea, 4% CHAPS) and pH was adjusted to 8.0-8.5 with NaOH to perform differential gel electrophoresis (DIGE) analysis. Samples were loaded onto IPG strips (24 cm, pH 4-7). Isoelectric focusing (IEF) was carried out in a PROTEAN IEF CELL (BioRad) according to the following program: active rehydration at 50V for 12 h, 500V for 1h, up to 3500V for 3h (linear voltage ramping method), 3500V for 3h and up to 5000V until 45000V were accumulated. Second dimension was carried out on 14% running gels using EttanDaltSix System (GE Healthcare). Gels were scanned using a Typhoon 9400 Variable Mode Imager (GE Healthcare) and spot maps were processed, analyzed and compared using the DeCyder Differential Analysis Software version 6.5 (GE Healthcare). Spot detection and normalized volume ratio calculations were performed in the Differential In-gel Analysis (DIA) module, while gel-to-gel matching and statistical analysis were performed in the Biological Variation Analysis (BVA) module. Student's t test was used to compare the expression of each spot. Spots found significantly varied (p-value ≤ 0.05) and with a fold change greater than 1.6 or lower than -1.6 were considered for further analysis.

Identification of the significantly varied proteins by MALDI-TOF/TOF

Protein spots were excised manually and automatically digested using the Ettan Digester (GE Healthcare). The digestion protocol used was that of Schevchenko *et al.* (16) with minor variations. 0.5 μl of each digested peptide solution were deposited using the thin layer method, onto a 384 Opti-TOF 123x81 mm MALDI plate (Applied

Biosystems) and allowed to dry at room temperature. The same volume of matrix (3mg/ml α-cyano-4-hydroxycinnamic acid (CHCA) (Sigma Aldrich) in 60% acetonitrile, 0.5% trifluoroacetic acid) was applied on every sample in the MALDI plate. Data were obtained in an automated analysis loop using a 4800 Plus MALDI TOF/TOF Analyzer (Applied Biosystems). Spectra were acquired in the reflector positive-ion mode with a Nd:YAG, 355 nm wavelength laser, at 200 Hz laser frequency, and 1000 to 2000 individual spectra were averaged. Automated analysis of mass data was performed using the 4000 Series Explorer Software version 3.5.3 (Applied Biosystems). MALDI-MS and MS/MS data were combined through the GPS Explorer Software Version 3.6 to search a nonredundant protein database (Swissprot 2011_09) using the Mascot software version 2.2 (Matrix Science) (17).

Metabolomic analysis of animal urine samples by ^{1}H NMR

Nuclear Magnetic Resonance (NMR) analysis was carried out as described previously (18). Briefly, animal urine samples were centrifuged at 31000g for 15 minutes and supernatants were frozen at -80ºC until processing. Frozen samples were thawed in a water bath at 37ºC and then 400µl sample were diluted (1:1) with 0.01mM sodium trimethylsilyl propionate (TSP) solution (as internal reference for spectra calibration) in D_2O buffered with Na_2HPO_4/NaH_2PO_4 (200 mM, each) to pH 7.0. All NMR experiments were performed at 277K on a Bruker AVANCE III 700 instrument with a 5mm TCI cryoprobe equipped with shielded z-gradient coil operating at 700.17 MHz ^{1}H resonance frequency. ^{1}H NMR spectra were measured with 256 scans into 32K data points over a spectral width of 8417.51 Hz, which results in an acquisition time of 1.94s. A relaxation delay (d1) of 2s ensured the T1-relaxation between successive scans. The signal of the solvent was suppressed by using noesypr1d pulse sequence (Bruker Biospin Ltd.) in which the residual water peak is irradiated during the relaxation delay and during the mixing time of 150 ms. All spectra were processed using TOPSPIN (version 1.3, Bruker Biospin Ltd.). Prior to Fourier transformation, the FIDs were multiplied by an exponential weight function corresponding to a line broadening of 0.3 Hz. Spectra were phased, baseline-corrected and referenced to the TSP singlet at δ 0 ppm. ^{1}H NMR spectra were data analyzed using the software program AMIX (Analysis of MIXtures version 3.6.8, Bruker Rheinstetten, Germany). Individual integral regions were normalized to the total sum of integral region following exclusion of the water resonance. Each spectrum from 10.00 to 0 ppm was partitioned into small spectral regions of 0.04ppm (buckets) thus reducing the number of total variables and compensating for small shifts in the spectra (19) prior to statistical analysis. Non-supervised principal components analysis (PCA) were applied to the bucket tables of spectra (no scaling). Loading plots were also calculated to show how principal component analysis is related to the original buckets.

Metabolites identification by two dimensional NMR (2D NMR)

For metabolites identification, spectra were analyzed by ACD/NMR Processor Academic Edition (Version 12.01, Advance Chemistry Development Inc). Unequivocal

identification of metabolites was accomplished by using Metabohunter tool (20) and 2D NMR experimental data: homonuclear correlation spectroscopy ^{1}H-^{1}H (COSY), total correlation spectroscopy (TOCSY) and heteronuclear single-quantum correlation spectroscopy (^{1}H-^{13}C HSQC).

Selected Reaction Monitoring (SRM) analysis of animal and human urine samples

Urine samples were analyzed in SRM mode (Selected Reaction Monitoring) (21) using a 6460 Triple Quadrupole LC-MS/MS on-line connected to: a) nano-chromatography in a Chip-format configuration (ChipCube interface, ProtID Zorbax 300B-C18-5µm chip, Agilent Technologies) constituted by 43x0.075-mm analytical column and 40 nL enrichment column for proteins analysis or b) a reversed-phase column (Atlantis T3, 3µm, 2.1x100mm, Waters) thermostated at 40ºC for metabolites analysis. The HPLC system consisted of a degasser, two binary pumps and thermostated autosampler maintained at 4ºC (1200 Series, Agilent Technologies). The system was controlled by Mass Hunter Software (v4.0 Agilent Technologies).

For protein analysis urine samples were concentrated in Amicon Ultra Centrifugal Filters, 10kDa cut-off (Millipore). Total protein content was quantified by Bradford assay. Protein samples were reduced, alkylated and digested with sequencing grade modified bovine trypsin (Roche) at a final concentration of 1:20 (trypsin:protein). Tryptic peptides solutions were cleaned with C18 spin columns (Protea Biosciences) according to manufacturer's instructions and mixed 1:1 with mobile phase A (0.1% formic acid in MilliQ water). Two microliters of sample was injected at 4 µL/min and separation took place at 0.4 µL/min in a continuous acetonitrile gradient as follows: 1) At 0 min 5% B (0.1% formic acid in acetonitrile), 2) At 1min 5% B, 3) At 5 min 40% B, 4) At 12 min 95% B, 5) At 14min 95% B, 6) At 14.2 min 5% B and 7) At 15min 5% B. The mass spectrometer operated in positive mode with capillary voltage of 1990V, 325ºC source gas temperature and 5 L/min source gas flow. Fragmentor was set to 130V, dwell time to 20 or 50 ms, delta EMV to 600 V and collision energy was optimized for each SRM transition. Theoretical SRM transitions were designed using Skyline (v.1.1.0.2905) (22) and peptide specificity was confirmed by protein blast. Only proteotypic peptides were selected.

For metabolites analysis, acetonitrile was added to urine samples (1:1) for protein precipitation and removal. Supernatants were taken, filtered through 0.20µm and diluted (1:2 or 1:6) with mobile phase A (0.1% formic acid in Milli-Q water). A sample volume of 10 µl was injected and separation took place at 0.4ml/min in an acetonitrile gradient: 1) at 0min 0% B (0.1% formic acid in acetonitrile), 2) at 0.5min 0%B, 3) at 2.5 min 95% B 4) at 2.51 min 0% B 5) at 3min 0%B and a post time of 2 minutes. The mass spectrometer operated in positive or negative mode with 300ºC source gas temperature and 5 L/min source gas flow. Fragmentor potential was optimized for each metabolite in the range 60-175 V, dwell time was fixed to 50 ms in positive mode and 100ms in negative mode (delta EMV was fixed to 600 V or 0V in positive or negative mode,

respectively). Collision energy was optimized for each metabolite by means of Optimizer Software (Agilent Technologies). Optimal SRM transitions were selected in direct infusion mode by previous analysis of commercial metabolite standards (see Suppl. Mat. Table 1). Individual signals were normalized based on total ion current (TIC) and normalized peak areas were calculated for comparison. Unpaired t-test was calculated by GraphPad Prism 6 (version 6.03) software.

Pathway analysis

Protein pathway analysis was carried out by STRING 9.0 software (23) consisting of a database of known and predicted protein interactions, including direct (physical) and indirect (functional) associations derived from genomics, high-throughput experiments, coexpression, and previous knowledge. High confidence filter (0.600) was applied and connections involving only 2 proteins were not considered. Metabolites pathway analysis was done using MetaboAnalyst 2.0 (24,25) by compound matching using Homo Sapiens library, performing Fishers' exact test.

RESULTS

Urine molecular variations in response to atherosclerosis silent development

This work aimed first at the identification of a molecular panel in urine associated with atherosclerosis development in an animal model. The high cholesterol diet rabbit model has been widely used for experimental atherosclerosis. The observed lesions resemble, at least partially, those seen in human plaques, mainly regarding the inflammatory component. Serum total cholesterol, LDL cholesterol, and triglycerides were measured at the beginning, middle and end of the experimental model showing a progressive increment (Suppl. Mat. Table 2). Histological characterization of aortic sections dissected from animals depicted atherosclerosis development in the special diet group (Figure 1). In this pathological group (1-4A), compared to control animals (1-4B), intimal thickening has occurred (1A), calcium deposits are observed (2A) and migration of VSMC to the thickened intima of the aorta (3A) together with abundant macrophage infiltrate (4A) can be appreciated.

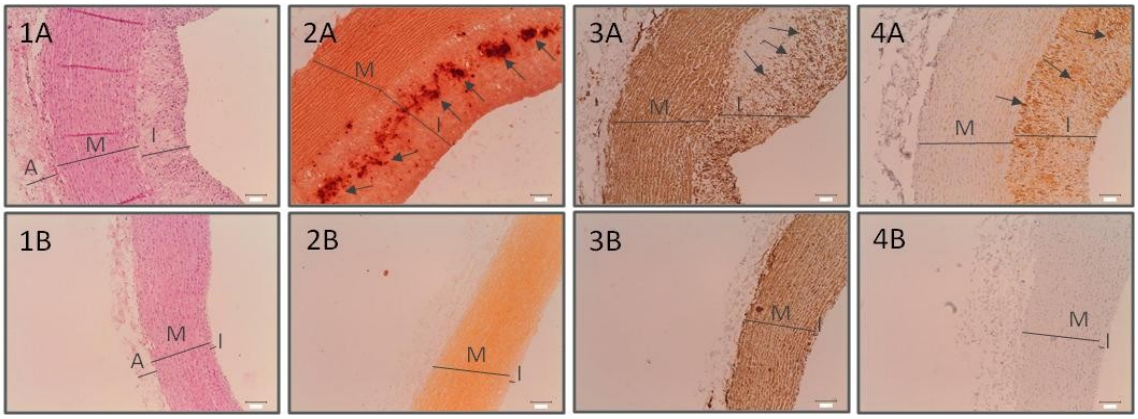

Figure 1. Histological characterization of aortic tissue from (A) pathological animals (special diet) and (B) control animals. 1: Hematoxilin-Eosin (H&E), 2: red alizarin staining, 3: actin and 4: RAM 11. Representative images (10X magnification, 100µm scale). Letter code, A: adventitia, M: media, I: intima. Arrows correspond to calcium deposits, SMCs and macrophages-foam cells on pictures 2A, 3A and 4A, respectively.

Proteins and metabolites significantly varied in urine from animals in response to atherosclerosis were investigated. PCA from proteome differential analysis by DIGE shows correct grouping of control and pathological groups and perfect separation by PC1 (Suppl. Mat. Figure 1). Proteins identification (Suppl. Mat. Table 3) revealed cathepsin D, and superoxide dismutase significantly increased in the special diet group, while hemopexin, kallikrein 1 (KLK1), and zymogen granule protein 16 homolog (ZG16B) significantly decreased. Protein variations were confirmed by Selected Reaction Monitoring (SRM)-LC-MS/MS analysis in animal urine samples for cathepsin D, hemopexin, KLK1, and ZG16B (see Table 2). Metabolomic analysis was performed by 1H-NMR. PCA showed a good clustering for cases and controls (Suppl. Mat. Figure 2). From a total of 96 chemical shifts in the spectra showing the strongest contribution to the PCA, 37 metabolites were identified as potentially significant and analyzed by (SRM)-LC-MS/MS (see Suppl. Table 4). 19 metabolites were confirmed as significantly varied between control and pathological animal groups. Table 2 shows the different trends and significant variations. A total of 7 metabolites increased in urine in response to atherosclerosis development: L-alanine, betaine, dimethylglycine, glycine, taurine, L-arabitol and 1-methylhydantoin. Twelve metabolites show the opposite trend (decreased in response to atherosclerosis): p-benzoquinone, pipecolic acid, L-serine, putrescine, 6-phosphogluconic acid, cyclohexanol, pyrocathecol, hypotaurine, L-lysine, spermidine, tyramine and scyllo-inositol.

PROTEINS		
Name	**Pathological/Control**	**Significance (p-value)**
Cathepsin D	↑	*
Hemopexin	↓	*
KLK1	↓	**
ZG16B	↓	*
METABOLITES		
Name	**Pathological/Control**	**Significance (p-value)**
1-Methylhydantoin	↑	*
6-Phosphogluconic	↓	***
Betaine	↑	****
Cyclohexanol	↓	*
Dimethylglycine	↑	***
Glycine	↑	*
Hypotaurine	↓	****
L-Alanine	↑	**
L-Arabitol	↑	**
L-Lysine	↓	**
L-Serine	↓	***
p-Benzoquinone	↓	***
Pipecolic acid	↓	****
Putrescine	↓	*
Pyrocatechol	↓	****
Scyllo-inositol	↓	****
Spermidine	↓	*
Taurine	↑	***
Tyramine	↓	***

Table 2. SRM confirmation analysis. Proteins and metabolites found significantly altered in urine from pathological animals (atherosclerosis) compared to control animal group (7 animals per group). *p-value<0.05,**p-value<0.01,***p-value<0.001,****p-value<0.0001.

Proteins and metabolites fingerprint in response to ACS and recovery

As detailed above, we initially defined a molecular panel which clearly responds to atherosclerosis pathology in animals (silently and asymptomatic). In a further step and as a proof of concept of animal data transference to humans, we investigated a potential alteration of those molecules in response to the ultimate fatal consequence of atherosclerosis development, i.e. an acute event. With this aim, those molecules were further analyzed in human urine samples from ACS patients. Human urine samples were collected both at the onset of ACS and at discharge, to elucidate changes in response to the acute syndrome but also related to patient's recovery. A detailed view of the workflow followed in the study is shown in Figure 2.

We quantitatively analyzed those proteins and metabolites which had been selected as responders to atherosclerosis in animal urine, in urine samples collected from individuals who had suffered ACS, both at admission (t0) and at discharge (t1) time points, and in comparison with healthy individuals' urine (control group). (SRM)-LC-MS/MS revealed different trends, providing with particular sub-sets of molecules which may serve as indicators of the acute event itself or recovery.

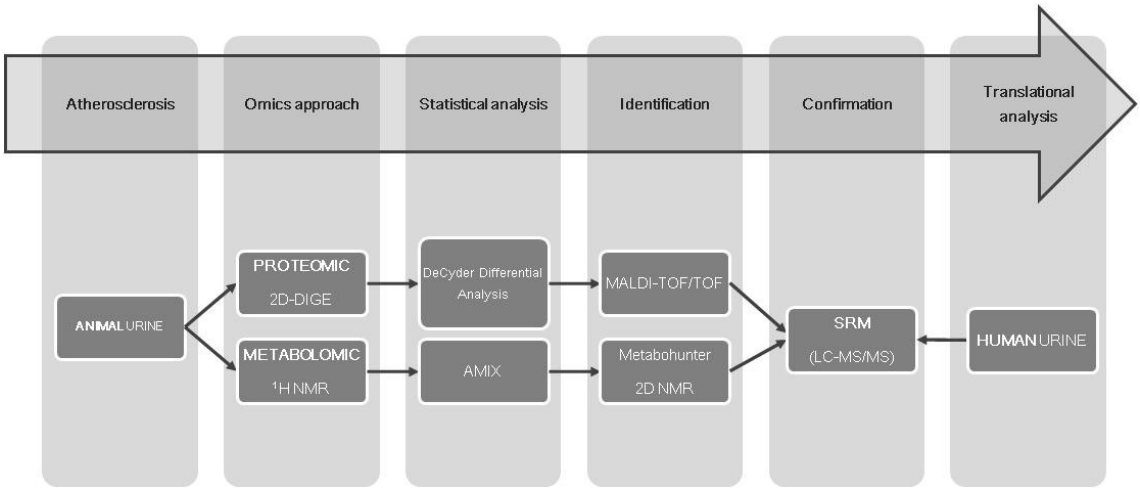

Figure 2. Workflow schema for proteomic and metabolomic analysis of urine. Candidate markers of atherosclerosis were discovered in an animal model and further confirmed by SRM. Translation into a human fingerprint was investigated in response to ACS.

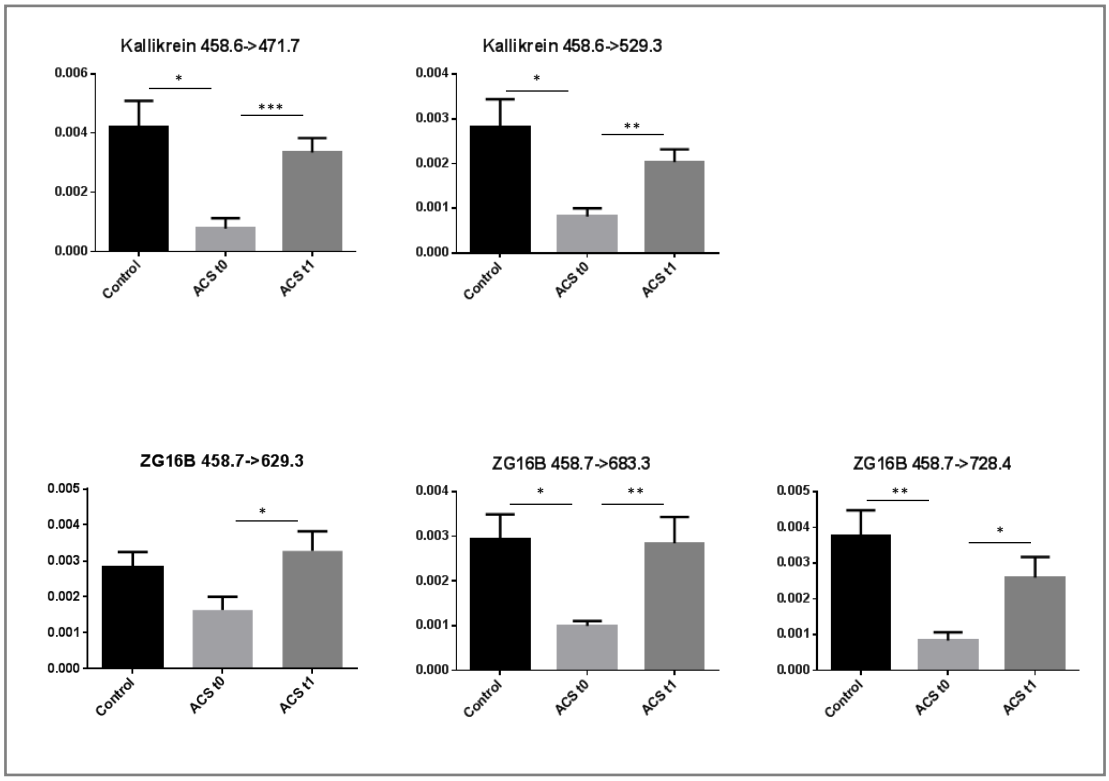

Figure 3. SRM data showing proteins significantly altered in urine from ACS patients. Urine samples were collected from healthy subjects (control group) (n=9) and patients at the onset (t0) and at discharge (t1) (n=5). Error bars represent SEM.

In particular, KLK1 and ZG16B were found significantly decreased in ACSt0 (onset), returning to control values at ACSt1 (discharge) and showing the same trend observed in the animal model (decreased in special diet group) (see Figure 3). Although without significant variation, trends observed in the animal model were also confirmed for cathepsin D and hemopexin in human urine samples collected at ACSt0 time point compared to control levels, showing partial normalization at ACSt1.

At metabolome level, L-alanine and L-arabitol were found significantly increased, and scyllo-inositol significantly decreased at ACS, both at t0 and t1, compared to control levels, showing the same trend observed in the animal model (increased or decreased in the special diet group, respectively). With opposite trend to that observed in the animal model, putrescine, spermidine, p-benzoquinone and cyclohexanol were found increased at ACSt0 versus control. Putrescine and cyclohexanol additionally showed total or partial recovery to normal values at ACSt1. 1-methylhydantoin significantly decreased at the onset (ACSt0), while normal levels are already reached at discharge (ACSt1). 2-hydroxyphenylacetic acid decreased at ACSt0, while N-acetylneuraminic acid and 3-hydroxybutyric acid increased. Interestingly, all these three metabolites showed significant variation in response to ACS, following the same trend to that observed in the animal model, although no significant differences have been found in animals' urine. Among the three, 3-hydroxybutyric acid showed normalized levels at discharge (see Figure 4).

Metabolic pathway analysis was performed by including metabolites found significantly altered during atherosclerosis progression (animal model) or in response to an ACS (human). Common altered pathways to both situations (p value <0.05) were "arginine and proline metabolism" (involving putrescine, spermidine and 1-methylhydantoin), and "glutathione metabolism" (including putrescine, spermidine and glycine) (Figure 5)

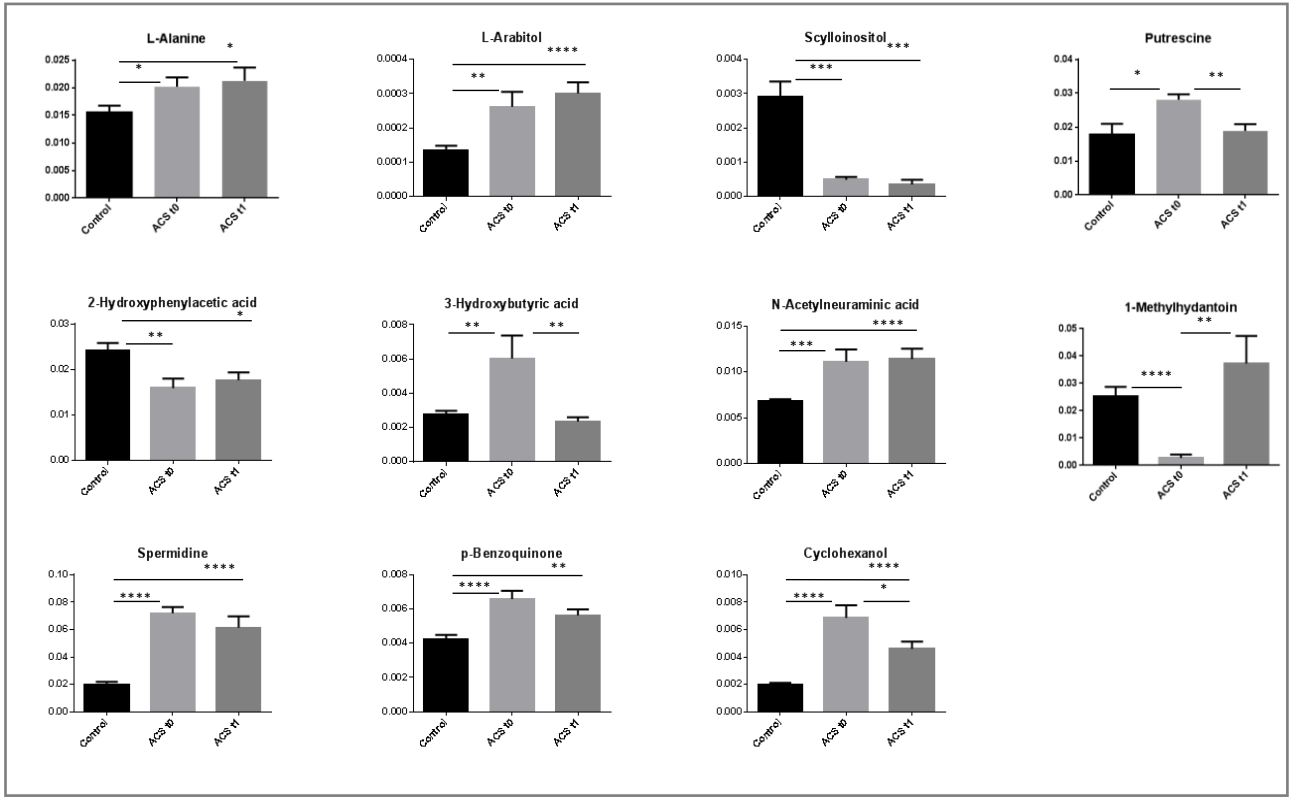

Figure 4. SRM data showing metabolites significantly altered in urine from ACS patients. Urine samples were collected from healthy subjects (control group) (n=9) and patients at the onset (t0) and at discharge (t1) (n=5). Error bars represent SEM.

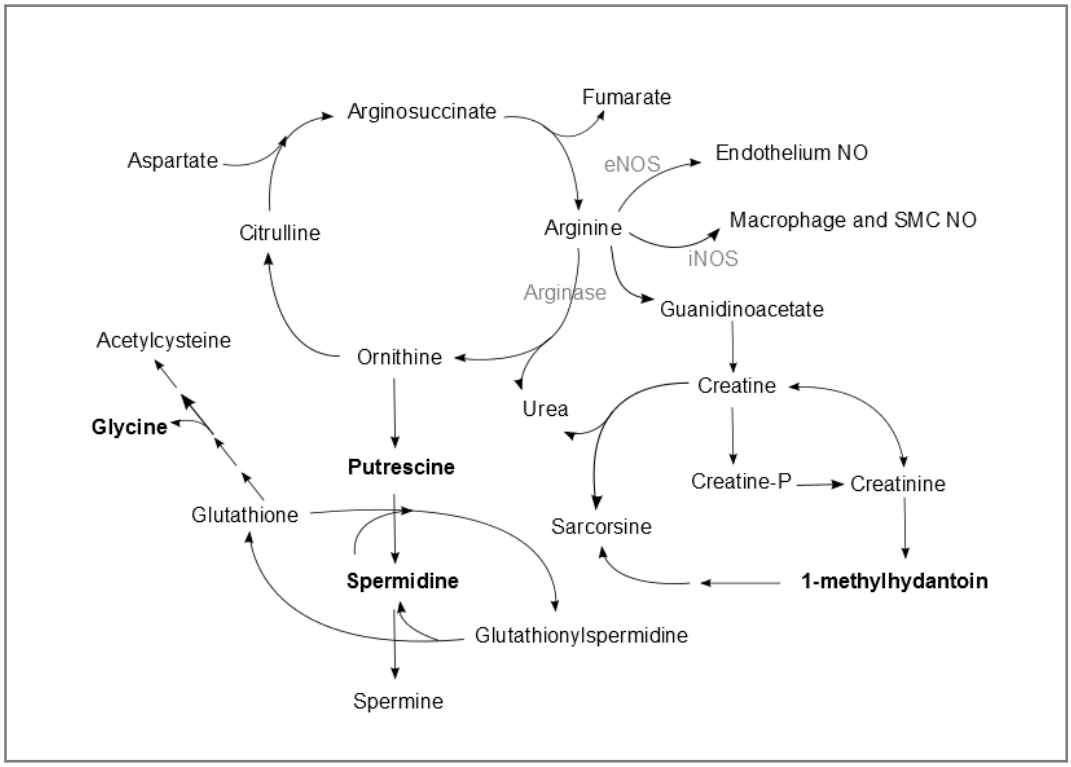

Figure 5. Overview of key altered metabolites found in animal model (atherosclerosis development) and human urine (acute event). Main pathways involved are glutathione and arginine-proline metabolism. This map was created from KEGG pathways database, highlighting only those which are relevant in the context of metabolites found altered in this study. Role of arginine as NO precursor is also included. Metabolites found significantly altered in this study are marked in black bold letters. Enzymes are in grey. Metabolites in glutathione pathway: acetylcysteine, glycine, glutathione, spermidine and glutathionylspermidine. Metabolites in arginine-proline pathway: aspartate, arginosuccinate, fumarate, arginine, ornithine, putrescine, spermidine, spermine, guanidinoacetate, creatine, creatinine, cretaine-P, 1-methylhydantoin, sarcorsine.

DISCUSSION

A significant alteration of the urine proteome and metabolome in response to atherosclerosis is demonstrated here. To investigate whether those molecules which respond to atherosclerosis development in the animal model and which of them correlate well with operating mechanisms in humans, we collected urine samples from individuals suffering from an acute event (ACS). This is the extreme situation and the latest effect of disease progression. Additionally, samples were collected at hospital discharge too, looking for a potential value of these markers as indicators of patients' recovery.

A sub-set of molecules showed significant variation in human urine in response to ACS and some of them returned to control values at patient discharge. A group of them responded with the same trend both to atherosclerosis development (animal model) and to the acute onset (in human). That is the case for proteins KLK1 and ZG16B and metabolites L-alanine, L-arabitol, scyllo-inositol, 2-hydroxyphenylacetic acid, 3-hydroxybutyric acid and N-acetylneuraminic acid. This panel allows monitoring disease

progression and may constitute a potential signature to evaluate individual cardiovascular risk, pending further research in additional patient cohorts.

In other cases, as for metabolites putrescine, spermidine, p-benzoquinone, cyclohexanol and 1-methylhydantoin, opposite trends (increase or decrease) were observed in response to atherosclerosis development (before an acute event occurs, animal model) and to the event itself. This observation points to a mixed response in opposite directions, i.e. different mechanisms are activated in particular conditions or particular stage of the disease. In this case, particular metabolites showed altered response following a certain trend during atherosclerosis development (still asymptomatic) but this alteration is in the opposite trend when an acute syndrome takes place, indicating overlapping responses.

In relation to recovery or follow-up, a panel composed by three metabolites, 3-hydroxybutyric acid, putrescine, 1-methylhydantoin and two proteins KLK1 and ZG16B clearly responds to an ACS event and additionally shows the capability to monitor recovery, as the urinary levels returned to control values at patient's hospital discharge. Figure 6 summarizes the most relevant findings of the study.

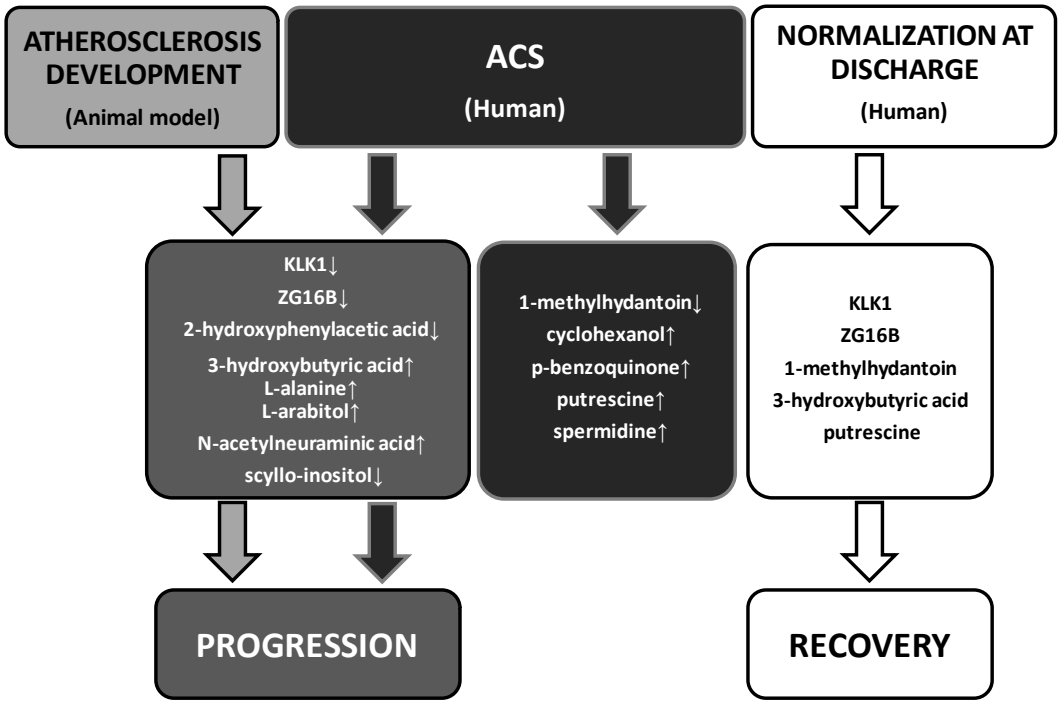

Figure 6. Panels of discovered metabolites and proteins as potential markers of disease progression, acute onset and/or recovery.

KLK-1 is a serine protease acting in the release of the vasoactive peptide, Lys-bradykinin, from low molecular weight kininogen. These kinins are inflammatory mediators (26). Kallikrein-kinin system is involved in the control of vascular smooth muscle tone and arterial blood pressure (27), playing a significant cardioprotective

effect mostly endothelium-mediated (28). It has been suggested (29) that reduced activity of the local kallikrein-kinin system may be instrumental in the induction of cardiovascular-related diseases. Tissue kallikrein measurement has been shown to be useful in diagnosis and monitoring of atherosclerosis (30) and it has been proved that tissue kallikrein infusion improvescardiac function and protect against myocardial ischemia injury after coronary artery occlusion (31). The protector mechanism is related with an inhibition of apoptosis, inflammation, hypertrophy and fibrosis, as well as an enhancement of neovascularization (32). These observations correlate with the observed decrease in urine for kallikrein-1 in response to atherosclerosis development and acute event (ACS), following normalization at patient's hospital discharge. The same behavior was observed for ZG16B. It has been described that ZG16B activate the chemokine CXCR4 (33), which is a receptor of CXCL12. Levels of CXCL12 were found diminished in plasma from patients with stable and unstable angina (34). In agreement, our study shows a decrease in ZG16B urinary levels, which may imply a reduced activation of CXCL12 receptor, CXCR4.

ZG16B and KLK-1 proteins are connected by toll like receptor 2 (TLR2); KLK1 via Kininogen and ZG16B via CXCR4 (suppl. Mat. Figure 3). TLR2 has been widely related with atherosclerosis playing different and controversial roles (35). From one side it has been described to have a beneficial effect by preserving endothelial cell function during vascular inflammatory diseases (36). From the other side, overactivation of the endothelium by excessive TLR2 activation may promote endothelial dysfunction. We observed here a decrease of ZB16B and KLK-1 levels in the context of atherosclerosis. In view of the controversial roles attributed to TLR2 in the literature (beneficial or detrimental), reduced levels of KLK1 and ZG16B found in this study in atherosclerosis are in better consonance with a potential diminution of TLR2 levels (Supplementary Figure 3), and thus more in agreement with a beneficial effect.

At the metabolome level, cardiovascular risk assessment of population from different geographical areas has been related to an increase in urinary L-alanine, and N-acetyl neuraminic acid, and to a decrease in urinary scyllo-inositol, in agreement with our findings (37). Plasma 3-hydroxybutyrate was found increased in stable carotid atherosclerosis patients, and in plasma from ACS patients, in accordance with our data in human urine where this metabolite was found increased at the ACS onset and normalized at discharge (38,39). Spermidine and putrescine have an antagonist action in platelet aggregation which explains the increase observed in this study in ACSt0 as a compensatory mechanism (40), (41). 1-methylhydantoin is a product of the creatinine metabolism (42) which has been widely described to increase in atherosclerosis (43), (44). We found this trend in atherosclerotic animals compared to the control group, but urinary levels in ACS conditions were found lower. Oxidative stress is a causative factor in this pathology and, particularly, plasma levels of oxidative stress indicators (isoprostanes) were found particularly increased in ACS, compared with stable coronary artery disease (CAD) and correlating with platelet activation (45). In mammals, the

metabolism of 1-methylhydantoin occurs via 5-hydroxymethylhydantoin, which is an intrinsic antioxidant against cellular damage (46). The observed decrease of urinary 1-methylhydantoin in response to an ACS correlates well with an activated metabolism in favor of 5-hydroxymethylhydantoin in response to increased levels of ROS produced by activated platelets. In vitro analysis have shown inhibition of Fc receptor- mediated phagocytosis in macrophages by benzoquinone (47). Deficiency of Fcgamma receptor has been pointed to a protective mechanism against atherosclerosis (48). In our study, benzoquinone was found decreased in atherosclerosis development but increased during ACS. This observation might point to a specific activation of this protective mechanism in extreme situations, although further research should be performed.

Metabolic pathway analysis was performed by including found metabolites significantly altered during atherosclerosis progression (animal model) or in response to an ACS (human). The common pathways were arginine and proline and glutathione metabolism. Figure 5 depicts a combined view of those KEGG pathways involved. The polyamines putrescine and spermidine are produced from ornithine. They inhibit platelet aggregation and their increment is closely related with arterial injury (49) as they contribute to arterial remodelling at sites of vascular damage (50). In particular, there are two competing mechanisms for arginine between arginase and NOS (nitric oxide synthase) in favour of NO (nitric oxide) or ornithine production (precursor of polyamines and proline), respectively (51) An increase in polyamine synthesis in tissue has been described in response to proliferation of VSMCs and development of intimal thickening (52). In atherosclerosis and arterial injury, arginase activity is increased showing different roles for arginase I and II in plaque development and vulnerability (53). The increase of arginase explains the synthesis of polyamines from ornithine and in consonance with previously reported elevation of polyamines levels in tissue. We found putrescine and spermidine decreased in urine during atherosclerosis development (animal model) in agreement with the expected accumulation in tissue. Once the acute event takes place, increased polyamines levels were found in urine from ACS patients which may be a consequence of a release of the intracellular content to the blood stream and ultimately filtrated into urine, or of an activation of the polyamines inhibitory response to platelet aggregation which takes place after an acute event occurs, or both., Taking part in to glutathione metabolism N-acetylcysteine (also called mercapturic acid) has antioxidant and anti-inflammatory properties and promotes plaque stabilization (54). It is an end product of four consecutive variations of glutathione. In the third step glycine is released, in agreement with our data showing increased levels in urine of atherosclerotic animals.

CONCLUDING REMARKS

This pilot study shows specific molecular panels associated with atherosclerosis, acute event and recovery in a non-invasive and easily accessible fluid used in routine clinical practice as urine.

Further investigation related to plaque development and instability, and evaluation of molecular panels identified here in patients without reported acute events but high cardiovascular risk, would help in defining specific signatures for disease progression and risk stratification and would cover a gap between atherosclerosis development and irreversible acute damage.

ACKNOWLEDGEMENTS

Instituto de Salud Carlos III (FIS PI080970, FIS PI11/01401, FIS PI13/01873, FIS PI11/02239, FIS IF08/3667-1, FIS PS09/00447, CP09/00229, RD12/0013/0013, RD12/0042/0071, PTI3/0001/0013, PIE13/00051), IDCSalud (3371/002), Fondos FEDER, Fundación Conchita Rábago de Jiménez Díaz. Authors thank personnel from the Cardiology Service in Hospital Virgen de la Salud (Toledo), Proteomics Facility UCM-PCM (a member of ProteoRed-ISCIII network), Unidad de Proteómica Hospital Nacional de Parapléjicos (Toledo) and CAI-RMN (UCM).

These results are lined up with the Spanish initiative on the Human Proteome Project (SpHPP).

DISCLOSURE

The authors declare no financial benefit from this work.

COMPLIANCE WITH ETHICAL REQUIREMENTS

All procedures performed in studies involving human participants were in accordance with the ethical standards of the institutional and/or national research committee and with the 1964 Helsinki declaration and its later amendments or comparable ethical standards.

All applicable international, national, and/or institutional guidelines for the care and use of animals were followed.

REFERENCES

1. Roger VL. Outcomes research and epidemiology: the synergy between public health and clinical practice. CircCardiovascQualOutcomes 2011;4:257-259.

2. Bassand JP, Hamm C. New European guidelines for the management of patients with unstable angina/non-ST-elevation myocardial infarction--what are the new and key messages. PolArchMedWewn 2007;117:391-393.

3. Libby P, Ridker PM, Hansson GK. Progress and challenges in translating the biology of atherosclerosis. Nature 2011;473:317-325.

4. Naghavi M, Libby P, Falk E et al. From vulnerable plaque to vulnerable patient: a call for new definitions and risk assessment strategies: Part II. Circulation 2003;108:1772-1778.

5. Naghavi M, Libby P, Falk E et al. From vulnerable plaque to vulnerable patient: a call for new definitions and risk assessment strategies: Part I. Circulation 2003;108:1664-1672.

6. Corti R, Hutter R, Badimon JJ, Fuster V. Evolving concepts in the triad of atherosclerosis, inflammation and thrombosis. JThrombThrombolysis 2004;17:35-44.

7. Libby P, Theroux P. Pathophysiology of coronary artery disease. Circulation 2005;111:3481-3488.

8. Darde VM, de la Cuesta F, Dones FG, Alvarez-Llamas G, Barderas MG, Vivanco F. Analysis of the plasma proteome associated with acute coronary syndrome: does a permanent protein signature exist in the plasma of ACS patients? JProteomeRes 2010;9:4420-4432.

9. de la Cuesta F, Barderas MG, Calvo E et al. Secretome analysis of atherosclerotic and non-atherosclerotic arteries reveals dynamic extracellular remodeling during pathogenesis. JProteomics 2012;75:2960-2971.

10. de la Cuesta F, Alvarez-Llamas G, Maroto AS et al. A proteomic focus on the alterations occurring at the human atherosclerotic coronary intima. MolCell Proteomics 2011;10:M110.

11. de la Cuesta F, Zubiri I, Maroto AS et al. Deregulation of smooth muscle cell cytoskeleton within the human atherosclerotic coronary media layer. JProteomics 2013;82:155-165.

12. Lewis GD, Asnani A, Gerszten RE. Application of metabolomics to cardiovascular biomarker and pathway discovery. JAmCollCardiol 2008;52:117-123.

13. Barderas MG, Laborde CM, Posada M et al. Metabolomic profiling for identification of novel potential biomarkers in cardiovascular diseases. JBiomedBiotechnol 2011;2011:790132.

14. Rhee EP, Gerszten RE. Metabolomics and cardiovascular biomarker discovery. ClinChem 2012;58:139-147.

15. Drolet MC, Arsenault M, Couet J. Experimental aortic valve stenosis in rabbits. JAmCollCardiol 2003;41:1211-1217.

16. Shevchenko A, Wilm M, Vorm O, Mann M. Mass spectrometric sequencing of proteins silver-stained polyacrylamide gels. AnalChem 1996;68:850-858.

17. Perkins DN, Pappin DJ, Creasy DM, Cottrell JS. Probability-based protein identification by searching sequence databases using mass spectrometry data. Electrophoresis 1999;20:3551-3567.

18. Posada-Ayala M, Zubiri I, Martin-Lorenzo M et al. Identification of a urine metabolomic signature in patients with advanced-stage chronic kidney disease. Kidney Int 2013.

19. Holmes E, Foxall PJ, Nicholson JK et al. Automatic data reduction and pattern recognition methods for analysis of 1H nuclear magnetic resonance spectra of human urine from normal and pathological states. AnalBiochem 1994;220:284-296.

20. Tulpan D, Leger S, Belliveau L, Culf A, Cuperlovic-Culf M. MetaboHunter: an automatic approach for identification of metabolites from 1H-NMR spectra of complex mixtures. BMCBioinformatics 2011;12:400.

21. Picotti P, Aebersold R. Selected reaction monitoring-based proteomics: workflows, potential, pitfalls and future directions. NatMethods 2012;9:555-566.

22. MacLean B, Tomazela DM, Shulman N et al. Skyline: an open source document editor for creating and analyzing targeted proteomics experiments. Bioinformatics 2010;26:966-968.

23. Jensen LJ, Kuhn M, Stark M et al. STRING 8--a global view on proteins and their functional interactions in 630 organisms. Nucleic Acids Res 2009;37:D412-D416.

24. Xia J, Psychogios N, Young N, Wishart DS. MetaboAnalyst: a web server for metabolomic data analysis and interpretation. Nucleic Acids Res 2009;37:W652-W660.

25. Xia J, Mandal R, Sinelnikov IV, Broadhurst D, Wishart DS. MetaboAnalyst 2.0--a comprehensive server for metabolomic data analysis. Nucleic Acids Res 2012;40:W127-W133.

26. Brain SD, Williams TJ. Inflammatory oedema induced by synergism between calcitonin gene-related peptide (CGRP) and mediators of increased vascular permeability. BrJPharmacol 1985;86:855-860.

27. Marcondes S, Antunes E. The plasma and tissue kininogen-kallikrein-kinin system: role in the cardiovascular system. CurrMedChemCardiovascHematolAgents 2005;3:33-44.

28. Dendorfer A, Wolfrum S, Dominiak P. Pharmacology and cardiovascular implications of the kinin-kallikrein system. JpnJPharmacol 1999;79:403-426.

29. Sharma JN, Sharma J. Cardiovascular properties of the kallikrein-kinin system. CurrMedResOpin 2002;18:10-17.

30. Porcu P, Emanueli C, Desortes E et al. Circulating tissue kallikrein levels correlate with

severity of carotid atherosclerosis. ArteriosclerThrombVascBiol 2004;24:1104-1110.

31. Yao YY, Yin H, Shen B, Chao L, Chao J. Tissue kallikrein infusion prevents cardiomyocyte apoptosis, inflammation and ventricular remodeling after myocardial infarction. RegulPept 2007;140:12-20.

32. Chao J, Shen B, Gao L, Xia CF, Bledsoe G, Chao L. Tissue kallikrein in cardiovascular, cerebrovascular and renal diseases and skin wound healing. BiolChem 2010;391:345-355.

33. Lee Y, Kim SJ, Park HD et al. PAUF functions in the metastasis of human pancreatic cancer cells and upregulates CXCR4 expression. Oncogene 2010;29:56-67.

34. Damas JK, Waehre T, Yndestad A et al. Stromal cell-derived factor-1alpha in unstable angina: potential antiinflammatory and matrix-stabilizing effects. Circulation 2002;106:36-42.

35. Mullick AE, Tobias PS, Curtiss LK. Modulation of atherosclerosis in mice by Toll-like receptor 2. JClinInvest 2005;115:3149-3156.

36. Wagner NM, Bierhansl L, Noldge-Schomburg G, Vollmar B, Roesner JP. Toll-like receptor 2-blocking antibodies promote angiogenesis and induce ERK1/2 and AKT signaling via CXCR4 in endothelial cells. ArteriosclerThrombVascBiol 2013;33:1943-1951.

37. Yap IK, Brown IJ, Chan Q et al. Metabolome-wide association study identifies multiple biomarkers that discriminate north and south Chinese populations at differing risks of cardiovascular disease: INTERMAP study. JProteomeRes 2010;9:6647-6654.

38. Teul J, Ruperez FJ, Garcia A et al. Improving metabolite knowledge in stable atherosclerosis patients by association and correlation of GC-MS and 1H NMR fingerprints. JProteomeRes 2009;8:5580-5589.

39. M.Laborde C, Mourino-Alavarez L, Posada-Ayala M et al. Plasma metabolomics reveals a potential panel of biomarkers for early diagnosis in acute coronary syndrome. Metabolomics 2014;10:414-424.

40. de la Pena NC, Sosa-Melgarejo JA, Ramos RR, Mendez JD. Inhibition of platelet aggregation by putrescine, spermidine, and spermine in hypercholesterolemic rabbits. ArchMedRes 2000;31:546-550.

41. Zhang F, Jia Z, Gao P et al. Metabonomics study of atherosclerosis rats by ultra fast liquid chromatography coupled with ion trap-time of flight mass spectrometry. Talanta 2009;79:836-844.

42. Wyss M, Kaddurah-Daouk R. Creatine and creatinine metabolism. Physiol Rev 2000;80:1107-1213.

43. Gentile M, Panico S, Mattiello A et al. Plasma creatinine levels, estimated glomerular filtration rate and carotid intima media thickness in middle-aged women: A population based cohort study. NutrMetab CardiovascDis 2013.

44. Rein P, Saely CH, Vonbank A, Fraunberger P, Drexel H. Impact of the albumin to creatinine ratio and the coronary artery state on vascular events. AmJCardiol 2014;113:1616-1620.

45. Szuldrzynski K, Zalewski J, Machnik A, Zmudka K. Elevated levels of 8-iso-prostaglandin F2alpha in acute coronary syndromes are associated with systemic and local platelet activation. PolArchMedWewn 2010;120:19-24.

46. Ienaga K, Park CH, Yokozawa T. Protective effect of an intrinsic antioxidant, HMH (5-hydroxy-1-methylhydantoin; NZ-419), against cellular damage of kidney tubules. ExpToxicolPathol 2013;65:559-566.

47. Manning BW, Adams DO, Lewis JG. Effects of benzene metabolites on receptor-mediated phagocytosis and cytoskeletal integrity in mouse peritoneal macrophages. ToxicolApplPharmacol 1994;126:214-223.

48. Hernandez-Vargas P, Ortiz-Munoz G, Lopez-Franco O et al. Fcgamma receptor deficiency confers protection against atherosclerosis in apolipoprotein E knockout mice. CircRes 2006;99:1188-1196.

49. Durante W, Liao L, Peyton KJ, Schafer AI. Lysophosphatidylcholine regulates cationic amino acid transport and metabolism in vascular smooth muscle cells. Role in polyamine biosynthesis. JBiolChem 1997;272:30154-30159.

50. Durante W, Liao L, Reyna SV, Peyton KJ, Schafer AI. Transforming growth factor-beta(1) stimulates L-arginine transport and metabolism in vascular smooth muscle cells: role in polyamine and collagen synthesis. Circulation 2001;103:1121-1127.

51. Getz GS, Reardon CA. Arginine/arginase NO NO NO. Arteriosclerosis, thrombosis, and vascular biology 2006;26:237-9.

52. Nishida K, Abiko T, Ishihara M, Tomikawa M. Arterial injury-induced smooth muscle cell proliferation in rats is accompanied by increase in polyamine synthesis and level. Atherosclerosis 1990;83:119-25.

53. Durante W. Role of arginase in vessel wall remodeling. Frontiers in immunology 2013;4:111.

54. Lu Y, Qin W, Shen T et al. The antioxidant N-acetylcysteine promotes atherosclerotic plaque stabilization through suppression of RAGE, MMPs and NF-kappaB in ApoE-deficient mice. Journal of atherosclerosis and thrombosis 2011;18:998-1008

SUPPLEMENTAL MATERIAL

Supplemental Table 1. SRM conditions for proteins and metabolites analysis

Protein	SRM Transition (m/z precursor ion→ m/z product ion)	Fragmentor Voltage (V)	Collision Energy (V)	Mode
Catepsin D (Oryctolagus cuniculus)	717.8 → 1055.5	130	21	Positive
Hemopexin (Orctolagu Cuniculus)	922.0 → 1013.5	130	31.5	Positive
Kallikrein (Oryctolagus Cuniclus)	667.9 → 817.4	130	18.5	Positive
Kallikrein (Homo Sapiens)	458.6 → 471.7	130	7.2	Positive
	458.6 → 529.3	130	7.2	Positive
Zymogen Granule Protein 16 homolog (Oryctolagus cuniculus)	435.6 → 435.8	130	6.3	Positive
Zymogen Granule Protein 16 homolog (Homo Sapiens)	458.7 → 629.3	130	7.8	Positive
	458.7 → 683.3	130	7.8	Positive
	458.7 →728.4	130	7.8	Positive
Metabolite	**SRM Transition (m/z precursor ion→ m/z product ion)**	**Fragmentor Voltage (V)**	**Collision Energy (V)**	**Mode**
1-Methylhydantoin	113.1 → 69.1	90	10	Negative
2-Hydroxyphenylacetic acid	151.2 → 107.1	72	10	Negative
3-Hydroxybutyric acid	103.1 → 59.1	60	10	Negative
6-Phosphogluconic	137.6 → 121.1	60	10	Positive
Betaine	117.9 → 58.0	175	29	Positive
Cyclohexanol	101.2 → 84.0	130	10	Positive
Dimethylglycine	104.9 → 59.2	60	14	Positive
Glycine	76.1 → 48.3	130	16	Positive
Hypotaurine	110.2 → 92.1	76	10	Positive
L-Alanine	90.1 → 44.1	130	22	Positive
L-Arabitol	153.2 → 61.2	60	34	Positive
L-Lysine	146.2 → 72.2	60	18	Positive
L-Serine	105.9 → 60.1	175	20	Positive
N-Acetylneuraminic	308.3 → 87.0	90	10	Negative
p-Benzoquinone	109.9 → 69.0	74	10	Positive
Pipecolic acid	130.2 → 84.1	72	14	Positive
Putrescine	89.2 → 72.2	60	10	Positive
Pyrocatechol	111.1 → 93.1	60	10	Positive
	111.1 → 65.1	60	18	Positive
Scylloinositol	181.2 → 137.1	130	14	Positive
Spermidine	146.3 → 72.2	60	14	Positive
Taurine	125.0 → 61.2	60	34	Positive
Tyramine	138.2 → 121.1	60	10	Positive

Supplemental Table 2. Average serum values for animals fed with control diet and special diet at three time points: beginning (t=0), middle (t=1) and end (after sacrifice) (t=2) of the model. Fourteen male New Zealand White rabbits were divided in two study groups (7 animals per group).

		Special Diet			Control Diet		
		t=0	t=1	t=2	t=0	t=1	t=2
BIOCHEMISTRY	Calcium (mg/dl)	1.2	2.6	3.7	1.5	1.4	1.7
	Phosphorous (mg/dl)	5.8	5.5	6.8	6.5	5.4	4.6
IONS	Potassium (mmol/L)	41.0	27.9	23.1	31.8	35.1	33.2
	Hemolysis (mg/dl)	74	68	<1	26	79	268.9
LIPIDS METABOLISM	Total Cholesterol (mg/dl)	81	1414	1410	63	48	53
	Triglycerides (mg/dl)	127	190	200	99	59	64
	HDL cholesterol (mg/dl)	29	20	14	29	25	22
	LDL cholesterol (mg/dl)	27	1366	1355	14	12	23
	No-HDL Cholesterol (mg/dl)	52	1395	1395	33	23	36

Supplemental Table 3. Proteins significantly altered in urine from pathological animals (special diet) vs. control animals (regular diet) (p value <0.05). 2D-DIGE analysis (n=5 animals per group).

Spot Num.	Special/Control		Protein Identification	Accession number (NCBInr or SwissProt) *Oryctolagus Cuniculus*	Unique peptides detected	Sequence Coverage (%)	Accesion number (NCBInr or SwissProt) *Homo Sapiens*
	t-test	Av. Ratio					
1	0,03	2,18	Catepsin D	gi|146386352	9	34	P07339
2	0,019	-2,12	Hemopexin precursor	gi|130500366	12	25	P02790
3	0,047	-5,01	Kallikrein 1	gi|145321068	5	31	P06870
4	0,0073	-4,19	ZG16b	gi|291415190	8	43	Q96DA0
5	0,0081	-2,92	ZG16b	gi|291415190	8	52	Q96DA0
6	0,0041	-12,22	ZG16b	gi|291390810	8	58	Q96DA0
7	0,0058	-5,55	ZG16b	gi|291415190	9	43	Q96DA0
8	0,0021	-9,07	ZG16b	gi|291415190	5	30	Q96DA0
9	0,003	-6,79	ZG16b	G1TYG4	6	-	Q96DA0
10	0,04	2,57	Superoxide dismutase [Cu-Zn]	G1TKH3	3	21	P00441
11	0,0021	-8,97	ZG16b	gi|291390810	7	40	Q96DA0
12	0,059	-2,51	Kallikrein 1	gi|153792063	29	75	P06870

Supplemental Table 4

METABOLITE	CHEMICAL SHIFTS (ppm) and mulyiplicity
1-Methylhydantoin	2.92 (s); 4.08(s)
2-Hydroxyphenylacetic acid	3.56 (S); 6.93 (m); 7.21(m)
3-Aminoisobutyric	1.19 (d); 2.60 (m); 3.02 (dd); 3.11(dd)
3-Hydroxybutyric acid	1.20 (d); 2.31 (m); 2.41 (m); 4.16 (m)
6-Phosphogluconic	3.84 (m); 3.96 (m); 4.09 (m); 4.19(d)
Acetylcholine	2.16 (s); 3.23 (s); 3.75 (t)
Allantoin	5.38 (s)
Betaine	3.25 (s); 3.89(s)
Citric Acid	2.56 (d); 2.65 (d)
Citrulline	1.56 (m); 1.87 (m); 3.14(q); 3.74 (dd)
Cyclohexanol	1.20 (m); 1.52 (dd); 1.69(dd); 1.85 (d); 3.60 (m)
Dimethylamine	2.50 (s)
Dimethylglycine	2.91 (s); 3.71(s)
Dimethylmalonic	1.43 (s)
Gamma-aminobutyric (GABA)	1.89 (m); 2.28 (t); 3.00 (t)
Gluconolactone	3.66 (dd); 3.76 (m); 3.82 (dd); 4.03 (t); 4.12 (t)
Glycine	3.54 (s)
Hypotaurine	2.66 (t); 3.34 (t)
Lactic acid	1.32 (d); 4.10 (q)
L-Alanine	1.46 (d); 3.76 (q)
L-Arabitol	3.57 (dd); 3.66 (m); 3.75(td); 3.83(dd); 3.93(m)
L-Arginine	1.68 (m); 1.90 (m); 3.23 (t); 3.73 (t)
L-Lysine	1.46 (m); 1.71 (m); 1.89 (m); 3.02 (t); 3.74 (t)
L-Serine	3.83 (dd); 3.96 (m)
Myoinositol	3.27 (t); 3.52(dd); 3.61 (t); 4.05 (t)
N-Acetylneuraminic	1.82 (t); 2.05 (s); 2.21 (dd); 3.52 (d); 3.61 (dd); 3.75 (m); 3.84 (dd); 3.90 (q); 3.96 (d); 4.03 (m)
p-Benzoquinone	6.79 (s)
Pipecolic acid	1.63 (m); 1.86 (m); 2.21 (m); 2.99 (td); 3.40 (d); 3.57 (dd)
Putrescine	1.75 (m); 3.04 (t)
Pyrocatechol	6.86 (m); 6.93 (m)
Sarcosine	2.73 (s); 3.60 (s)
Scyllo-inositol	3.33 (s)
Shikimic acid	2.21 (dd); 2.76 (dd); 3.74 (dd); 4.01 (m); 4.42 (t); 6.62 (m)
Spermidine	1.46 (m); 1.61 (m); 2.60 (m)
Taurine	3.25 (t); 3.42(t)
Trymethyamine-N-Oxide (TMANO)	3.25 (s)
Tyramine	2.92 (t); 3.23 (t); 6.90 (d); 7.21 (d)

Supplemental Figure 1. PCA of DIGE data. Five animals per group.

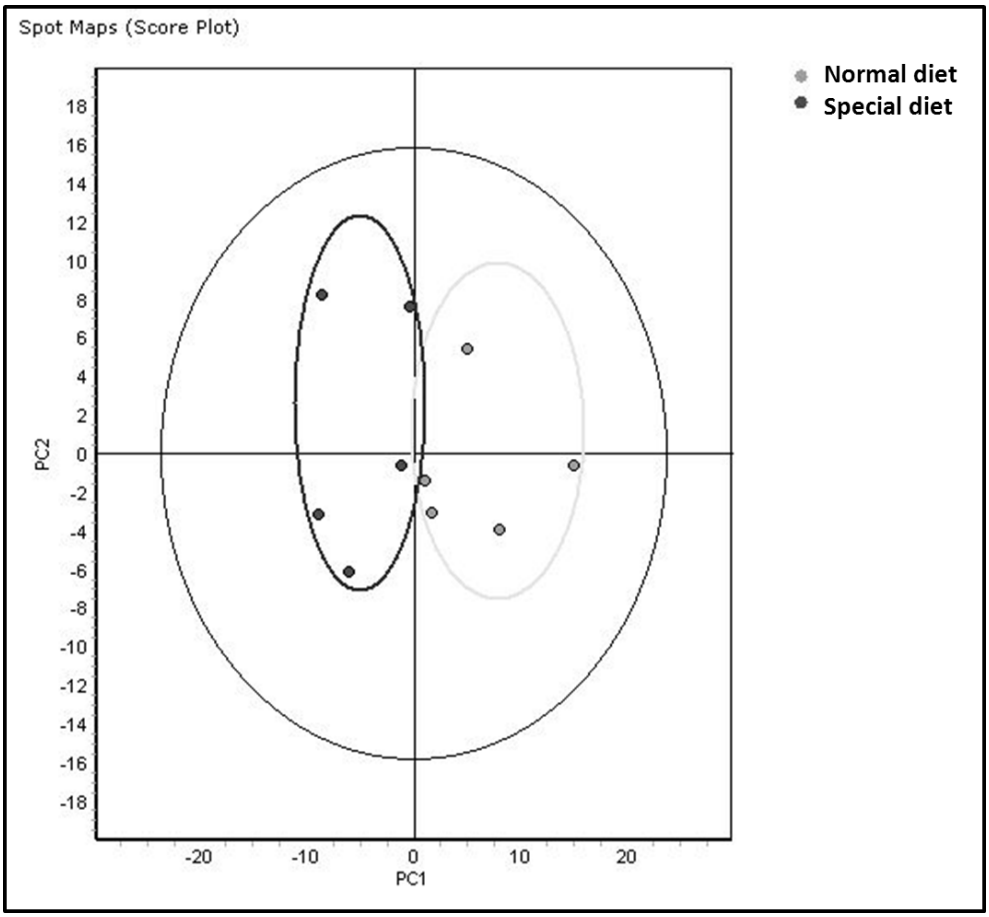

Supplemental Figure 2. PCA of 1H NMR data. Seven animals per group.

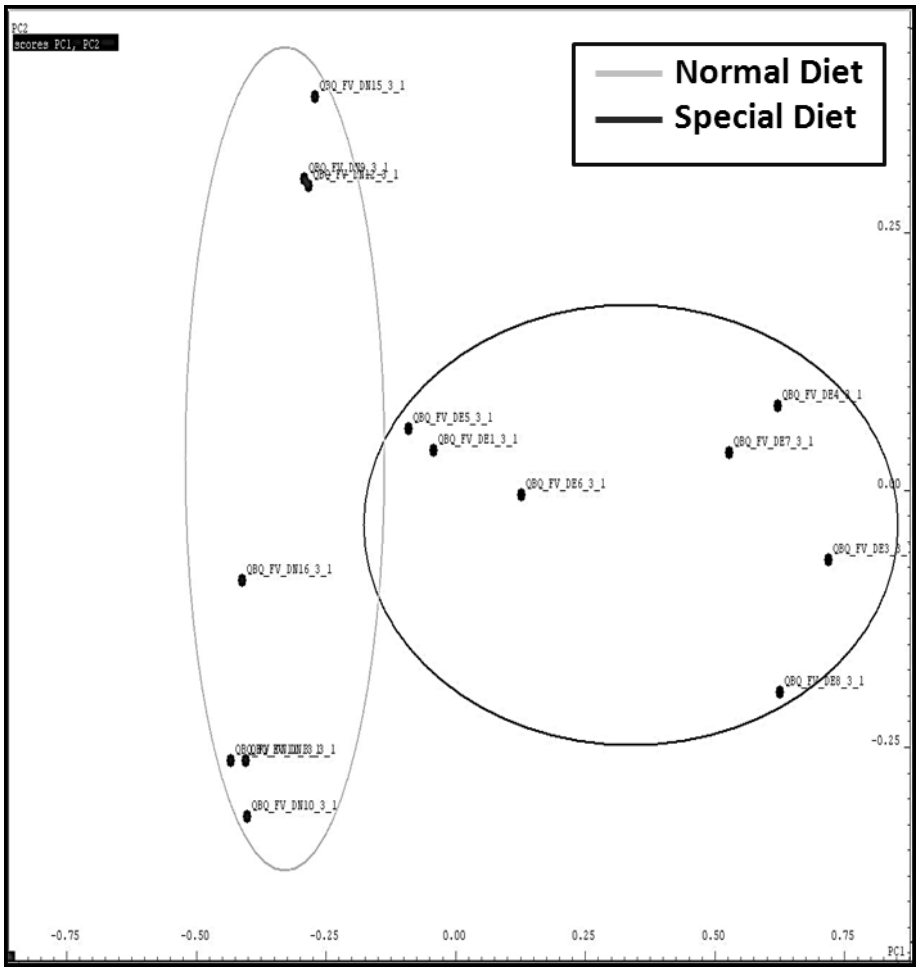

Supplemental Figure 3. Proteins pathway analysis by STRING. Known and predicted interactions between KLK1 and ZG16B, together with other proteins in the STRING database are shown. The interactions include direct (physical) and indirect (functional) associations. Action view is shown. Green arrows: activation. Blue line: binding evidence. Grey line: other evidence.

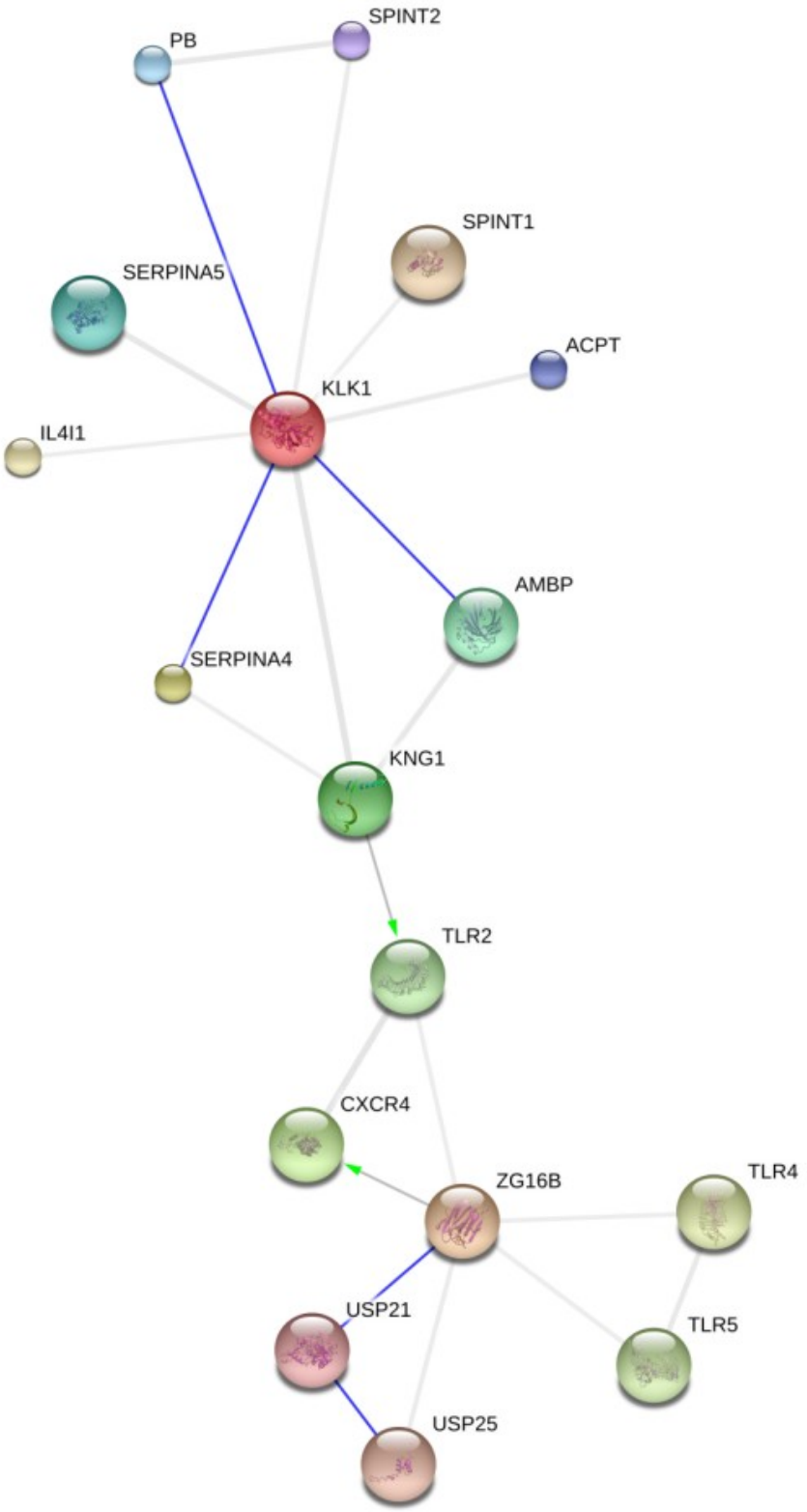

Chapter 3

Cytoskeleton deregulation and impairment in amino acids and energy metabolism in subjacent early atherosclerosis at aortic tissue with reflection in plasma

Marta Martin-Lorenzo, *Laura Gonzalez-Calero, Aroa S. Maroto, Irene Zubiri, Fernando de la Cuesta, Laura Mourino-Alvarez, Luis F. Lopez-Almodovar, Luis R. Padial, Maria G. Barderas, Fernando Vivanco, Gloria Alvarez-Llamas.*

Manuscript in Preparation.

En línea con el capítulo anterior que buscaba alteraciones en orina en los estadios iniciales de la aterosclerosis, se realizó un estudio con similar flujo de trabajo pero esta vez empleando aortas. El objetivo en este caso fue examinar los cambios latentes directamente en el tejido evitando así cualquier sesgo debido a procesos de naturaleza diferente que confluyen en los fluidos tales como el plasma o la orina. Esto nos permite evaluar los procesos dinámicos de moléculas interconectadas entre sí en aterosclerosis que están ocurriendo simultáneamente. En este caso estaremos en una situación inicial donde fundamentalmente se está dando un engrosamiento de la capa íntima y están comenzando a tener lugar algunos depósitos de calcio.

Para asegurar una amplia cobertura de estos cambios, nuevamente se ha utilizado una combinación de estrategias proteómicas y metabolómicas. Las alteraciones de las proteínas en los estados iniciales de la aterosclerosis se han estudiado de nuevo por electroforesis bidimensional diferencial (2D-DIGE) a través de lisados del tejido y extracción proteica y en el caso de los metabolitos, por similitud, se ha empleado resonancia magnética nuclear (NMR). Sin embargo, se ha utilizado una variante de la técnica clásica de resonancia más adecuada para la investigación en tejido que se conoce como resonancia de ángulo mágico (HR-MAS: high resolution magic angle spinning). Está técnica permite el análisis por resonancia directamente en tejido, sin ningún pre-tratamiento y permitiendo la recuperación del tejido tal cual, si fuese necesario. Ha demostrado ser muy útil en la investigación clínica en estudios de oncología, renales, relacionados con el cerebro y también en enfermedades cardiovasculares por análisis directo del tejido cardiaco. Sin embargo, y en nuestro conocimiento, esta es la primera vez que se aplica directamente a arterias. Como cualquier técnica de resonancia es prácticamente un detector universal y aunque otras técnicas presenten una mayor sensibilidad, ésta es muy reproducible, rápida y robusta.

Las alteraciones del conjunto de moléculas estudiadas señalan a cambios en el citoesqueleto, variaciones en el metabolismo de la energía, de diferentes aminoácidos interconectados entre sí y al metabolismo de los glicerofosfolípidos en su rama de la colina y compuestos relacionados. Proteínas y metabolitos parecen cooperar en todos estos cambios como mecanismo de defensa ante los cambios de remodelado que está sufriendo la aorta. En un intento de ver si alguna de estas moléculas alteradas pudiera ser también un buen marcador de progresión para una detección precoz, se hizo un estudio traslacional dirigido de evaluación de dichas variaciones en el plasma, como reflejo directo de los cambios encontrados en el tejido arterial. En el trabajo se propone un panel compuesto por 6 moléculas que pueden servir para monitorizar los inicios de la aterosclerosis.

El estudio presentado a continuación junto con el presentado en el capítulo anterior constituyen un estudio exhaustivo de los mecanismos subyacentes al inicio de la enfermedad aterosclerótica. Empleando un modelo animal se han estudiado con un abordaje sin sesgo todas las moléculas potencialmente implicadas a nivel de tejido (aorta) y de orina. Además, estudios dirigidos en plasma completan esta visión y

permiten la identificación de moléculas específicas monitorizables y por tanto con un gran potencial de aplicabilidad clínica, particularmente considerando que la principal limitación actual es la incapacidad de prevenir y evitar un evento agudo fatal. Cabe destacar que la alteración del metabolismo de los aminoácidos arginina-prolina es común a todos los enfoques y que por ello, desde nuestro punto de vista, es un nuevo campo sobre el que más estudios de enfermedad cardiovascular deberían dirigirse.

ABSTRACT

INTRODUCTION

Cardiovascular disease (CVD) remains the leading cause of premature death worldwide being atherosclerosis the main subjacent cause. Of all deaths occurring before the age of 75 in Europe around 40% are due to CVD, both in women and men. Main risk factors are age, male sex, smoking, high blood pressure, diabetes mellitus, and high cholesterol. Despite that over 50% of the observed decrease in mortality caused by coronary heart disease can be attributed to changes in those risk factors, further knowledge is needed to better stratify individual risk and improve prevention . Unfortunately, the symptoms only become evident when the disease is in an advanced and irreversible state and underlying mechanisms involve a complex network of acting molecules, not fully understood and no early diagnosis markers are available to date that may undoubtedly predict future events on healthy subjects. In this clinical scenario, there is urgent need to find out novel molecular indicators, alone or combined with existing ones. It is essential, too, a better knowledge of operating mechanisms causing disease progression.

Different strategies have been applied by our group and others (1, 2) searching for alterations in biological fluids (urine (3), plasma (4)), arterial tissular layers (5-7) and arterial tissue secretomes (8). Here we investigate molecular changes taking place, directly, in aortic tissue when atherosclerosis starts developing, i.e. at early and asymptomatic stages, to identify main alterations occurring both at protein and metabolite level which may ultimately have reflection in plasma. A novel *ex-vivo* approach which is a variation of magnetic nuclear resonance (HRMAS: high resolution magic angle spinning) is applied here for the first time in atherosclerosis research with the unique advantage of allowing direct metabolites analysis in-tissue (9).

METHODS

Animal model of early atherosclerosis.

A rabbit model of atherosclerosis was developed as previously published (3) Briefly, twelve male New Zealand White rabbits were divided in two study groups fed with standard (control group) or 1% cholesterol-enriched chow plus 50,000 IU/Kg vitamin D2 (Harlan, Indianapolis, Indiana) diet (atherosclerosis group). Principles of laboratory animal care were followed and all experimental procedures were approved by the Animal Care and Use Committee of the IIS-Fundación Jiménez Díaz, according to the guidelines for ethical care of the European Community. Animals were sacrificed after 13 weeks.

Identification of aortic tissue differential proteins in early atherosclerosis

Differential analysis was performed as previously published with minor modifications. Briefly, tissue proteins were extracted in lysis buffer (7M urea, 2M thiourea, 4% CHAPS, 30mM Tris and 1% DTT) and cleaned by 2D clean-up kit (GE Healthcare). Total protein was quantified by Bradford method. Differential Gel Electrophoresis (DIGE) was carried out following manufacturer's protocol. Labeled samples were loaded onto IPG strips (24 cm, pH 3-11), isoelectric focusing (IEF) was carried out in a

PROTEAN IEF CELL (BioRad) with a final accumulation step of 56000V and second dimension was performed on 12% running gels using EttanDaltSix System (GE Healthcare). Gels were scanned using a Typhoon 9400 Variable Mode Imager (GE Healthcare) and spot maps were digitalized and compared using DeCyder Differential Analysis Software version 6.5 (GE Healthcare). Spots satisfying cut-off criteria (p-value <0.05 and minimum fold change of 2.0 or p-value <0.05 when data was corrected for multiple comparisons and FDR applied) were considered significant and selected for identification. Differential protein spots were excised, reduced, alkylated and digested with trypsin (10) and protein identification was performed in a 4800 Proteomics Analyzer MALDITOF/TOF mass spectrometer (Applied Biosystems, Framingham, MA, USA) as previously described (3). The UniProtKB/Swiss-Prot Data Base was searched in batch mode using GPS Explorer v3.6 software (Applied Biosystems) with a licensed version 2.1 of MASCOT.

Identification of aortic tissue differential metabolites in early atherosclerosis

Intact arterial tissue was analysed by high resolution magic angle spinning (HR-MAS) nuclear magnetic resonance (NMR) at 4ºC. ^{1}H-NMR spectroscopy was performed at 500.13 MHz in a Bruker AMX500 spectrometer 11.7 T. Samples were placed within a 50µl zirconium oxide rotor with cylindrical insert and spun at 4000 Hz spinning rate.

Spectra were processed using TOPSPIN software, version 1.3 (Bruker Rheinstetten, Germany). Standard solvent signal was suppressed and spectra were phased, baseline-corrected and referenced to the sodium (3-trimethylsilyl)-2,2,3,3-tetradeuteriopropionate singlet at δ 0ppm. Second dimension homonuclear correlation spectroscopy ^{1}H-^{1}H (COSY and TOCSY) and gradient-selected HSQC spectra were also acquired. ^{1}H NMR spectra were data reduced using the software program AMIX (Analysis of MIXtures version 3.6.8, Bruker Rheinstetten, Germany) by subdivision into integral regions of 0.04ppm between δ 0.4 and 9ppm (excluding the water region). Individual integral regions were normalized to the total sum of integral region by combination of one- and two-dimensional-HRMAS experiments using ACD/NMR Processor Academic Edition (Version 12.01, Advance Chemistry Development Inc) and Metabohunter tool (11).

Confirmation of protein and metabolite tissue variations by Selected Reaction Monitoring (SRM)-LC-MS/MS

Selected reaction monitoring (SRM)-LC-MS/MS technique has been previously applied by our group and others for data confirmation (3, 12, 13). Protein extracts were cleaned in Protein Desalting Spin Columns (Thermo Scientific) following manufacturer's instructions. Total protein content was quantified by Bradford assay and samples containing 30µg were reduced, alkylated and digested with sequencing grade modified bovine trypsin (Roche) . Tryptic peptides solutions were cleaned with C18 spin columns (Protea Biosciences) according to manufacturer's instructions and mixed 1:1 with mobile phase A (0.1% formic acid in MilliQ water). 2µL of sample was injected in a HPLC system (1200Series) and protein digests were analysed using a 6460 Triple

Quadrupole LC-MS/MS on-line connected to nano-chromatography in a Chip-format configuration (ChipCube interface, ProtID Zorbax 300B-C18-5µm chip, Agilent Technologies) constituted by 43x0.075-mm analytical column and 40nL enrichment column controled by Mass Hunter software (B.0.4.0.1) (Agilent Technologies). Separation took place at 0.4 µL/min in a continuous acetonitrile gradient as follows: 1) At 0 min 5% B (0.1% formic acid in acetonitrile), 2) At 1min 5% B, 3) At 5 min 40% B, 4) At 12 min 95% B, 5) At 14min 95% B, 6) At 14.2 min 5% B and 7) At 15min 5% B. Fragmentor was set to 130V, dwell time to 20ms, delta EMV to 600 V and collision energy was optimized for each SRM transition. Theoretical SRM transitions were designed using Skyline (v.1.1.0.2905) (14) and manually inspected according to Lange *et al*. recomendations (15). Protein specificity was confirmed by protein blast and only proteotypic peptides were selected (see Suppl. Table1). Individual signals were normalized based on TIC (total ion current) and normalized peak areas were used for comparison.

Tissue metabolites were extracted as described (16) with minor modifications. Briefly, ten milligrams of aortic tissue were treated with 1mL of pre-chilled MeOH:H_2O (1:1) supernatant taken and evaporated up to dryness. Pellets were solved in 100µl MeOH:H_2O (1:1) for analysis. Samples were analyzed in a reversed-phase column (Atlantis T3, 3µm, 2.1x100mm, Waters) thermostated at 40ºC. A sample volume of 10µL was injected and separation took place at 0.4mL/min in an acetonitrile gradient: 1) At 0min 0% B (0.1% formic acid in acetonitrile), 2) At 0.5min 0% B, 3) At 2.5 min 95% B 4) At 2.51 min 0% B 5) At 5min 0% B. Dwell time was fixed to 50 ms for positive analysis and 100 ms for negative ones and so delta EMV to 400 V in positive mode and 600 V in negative one. Collision energy and fragmentor in the range range 60-175 V were optimized for each metabolite by means of Optimizer Software (Agilent Technologies). Optimal SRM transitions were selected in direct infusion mode by previous analysis of commercial metabolite standards (see Suppl. Table 1). Individual signals were normalized based on TIC (total ion current) and normalized peak areas were used for comparison.

Analysis of protein and metabolite signatures in plasma

For protein analysis, 25µL of plasma was depleted using ProteoPrep Immunoaffinity Albumin and IgG Depletion Kit (Sigma-Aldrich) according to manufacturer's protocol and as previously published (17). Depleted plasma samples were reduced, alkylated and tryptic digested. For metabolite analysis protein removal was performed by precipitation in pre-chilled 50% MeOH, and supernatant was diluted (1:3) with mobile phase A (0.1% formic acid in Milli-Q water) and filtered through 0.20µm. Samples were analyzed by (SRM)-LC-MS/MS as described.

Statistical analysis and pathway analysis

Non-parametric Mann-Whitney test was applied using GraphPad Prism 6 software. Comparisons resulting in p-values lower than 0.05 were considered significant. Marker

candidates were further analyzed with Metaboanalyst 3.0 (18) in biomarker analysis module using normalized peak intensity to calculate clasical univariate ROC curves.

Protein pathway analysis was carried out by STRING 9.0 software (19) consisting of a database of known and predicted protein interactions, including direct (physical) and indirect (functional) associations derived from genomics, high-throughput experiments, coexpression, and previous knowledge. High confidence filter (0.700) was applied and 20 interactions were shown. Enrichment analysis was performed under these conditions. Pathways including more altered molecules and FDR<0.05 were considered of special interest. Metabolites pathway analysis was done using MetaboAnalyst 3.0 by compound matching using Homo Sapiens library, and performing Fishers' exact test. Only pathways with $p < 0.05$ and four or more metabolites involved are consider for in-depth revision.

RESULTS

A combined proteomic and metabolomic double-approach was used to investigate main molecular alterations in response to early atherosclerosis at aortic tissue and with furher reflection in plasma. (Figure 1)

In-tissue protein alterations in response to atherosclerosis development

Comparative tissue proteome analysis of control and pathological aortas was performed. From 21 protein spots found significantly altered, a total of fifteen proteins and one conserved region of a not characterized protein were identified (See Suppl. Table 2 and Suppl. Figure 1). The alteration of 12 proteins were confirmed using SRM, 10 proteins being upregulated in tissue in response to early atherosclerosis condition and 2 proteins being downregulated. (Table 1).

Involved in cytoskeleton organization vinculin isoform 2 (VCL), capping protein gelsolin-like (CAPG) and tropomyosin (isoform 2 (TM2) were identified and confirmed. VCL is downregulated in atherosclerotic tissue meanwhile CAPG and TM2 are upregulated. Integrin linked kinase (ILK) was found increased in tissue. Two heat shock proteins involved in protein folding and showing chaperone or chaperone-like properties were identified significantly altered: HSP70 (increased) and HSPB6-alpha-crystallin like (decreased). Other protein alterations directly point to amino acids and energy metabolism. In particular, pyruvate kinase isozymes M1/M2 (PKM) and phosphoglycerate kinase (PGK) are involved in the glucose metabolism and were found increased at tissue level. PKM catalyzes the last step of glycolysis to generate pyruvate as last product, while PGK participates in the first step of ATP generation. CNDP dipeptidase 2 isoform 1, also increased, is a metallopeptidase M20 family involved in the metabolism of different amino acids. An accumulation of serum proteins in tissue was also observed, particularly for serotransferrin (TF), serine proteinase ATS-22 and fibrinogen beta chain (FGB).

Pathway enrichment analysis showed different KEEG altered pathways, among which three stand: focal adhesion (p=2.250E-6), coagulation (p=5.21E-6) and glycolisis/gluconeogénesis (p=4.000E-3) (Suppl. Figure 2).

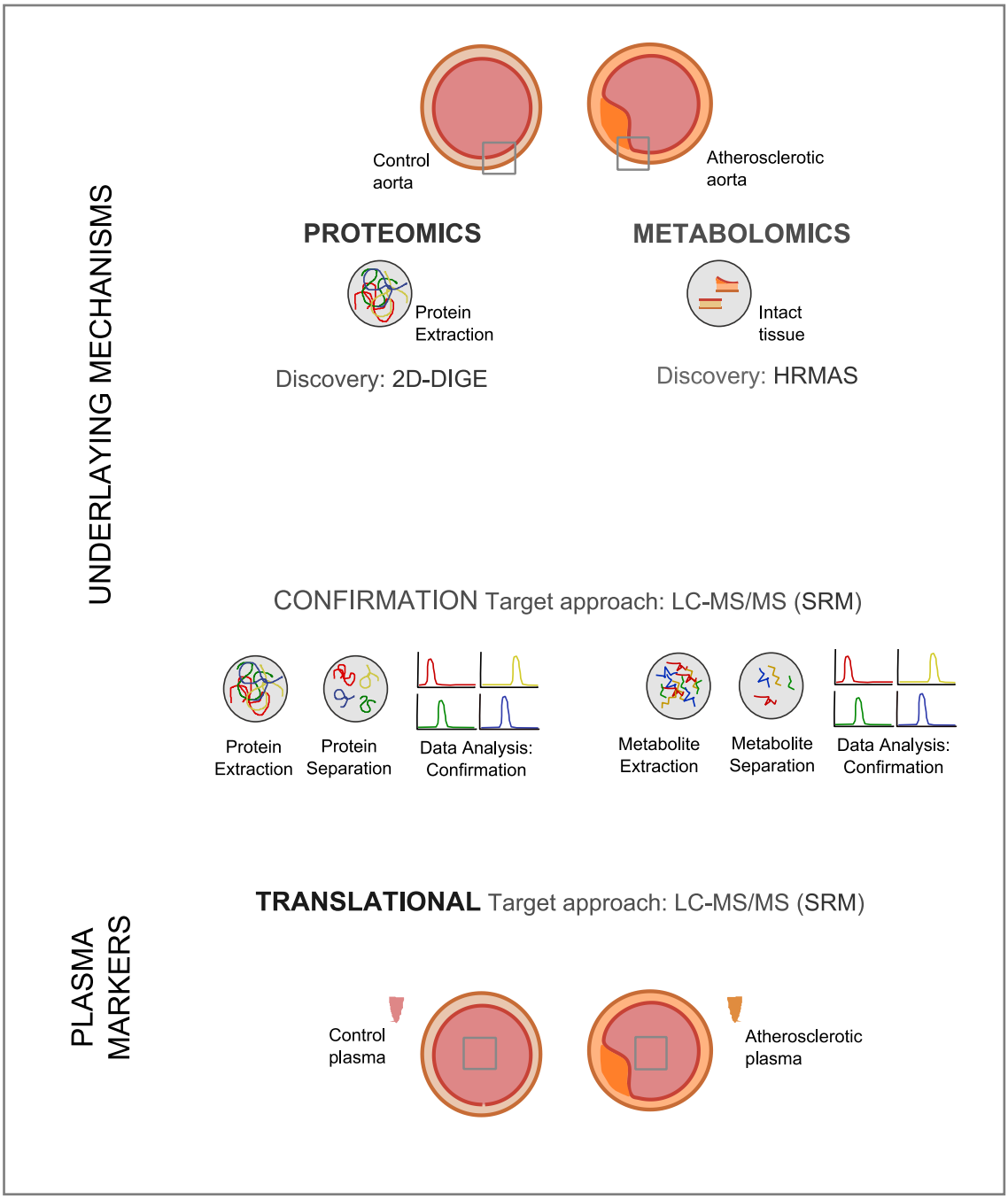

Figure 1. Workflow of combined omic approach applied here using aortic tissue and plasma.

	Aorta		Plasma	
	Pathological/Control	p-Value	Pathological/Control	p-Value
PROTEINS				
Myofilaments and associated proteins				
Vinculin (VCL)	↓	0.014		
Capping protein gelsolin-like	↑	0.022		
Tropomyosin 2, beta-like isoform 2	↑	0.0058		
Plasma Proteins				
Serotransferrin	↑	0.017		
ATS-22 (A1AT)	↑	0.018	↓	0.023
Fibrinogen β-chain	↑	0.019		
Glucose metabolism				
Phosphoglycerate kinase (PK)	↑	0.00017	↑	0.00025
Pyruvate kinase (PKM)	↑	0.0029	↓	0.011
Protein folding				
HSP70	↑	0.0098		
α-Crystallin	↓	0.00065		
Other enzymes				
CNDP (dipeptidase 2 isoform 1)	↑	0.018		
Integrin linked kinase (ILK)	↑	<0.0001	↓	0.0038
METABOLITES				
Choline and related metabolites				
Acetylcholine	↓	0.0007	↓	0.0009
Choline	↓	0.040	↓	0.016
Glycerophosphocholine	↑	<0.0001		
Phosphocholine	↓	0.043		
TMAO	↓	0.0014		
Amino acids and derivatives				
Guanidoacetic acid	↑	<0.0001		
L-Aspartic acid	↑	0.00060		
L-Glutamic acid	↓	<0.0001	↓	0.0012
L-Glutamine	↓	<0.0001		
L-Threonine	↑	0.00030		
L-Valine	↓	0.00050	↓	0.0328
N-acetyl-L-alanine	↓	<0.0001	↓	0.0018
Tyramine	↓	0.017		
Other metabolites				
Glucuronic acid	↑	0.00040	↑	<0.0001
Glutathione	↓	0.0051	↓	0.022
Pyruvic acid	↑	0.0005	↑	<0.0001
Threitol	↓	0.0086		

Table 1. Confirmed protein and metabolite alterations in aortic tissue and plasma in response to early atherosclerosis.(*p-value<0.05,**p-value<0.01,***p-value<0.001,****p-value<0.0001.)

In-tissue metabolic alterations in response to atherosclerosis development

To investigate the metabolic changes taking place in the aorta in response to early atherosclerosis, intact tissue (control and pathological) was investigated by HR-MAS. Statistical analysis of main components reveals a good clustering for cases and controls and a region of special interest in the range to 3-4ppm, where highest contributions take place (Figure 2). NMR spectral analysis revealed that region between 1-4.5ppm codifies a total of 24 metabolites (Suppl. Table 3), among which a total of 17 metabolites are significantly varied ($p<0.05$) as confirmed by target analysis (See Table 1).

Pathological aorta shows lower levels of: choline, acetylcholine, phosphocholine and TMAO. In contrast, an accumulation of glycerophosphocholine has been detected in pathological condition. All these molecules are important players in the glycerophospholipids metabolism pathway except TMAO which is a direct metabolite of choline. Additionally, guanidoacetate, L-aspartate and L-threonine were found accumulated and lower levels of L-glutamate, L-glutamine, L-valine, N-acetyl-L-alanine and tyramine were found in pathological conditions. Glutathione and threithol were found downregulated in pathological samples and with the opposite trend glucuronic acid and pyruvic acic were detected.

A total of eight amino acid and amino acid derivatives were found altered. Metabolic pathway analysis revealed "glycine, serine and threonine metabolism" (p= 9.4557E-6, FDR= 5.1176E-4)*;* "alanine, aspartate and glutamate metabolism" (p= 1.2794E-4 ; FDR= 5.1176E-4)*;* "aminoacyl-tRNA biosynthesis" (p= 8.5839E-5 ; FDR= 0.001560)*;* "glycerophospholip metabolism" (p= 9.3233E-5; FDR= 0.0015601)*;* and "arginine and proline metabolism" (p= 9.7503 E-5; FDR= 0.0015601*)* , as main pathways involved in response to early atherosclerosis (Suppl. Figure 3).

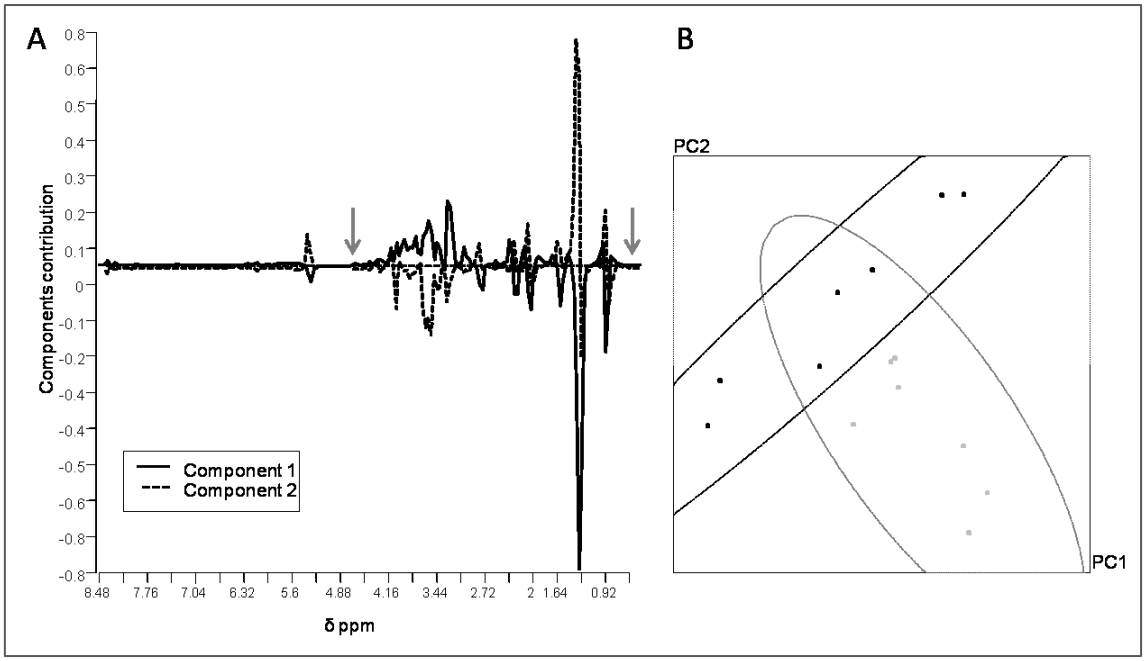

Figure 2. HRMAS data analysis for identification of main altered features at tissue metabolome. The component contribution chart (A) shows that the main changes between atherosclerotic and control groups are taking place in the region of 0-4.5 ppm chemical shift (δ) (marked with grey arrows) corresponding to the metabolites of interest (Suppl Table 3). Of special interest is the region btween 3-4ppm where more changes are obseved. The PCA for this regions (3-4ppm) (B) confirms the good clasiffication between groups (black: control, grey: atherosclerosis).

Molecular alterations in tissue with reflection in plasma compose a panel of measurable indicators of atherosclerosis development

A direct reflection of tissue molecular alterations identified here was pursued in plasma. A total of four proteins (enzymes) were found altered in plasma: integrin linked kinase (ILK), phosphoglycerate kinase (PGK), pyruvate kinase (PKM) and ATS22 (similar to A1AT in humans). Plasma PGK is upregulated in pathological animals presenting the same trend observed in tissue. ILK, PKM and ATS22 were found downregulated with an opposite trend, to that observed in aorta. A total of eight metabolites were found altered in plasma, with the same trend in tissue: acetylcholine, choline, L-glutamate, L-valine, N-acetyl-L-alanine, glucuronic acid, glutathione and piruvate. ROC curves are shown in figure 3 for the most featured marker candidates (AUC>0.8): PGK, PKM, ILK, glutamate, N-acetyl-L-alanine and valine.

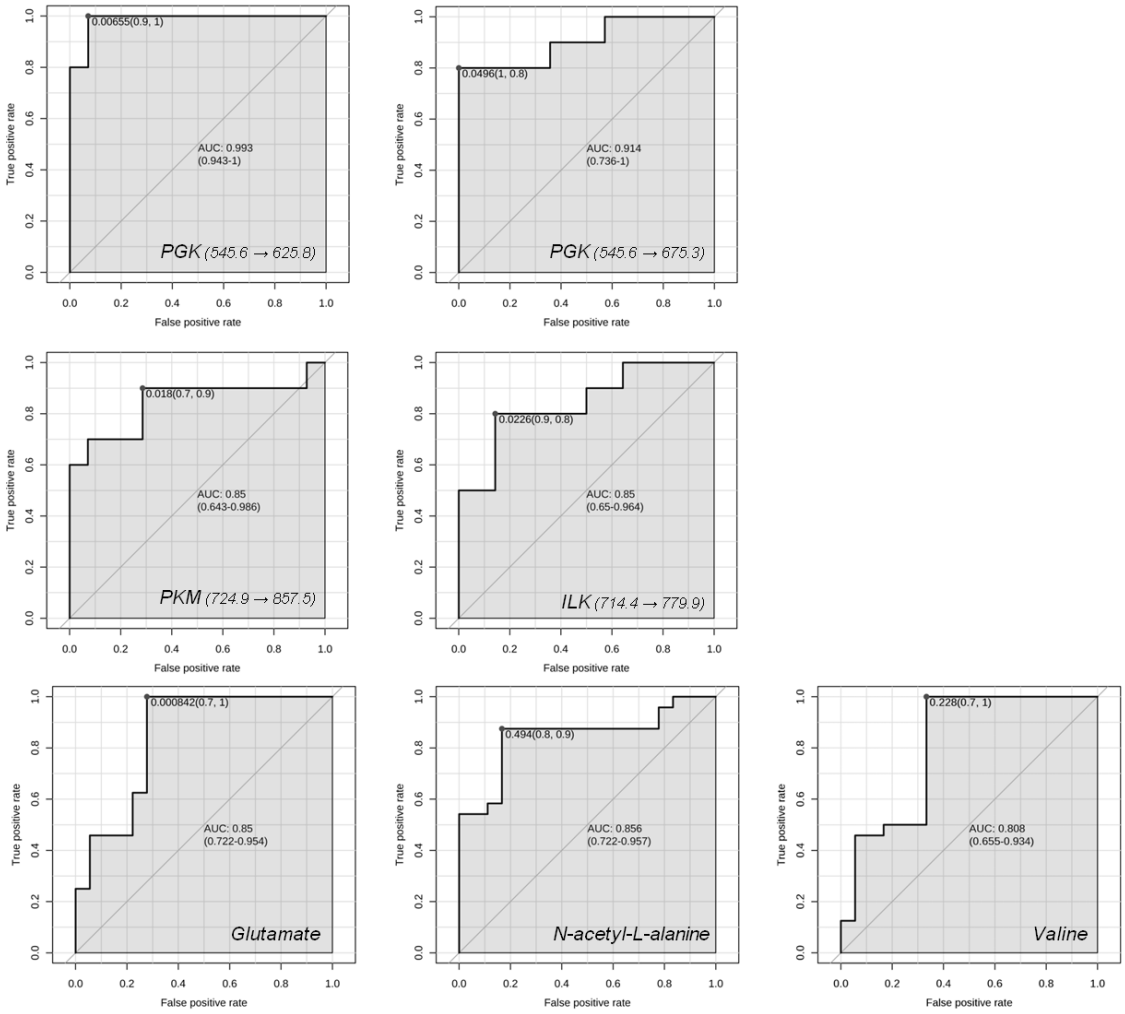

Figure 3. ROC curves for molecules proposed as early diagnosis markers of atherosclerosis. The panel is composed by three enzymes, PGK, PKM and ILK and three metabolites, glutamate, N-acetyl-l-alanine, valine. (Numbers in brackets show SRM transition measured)

DISCUSSION

Our study in early atherosclerosis scenario investigates main alterations both at protein and metabolite levels. This double approach pursues looking in depth into interconnected dynamic processes taking place in atherosclerosis at early development where thousands of molecules operate simultaneously. We intended to find out the strongest variations at tissue level which can be ultimately measured in plasma so that they can serve as potential markers of subjacent atherosclerosis to be further confirmed in wider studies.

Molecular response to oxidative stress

Miss-balance in energy metabolism is known to have an important role in atherosclerosis development (20, 21). Here, we identified up-regulation of two of the

main enzymes of glycolysis, PKM and PGK (also observed in Atrial Fibrillation (22)), increased of pyruvate, and down- regulation of glutathione. The formation of reactive oxygen species (ROS) is widely described to be an important factor in atherogenesis (23, 24) and one of the first cellular defense mechanism is played by glutathione (25). Glutathione is the major antioxidant produced by cells, neutralizes free radicals and ROS, and regulates the NO cycle. Oxidized LDL taking place in atherosclerosis initial stages, implies rapid depletion of intracellular glutathione (26) and we found both glutathione and its precursor glutamate decreased in pathological conditions, in tissue and plasma. Pyruvate, is also antioxidant, a fuel for cardiac function (27) which promotes contractile recovery of injured myocardium (28) and it was found here to be increased both in tissue and plasma in atherosclerotic condition, which may point to a compensatory mechanism to counteract glutathione diminished levels.

Structural changes and arterial remodeling

Deregulation of cytoskeleton in atherosclerosis has been described as a mixture of different changes happening in the media layer (7). Actin cytoskeleton disorganization, modifications in cell-matrix adhesions and cell-cell junctions, deconstruction of filaments and microtubules, and vascular smooth muscle cells (VSMC) migration and phenotype switch from contractile to synthetic, are known alterations taking place. Our study shows a number of molecules taking part in this deregulation. Vinculin (VCL) downregulation was observed in aortic atherosclerotic tissue. Decreased levels of VCL at cell-cell junctions leading in not fully functional junctions (29). Dismissed expression of Integrin linked kinase (ILK) results in the inhibiton of cell attachment and inhibiton of cell migration (30). Here we found and up-regualtion that combinated VCL downregualtion point to poor focal adhesions and a favored cell migration situation. Additionally, higher levels of TPM2 and CAPG were found in atherosclerotic tissue. α-Tropomyosin is overexpressed in plaque VSMCs (31) and CAPG has been found augmented in conditions of increased motility of stimulated SMC by hypoxia (32).

On the other hand, the observed reduction of glutathione levels and the increase of glycolytic enzymes has important contribution in macrophage polarization and its functions. In particular, PKM2 is directly involved in the preferential M2-polarized macrophages (33) which is the polarized form involved in tissue repair. Observed changes in valine levels also reflect alterations taking place in response to arterial injury. This amino acid was shown to improve endothelial dysfunction related to atherosclerosis when dietary supplemented (34) and here was found dismished. In arterial remodeling, VSMC proliferation and migration occurs and one of these mechanisms promoters is hyaluronan acid (HA), which accumulates during neointimal hyperplasia (35). A component of HA is glucuronic acid which was found increased in this study, both in tissue and plasma.

All these measurable observations are a reflection of structural remodeling taking place in atherosclerotic arteries, pointing to a loss of contractile properties and favored migration of VSMC.

Amino acids metabolism

Aspartate resulted to be a common metabolite in main pathways revealed to be altered in response to atherosclerosis development (Figure 4). Aspartate is a dicarboxylic amino acid related with inhibition of fatty streak formation and atherogenesis progression (36), thus it has been attributed a protective role. In this study, higher levels of aspartate were found in tissue. Furthermore, asparte is one of the intermediates in the urea cycle of arginine and proline metabolism and previous studies in our laboratory pointed to a preferential synthesis of polyamines in that cycle (3). Here, valine levels were found lower in atherosclerosis. Since valine inhibits arginase activity (37), polyamine synthesis is expected to be favored too in this study. As consequence of this preferred synthesis, due to the competition of arginase and NOS (nitric oxide synthase), less NO is being produced. This is in aliment with the observed inhibition of NO release by glutamine in the presence of acetylcholine from aortic rings, without affecting beneficial endothelial NO (eNOS) (38).

Another identified molecular fingerprint reflecting amino acids metabolism shows increased threonine levels and decreased glutamine in response to pathological conditions, in consonance with improved glucose tolerance and lowered blood pressure observed when glutamine is supplemented (39).

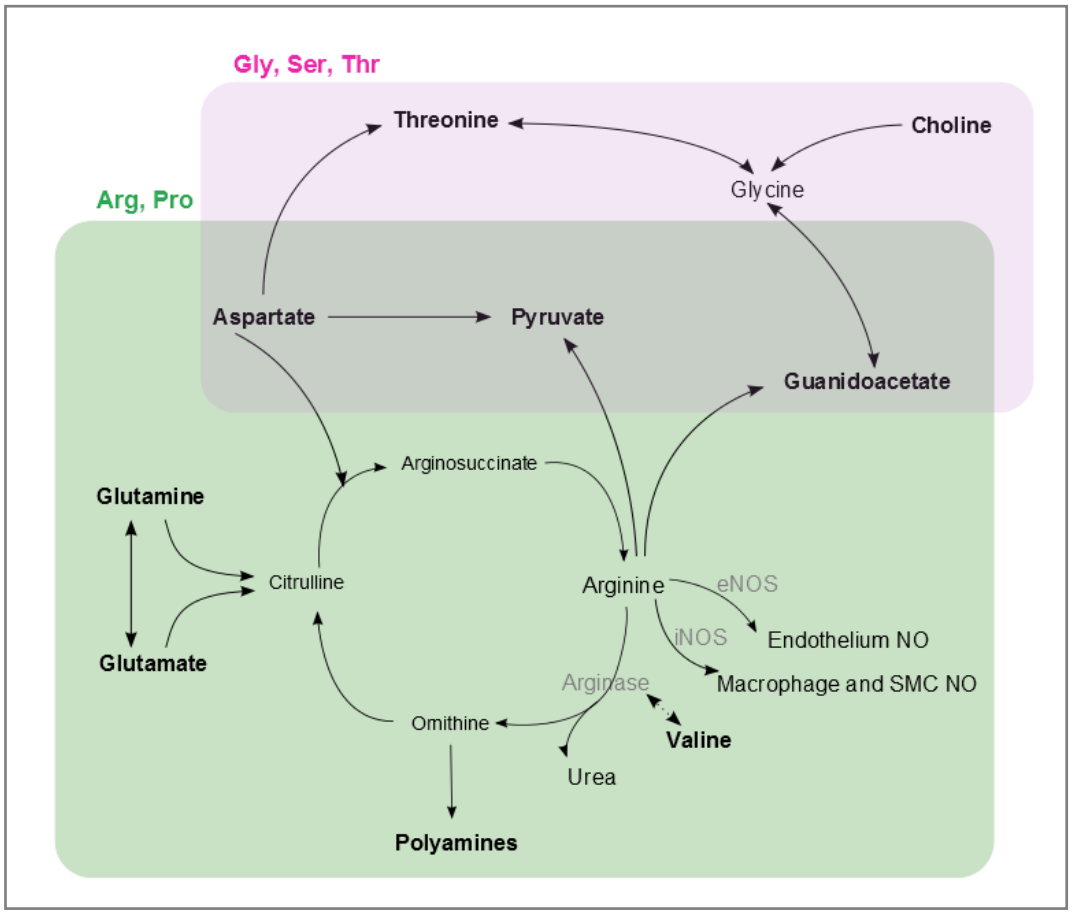

Figure 4. Overview of the main amino acid metabolisms atered based in KEGG pathways.

Glycerophospholipid metabolism

In the glycerophospholipid metabolism there are two different routes. One toward phosphatydilethanolamine and the other toward phosphatydilcholine (KEGG map00564). Our research found changes in the phosphatydilcholine part. Choline, phosphocholine, acetylcholine and glycerophosphocholine were found here altered in early atherosclerosis condition. The first three, choline, phosphocholine and acetylcholine, are down regulated while glycerophosphocholine is upregulated. Furthermore TMAO, a common metabolite of choline (40), was found decreased in atherosclerotic tissue. Choline low levels are associated to lipid accumulation in arterial tissue (41). It is a precursor of acetylcholine which induces vasoconstriction in situations of endothelial dysfunction (42) and is known to cause endothelium-dependent contraction of mouse arteries (43). Choline and acetylcholine participate in the biosynthesis of phosphatidylcholine, which is a precursor of platelet-activation factor (PAF). PAF is synthesized mainly in the remodeling pathway under inflammation environment. In fact, PAF is produced during LDL oxidation, leading to endothelial dysfunction. It activates the formation of active oxygen species, VSMC proliferation and migration, and it has been proposed as initiator of atherosclerosis at early stages (44). These processes are taking place during atherosclerosis development in agreement with the reducted levels observed here for choline and phosphocholine. Glycerophosphocholine, the only one found increased, is a natural choline compound with associated beneficial effects in stroke conditions (45) which can reflect here a defense compensatory mechanism.

Conclusions

We found here 12 proteins and 17 metabolites to be involved in underlying mechanisms of atherosclerosis development. Oxidative stress, arterial remodeling, amino acid alterations and glycerophospholipids metabolism have been identified to be important changes happening at the early stage of atherosclerosis. Additionally, a molecular panel in plasma constituted by ILK, PGK, PKM, glutamate, N-acetyl-L-alanine and valine is proposed here in response to early development of atherosclerosis.

REFERENCES

1. Barderas MG, Vivanco F, Alvarez-Llamas G. Vascular proteomics. Methods Mol Biol 2013; 1000:1-20.

2. Alvarez-Llamas G, Barderas MG, Posada-Ayala M, Martin-Lorenzo M, Vivanco F. Chapter 11 - Application of Metabolomics to Cardiovascular and Renal Disease Biomarker Discovery. In: Virginia GarcÃ-a-CaÃ±as ACaCS, editor. Comprehensive Analytical Chemistry. Applications of Advanced Omics Technologies: From Genes to Metabolites. Elsevier, 2014:279-308.

3. Martin-Lorenzo M, Zubiri I, Maroto A, et al. KLK1 and ZG16B proteins and arginine-proline metabolism identified as novel targets to monitor atherosclerosis, acute coronary syndrome and recovery. Metabolomics 2014.

4. Laborde CM, Mourino-Alvarez L, Posada-Ayala M, et al. Plasma metabolomics reveals a potential panel of biomarkers for early diagnosis in acute coronary syndrome. Metabolomics 2014; 10:414-24.

5. Bagnato C, Thumar J, Mayya V, et al. Proteomics analysis of human coronary atherosclerotic plaque: a feasibility study of direct tissue proteomics by liquid chromatography and tandem mass spectrometry. Mol Cell Proteomics 2007; 6:1088-102.

6. de la Cuesta F, Alvarez-Llamas G, Maroto AS, et al. A proteomic focus on the alterations occurring at the human atherosclerotic coronary intima. Mol Cell Proteomics 2011; 10:M110.

7. de la Cuesta F, Zubiri I, Maroto AS, et al. Deregulation of smooth muscle cell cytoskeleton within the human atherosclerotic coronary media layer. J Proteomics 2013; 82:155-65.

8. de la Cuesta F, Barderas MG, Calvo E, et al. Secretome analysis of atherosclerotic and non-atherosclerotic arteries reveals dynamic extracellular remodeling during pathogenesis. J Proteomics 2012; 75:2960-71.

9. Hennel J, Klinowski J. Magic-Angle Spinning: a Historical Perspective.

10. Sechi S, Chait BT. Modification of cysteine residues by alkylation. A tool in peptide mapping and protein identification. Anal Chem 1998; 70:5150-8.

11. Tulpan D, Leger S, Belliveau L, Culf A, Cuperlovic-Culf M. MetaboHunter: an automatic approach for identification of metabolites from 1H-NMR spectra of complex mixtures. BMC Bioinformatics 2011; 12:400.

12. Picotti P, Aebersold R. Selected reaction monitoring-based proteomics: workflows, potential, pitfalls and future directions. Nat Methods 2012; 9:555-66.

13. Posada-Ayala M, Zubiri I, Martin-Lorenzo M, et al. Identification of a urine metabolomic signature in patients with advanced-stage chronic kidney disease. Kidney Int 2014; 85:103-11.

14. MacLean B, Tomazela DM, Shulman N, et al. Skyline: an open source document editor for creating and analyzing targeted proteomics experiments. Bioinformatics 2010; 26:966-8.

15. Lange V, Picotti P, Domon B, Aebersold R. Selected reaction monitoring for quantitative proteomics: a tutorial. Mol Syst Biol 2008; 4:222.

16. Want EJ, Masson P, Michopoulos F, et al. Global metabolic profiling of animal and human tissues via UPLC-MS. Nat Protoc 2013; 8:17-32.

17. Zubiri I, Posada-Ayala M, Sanz-Maroto A, et al. Diabetic nephropathy induces changes in the proteome of human urinary exosomes as revealed by label-free comparative analysis. J Proteomics 2014; 96:92-102.

18. Xia J, Mandal R, Sinelnikov IV, Broadhurst D, Wishart DS. MetaboAnalyst 2.0--a comprehensive server for metabolomic data analysis. Nucleic Acids Res 2012; 40:W127-W133.

19. Jensen LJ, Kuhn M, Stark M, et al. STRING 8--a global view on proteins and their functional interactions in 630 organisms. Nucleic Acids Res 2009; 37:D412-D416.

20. Mayr M, Yusuf S, Weir G, et al. Combined metabolomic and proteomic analysis of human atrial fibrillation. J Am Coll Cardiol 2008; 51:585-94.

21. Mayr M, Chung YL, Mayr U, et al. Proteomic and metabolomic analyses of atherosclerotic vessels from apolipoprotein E-deficient mice reveal alterations in inflammation, oxidative stress, and energy metabolism. Arterioscler Thromb Vasc Biol 2005; 25:2135-42.

22. Barth AS, Merk S, Arnoldi E, et al. Reprogramming of the human atrial transcriptome in permanent atrial fibrillation: expression of a ventricular-like genomic signature. Circ Res 2005; 96:1022-9.

23. Khatri JJ, Johnson C, Magid R, et al. Vascular oxidant stress enhances progression and angiogenesis of experimental atheroma. Circulation 2004; 109:520-5.

24. Brown DI, Griendling KK. Regulation of Signal Transduction by Reactive Oxygen Species in the Cardiovascular System. Circ Res 2015; 116:531-49.

25. Prasad A, Andrews NP, Padder FA, Husain M, Quyyumi AA. Glutathione reverses endothelial dysfunction and improves nitric oxide bioavailability. J Am Coll Cardiol 1999; 34:507-14.

26. Shen L, Sevanian A. OxLDL induces macrophage gamma-GCS-HS protein expression: a role for oxLDL-associated lipid hydroperoxide in GSH synthesis. J Lipid Res 2001; 42:813-23.

27. Ojha S, Goyal S, Kumari S, Arya DS. Pyruvate attenuates cardiac dysfunction and oxidative stress in isoproterenol-induced cardiotoxicity. Exp Toxicol Pathol 2012; 64:393-9.

28. Mallet RT, Squires JE, Bhatia S, Sun J. Pyruvate restores contractile function and antioxidant defenses of hydrogen peroxide-challenged myocardium. J Mol Cell Cardiol 2002; 34:1173-84.

29. Carisey A, Ballestrem C. Vinculin, an adapter protein in control of cell adhesion signalling. Eur J Cell Biol 2011; 90:157-63.

30. Attwell S, Mills J, Troussard A, Wu C, Dedhar S. Integration of cell attachment, cytoskeletal localization, and signaling by integrin-linked kinase (ILK), CH-ILKBP, and the tumor suppressor PTEN. Mol Biol Cell 2003; 14:4813-25.

31. Zhang QJ, Goddard M, Shanahan C, Shapiro L, Bennett M. Differential gene expression in vascular smooth muscle cells in primary atherosclerosis and in stent stenosis in humans. Arterioscler Thromb Vasc Biol 2002; 22:2030-6.

32. Zhang R, Zhou L, Li Q, Liu J, Yao W, Wan H. Up-regulation of two actin-associated proteins prompts pulmonary artery smooth muscle cell migration under hypoxia. Am J Respir Cell Mol Biol 2009; 41:467-75.

33. Palsson-McDermott EM, Curtis AM, Goel G, et al. Pyruvate Kinase M2 Regulates Hif-1alpha Activity and IL-1beta Induction and Is a Critical Determinant of the Warburg Effect in LPS-Activated Macrophages. Cell Metab 2015; 21:65-80.

34. Cojocaru E, Filip N, Ungureanu C, Filip C, Danciu M. Effects of Valine and Leucine on Some Antioxidant Enzymes in Hypercholesterolemic Rats. Health 2014; 6:2313-21.

35. Evanko SP, Angello JC, Wight TN. Formation of hyaluronan- and versican-rich pericellular matrix is required for proliferation and migration of vascular smooth muscle cells. Arterioscler Thromb Vasc Biol 1999; 19:1004-13.

36. Yanni AE, Agrogiannis G, Nomikos T, et al. Oral supplementation with L-aspartate and L-glutamate inhibits atherogenesis and fatty liver disease in cholesterol-fed rabbit. Amino Acids 2010; 38:1323-31.

37. Suschek CV, Schnorr O, Hemmrich K, et al. Critical role of L-arginine in endothelial cell survival during oxidative stress. Circulation 2003; 107:2607-14.

38. Arnal JF, Munzel T, Venema RC, et al. Interactions between L-arginine and L-glutamine change endothelial NO production. An effect independent of NO synthase substrate availability. J Clin Invest 1995; 95:2565-72.

39. Cheng S, Rhee EP, Larson MG, et al. Metabolite profiling identifies pathways associated with metabolic risk in humans. Circulation 2012; 125:2222-31.

40. Wang Z, Klipfell E, Bennett BJ, et al. Gut flora metabolism of phosphatidylcholine promotes cardiovascular disease. Nature 2011; 472:57-63.

41. Rajaie S, Esmaillzadeh A. Dietary choline and betaine intakes and risk of cardiovascular diseases: review of epidemiological evidence. ARYA Atheroscler 2011; 7:78-86.

42. Ludmer PL, Selwyn AP, Shook TL, et al. Paradoxical vasoconstriction induced by acetylcholine in atherosclerotic coronary arteries. N Engl J Med 1986; 315:1046-51.

43. Zhou Y, Varadharaj S, Zhao X, Parinandi N, Flavahan NA, Zweier JL. Acetylcholine causes endothelium-dependent contraction of mouse arteries. Am J Physiol Heart Circ Physiol 2005; 289:H1027-H1032.

44. Brocheriou I, Stengel D, Mattsson-Hulten L, et al. Expression of platelet-activating factor receptor in human carotid atherosclerotic plaques: relevance to progression of atherosclerosis. Circulation 2000; 102:2569-75.

45. Barbagallo SG, Barbagallo M, Giordano M, Meli M, Panzarasa R. alpha-Glycerophosphocholine in the mental recovery of cerebral ischemic attacks. An Italian multicenter clinical trial. Ann N Y Acad Sci 1994; 717:253-69

SUPPLEMENTAL MATERIAL

Supplemental Table 1. SRM conditions.

Protein	SRM Transition (ms precursor ion → ms product ion)	Fragmentor Voltage (V)	Collision Energy (V)	Mode
α-Crystallin	881.4 → 1168.6	130	22.8	Positive
	1321.6 → 1328.6	130	51.8	Positive
ATS-22	699.7 → 716.4	130	16.1	Positive
	699.7 → 862.0	130	16.1	Positive
	827.1 → 846.5	130	20.8	Positive
	827.1 → 931.5	130	20.8	Positive
	827.1 → 961.5	130	20.8	Positive
	827.1 → 1010.5	130	20.8	Positive
	1049.1 → 1123.6	130	37.9	Positive
CNDP (dipeptidase 2 isofrom 1)	579.0 → 766.4	130	11.6	Positive
	626.7 → 802.4	130	13.4	Positive
	626.7 → 809.4	130	13.4	Positive
	830.0 → 1019.5	130	26.8	Positive
	867.9 → 955.5	130	28.7	Positive
Fibrinogen β-chain	513.9 → 572.2	130	9.2	Positive
	665.0 → 699.4	130	14.8	Positive
	809.9 → 973.5	130	25.7	Positive
	890.9 → 1150.4	130	29.9	Positive
	922.5 → 999.6	130	31.5	Positive
Gelsolin-like capping protein	933.5 → 978.5	130	24.8	Positive
	933.5 → 1034.0	130	24.8	Positive
	933.5 → 1114.5	130	24.8	Positive
HSP70	661.3 → 885.5	130	14.7	Positive
	741.4 → 788.4	130	22.2	Positive
	830.4 → 881.4	130	26.8	Positive
	846.3 → 1022.5	130	27.6	Positive
Integrin linked kinase	714.4 → 779.9	130	16.6	Positive
Phosphoglycerate kinase	545.6 → 625.8	130	10.4	Positive
	545.6 → 675.3	130	10.4	Positive
	581.0 → 688.4	130	11.7	Positive
Pyruvate kinase	546.3 → 683.9	130	10.4	Positive
	724.9 → 857.5	130	21.4	Positive
	822.4 → 915.0	130	20.6	Positive
	822.4 → 988.5	130	20.6	Positive
	822.4 → 1032.1	130	20.6	Positive
Serotransferrin	469.5 → 574.3	130	7.6	Positive
	671.3 → 811.5	130	15.1	Positive
	703.8 → 759.4	130	20.3	Positive
	712.0 → 866.4	130	16.6	Positive
	712.0 → 866.9	130	16.6	Positive
	1006.5 → 1201.5	130	35.8	Positive
Tropomyosin 2, beta-like isoform 2	780.7 → 781.3	130	19.1	Positive
	780.7 → 849.9	130	19.1	Positive
	780.7 → 976.5	130	19.1	Positive
	807.9 → 881.5	130	25.6	Positive
Vinculin	692.7 → 695.4	130	15.8	Positive
	692.7 → 697.9	130	15.8	Positive
	692.7 → 758.5	130	15.8	Positive
	742.9 → 869.5	130	22.3	Positive
	742.9 → 1029.6	130	22.3	Positive
	816.4 → 1161.6	130	20.4	Positive
	816.4 → 1189.5	130	20.4	Positive

Metabolite	SRM Transition (ms precursor ion → ms product ion)	Fragmentor Voltage (V)	Collision Energy (V)	Mode
Acetylcholine	147.2 → 88.1	60	14	Positive
Choline	105.18 → 64.2	60	10	Positive
D-Glucuronic acid	193.1 → 112.9	120	10	Negative
DL-Threitol	121.13 → 75.1	60	10	Negative
Glutathione	308 → 84.1	175	40	Positive
Glycerophosphocholine	258.24 → 104	132	10	Positive
Guanidoacetic acid	118.1 → 72.1	120	10	Positive
L-Aspartic acid	134.11 → 74.2	60	10	Positive
L-Glutamic acid	147.9 → 102.0	175	18	Positive
L-Glutamine	147.15 → 84.1	84	18	Positive
	147.15 → 130	84	10	Positive
L-Threonine	120.13 → 102.9	130	18	Positive
	120.13 → 77.1	130	30	Positive
L-Valine	118.16 → 58.1	130	30	Positive
	118.16 → 59.1	130	18	Positive
N-acetyl-L-alanine	132.14 → 44.3	120	26	Positive
Phosphocholine	185.16 → 57.2	60	14	Positive
	142.1 → 44.3	80	10	Positive
Pyruvic acid	87.1 → 43.3	60	10	Negative
Trymethyamine-N-Oxide (TMAO)	76.1 → 59.0	175	22	Positive
Tyramine	138.2 → 121.1	60	10	Positive

Suppl. Table 2. Protein spots identified as significantly altered in DIGE analysis.

Protein Identification	Pathological/Control		Accesion number (NCBInr or SwissProt) *Oryctolagus Cuniculus*	Unique peptides detected	Sequence Coverage (%)	Accesion number (NCBInr or SwissProt) *Homo Sapiens*
	t-test	Av. Ratio				
Myofilaments and associated proteins						
PREDICTED: Vinculin Isoform 2	0.015	-2.05	gi|291404138|XP_002718452.1	35/8	34/19	G1U7Q7 + G1TRT2
PREDICTED: ARP3 actin-related protein 3 homolog isoform 3	0.039	2.64	gi|291391456|XP_002712452.1	23	48	G1SLQ4
PREDICTED: ARP3 actin-related protein 3 homolog isoform 3	0.00016	1.27	gi|291391456|XP_002712452.1	24	51	G1SLQ4
PREDICTED: gelsolin-like capping protein	0.015	2.8	gi|291386425|XP_002709720.1	11	34	G1SHB9
Actin, aortic smooth muscle	0.013	2.3	gi|156119362|NP_001095152.1	7	17	P62740
PREDICTED: tropomyosin 2, beta-like isoform 2	0.014	2.14	gi|291411755|XP_002722136.1	10	31	G1U5H1
PREDICTED: tropomyosin 4	0.042	2.14	gi|291384021|XP_002708655.1	13	43	G1SSK9
PREDICTED: transgelin	0.023	3.09	gi|291383827|XP_002708427.1	25	65	G1T2C4
Plasma proteins						
Serotransferrin	0.00061	2.06	gi|6175087|P19134.4	23	34	P19134
Serotransferrin	0.0032	2.19	gi|6175087|P19134.4	34	50	P19134
Serotransferrin	0.0028	2.23	gi|6175087|P19134.4	42	57	P19134
ATS-22	0.0084	2.4	gi|126723362|NP_001075463.1	15	38	G1TFX2
Glucose metabolism						
Pyruvate kinase isozymes M1/M2	0.0000083	1.8	gi|2851533|P11974.4	27	50	P11974
PREDICTED: phosphoglycerate kinase 1	0.00017	1.14	gi|291384724|XP_002709046.1	15	44	G1TLE3
Coagulation						
Fibrinogen beta chain	0.02	2.12	gi|291401109|XP_002716936.1	33	63	G1T0W8
Fibrinogen beta chain	0.034	2.18	gi|291401109|XP_002716936.1	24	56	G1T0W8
Protein folding						

PREDICTED: heat shock 70kDa protein 8	0.00017	1.23	gi|291400199|XP_002716475.1	29	37	G1T9M9
PREDICTED: heat shock protein, alpha-crystallin-related, B6	0.035	-2.06	gi|291412016|XP_002722271.1	7	47	G1U1F6
Other enzymes						
CNDP dipeptidase 2 isoform 1	0.046	2.39	gi|291394489|ref|XP_002713697.1	14	35	G1SKV7
Uncharacterized protein. Region: Integrin-linked-kinase	0.0035	2.28	-	16	36	G1SRA9

Supplemental Table 3. Identified metabolites from HRMAS experiment.

METABOLITE	CHEMICAL SHIFTS (ppm) and MULTIPLICITY
Acetylcholine	2.16 (s); 3.23 (s); 3.75 (t)
Agmatine	1.67 (m); 1.73 (m); 3.02 (t); 3.22 (t)
Choline	3.19 (s); 3.51 (dd); 4.06 (ddd)
D-Glucuronic acid	3.29 (t); 3.51 (m); 3.58 (dd); 3.73 (m); 4.08 (d); 4.65 (d); 5.25 (d)
DL-Threitol	3.61 (m); 3.70 (m) L: 3.65 (m); 3.77 (d)
Glutathione	2.15 (m); 2.54 (m); 2.97 (dd); 3.78 (m); 4.20 (q)
Glycerol	3.55 (m); 3.64 (m) ; 3.78 (tt)
Glycerophosphocholine	3.20 (s); 3.63 (m); 3.90 (m); 4.30 (m)
Glycolic acid	3.94 (s)
Guanidoacetic acid	3.78 (s)
L-Aspartic acid	2.66 (dd); 2.80 (dd); 3.89 (dd)
L-Glutamic acid	2.04 (m); 2.12 (m); 2.34 (m); 3.75 (dd)
L-Glutamine	2.13 (m); 2.45 (m); 3.77 (t)
L-Threonine	1,32 (d); 3,58 (d); 4,24 (m)
L-Serine	3.83 (dd); 3.96 (m)
L-Valine	0.98 (d); 1.03 (d); 2.26 (m); 3.60 (d)
Malic acid	2.33 (dd); 2.66 (dd); 4.29 (dd)
N-acetyl-L-alanine	1.32 (d); 2.00 (s); 4.11 (t)
Phosphocholine	3.21 (s); 3.59 (t); 4.16 (dddd)
Phosphoethanolamine	3.24 (t); 4.01 (td)
Pyruvic acid	2.46 (s)
Ribitol	3.64 (dd); 3.69 (dd); 3.80 (dd); 3.83 (ddd)
Trymethyamine-N-Oxide (TMAO)	3.25 (s)
Tyramine	2.92 (t); 3.23 (t); 6.90 (d); 7.21 (d)

Supplemental Figure 1. PCA resulting from DIGE analysis. Seventy three spots of the non biased proteomic DIGE experimens were considered of interest. PCA analysis was performed with those 73 points of interest showing good clasiffication between control and atherosclerotic group which are discriminated by PC1.

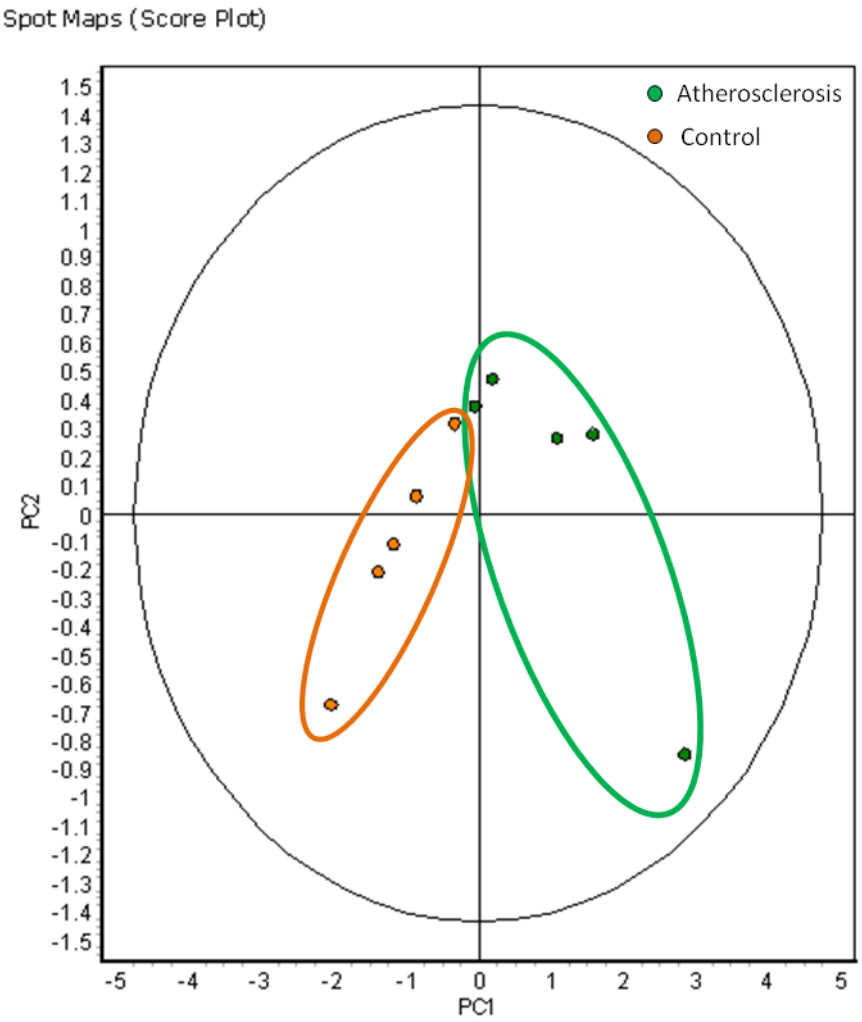

Supplemental Figure 2 . **Pathway analysis of the proteins found altered directly in aoritc atherosclerotic tissue**. Three main KEEG pathways involved are revealed **A:** Complement and coagulation cascades (p= 5.21E-6) that involves FGB and ATS22 ; **B:** Focal adhesion (p=2.250E-6) involving VCL, ILK, CAPG and TPM2; **C:** glycolisis/gluconeogenesis (p=4.000E-3) with important contribution of PKM2, PGK, ATS22 and ST.

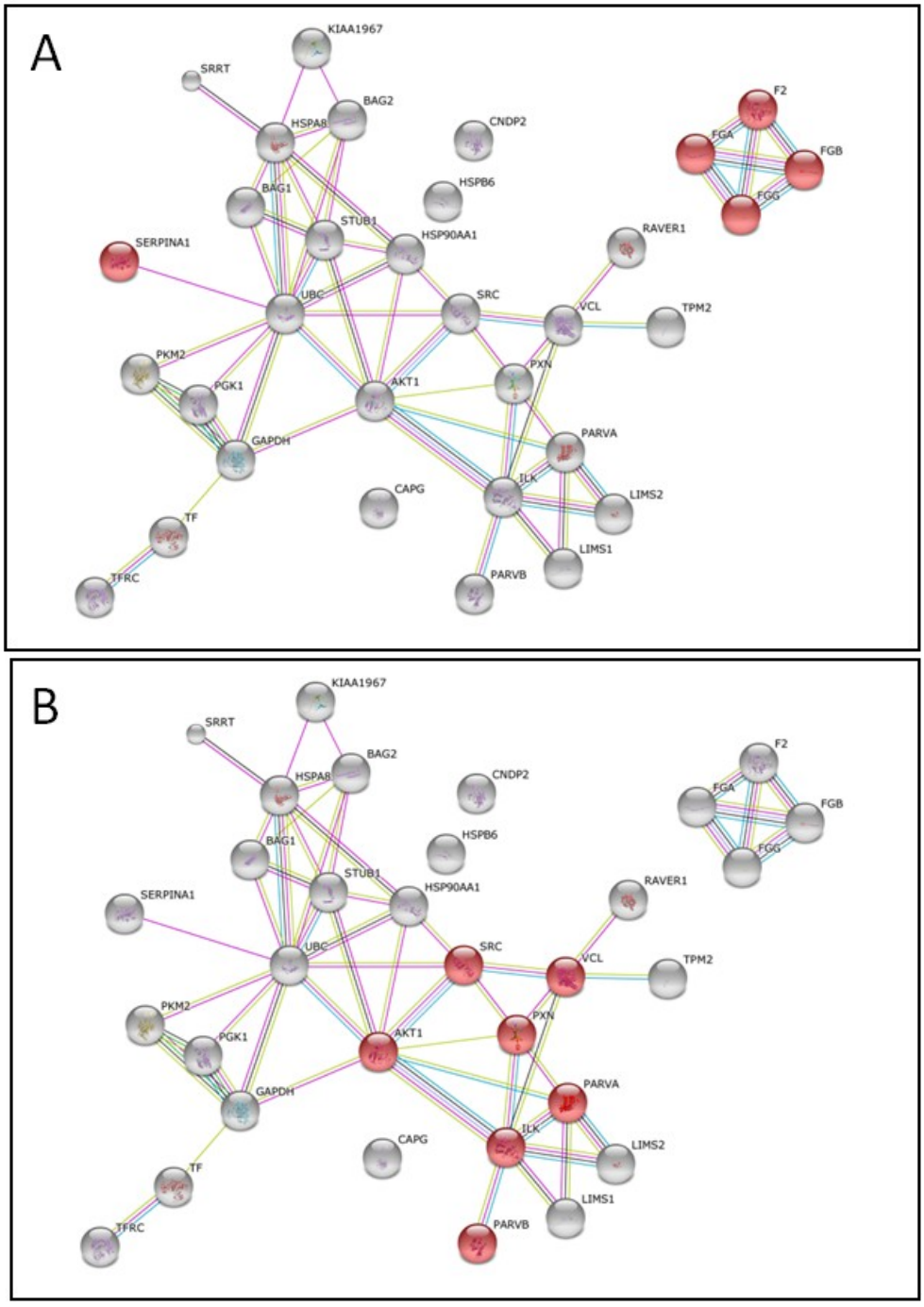

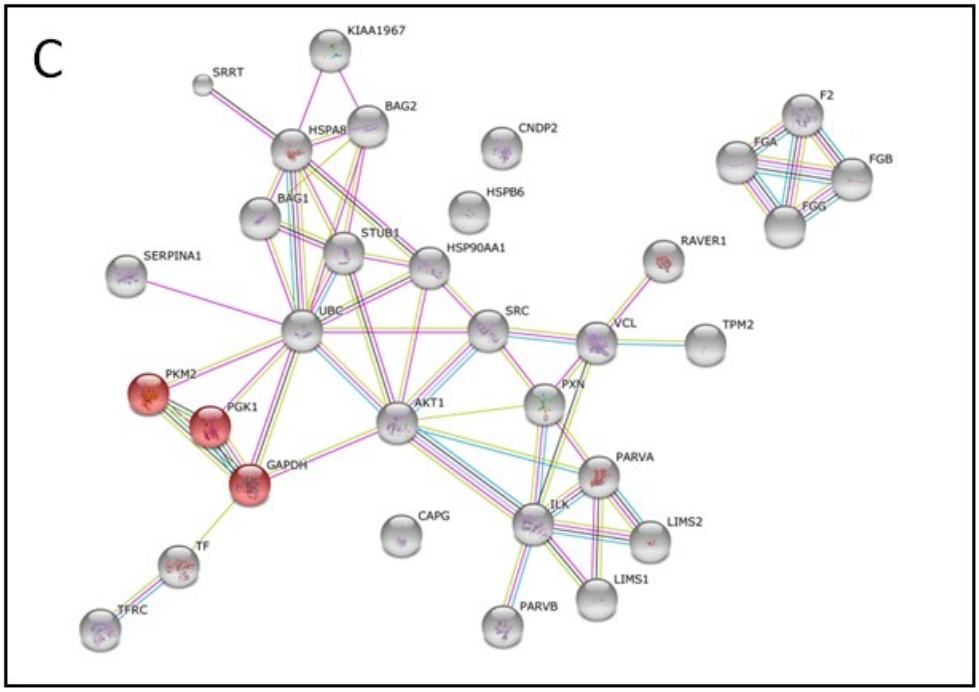
C
KIAA1967
SRRT
BAG2
HSPA8
CNDP2
F2
FGA
FGB
FGG
BAG1
HSPB6
STUB1
HSP90AA1
RAVER1
SERPINA1
UBC
SRC
VCL
TPM2
PKM2
PXN
PGK1
AKT1
PARVA
GAPDH
ILK
CAPG
LIMS2
TF
LIMS1
TFRC
PARVB

Suppl. Fig 3. Most relevant found altered in aortic tissue. Classification is performed according to its impact and the p value. "glycine, serine and threonine metabolism" (p= 9.4557E-6, FDR= 5.1176E-4), *involving L-aspartate, L-threonine, choline, guanidoacetate and pyutvate;* "alanine, aspartate and glutamate metabolism" (p= 1.2794E-4 ; FDR= 5.1176E-4), *involving L-aspartic acid, pyruvate, L-glutamine and L-glutamate;* "aminoacyl-tRNA biosynthesis" (p= 8.5839E-5 ; FDR= 0.001560), *involving L-aspartate, L-glutamate, L-glutamine, L-valine and L-threonine;* "glycerophospholip metabolism" (p= 9.3233E-5; FDR= 0.0015601), *involving phosphocholine, glycerophosphocholine, choline and acetylcholine;* and "arginine and proline metabolism" (p= 9.7503 E-5; FDR= 0.0015601*) involving L-glutamine, L-aspartate, L-glutamate, guanido acetic acid and piruvate*..

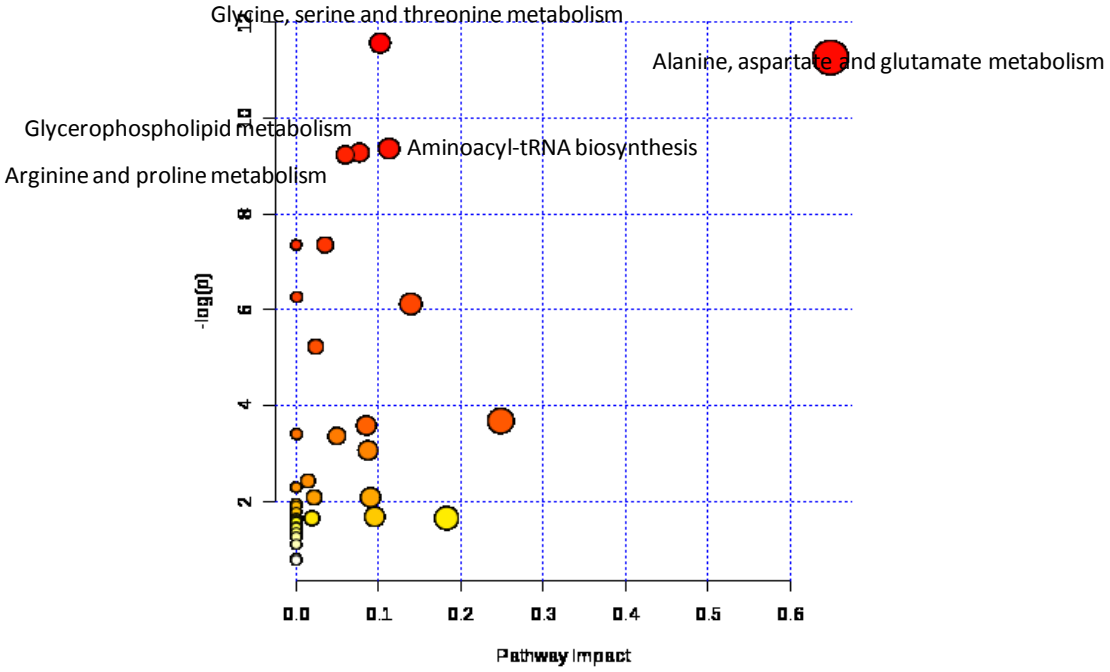

Chapter 4

30µm spatial resolution protein MALDI MSI: In-depth comparison of five sample preparation protocols applied to human healthy and atherosclerotic arteries

Marta Martin-Lorenzo, *Benjamin Balluff, Aroa Sanz-Maroto, René J.M. van Zeijl, Fernando Vivanco, Gloria Alvarez-Llamas, Liam A. McDonnell.*

J Proteomics. 2014 Aug 28;108:465-8. doi: 10.1016/j.jprot.2014.06.013

La técnica de espectrometría de masas de imagen basada en ionización por fuente MALDI (MALDI-MSI) representa una novedosa técnica de histología molecular. Permite estudiar simultáneamente diferentes tipos de moléculas (lípidos, metabolitos, péptidos, proteínas...) directamente en el tejido, conservando su distribución espacial al mismo tiempo que se mantiene la integridad morfológica del tejido. Gracias a ello se obtienen mapas bidimensionales de distribuciones moleculares y se pueden seguir los cambios fisiopatológicos que están teniendo lugar directamente en el tejido. En el estudio que se presenta a continuación hemos establecido un protocolo óptimo pionero para el análisis de proteínas por MALDI-MSI en arterias control y arterias ateroscleróticas de alta resolución.

Desde los primeros estudios de MALDI-MSI en 1997 por *Caprioli et al.* se ha visto que la clave de la obtención de buenos perfiles moleculares con la sensibilidad adecuada y que permitan una elevada resolución espacial es la correcta preparación del tejido. En los estudios proteicos de especial interés para el análisis son los pre-tratamientos basados en un lavado óptimo del tejido. Los lavados se hacen con el fin de aumentar la sensibilidad y mantener la distribución espacial nativa de las diferentes moléculas biológicas del tejido y siempre controlando que no se dé una difusión indeseada de los analitos. Tienen como funciones fundamentales eliminar los lípidos libres y las sales presentes en el tejido que afectan a la sensibilidad de la medida y mejorar la relación señal/ruido. En algunos casos, los lavados con disolventes orgánicos, también pueden ayudar a la fijación del tejido al cristal. La principal precaución a tener en cuenta es que dichos lavados no pueden provocar una deslocalización de las moléculas.

Estos lavados deben ser optimizados para cada aplicación concreta de MSI y de especial relevancia es esta optimización en el caso de las arterias donde además de la dificultad añadida de tener dimensiones reducidas, coexisten zonas con muy diferentes propiedades moleculares y físicas como son zonas ricas en grasas o calcificadas típicas del desarrollo de la aterosclerosis. En el siguiente trabajo realizado en colaboración con el Dr. Liam McDonnell del LUMC ("Leiden University Medical Center"), Holanda que está publicado en *Journal of Proteomics* se realiza una comparación exhaustiva de cinco lavados de diferente naturaleza; lavados con base acuosa que son indicados para la eliminación de sales, lavados de base orgánica que ayudan a preservar el tejido a la vez que eliminan sales y lípidos y lavados que incluyen tampones que están descritos como idóneos para mejorar la detección de los perfiles proteicos. Los parámetros de evaluación implicados fueron la sensibilidad, considerando el número de picos y su relación señal ruido; la reproducibilidad, realizando medidas en cortes contiguos y la calidad de la imagen espectral, en función del número de espectros excluidos en cada corte y la localización de diferentes valores de masa/carga en función de la histología del mismo corte evaluado.

La conclusión final fue que lavados sucesivos por inmersión en isopropanol son los más adecuados en el estudio de tejido arterial tanto control como patológico en la enfermedad aterosclerótica, ya que se obtienen perfiles proteicos de calidad que van unidos a una distribución espacial de esas proteínas de una manera fiable y veraz.

Además este protocolo permite trabajar a muy alta resolución, 30µm, tal y como requieren las muestras de arterias. En el campo de la aterosclerosis el estudio desarrollado a continuación representa el primer intento de investigar las proteínas implicadas en los cambios subyacentes de la enfermedad conservando la localización original.

JOURNAL OF PROTEOMICS 108 (2014) 465–468

Available online at www.sciencedirect.com

ScienceDirect

www.elsevier.com/locate/jprot

Technical note

30 μm spatial resolution protein MALDI MSI: In-depth comparison of five sample preparation protocols applied to human healthy and atherosclerotic arteries

Marta Martin-Lorenzo[a], Benjamin Balluff[b], Aroa Sanz-Maroto[a], René J.M. van Zeijl[b], Fernando Vivanco[a,c], Gloria Alvarez-Llamas[a,1], Liam A. McDonnell[b,*,1]

[a]Department of Immunology, IIS-Fundacion Jimenez Diaz, Madrid, Spain
[b]Center for Proteomics and Metabolomics, Leiden University Medical Center, Leiden, The Netherlands
[c]Department of Biochemistry and Molecular Biology I, Universidad Complutense, Madrid, Spain

ARTICLE INFO

Artide history:
Received 5 April 2014
Accepted 11 June 2014
Available online 25 June 2014

Keywords:
MALDI mass spectrometry imaging
High spatial resolution
Atherosclerosis
Sample preparation

ABSTRACT

Tissue preparation is the key to a successful MALDI mass spectrometry imaging experiment. A number of different tissue preparations methods have recently been reported for increased sensitivity and/or high spatial resolution analysis. In order to better benchmark these methods in terms of the information content and their suitability for analyzing small tissues containing small but distinct regions, we have performed an extensive comparison using technical and biological repeats as well as a fully randomized measuring sequence. We then demonstrate how the optimized tissue preparation method enables 30 μm spatial resolution analysis of proteins from atherosclerotic arterial tissues, revealing proteins specific to the intima and media layers.

© 2014 Elsevier B.V. All rights reserved.

Tissue preparation is the key to a successful MALDI mass spectrometry imaging (MALDI MSI) experiment [1]. Washing the tissues prior to matrix deposition can effectively reduce the free lipid and salt content and thus increase protein detection sensitivity [2]. Organic solvents, as widely used in histology for fixation and preservation of tissues, extract lipids rapidly and efficiently [2,3]. Aqueous washes can be effective at removing salts but care must be taken to limit delocalization of water-soluble proteins [4]. A combination of organic and aqueous washes has been proposed in order to benefit from both characteristics, namely the removal of interfering molecular material while preserving protein localization and tissue integrity [5]. A number of different washes have recently been reported, each reporting increases in sensitivity and their suitability for high spatial resolution analysis [5–7].

In order to better benchmark these tissue washes in terms of the information content provided by MALDI MSI, and their suitability for analyzing small tissues containing small but

* Corresponding author at: Center for Proteomics and Metabolomics, Leiden University Medical Center, Einthovenweg 20, 2333 ZC Leiden, The Netherlands. Tel.: +31 71 526 8744; fax: +31 71 526 6907.
E-mail address: L.A.Mcdonnell@lumc.nl (L.A. McDonnell).
[1] Equal contributions.

http://dx.doi.org/10.1016/j.jprot.2014.06.013
1874-3919/© 2014 Elsevier B.V. All rights reserved.

ABSTRACT

Tissue preparation is key to a successful MALDI mass spectrometry imaging experiment. A number of different tissue preparations methods have recently been reported for increased sensitivity and/ high spatial resolution analysis. In order to better benchmark these methods in terms of the information content and their suitability for analyzing small tissues containing small but distinct regions, we have performed an extensive comparison using technical and biological repeats as well as a fully randomized measuring sequence. We then demonstrate how the optimized tissue preparation method enables high spatial resolution analysis of proteins from atherosclerotic arterial tissues, revealing proteins specific to the intima and media layers.

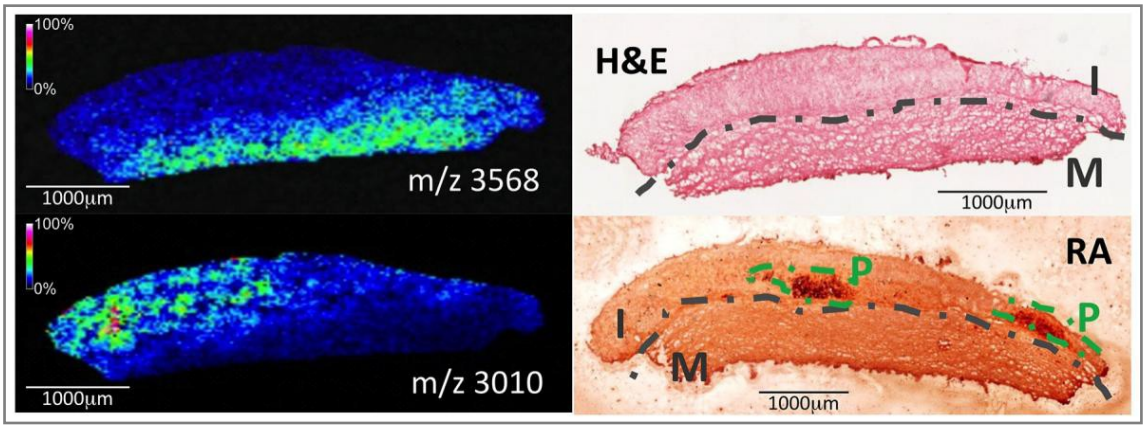

Tissue preparation is key to a successful MALDI mass spectrometry imaging (MALDI MSI) experiment (1). Washing the tissues prior to matrix deposition can effectively reduce the free lipid and salt content and thus increase protein detection sensitivity (2). Organic solvents, as widely used in histology for fixation and preservation of tissues, extract lipids rapidly and efficiently (2,3). Aqueous washes can be effective at removing salts but care must be taken to limit delocalization of water-soluble proteins (4). A combination of organic and aqueous washes has been proposed in order to benefit from both characteristics, namely the removal of interfering molecular material while preserving protein localization and tissue integrity (5). A number of different washes have recently been reported, each reporting increases in sensitivity and their suitability for high spatial resolution analysis (5-7).

In order to better benchmark these tissue washes in terms of the information content provided by MALDI MSI, and their suitability for analyzing small tissues containing small but distinct regions, we have performed an extensive comparison using human arterial tissue samples. Five different washing protocols were compared:-

1) 70% EtOH followed by 100% EtOH wash (7);

2) Carnoy's wash (6)*;*

3) Ammonium formate buffer wash (5);

4) 70% EtOH, 90% EtOH, then 90:9:1 EtOH:acetic acid:water wash (2);

5) 70% Isopropanol followed by 95% Isopropanol (2).

The experiments have been performed as part of an optimization process for the application of MALDI MSI to atherosclerosis. As molecular alterations are known to occur in specific arterial layers (8-10) the application places high demands on measurement sensitivity, spatial resolution and retaining the spatial integrity of the protein signals. The comparison was performed using pathological arteries obtained from patients subjected to carotid endarterectomy and healthy mammary arteries obtained from patients admitted for coronary artery bypass. All experiments involved multiple technical and biological repeats, identical MALDI matrix solution and were measured in a randomized order to avoid any systemic bias affecting the result. Detailed material and methods can be found in the supplementary information.

The different washing protocols were first compared using eight carotid sections for each protocol, analyzed using 100µm spatial resolution. Figure 1A shows example average mass spectra (average of a single MALDI MSI dataset) obtained for each tissue wash protocol. The results were evaluated in terms of both the quality of the mass spectra as well as the mass spectral images. Mass spectral quality was evaluated by calculating the number and signal-to-noise ratio of the detected protein-ion peaks. The quality of the mass spectral images is dependent on retaining the protein's original

localization as well as each pixel generating a rich mass spectrum; accordingly, mass spectral image quality was evaluated by comparing the *m/z* distributions with the morphological structure of the tissue and by recording the number of low quality and therefore excluded mass spectra (the low quality prevents their alignment to the rest of the MALDI MSI dataset, a routine step prior to further statistical analysis).

The carotid tissue sections washed with organic solvents or Carnoy's protocol provided the highest number of protein ions and average s/n ratio (Figure 1B). With the exception of Carnoy's protocol the number of excluded spectra was low and the sections well adhered to the slide, enabling the MALDI MSI dataset to be co-registered with the histological images (tissues H&E stained after MALDI MSI measurements (11)). The arteries washed with the acetic acid-containing solution generated fewer protein ions and with a lower mean intensity. The ammonium formate buffer wash resulted in the poorest spectral quality for all metrics.

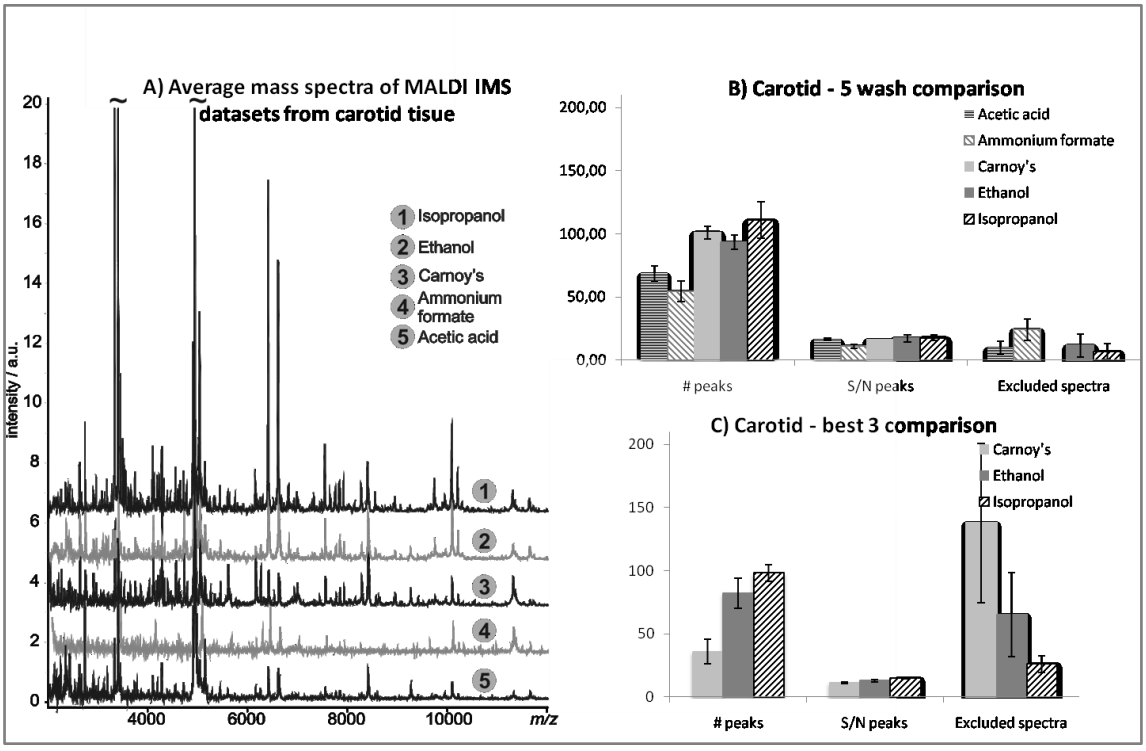

Figure 1. Comparison of MALDI IMS datasets using different washing protocols. A) Examples of the average mass spectra from atherosclerotic carotid arteries using five different washing protocols; B) Comparison of detected peak numbers, average peak signal-to-noise ratio, and number of excluded spectra for MALDI IMS datasets for the five tissue washes; C) Repeated analysis of 3-best tissue wash protocols using sequential sections and randomized measurement sequence.

The three protocols that gave the best results (ethanol, isopropanol, and Carnoy's wash) were investigated further using three additional carotid samples, and six mammary arteries. The different washes were applied to serial tissue sections and the MALDI MSI data acquisition sequence randomized. These results clearly demonstrated that the longest established methods, based on alcohol washes, generated spectra with the

highest number of peaks and signal-to-noise (Figures 1C and supplementary figure 1). Almost all protein ions detected from the sections prepared using Carnoy's wash were also present in the isopropanol- and ethanol-wash data sets (which exhibited substantial overlap).

Most of the carotid tissue sections consisted of the intima layer owing to the nature of the carotid endarterectomy from which the tissues were obtained. Accordingly protein delocalization during the tissue wash must be minimized to avoid proteins signals from the larger intima layer overwhelming those from the media. Visual inspection revealed protein ion signals that follow the tissue's histology were in the order isopropanol >> ethanol >Carnoy's, supplementary figure 2. Indeed the MS images revealed that only the carotid sections washed with isopropanol generated images consistent with the tissue's morphology *m/z* 4307 and m/z 10089 co-localize with the media layer, whereas m/z 5000 co-localizes with the intima layer, supplementary figure 2. Once established the MALDI MSI tissue preparation protocol enabled high spatial resolution analysis of arterial tissues. Figure 2 shows an example of a 30μm pixel-size, protein MALDI MSI dataset, showing proteins localized within the intima and media layers. The images and average mass spectrum demonstrate the high quality of the MALDI MSI data. The figures of merit for MALDI MSI datasets measured with 30 μm spatial resolution also compare well with those measured with 100 μm spatial resolution: number of peaks = 88 ± 9.5 (98 ± 24 for 100 μm), S/N = 15.2 ± 0.5 (18.5 ± 2 for 100 μm), excluded spectra = 2 ± 3 (10 ± 13 for 100 μm dataset).

Many sample preparation protocols for protein MALDI MSI have been reported. In one of the first studies Seeley *et al.* compared the number of proteins and total protein ion-count detected from mouse liver tissue sections for twelve washing protocols (2), five of which were also compared for clear cell renal carcinoma tissue sections. It is noteworthy that the extensive comparison reported here, which includes several recent methods developed explicitly for higher spatial resolution analysis, results in the same conclusions as those initially reported by Seeley *et al.* "…that alcohol-based washes of sections, in particular isopropanol, [were found] to be most effective for protein analysis when considering MS signal quality, matrix deposition regularity, and preservation and histological integrity of the tissue" (matrix regularity and histological integrity being necessary to produce high quality MS images that can be compared with the tissue's morphology).

The results indicate that the transfer of previously reported protocols to different applications is not straightforward. While it may be argued that the high fat content and calcification of atherosclerotic arteries make them somewhat atypical, the findings were also confirmed in the control mammary arteries, and the common test sample for MALDI MSI method development (and used in the cited studies (6)) is rodent brain, a high fat content tissue.

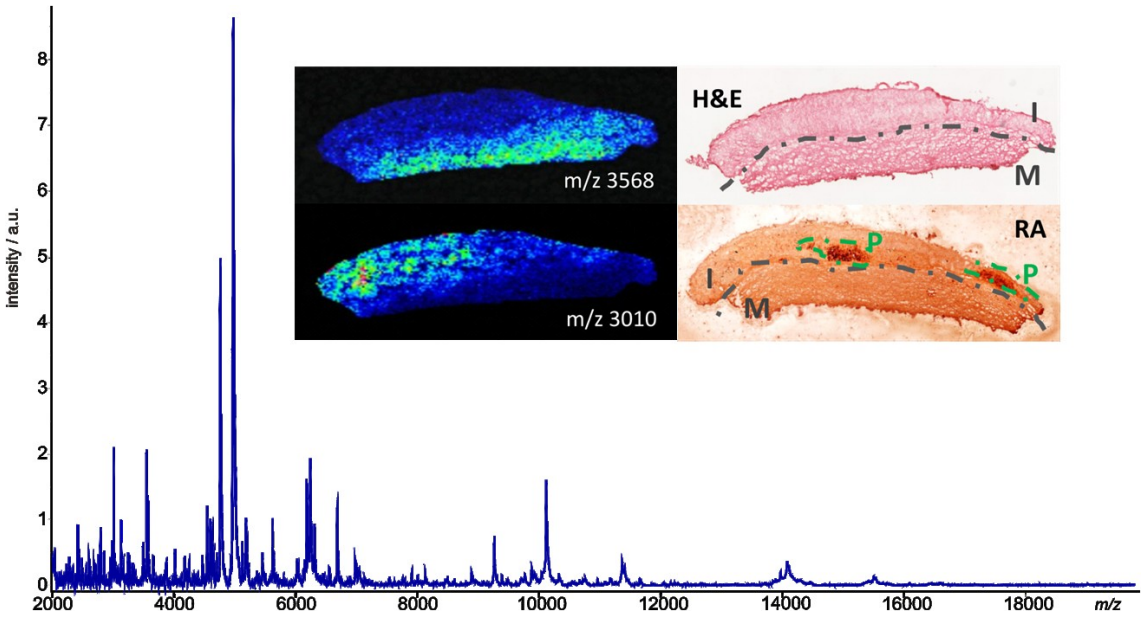

Figure 2. 30 μm spatial resolution MALDI IMS of proteins in atherosclerotic arterial tissue. The average mass spectrum demonstrates the detection of many distinct protein ions. Inset shows example mass spectral images localized to the media (m/z 3568) and intima (m/z 3010). The histological image and Red Alizarin (RA) image are included to contextualize the mass spectral images in terms of the tissue morphology and atherosclerotic (calcified) plaques; M = media; I = intima; P = plaque.

This study utilized standardized tissue handling, multiple biological and technical repeats as well as fully randomized measurement sequences utilizing sequential tissue sections in order to ensure all conclusions were verifiable and to minimize the impact of any potential source of systematic bias. Tissue washes are arguably the most straightforward aspect of the entire tissue preparation step yet it is known that small differences in tissue processing can have big consequences for MALDI MSI (1) and similar unexpected sources of bias have been reported for peptide profiling (12). The wide adoption of an imaging mass spectrometry analogue of a MIAPE (Minimum Information About a Proteomics Experiment) (13), would help identify the factors that can influence the results obtained by MSI.

A recent study indicates that provided they are detected the biomarkers reported by MALDI MSI can be insensitive to differences in tissue preparation protocols (14). MALDI MSI based identification of protein markers of stromal activation, performed in two centers using independent tissue banks, infrastructure, tissue preparation methods and even practitioners, found that of the four statistically-significant biomarkers found at the discovery center, three were also detected in the validation center and were all statistically significant. Reproducible tissue preparation would have enabled all four biomarkers to be detected in both centers. Standardized methods that reproducibly generate the same protein ions will be necessary for the large scale multicenter studies needed to realize the full clinical application of imaging mass spectrometry.

ACKNOWLEDGEMENTS

The authors would like to acknowledge financial support from Instituto de Salud Carlos III (FIS PI13/01873, PI11/01401, CP09/00229), BMBS COST Action BM1104, Cyttron II, Fundación Conchita Rábago de Jiménez Díaz, Spanish Proteomics Society (SeProt) and Cyttron II. BB is funded by the Marie Curie Action of the European Union (No. 331866, SITH FP7-PEOPLE-2012-IEF). Authors also thank Mª Teresa Tejerina and Luis F. Lopez-Almodovar for their help on the recruitment of the samples.

REFERENCES

1. Goodwin RJA. Sample preparation for mass spectrometry imaging: Small mistakes can lead to big consequences. J Proteomics 2012;75:4893-4911.

2. Seeley EH, Oppenheimer SR, Mi D, Chaurand P, Caprioli RM. Enhancement of protein sensitivity for MALDI imaging mass spectrometry after chemical treatment of tissue sections. J Am Soc Mass Spectrom 2008;19:1069-77.

3. Lemaire R, Wisztorski M, Desmons A et al. MALDI-MS Direct Tissue Analysis of Proteins: Improving Signal Sensitivity Using Organic Treatments. Anal Chem 2006;78:7145-7153.

4. Grey AC, Chaurand P, Caprioli RM, Schey KL. MALDI Imaging Mass Spectrometry of Integral Membrane Proteins from Ocular Lens and Retinal Tissue. J Proteome Res, 2009;8:3278–3283.

5. Thomas A, Patterson NH, Laveaux Charbonneau J, Chaurand P. Orthogonal organic and aqueous-based washes of tissue sections to enhance protein sensitivity by MALDI imaging mass spectrometry. J Mass Spectrom 2013;48:42-8.

6. Deutskens F, Yang J, Caprioli RM. High spatial resolution imaging mass spectrometry and classical histology on a single tissue section. J Mass Spectrom 2011;46:568-571.

7. Yang J, Caprioli RM. Matrix Sublimation/Recrystallization for Imaging Proteins by Mass Spectrometry at High Spatial Resolution. Anal Chem 2011;83:5728-5734.

8. Bagnato C, Thumar J, Mayya V et al. Proteomics Analysis of Human Coronary Atherosclerotic Plaque: A Feasibility Study of Direct Tissue Proteomics by Liquid Chromatography and Tandem Mass Spectrometry. Molecular & cellular proteomics : MCP 2007;6:1088-1102.

9. de la Cuesta F, Alvarez-Llamas G, Maroto AS et al. A Proteomic Focus on the Alterations Occurring at the Human Atherosclerotic Coronary Intima. Molecular & cellular proteomics : MCP 2011;10:M110.

10. de la Cuesta F, Zubiri I, Maroto AS et al. Deregulation of smooth muscle cell cytoskeleton within the human atherosclerotic coronary media layer. J Proteomics 2013;82:155-165.

11. Rauser S, Deininger S-O, Suckau D, Höfler H, Walch A. Approaching MALDI Molecular Imaging for Clinical Proteomic Research: Current State and Fields of Application. Expert Rev Proteomic 2010;7:927-941.

12. Villanueva J, Philip J, Chaparro CA et al. Correcting Common Errors in Identifying Cancer-Specific Serum Peptide Signatures. J Proteome Res 2005;4:1060–1072.

13. Taylor CF, Paton NW, Lilley KS et al. The minimum information about a proteomics experiment (MIAPE). Nat Biotech 2007;25:887-893.

14. Dekker TJA, Balluff BD, Jones EA et al. Multicentre matrix-assisted laser desorption/ionization mass spectrometry imaging (MALDI MSI) identifies proteomic differences in breast cancer-associated stroma J Proteom Res 2014; 7;13(11):4730-8.

SUPPLEMENTAL MATERIAL

MATERIALS AND METHODS

Chemicals and Reagents

Ethanol, acetic acid, chloroform, trifluoroacetic acid (TFA), methanol and acetonitrile were purchased from Merck (Merck KGaA, Darmstadt, Germany). Isopropanol, ammonium formate and triton X-100 were obtained from Sigma-Aldrich (Sigma Aldricht Co., St Louis, USA), and sinapinic acid (SA) from Fluka (Sigma Aldricht Co., St Louis, USA).

Human tissue collection

Human pathological arteries were obtained from patients subjected to carotid endarterectomy at Hospital Clinico San Carlos in Madrid, Spain. Human healthy mammary arteries were obtained from patients admitted for coronary artery bypass surgery at Hospital Virgen de la Salud in Toledo, Spain. Signed informed consent was obtained from patients and sample collection procedures were approved by the local ethics committee.

Tissue collection, storage and sample processing

To retain the native shape of the tissue, surgically removed arterial tissue (human carotids and mammary) was immediately transported to the laboratory at 4°C in a period no longer than 30 minutes. Tissue sections were washed in saline solution, loosely wrapped in aluminium foil and frozen by gently lowering the tissue into the liquid nitrogen over a period of 30–60 s to avoid cracking. Samples were stored at -80°C until analysis. For MALDI-IMS experiments, 15µm thick tissue sections were cut at − 22°C on a 1720 digital Leica Cryostat (Leica Microsystems GmbH, Wetzlar, Germany) and thaw-mounted onto conductive glass slides (Delta Technologies, Stillwater, MN, USA). The tissues sections were dehydrated in a freeze drierfor 1 hour and then prepared for MALDI-IMS experiments.

Sample preparation: tissue washing optimization

Five different washing protocols were systematically tested on two human carotid samples. Duplicate sections were taken from two different regions of each artery (plaque rich and plaque poor). In total eight carotid sections were used per condition for each washing protocol (two technical repeats for two different regions of artery for two biological samples). The slides were washed by immersion in a series of 50mL solutions, testing the following five protocols:

1) 70% EtOH followed by 100% EtOH wash (1);

2) Carnoy's wash (2)*;*

3) Ammonium formate buffer wash (3);

4) 70% EtOH, 90% EtOH, then 90:9:1 EtOH:acetic acid:water wash (4);

5) 70% Isopropanol followed by 95% Isopropanol (4).

An additional exploration of the three best-performing washing protocols was performed. To reduce the contribution of user and instrumental variability the three washes were performed on consecutive sections and using the same mounting slide. Each carotid sample was analyzed in triplicate for each of the three washing protocols (two biological samples, three technical repeats). For mammary arteries, which are much smaller than the carotids six biological samples per wash were measured.

MALDI Imaging Mass Spectrometry analysis of proteins in human arterial samples

All experiments were performed using an identical matrix solution; 20 mg/mL sinapinic acid (SA) in 10mL 4:4.2:1.8 acetonitrile: methanol: 0.5% TFA was uniformly deposited onto the washed tissues using an automated spraying device (ImagePrep, BrukerDaltonik, Bremen, Germany). The slides were then placed into a desiccator for 10 minutes prior to MALDI-IMS analysis. The experiments were performed using an UltrafleXtreme MALDI-ToF/ToF (BrukerDaltonik) with 100µm pixel size and 1000 laser shots per pixel (100 laser shots per position of a random walk within each pixel) in linear positive mode. Protein ions were detected in the range 2 -19k m/z. Data acquisition and data visualization were performed using the Flex software suite (FlexControl 3.0, FlexImaging 2.1, both from BrukerDaltonik). After MALDI-IMS data acquisition the remaining matrix was removed using an ethanol wash and the arterial tissue sections stained with haematoxylin and eosin.

Data Analysis – Comparison of performance of different washing protocols

Protein mass spectral data were compared using ClinProTools 3.0, ClinProtSpectra Import XML Generator (both from Bruker Daltonik), Microsoft Excel, and R (R Foundation for Statistical Computing, Vienna, Austria).

For each measured tissue section 150 mass spectra were randomly selected using ClinProtSpectra Import XML Generator and processed in ClinProTools 3.0. Mass spectral processing was performed with a mass resolution of 800, top-hat baseline subtraction (10%), Savitzky Golay smoothing, a data reduction factor of 5, activated null spectra exclusion and a recalibration of 2000 ppm as maximum peak shift. Peak detection was performed on the total average spectrum witha signal-to-noise (s/n) threshold of 5.0. The processed datasets were then compared in terms of number of peaks, mean intensity of spectra, signal-to-noise ratio (s/n), and the number of excluded spectra.

For the closer-examination of the 3-best performing tissue washes 500 spectra were randomly selected from each triplicate carotid tissue section; a total of 100 spectra were collected for the smaller mammary arteries. These spectra collections were individually processed to assess repeatability within washes and pooled to compare the results

between the washes. The performance was evaluated by comparing the mean intensities of spectra, number of excluded spectra, number of detected peaks, their mean signal-to-noise ratio (s/n), and finally the image quality. Venn diagrams were used to evaluate overlaps in detected peaks between washes using a mass tolerance of 2000 ppm. The visualization quality of selected mass signals was benchmarked by calculating Pearson correlation coefficients between the spatial distributions of mass intensities and a ground-truth image based on a previous histological annotation of the tissues.

Supporting Figure 1. Comparison of MALDI IMS datasets using 3-best tissue wash protocols using sequential sections of from six artery tissues and randomized measurement sequence.

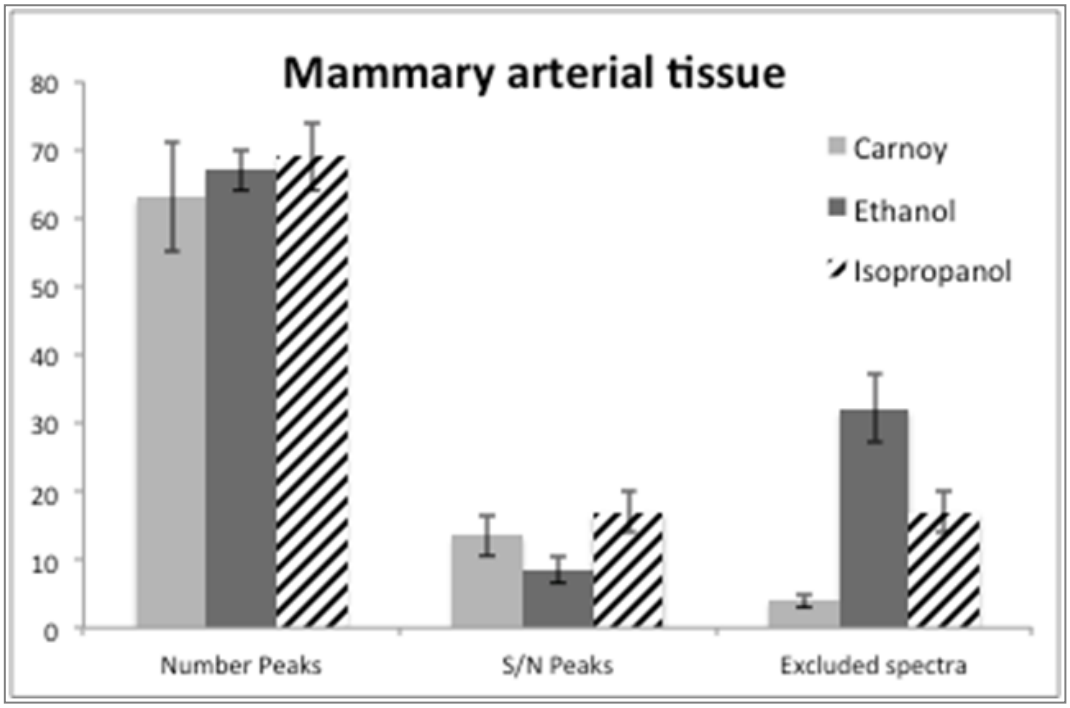

Supporting figure 2. Example MALDI MS images obtained from atherosclerotic carotid arteries for the different tissue washes. M=media, I=intima, and the insert number refers to the Pearson correlation coefficient for the correlation of the MS image with the media. Correlation coefficient calculated according to McDonnell *et al. J. Proteome Res.* **7**, 3619-3627 (2008).

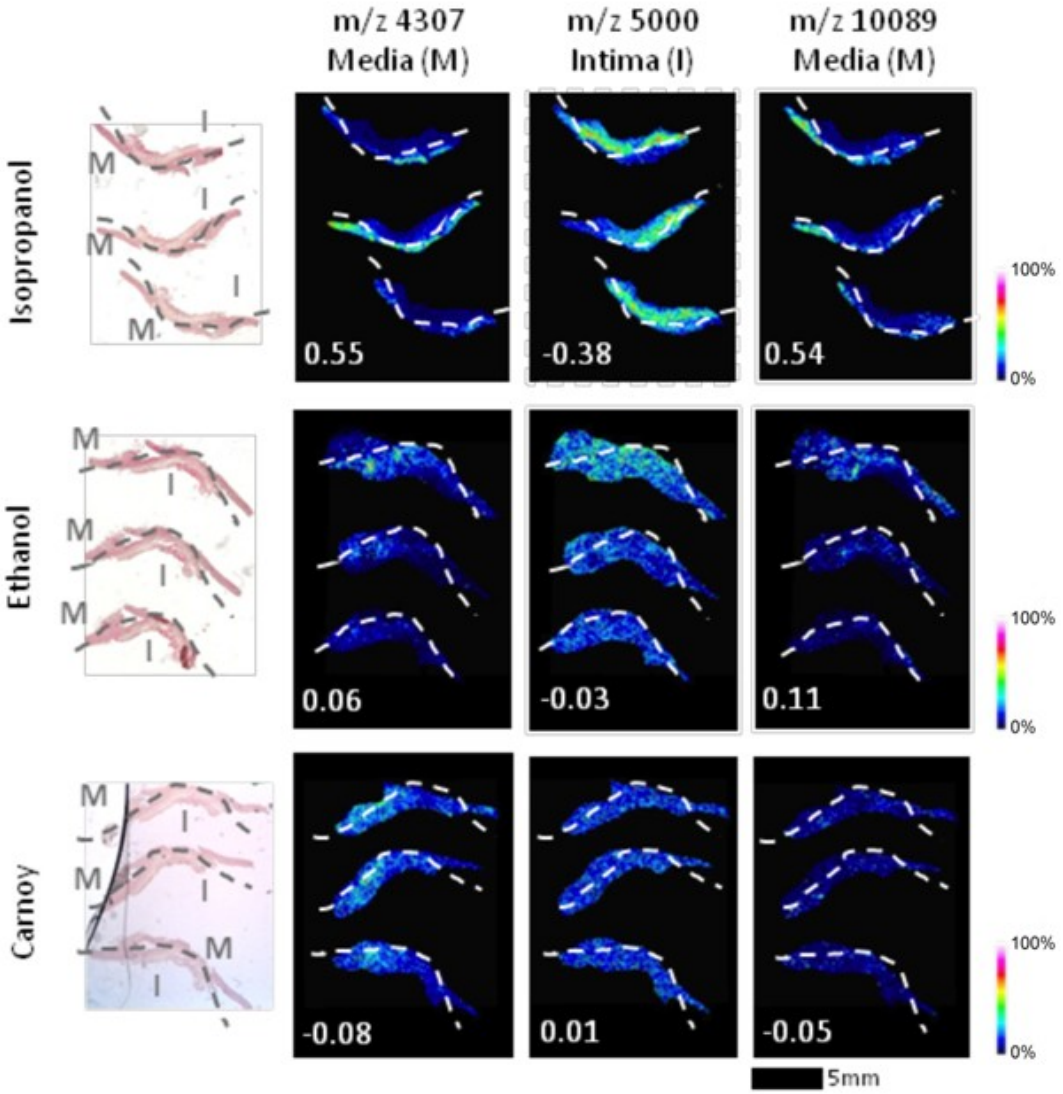

REFERENCES

1. Yang J, Caprioli RM. Matrix Sublimation/Recrystallization for Imaging Proteins by Mass Spectrometry at High Spatial Resolution. Anal Chem 2011;83:5728-5734.

2. Deutskens F, Yang J, Caprioli RM. High spatial resolution imaging mass spectrometry and classical histology on a single tissue section. J Mass Spectrom 2011;46:568-571.

3. Thomas A, Patterson NH, Laveaux Charbonneau J, Chaurand P. Orthogonal organic and aqueous-based washes of tissue sections to enhance protein sensitivity by MALDI imaging mass spectrometry. J Mass Spectrom 2013;48:42-8.

4. Seeley EH, Oppenheimer SR, Mi D, Chaurand P, Caprioli RM. Enhancement of protein sensitivity for MALDI imaging mass spectrometry after chemical treatment of tissue sections. J Am Soc Mass Spectrom 2008;19:1069-77.

Chapter 5

Molecular anatomy of ascending aorta in atherosclerosis by MS Imaging: specific lipid and protein patterns reflect pathology.

Running Title: New *ex vivo* imaging applied to atherosclerosis

Marta Martin-Lorenzo*, Benjamin Balluff, Aroa S. Maroto, Ricardo J. Carreira, Rene J.M. van Zeijl, Laura Gonzalez-Calero, Fernando de la Cuesta, Maria G Barderas, Luis F Lopez-Almodovar, Luis R Padial, Liam A. McDonnell, Fernando Vivanco, Gloria Alvarez-Llamas.*

Under Review. *Journal of Proteomics* Ref: JPROT-D-15-00238

El abordaje del estudio de la aterosclerosis directamente en tejido permite evaluar *in situ* los mecanismos y cambios sufridos por las arterias durante el desarrollo silente de la enfermedad. Numerosos trabajos han utilizado las arterias como un todo en lo que se denominan estudios de tejido completo en los que se realiza una extracción proteica del mismo tal y como se ha presentado previamente en esta tesis doctoral, dando lugar a la identificación de alteraciones en la fase subyacente de la aterosclerosis. Tratando de afinar y dando un paso más, las diferentes capas de la arteria se han analizando empelado microdisección por láser, centrando así las alteraciones particulares que ocurren en íntima y media en el desarrollo de enfermedad cardiovascular (*F. de la Cuesta et al.*). En este sentido, la técnica de espectrometría de imagen MALDI-MSI representa un paso más allá al permitir analizar las alteraciones del todo manteniendo la localización original dentro del vaso de dichas alteraciones.

La capacidad de analizar cientos de analitos simultáneamente para proporcionar mapas moleculares convierte al MALDI-MSI en una herramienta extremadamente valiosa en la investigación clínica. De hecho, esta técnica ya ha mostrado importantes contribuciones en la investigación de diferentes enfermedades como el cáncer permitiendo la identificación de nuevos marcadores, la evaluación de prognosis y supervivencia de los pacientes, el análisis de la heterogeneidad de los tumores o la respuesta a tratamientos farmacológicos. En el caso de la aterosclerosis el MALDI MSI se ha utilizado previamente en el estudio de perfiles lipídicos de las diferentes capas arteriales. En el trabajo presentado a continuación, en revisores en *Journal of Proteomics*, se aborda el análisis no sólo de lípidos sino también de proteínas como analitos de interés. Esto representa la primera aplicación proteómica de una nueva técnica *ex-vivo* de imagen que previamente ha sido puesta a punto tal y como se ha descrito en el capítulo anterior de esta tesis y que permite un análisis a alta resolución espacial (30µm) tal y como requieren las arterias dado su tamaño y sus estructuras internas. Los objetivos del estudio fueron principalmente dos, primero encontrar e identificar las moléculas características de la región de placa así como las de capa íntima y media y segundo evaluar la alteración de dichas moléculas en la aterosclerosis por comparación de tejido arterial control y patológico.

Los resultados obtenidos han dado lugar al primer mapa proteico diferenciando entre capa íntima y media y a un mapa lipídico que además de diferenciar entre capas es capaz de localizar lípidos específicos de zonas calcificadas previas a la formación de la placa aterosclerótica. Esto abre camino y pone de manifiesto la potencial aplicación de esta técnica de imagen molecular en el campo de las enfermedades cardiovasculares. Además, a falta de un estudio trasnacional a un fluido accesible y una ampliación a una cohorte superior de individuos, se propone la Timosina β4 localizada en la capa íntima y aumentada en aterosclerosis como posible marcador de la enfermedad y diana terapéutica.

ABSTRACT

The molecular anatomy of healthy and atherosclerotic tissue is pursued here to identify ongoing molecular changes in atherosclerosis development. Subclinical atherosclerosis cannot be predicted and novel therapeutic targets are needed. Mass Spectrometry Imaging (MSI) is a novel unexplored *ex vivo* imaging approach in CVD able to provide in-tissue molecular maps. A rabbit model of early atherosclerosis was developed and high-spatial-resolution MALDI-MSI was applied to comparatively analyze histologically-based arterial regions of interest from control and early atherosclerotic aortas. Specific protocols were applied to identify lipids and proteins significantly altered in response to atherosclerosis. Observed protein alterations were confirmed by immunohistochemistry in rabbit tissue, and additionally in human aortas. Molecular features specifically defining different arterial regions were identified. Localized in the intima, increased expression of SFA and lysolipids and intimal spatial organization showing accumulation of PI, PG and SM point to endothelial dysfunction and triggered inflammatory response. TG, PA, SM and PE-Cer were identified specifically located in calcified regions. Thymosin β4 (TMSB4X) protein was upregulated in intima *versus* media layer and also in response to atherosclerosis. This overexpression and localization was confirmed in human aortas. In conclusion, molecular histology by MS Imaging identifies spatial organization of arterial tissue in response to atherosclerosis.

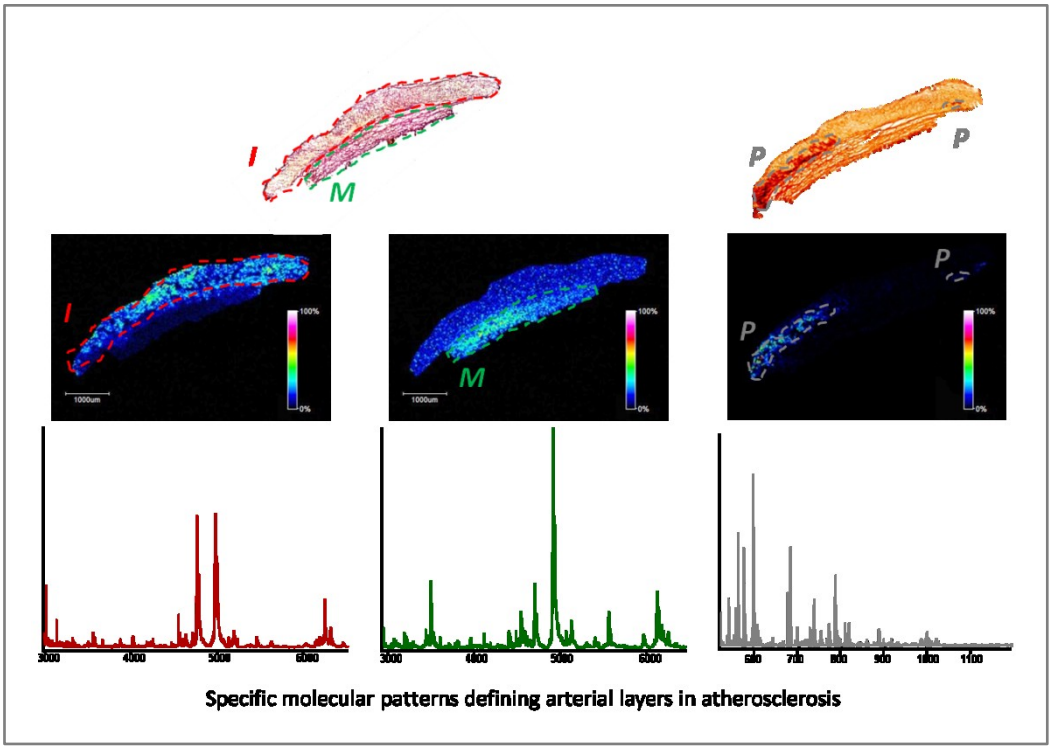

Specific molecular patterns defining arterial layers in atherosclerosis

INTRODUCTION

Atherosclerosis is usually the underlying cause of a fatal event (e.g. myocardial infarction, stroke) following the silent and progressive occlusion of the arteries. The lesion starts with the formation of fatty streaks and endothelial activation, followed by lipid accumulation and monocytes and platelets recruitment and inducing proliferation and migration of vascular smooth muscle cells (VSMC) from the media to the intima layer (1-3). Progressively, atheroma plaque develops silently and this complex scenario cannot be seen as a simple sequence of unrelated facts, but as a complex network of interconnected molecules involved in multiple reactions operating simultaneously (4, 5).Thus, mechanisms underlying atherosclerosis development are still not fully understood.

Molecule-specific localization is essential in the study of atherosclerosis disease, considering that specific alterations occur in the different arterial layers (intima and media). Spatial resolved mass spectrometry imaging (MSI) can generate molecular profiles directly from tissue, providing its molecular histology, allowing visualization of proteins, lipids and metabolites at their tissular location (6-8). Clinical investigation using spatial resolved mass spectrometry imaging has provided important contributions for a range of diseases (9, 10) in biomarker discovery, patient prognosis and survival (11, 12), response to treatment (13, 14) or evaluation of heterogeneous tumors (15, 16). In cardiovascular diseases, MALDI-MSI represents a novel *ex vivo* imaging tool to investigate atherosclerosis, offering the unique advantage to investigate the physiopathological changes taking place directly in-tissue and retaining the histopathological context of the observations. Importantly, MALDI-MSI allows high spatial integrity as demanded by the small dimensions of these structures.

Using MALDI-MSI, this is the first approach map combining proteins and lipids in the atherosclerotic lesion and healthy arterial tissue, pursuing a look into atherosclerotic mechanisms, and identification of novel therapeutic targets directly at tissue level and which may be potentially released to plasma.

MATERIAL AND METHODS

Animal model

A rabbit model of atherosclerosis was developed as previously published (17) . Briefly, twelve male New Zealand White rabbits were divided in two study groups fed with standard or cholesterol enriched diet. All animals were housed in individual cages in an air-conditioned room under a 12:12-h light-dark cycle. Principles of laboratory animal care were followed and all experimental procedures were approved by the Animal Care and Use Committee of the IIS-Fundación Jiménez Díaz, according to the guidelines for ethical care of the European Community. Animals were sacrificed after 13 weeks.

Tissue collection, matrix deposition and MSI spectral acquisition

We followed standard guidelines for tissue collection and preservation prior to MS imaging analysis (18, 19). In synthesis, the ascending aortic section of each animal was dissected, rinsed in phosphate-buffered saline and immediately snap frozen by immersion in liquid nitrogen without any fixation. Aortas samples were stored at -80 °C. For the MALDI-MSI experiments, a total of 36 tissue sections (3 sections per animal, 12 animals), 15 μm thick, were cut at − 22 °C and mounted onto indium-tin-oxide coated glass slides (Bruker Daltonik, Bremen, Germany) using a cryostat (Leica Mycrosystems GmbH, Wetzlar, Germany). The tissue sections (n=36) were stored at -80 °C before measurements, for which they were slowly brought to temperature in a freeze dryer. The matrix solution was uniformly deposited onto the washed tissue using the ImagePrep automated spraying device (Bruker Daltonik). MSI experiments were performed with an UltrafleXtreme MALDI-ToF (Bruker Daltonik), using 30 μm pixel size and 500 laser shots per pixel (100 laser shots per position of a random walk within each pixel) as previously described (20). Data acquisition and visualization were performed using FlexControl 3.0 and FlexImaging 2.1, respectively (both from Bruker Daltonik).

Three different MALDI-MSI protocols were applied for the detection of proteins (20), lipids (16) and metabolites (21, 22). Briefly, aortic tissue sections were washed in isopropanol by immersion prior to proteins analysis. A solution of 20mg/mL sinapinic acid (SA) in 10mL 4:4.2:1.8 acetonitrile:methanol:0.05% TFA was used as matrix. Spectra were acquired in linear positive mode. The m/z values measured were in the range from 2 to 20 kDa. As previously published (23) public libraries of MALDI-MSI data, MSiMass list database (24) and MaTisse (25) were used to assign identity of the most significantly altered protein molecular fearture using a mass tolerance of ±3Da, as commonly used cut-off criteria for tentative identification in maldi-msi experiments (26). Confirmation of protein identification was performed by IHC analysis as detailed below. For lipid analysis 20mg/mL DHB in 10mL 4:4.2:1.8 acetonitrile: methanol:0.05 % TFA was used as matrix. Spectra were acquired in reflector negative and positive mode in the mass range 500-1200Da. 9-Aminoacridine (9AA) (10mg/mL) in 70%MeOH was used for metabolites/lipids, and spectra were acquired in reflector negative mode in the mass range 0-1000 Da. For identity assignment, tissue samples were also analyzed on a 9.4T Solarix FT-ICR (BrukerDaltonik, Bremen, Germany) mass spectrometer. Lipid molecular identification was performed by using exact mass measurements, peak peaking and spatial filtering combined with Lipidsmap database using a tolerance of ≤ 0.005Da, as previously published (27, 28).

MALDI-MSI differential analysis of arterial layers and control/atherosclerotic tissue

Two approaches were performed by MALDI-MSI: 1) in depth comparison of histologically-distinct, regions of interest (media, intima, plaque), and 2) comparison of control and atherosclerotic tissue. For comparison between control and atherosclerotic tissue, only those masses specifically defining an arterial region of interest (intima, media, or plaque) were selected. Additionally, we selected only those present in a

minimum of two thirds of the total number of assayed samples. A random selection of the whole spectra sets from these regions were then imported into ClinProTools 3.0 (Bruker Daltonik) where they underwent smoothing, baseline substraction, mass spectral alignment and normalization. In both cases, proteins and lipids, recalibration was performed using 2000ppm of maximal peak shift and 10% match to calibrant peaks. The resulting peak intensity data was then subject to statistical analysis using GraphPad Prism (Graphpad Software, La Jolla, CA, USA). We performed D'Agostino-Pearson normality test but the number of values was too small. As Gaussian distribution could not be assumed, we perform more stringent Mann-Whitney non-parametric test to calculate p-values.

Histochemical analysis and correlation with MALDI-MSI images

After the MALDI experiments the remaining matrix was removed by immersion in a 70% ethanol solution. The tissue sections were then stained with hematoxylin and eosin (H&E) and scanned with a digital iScan Coreo slide scanner (Roche, Ventana Medical Systems Inc, Arizona,USA). In FlexImaging, the H&E stained sections were co-registered to the MALDI-MSI results to align mass spectrometric data with the histological features. Consecutive sections were subjected to H&E staining, red alizarin staining to visualize calcium deposits, and oil red staining to localize lipids. α-Actin (Dako) immunohistochemistry (IHC) was performed to localize vascular smooth muscle cells (VSMCs).

Human aortic tissue collection

Human healthy and atherosclerotic aortic tissues were from necropsy origin collected in a timeframe of 4-10h at Hospital Virgen de la Salud (Toledo, Spain). Tissue samples were obtained from 10 subjects (male:7 , average age: 76) with atherosclerotic lesions previously characterized (29) which show a well formed lipid core, presence of an inflammatory infiltrate, and evidence of sporadic calcification. Control arteries were obtained from 4 individuals who did not die from cardiovascular events and with no evidences of atherosclerotic lesions in any of the most frequently affected arteries (male: 2, average age: 48). Samples were immediately washed in saline, embedded in OCT, frozen with liquid nitrogen and stored at -80ºC until use. Procedures of sample collection were approved by the local ethics committee.

Immunohistochemistry analysis of TMSB4X in rabbit and human aortic tissue.

Sections of 4µm of formalin-fixed, paraffin-embedded FFPE rabbit aortic tissue from control (n=4) and pathological (n=4) were analyzed using a dilution 1/100 of primary antibody against TMSB4X (Abnova corporation). Sections of 6 µm of OCT embedded human aortas from control (n=4) and atherosclerotic tissue (n=10) were analyzed using a dilution of 1/10000 of primary antibody against TMSB4X (Abcam, Cambridge, UK). Detection was performed by using EnVision+DAB system (Dako). Image analysis of the staining was conducted with Image-Pro Plus software (Media Cybernetics, Inc). For this purpose the stained slides were scanned at X20 (human tissue) or X40 (rabbit

tissue) objective magnification in a digital slide scanner (iScan Coreo slide scanner, Roche, Ventana Medical Systems Inc, Arizona, USA).

RESULTS

A previously set-up methodology was here applied to identify specifically located alterations in response to atherosclerosis development (20). Control and atherosclerotic aortic tissues from animals were analyzed by MALDI-MSI. On average, around 150 and 200 m/z signals for proteins and lipids, respectively, were detected. Detected masses were evaluated in all spectra collected from 36 tissue sections (3 per animal) in two different approaches. Firstly, by comparing control and atherosclerotic samples and, secondly, by comparing the different regions defining within the samples (intima layer, media layer or calcified region). Molecular mass signals were found to correlate with the artery's anatomy as well as to be differently expressed in response to atherosclerosis. A total of 29 m/z values matched to a specific localization in the arterial tissue according to histology staining: a) intima layer, b) media layer or c) atheroma plaque as defined by calcified regions. Out of these 29 m/z values, 21 showed differential expression levels between intima and media layers with statistical significance. See supplementary data Table S1.

Molecular lipid maps define the anatomy of healthy and atherosclerotic arteries

Fifteen lipid molecular features (m/z) showed significant increase in atherosclerotic tissue (Table 1). Located in the calcified region PA(34:2), PA(34:1), SM(d16:1/17:0), SM(d18:1/15:0), PE-Cer(d14:1/22:0) and PE-Cer(d16:1/20:0) were identified (Figure 1). Located in the intima, we found SFA, SM(d17:1/24:1), SM(d18:2/23:0), PI(O-37:2), PI(P-37:1), PG(41:6), and lysolipids (Figure 2).

MALDI-MSI identifies Thymosin beta 4 overexpression in the intima layer of atherosclerotic tissue

The strongest and most significant alteration observed at the protein level with a fold change of 3.0 between healthy and atherosclerostic aortic tissue corresponded to the peak detected at m/z 4762 and tentatively identified as TMSB4X (Table 1). In this study, MALDI-MSI reveals TMSB4X to be significantly located in the intima layer, as shown in Figure 3A and 3B. IHC analysis of rabbit aortas confirmed TMSB4X expression in aortic tissue and localization in the intima (Figure 3C1, 3C2). This localization was further confirmed in human aortas (Figure 3D1, 3D2). Statistical analysis showed significantly increased expression of TMSB4X not only in the rabbit (Figure 3E-G) and human (Figure 3H) intima compared to media but also in rabbit atherosclerotic aortas (Figure 3I-K) and in human atherosclerotic aortas (Figure 3L) compared to healthy tissue, by MALDI-MSI and IHC.

MSI m/z	Molecule	Arterial localization			Atherosclerosis		
		Intima	Plaque	p-value	Trend	Fold Change (P/C)	p-value
Proteins							
4762	TMSB4X	x		**0.0303**	↑	3.00	**0.0022**
Lipids							
255	SFA	x		**0.0152**	↑	4.98	**0.0022**
518	lysolipids	x		**0.0022**	↑	8.74	**0.0022**
520	lysolipids	x		**0.0260**	↑	4.58	**0.0260**
522	lysolipids	x		**0.0022**	↑	5.64	**0.0022**
675	PA(34:2)		x^P	0.0667	↑	6.84	**0.0190**
676	PA(34:1)		x^P	0.1143	↑	4.61	**0.0381**
691	SM(d16:1/17:0)/ SM(d18:1/15:0)/ PE-Cer(d14:1/22:0)/ PE-Cer(d16:1/20:0)		x^P	0.0667	↑	4.43	**0.0381**
800	SM(d17:1/24:1)/ SMd18:1/23:0	x		**0.0022**	↑	3.74	**0.0022**
838	PG(41:6)	x		**0.0411**	↑	3.42	**0.0022**
864	PI(O-37:2) PI(P-37:1)	x		**0.0087**	↑	9.77	**0.0022**
895	TG		x^P	0.3874	↑	1.51	0.1320

Table 1. Molecules with specific localization in the intima or calcified region here identified by MSI are shown in arterial localization column. Molecular comparison between healthy and atherosclerotic tissues is also included (right column): ↑ increased in atherosclerosis; ↓ decreased in atherosclerosis; P: pathologic (atherosclerotic) tissue; C: control (healthy) tissue; X^P: localized in calcified region (plaque) Bold numbers show statistical significance (p value <0.05, Mann-Whitney test).

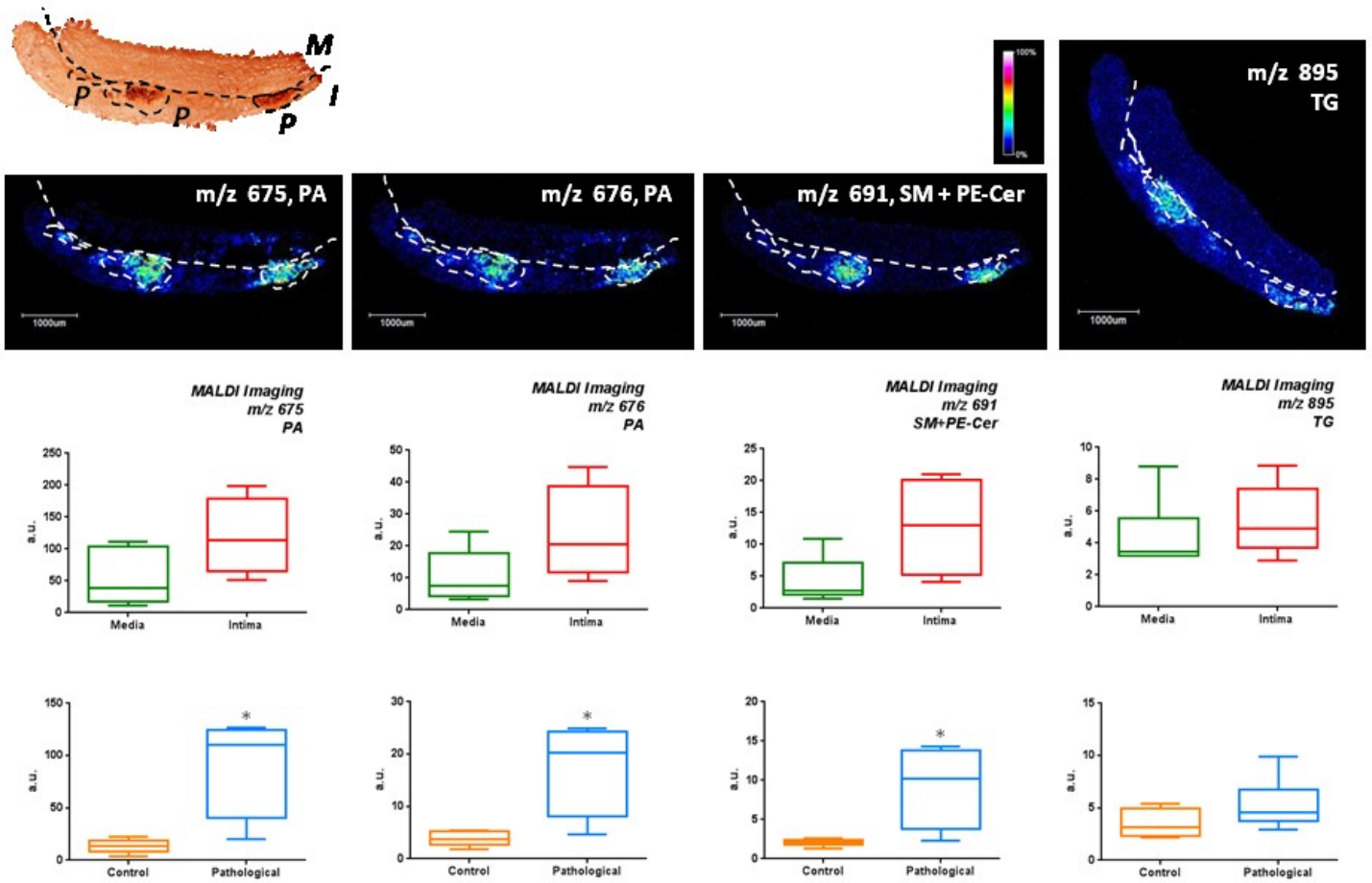

Figure 1. **Lipids defining calcified region in rabbit arterial tissue**. Histological annotation was made using Red Alizarin (M: media layer, I: intima layer, P: calcified plaque region) (A). MALDI-MSI reveals PA (m/z 675 (B1) and m/z 676 (B2)), SM+PE-Cer (m/z 691) (B3) and TG (m/z 895) (B4) localization in the intima. Significantly overexpression in intima versus media (C1-4) and in atherosclerotic aortas compared to healthy tissue (D1-4) were also found. *: p-value<0.05.

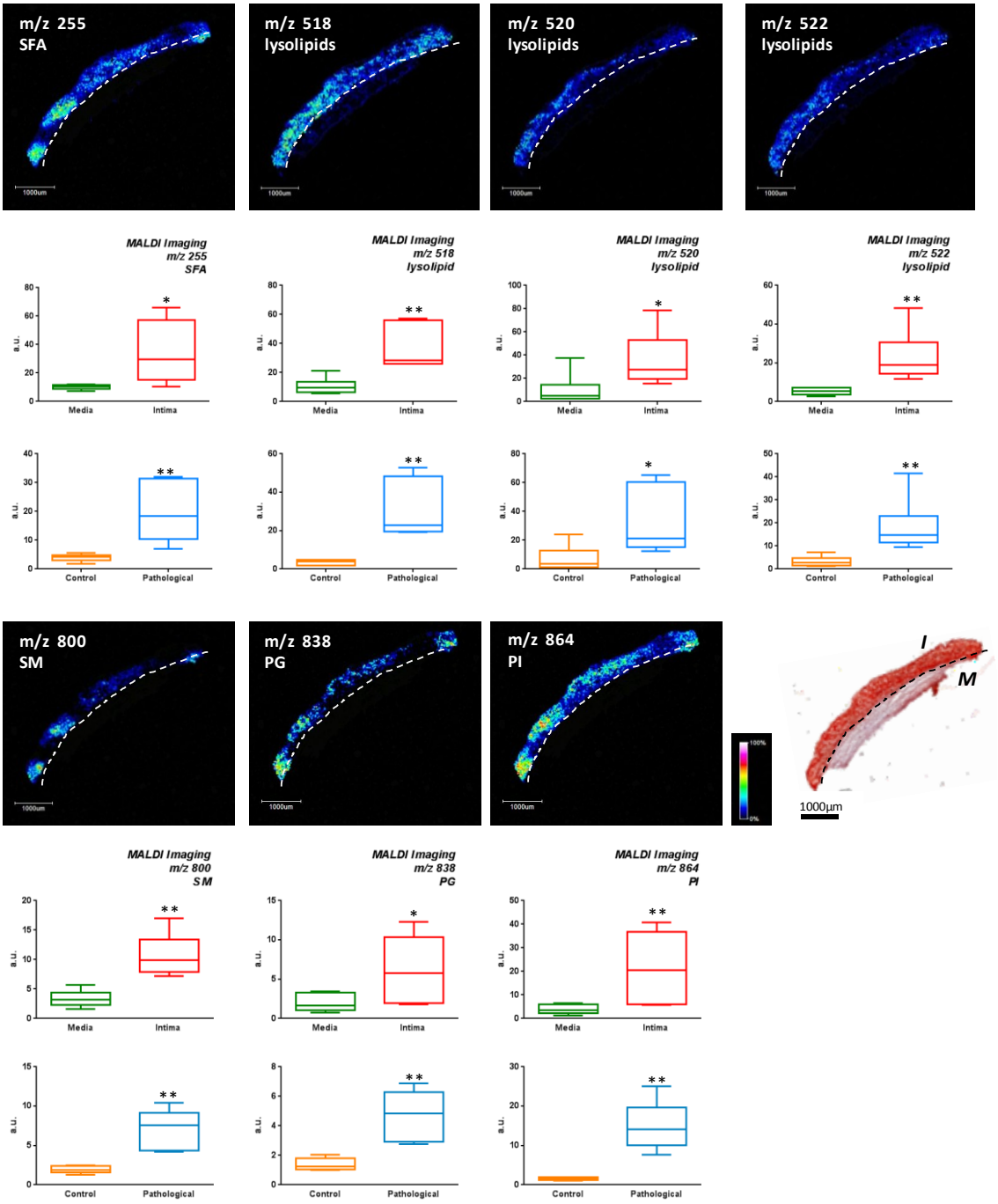

Figure 2. Lipids defining intima layer in rabbit arterial tissue. MALDI-MSI reveals SFA (m/z 255) (A1) and lysolipids (m/z 518 (A2), 520 (A3) and 522 (A4)) localization in the intima. Significantly overexpression in intima versus media (B1-4) and in atherosclerotic aortas compared to healthy tissue were also found (C1-4). The same localization (D1-3) and trends (E1-3 and F1-3) were observed for SM (m/z 800), PG (m/z 838) and PI (m/z 864). Oil Red tissue staining was used for histological annotation (M:Media, I: Intima) (G). *: p-value<0.05. **: p-value<0.005

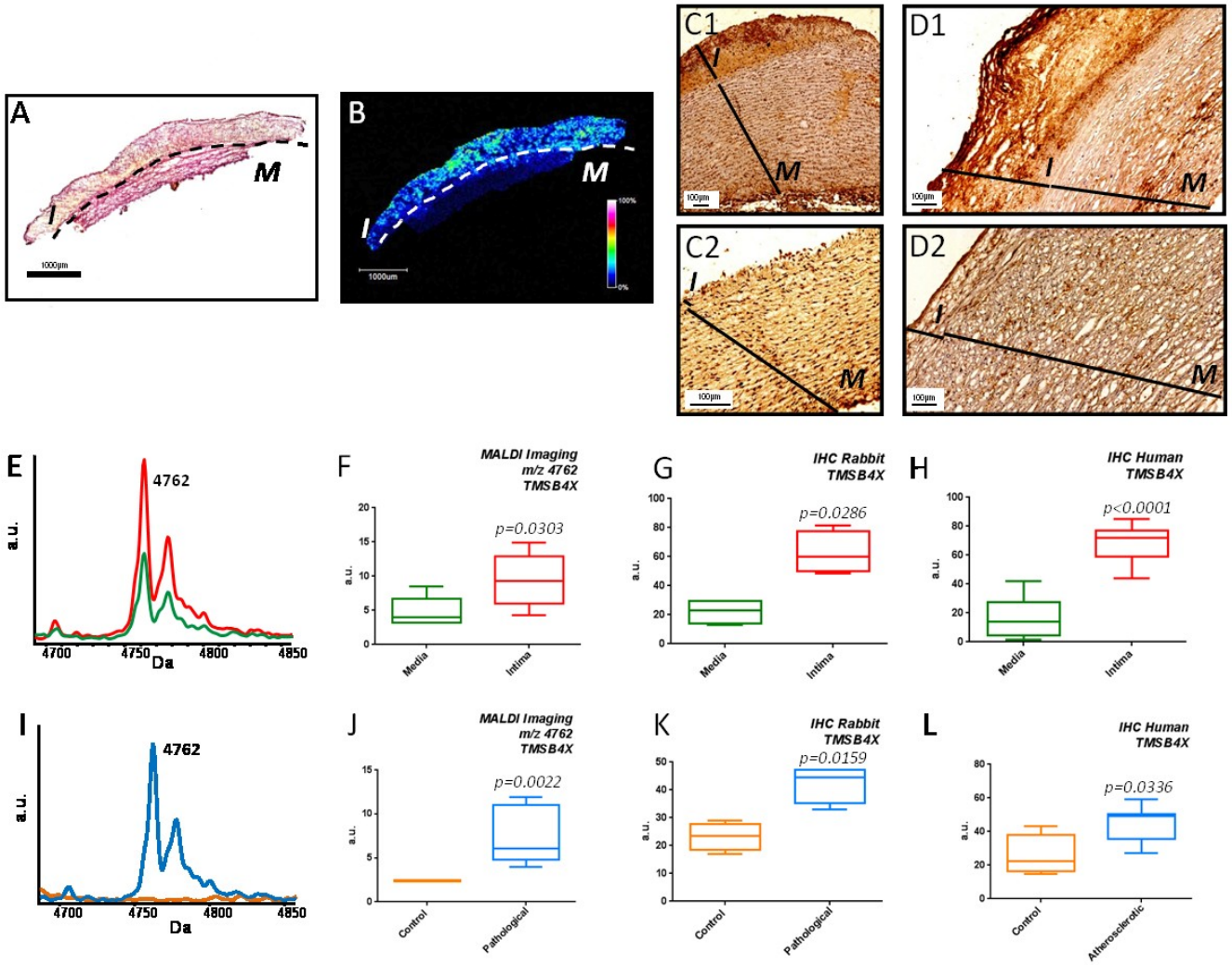

Figure 3. TMSB4X is overexpressed in intima layer and in atherosclerosis condition as shown by MALDI-MSI and confirmed by IHC. A) Representative rabbit atherosclerotic aorta (H&E staining). B) MALDI-MSI reveals TMSB4X (m/z 4762) localization in the rabbit aortic intima, confirmed by IHC (10X) (C1: pathological, C2: control). Translational studies confirm TMSB4X localization in human aortic intima by IHC (D1: atherosclerotic, D2: control). E) Overlapped intensity spectra obtained for m/z 4762 in the rabbit intima (red) and media (green) layers. The observed overexpression in the rabbit intima by MALDI-MSI (F) and by IHC in rabbit (G) and human (H) was significant in all cases. Significantly overexpression of TMSB4X in rabbit atherosclerotic aortas (blue) compared to healthy tissue (yellow) was also found (I, J, K, L)

DISCUSSION

We show here for the first time a combined molecular map of proteins and lipids in their original localization in healthy and atherosclerotic arterial tissue. This has been accomplished by means of new imaging technique MALDI-MSI particularly operated in high spatial resolution mode, which enables to differentiate, not only intima and media arterial layers, but also specific regions within the intima as calcified regions.

We found that the intima layer as a whole is characterized by increased levels of SFA, lysolipids, PI, PG and SM, which were not only differentially present in this layer but also significantly increased in atherosclerotic tissue, which could suggest a response to initial endothelial dysfunction and inflammatory process (Figure 2) (30). Accumulation of SFA and observed increased in atherosclerotic tissue is in agreement with previously reported endothelial dysfunction caused by SFA in vitro, including pro-inflammatory signaling and apoptosis (31). Overexpression of lysolipids in the intima layer in response to atherosclerosis may negatively affect endothelial regeneration after injury by impairment of endothelium-dependent relaxation (32, 33). PI clearly increases in atherosclerotic intima in relation with monocyte activation and matrix metalloproteinase production. PG also localizes in the intima increasing in response to atherosclerosis development, which is in agreement with a preferential recognition and internalization of negatively charged lipids by macrophages (34, 35). SM represents an independent risk factor of cardiovascular diseases (36-38) and we show here how SM accumulates in the intima, either from circulating SM or from in-situ synthesis (38, 39).

Following endothelium dysfunction, and recruitment of monocytes and macrophages, these cells start accumulating low-density lipoprotein (LDL) and transform themselves into foam cells. In advanced lesions, necrosis of macrophages and VSMCs forms a protective fibrous cap surrounding a lipid-rich core. The LDL present in the lipid core are mainly composed of cholestearyl esters and TG in an apolar core (40, 41), and surrounded by a polar monolayer of phospholipids in the surface (42). According to the MALDI-MSI data shown here, TG, glycerophospholipids (PA) and sphingolipids (SM and PE-Cer) are located in calcified regions (Figure 1). It is described that lysophosphatidic acids (LPA) typically accumulate in the lipid rich-core lesion of the atheromas by two ways: a) deposited directly by LDL-ox and b) from the PG of macrophages and VSMCs present in developing atherosclerosis (43-45). We show here localization of PA in calcified areas, which are most commonly synthesized from acylation of LPA. Additionally, local SM production involve ceramides (46), and PE-Cer were identified here in the intima calcified region correlating with mentioned in-situ synthesis of SM. Figure 4 summarizes MALDI-MSI main findings related to arterial spatial organization.

TMSB4X protein was here identified to be specifically localized in the intima layer and significantly increased in atherosclerotic tissue. TMSB4X is not secreted by a classical pathway (it could be through microvesicles) and it is present in the cytoplasm of circulating cells, with high levels in platelets, which are key mediators in acute coronary

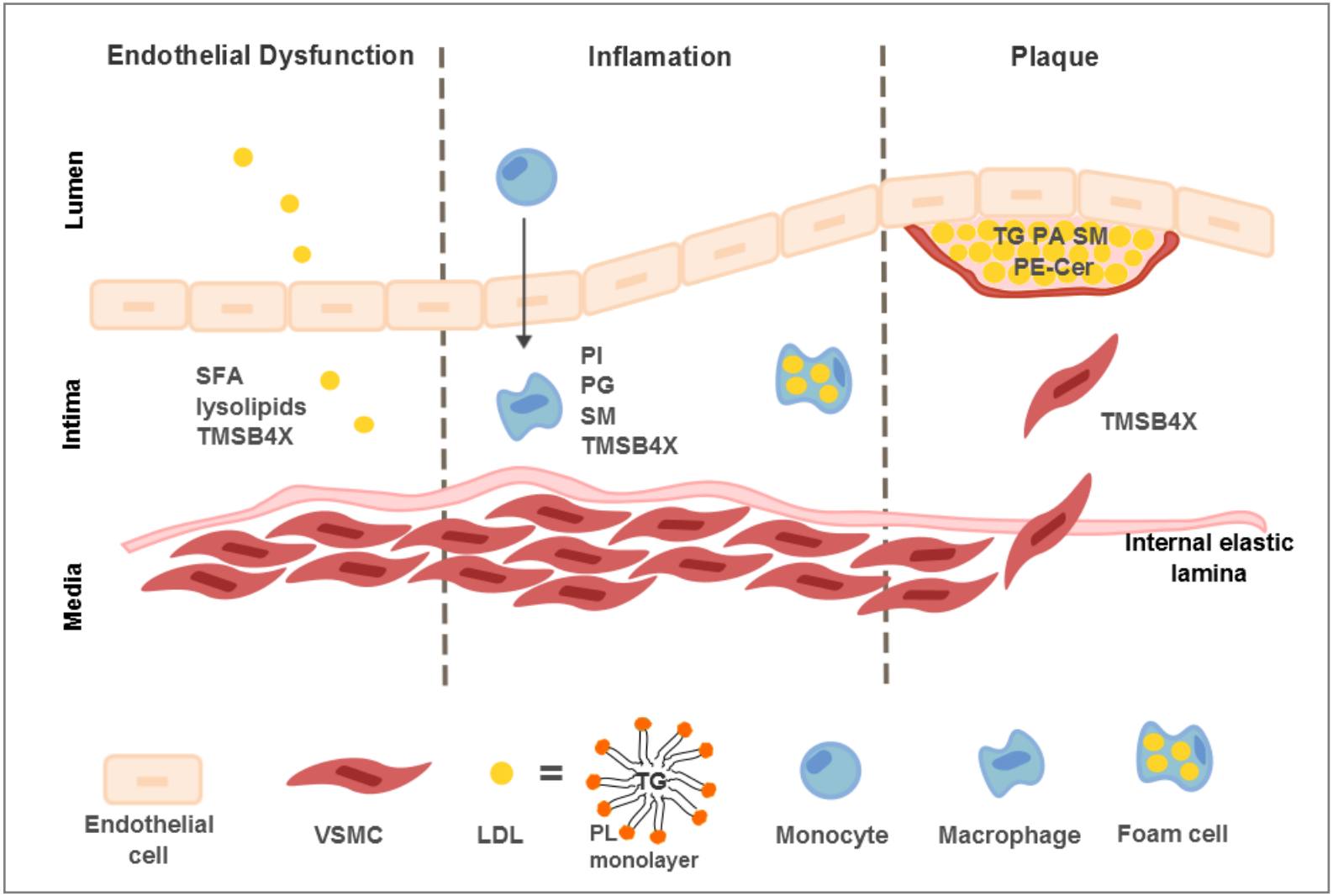

Figure 4. Overview of the specific arterial location of lipids and TMSB4X protein identified here by MALDI-MSI.

syndrome. TMSB4X plays a role in the organization of the actin cytoskeleton, down-regulation of inflammatory chemokines and cytokines, and promotion of cell migration, and blood vessel formation, among others. In atherosclerosis, an initial inflammatory response is triggered and inflammation takes active part in all stages of pathology development (47). Additionally, endothelial dysfunction, monocyte adhesion and migration into the subendothelial space, modification into macrophages and foam cells and proliferation of vascular smooth muscle cells within the intima are known process in initial stages which further progress to in-depth arterial remodeling. In this context, physiological roles attributed to TMSB4X are in consonance with a protective role (48). TMSB4X has been found expressed in human aorta localized closely to tissue damage and clot areas (49, 50) and a potential clinical use has also been previously suggested in view of TMSB4X wound healing properties (51). We show here specific location of TMSB4X in the intima layer and up-regulation in pathological condition by MALDI-MSI and IHC in rabbit. In human aortas, up-regulation could be confirmed despite of the age difference between the subjects from whom the atherosclerotic lesions were obtained and the individuals from whom control aortas were taken. This difference should be acknowledged, as it could be affecting the observed differences between both groups as ageing affects vascular wall by mechanisms independent of atherosclerosis. TMSB4X down-regulation was observed in blood from acute myocardial infarction patients (52). Together with the increased levels here found in tissue, it is suggested an accumulation of circulating plasma thymosin into de arteries, that stay in the intima layer according to IHC, and reinforces the wound repair role and its clinical use as a potential therapy target previously suggested for this protein. This is the first time the localization of TMSB4X has been shown. Further studies in individual subjects should follow to further confirm previous observation in blood, which points to a potential translation of TMSB4X overexpression here localized in atherosclerotic intima into a molecular response measurable in plasma.

Is important to stand out the main limitation of the study, which is the absence of a direct application to human non-invasive diagnosis so far. In this sense, mass spectrometry imaging is in a developing stage. However, it already allows investigating molecular dynamics taking place in-situ, inside the artery, even at initial stages when advanced plaques have not been yet developed. Additional studies should follow to confirm a potential use of TMSB4X as marker of subjacent atherosclerosis.

CONCLUSIONS

MALDI-MSI is proved here to be a new powerful imaging technique, especially when operated in high spatial resolution mode, offering simultaneous analysis of dozens of molecules, visualization of in-tissue molecular profiles and identification of main altered features in a specific location inside the artery, pursuing a step further in the full understanding of the mechanisms involved in atherosclerosis. This is the first time that MSI allows the identification of a specific distribution map for TMSB4X in this clinical scenario.

ACKNOWLEDGEMENTS

This work is financially supported by the Cyttron II project "Imaging Mass Spectrometry", ISCIII (PI11/01401, PI13/01873, CP09/00229) and IDCSalud. MML is funded by Fundación Conchita Rabago and gratefully acknowledges the travel funding supplied by SePROT and COST Action BM1104 for the Short Term Scientific Missions to LUMC. BB and RC are funded by Marie Curie Actions of the European Union (BB No. 331866, SITH FP7-PEOPLE-2012-IEF, RC No. 303344, ENIGMAS FP7-PEOPLE-2011-IEF).

REFERENCES

[1] Hansson GK, Robertson AK, Soderberg-Naucler C. Inflammation and atherosclerosis. Annu Rev Pathol 2006;1:297-329.

[2] Virmani R, Kolodgie FD, Burke AP, Farb A, Schwartz SM. Lessons from sudden coronary death: a comprehensive morphological classification scheme for atherosclerotic lesions. Arterioscler Thromb Vasc Biol 2000 May;20(5):1262-75.

[3] Libby P, Aikawa M. Stabilization of atherosclerotic plaques: new mechanisms and clinical targets. Nat Med 2002 Nov;8(11):1257-62.

[4] Corti R, Hutter R, Badimon JJ, Fuster V. Evolving concepts in the triad of atherosclerosis, inflammation and thrombosis. J Thromb Thrombolysis 2004 Feb;17(1):35-44.

[5] Libby P, Theroux P. Pathophysiology of coronary artery disease. Circulation 2005 Jun 28;111(25):3481-8.

[6] Chaurand P, Sanders ME, Jensen RA, Caprioli RM. Proteomics in diagnostic pathology: profiling and imaging proteins directly in tissue sections. Am J Pathol 2004 Oct;165(4):1057-68.

[7] Cornett DS, Reyzer ML, Chaurand P, Caprioli RM. MALDI imaging mass spectrometry: molecular snapshots of biochemical systems. Nat Methods 2007 Oct;4(10):828-33.

[8] McDonnell LA, Heeren RM. Imaging mass spectrometry. Mass Spectrom Rev 2007 Jul;26(4):606-43.

[9] Balluff B, Schone C, Hofler H, Walch A. MALDI imaging mass spectrometry for direct tissue analysis: technological advancements and recent applications. Histochem Cell Biol 2011 Sep;136(3):227-44.

[10] Neubert P, Walch A. Current frontiers in clinical research application of MALDI imaging mass spectrometry. Expert Rev Proteomics 2013 Jun;10(3):259-73.

[11] Balluff B, Rauser S, Meding S, Elsner M, Schone C, Feuchtinger A, et al. MALDI imaging identifies prognostic seven-protein signature of novel tissue markers in intestinal-type gastric cancer. Am J Pathol 2011 Dec;179(6):2720-9.

[12] Hardesty WM, Kelley MC, Mi D, Low RL, Caprioli RM. Protein signatures for survival and recurrence in metastatic melanoma. J Proteomics 2011 Jun 10;74(7):1002-14.

[13] Aichler M, Elsner M, Ludyga N, Feuchtinger A, Zangen V, Maier SK, et al. Clinical response to chemotherapy in oesophageal adenocarcinoma patients is linked to defects in mitochondria. J Pathol 2013 Aug;230(4):410-9.

[14] Reyzer ML, Caldwell RL, Dugger TC, Forbes JT, Ritter CA, Guix M, et al. Early changes in protein expression detected by mass spectrometry predict tumor response to molecular therapeutics. Cancer Res 2004 Dec 15;64(24):9093-100.

[15] Jones EA, Schmitz N, Waaijer CJ, Frese CK, van Remoortere A, van Zeijl RJ, et al. Imaging Mass Spectrometry-based Molecular Histology Differentiates Microscopically Identical and Heterogeneous Tumors. J Proteome Res 2013 Mar 25.

[16] Willems SM, van RA, van ZR, Deelder AM, McDonnell LA, Hogendoorn PC. Imaging mass spectrometry of myxoid sarcomas identifies proteins and lipids specific to tumour type and grade, and reveals biochemical intratumour heterogeneity. J Pathol 2010 Dec;222(4):400-9.

[17] Martin-Lorenzo M, Zubiri I, Maroto A, Gonzalez-Calero L, Posada-Ayala M, de la Cuesta F, et al. KLK1 and ZG16B proteins and arginine-proline metabolism identified as novel targets to monitor atherosclerosis, acute coronary syndrome and recovery. Metabolomics 2014.

[18] Chughtai K, Heeren RM. Mass spectrometric imaging for biomedical tissue analysis. Chem Rev 2010 May 12;110(5):3237-77.

[19] Meding S, Walch A. MALDI imaging mass spectrometry for direct tissue analysis. Methods Mol Biol 2013;931:537-46.

[20] Martin-Lorenzo M, Balluff B, Sanz-Maroto A, van Zeijl RJ, Vivanco F, Alvarez-Llamas G, et al. 30mum spatial resolution protein MALDI MSI: In-depth comparison of five sample preparation protocols applied to human healthy and atherosclerotic arteries. J Proteomics 2014 Aug 28;108:465-8.

[21] Jones EA, Shyti R, van Zeijl RJ, van Heiningen SH, Ferrari MD, Deelder AM, et al. Imaging mass spectrometry to visualize biomolecule distributions in mouse brain tissue following hemispheric cortical spreading depression. J Proteomics 2012 Aug 30;75(16):5027-35.

[22] Dekker TJ, Jones EA, Corver WE, van Zeijl RJ, Deelder AM, Tollenaar RA, et al. Towards imaging metabolic pathways in tissues. Anal Bioanal Chem 2014 Nov 9.

[23] Dekker TJ, Balluff BD, Jones EA, Schone CD, Schmitt M, Aubele M, et al. Multicenter Matrix-Assisted Laser Desorption/Ionization Mass Spectrometry Imaging (MALDI MSI) Identifies Proteomic Differences in Breast-Cancer-Associated Stroma. J Proteome Res 2014 Nov 7;13(11):4730-8.

[24] McDonnell LA, Walch A, Stoeckli M, Corthals GL. MSiMass List: A Public Database of Identifications for Protein MALDI MS Imaging. J Proteome Res 2013 Dec 13.

[25] Maier SK, Hahne H, Gholami AM, Balluff B, Meding S, Schoene C, et al. Comprehensive identification of proteins from MALDI imaging. Mol Cell Proteomics 2013 Oct;12(10):2901-10.

[26] Balluff B, Rauser S, Meding S, Elsner M, Schone C, Feuchtinger A, et al. MALDI imaging identifies prognostic seven-protein signature of novel tissue markers in intestinal-type gastric cancer. Am J Pathol 2011 Dec;179(6):2720-9.

[27] Chughtai K, Jiang L, Greenwood TR, Glunde K, Heeren RM. Mass spectrometry images acylcarnitines, phosphatidylcholines, and sphingomyelin in MDA-MB-231 breast tumor models. J Lipid Res 2013 Feb;54(2):333-44.

[28] Schiller J, Zschornig O, Petkovic M, Muller M, Arnhold J, Arnold K. Lipid analysis of human HDL and LDL by MALDI-TOF mass spectrometry and (31)P-NMR. J Lipid Res 2001 Sep;42(9):1501-8.

[29] de la Cuesta F, Alvarez-Llamas G, Maroto AS, Donado A, Zubiri I, Posada M, et al. A proteomic focus on the alterations occurring at the human atherosclerotic coronary intima. Mol Cell Proteomics 2011 Apr;10(4):M110.

[30] De Caterina R, Liao JK, Libby P. Fatty acid modulation of endothelial activation. Am J Clin Nutr 2000 Jan;71(1 Suppl):213S-23S.

[31] Harvey KA, Walker CL, Pavlina TM, Xu Z, Zaloga GP, Siddiqui RA. Long-chain saturated fatty acids induce pro-inflammatory responses and impact endothelial cell growth. Clin Nutr 2010 Aug;29(4):492-500.

[32] Murugesan G, Fox PL. Role of lysophosphatidylcholine in the inhibition of endothelial cell motility by oxidized low density lipoprotein. J Clin Invest 1996 Jun 15;97(12):2736-44.

[33] Choy PC, Siow YL, Mymin D, O K. Lipids and atherosclerosis. Biochem Cell Biol 2004 Feb;82(1):212-24.

[34] Ahsan F, Rivas IP, Khan MA, Torres Suarez AI. Targeting to macrophages: role of physicochemical properties of particulate carriers--liposomes and microspheres--on the phagocytosis by macrophages. J Control Release 2002 Feb 19;79(1-3):29-40.

[35] Fidler IJ, Raz A, Fogler WE, Kirsh R, Bugelski P, Poste G. Design of liposomes to improve delivery of macrophage-augmenting agents to alveolar macrophages. Cancer Res 1980 Dec;40(12):4460-6.

[36] Tabas I. Sphingolipids and atherosclerosis: a mechanistic connection? A therapeutic opportunity? Circulation 2004 Nov 30;110(22):3400-1.

[37] Jiang XC, Paultre F, Pearson TA, Reed RG, Francis CK, Lin M, et al. Plasma sphingomyelin level as a risk factor for coronary

artery disease. Arterioscler Thromb Vasc Biol 2000 Dec;20(12):2614-8.

[38] Nelson JC, Jiang XC, Tabas I, Tall A, Shea S. Plasma sphingomyelin and subclinical atherosclerosis: findings from the multi-ethnic study of atherosclerosis. Am J Epidemiol 2006 May 15;163(10):903-12.

[39] Chatterjee S. Sphingolipids in atherosclerosis and vascular biology. Arterioscler Thromb Vasc Biol 1998 Oct;18(10):1523-33.

[40] Stegemann C, Drozdov I, Shalhoub J, Humphries J, Ladroue C, Didangelos A, et al. Comparative lipidomics profiling of human atherosclerotic plaques. Circ Cardiovasc Genet 2011 Jun;4(3):232-42.

[41] Zaima N, Sasaki T, Tanaka H, Cheng XW, Onoue K, Hayasaka T, et al. Imaging mass spectrometry-based histopathologic examination of atherosclerotic lesions. Atherosclerosis 2011 Apr 9.

[42] Prassl R. Human low density lipoprotein: the mystery of core lipid packing. J Lipid Res 2011 Feb;52(2):187-8.

[43] Spector AA. Plaque rupture, lysophosphatidic acid, and thrombosis. Circulation 2003 Aug 12;108(6):641-3.

[44] Siess W, Zangl KJ, Essler M, Bauer M, Brandl R, Corrinth C, et al. Lysophosphatidic acid mediates the rapid activation of platelets and endothelial cells by mildly oxidized low density lipoprotein and accumulates in human atherosclerotic lesions. Proc Natl Acad Sci U S A 1999 Jun 8;96(12):6931-6.

[45] Pages C, Simon MF, Valet P, Saulnier-Blache JS. Lysophosphatidic acid synthesis and release. Prostaglandins Other Lipid Mediat 2001 Apr;64(1-4):1-10.

[46] Bismuth J, Lin P, Yao Q, Chen C. Ceramide: a common pathway for atherosclerosis? Atherosclerosis 2008 Feb;196(2):497-504.

[47] Libby P, Ridker PM, Maseri A. Inflammation and atherosclerosis. Circulation 2002 Mar 5;105(9):1135-43.

[48] Wei C, Kumar S, Kim IK, Gupta S. Thymosin beta 4 protects cardiomyocytes from oxidative stress by targeting anti-oxidative enzymes and anti-apoptotic genes. PLoS One 2012;7(8):e42586.

[49] Huff T, Otto AM, Muller CS, Meier M, Hannappel E. Thymosin beta4 is released from human blood platelets and attached by factor XIIIa (transglutaminase) to fibrin and collagen. FASEB J 2002 May;16(7):691-6.

[50] Huo Y, Ley KF. Role of platelets in the development of atherosclerosis. Trends Cardiovasc Med 2004 Jan;14(1):18-22.

[51] Philp D, Kleinman HK. Animal studies with thymosin beta, a multifunctional tissue repair and regeneration peptide. Ann N Y Acad Sci 2010 Apr;1194:81-6.

[52] Yesilay AB, Karakurt O, Akdemir R, Erden G, Kilic H, Acikel S, et al. Thymosin beta4 levels after successful primary percutaneous coronary intervention for acute myocardial infarction. Turk Kardiyol Dern Ars 2011 Dec;39(8):654-60.

SUPPLEMENTAL MATERIAL

Supplementary Table S1. MALDI-MSI m/z values with specific localization in the intima or media layer are shown (left column): X^P means specifically located in the calcified region of the intima layer. Comparison between healthy and atherosclerotic tissues is also included (right column): ↑ increased in atherosclerosis; ↓ decreased in atherosclerosis; P: pathologic (atherosclerotic) tissue; C: control (healthy) tissue. Bold numbers show statistical significance (p value <0.05, Mann-Whitney test). Identification was performed by FT-ICR measurements, MaTisse database, MSiMass list database and literature [J Lipid Res. 2013 Feb;54(2):333-44] [J Lipid Res. 2001 42:1501-1508].

m/z	Arterial localization			Atherosclerosis			Molecule
	Media	Intima	p-value	Trend	Fold Change (P/C)	p-value	
PROTEINS							
3011		x	**0.0108**	↑	1.67	**0.0022**	SEL1L, IQGAP1, GANAB, NCSTN, UGDH, CYBA, YWHAG, MIF, EIF2S3, SYNM, ITGA5, NDUFS7, COL12A1, VASN, EEF1A1, MYBPC1, HBA1-2, ENO1, UBA1, CA3, MUC5B
3553	x		**0.0022**	↓	0.64	**0.0152**	NSF, PSMC4, ACTB, MYL2, PKM2, HSPD1
3569	x		**0.0022**	↓	0.67	**0.0303**	DHRS7, ACTB, MYL2, PKM2, ERP44, S100A6
4597	x		**0.0022**	↓	0.92	0.4589	-
4614	x		**0.0022**	↓	0.93	0.6494	HBB
4762		x	**0.0303**	↑	3.00	**0.0022**	TMSB4X
4778		x	**0.0303**	↑	2.07	**0.0022**	-
5620	x		**0.0022**	↓	0.58	**0.0087**	-
6182	x		**0.0022**	↓	0.49	**0.0022**	-
6199	x		**0.0022**	↓	0.57	**0.0152**	-
LIPIDS							
255		x	**0.0152**	↑	4.98	**0.0022**	SFA
518		x	**0.0022**	↑	8.74	**0.0022**	lysolipids
520		x	**0.0260**	↑	4.58	**0.0260**	lysolipids
522		x	**0.0022**	↑	5.64	**0.0022**	LPC (0:0/18:1), lysolipids
535		X^P	**0.0381**	↑	4.21	**0.0381**	-
536		x^P	0.3524	↑	1.42	0.1714	-
568		x^P	0.1714	↑	3.57	0.0667	-
675		x^P	0.0667	↑	6.84	**0.0190**	PA
676		x^P	0.1143	↑	4.61	**0.0381**	PA+PG
691		x^P	0.0667	↑	4.43	**0.0381**	SM+PA+PE-Cer
722		x^P	0.1143	↑	4.76	0.1143	PC+PE
800		x	**0.0022**	↑	3.74	**0.0022**	SM
838		x	**0.0411**	↑	3.42	**0.0022**	-
864		x	**0.0087**	↑	9.77	**0.0022**	PG
865		x	**0.0087**	↑	6.54	**0.0022**	PI
866		x	**0.0260**	↑	1.03	**0.0022**	PC
891		x	0.0931	↑	6.52	**0.0022**	Glc-GP+PI
893		x	**0.0433**	↑	6.18	**0.0411**	PS
895		x^P	0.3874	↑	1.51	0.1320	TG

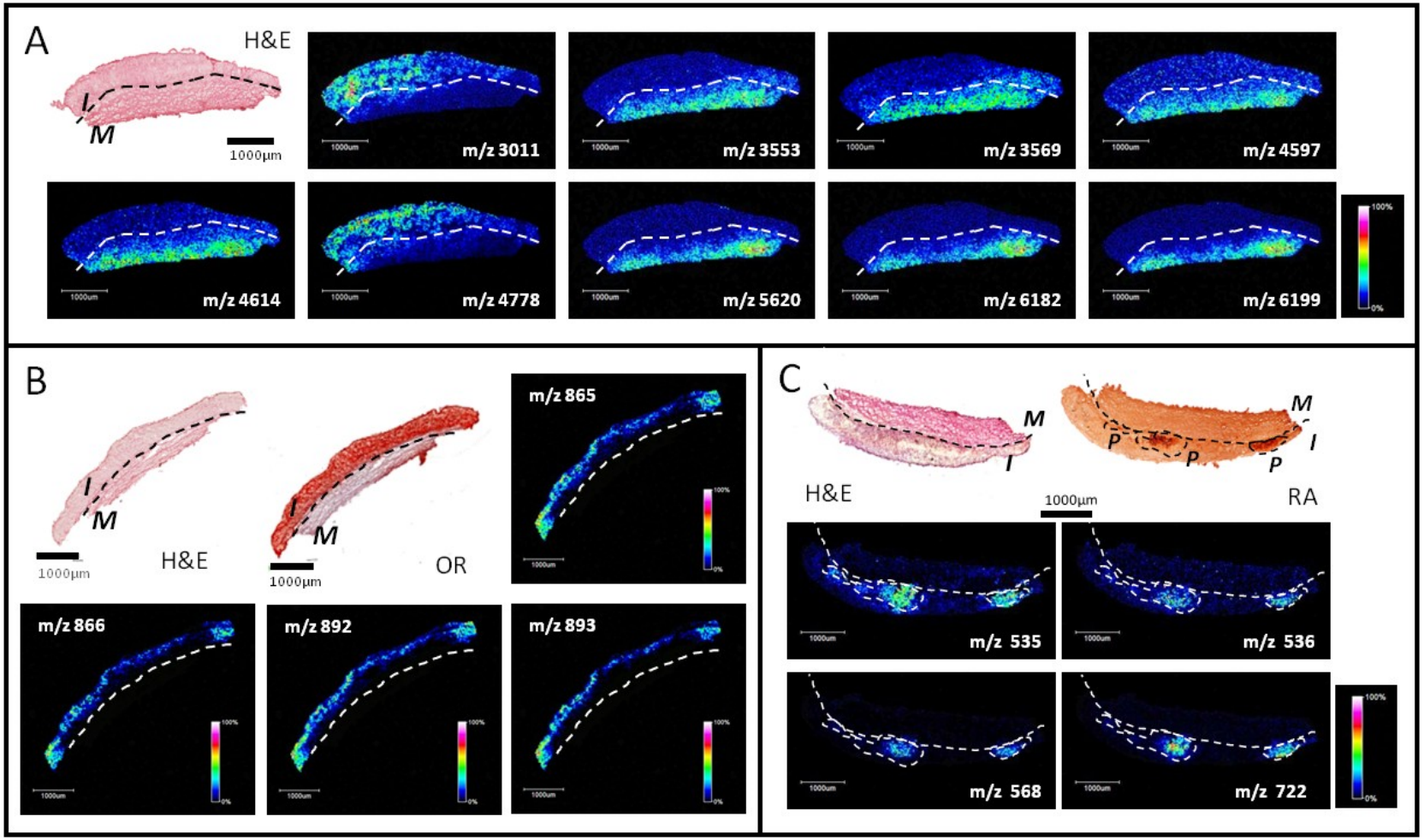

Supplementary Figure S1. Representative MALDI-MSI images for proteins (A) and lipids (B,C) in rabbit aorta. Intima (I) and media (M) layers and calcified regions (P) in the intima are defined by specific m/z values. Characterization of samples is made according to histology: H&E, Oil-Red (OR) and Red Alizarin (RA).

DISCUSIÓN

IDENTIFICACIÓN DE MARCADORES MOLECULARES (PROTEÍNAS Y METABOLITOS) EN ORINA EN RESPUESTA AL DESARROLLO DE ATEROSCLEROSIS

Análisis proteómico diferencial. Desarrollo metodológico.

La orina es un fluido biológico de gran interés clínico y que se emplea rutinariamente en ensayos diagnóstico de enfermedades y seguimiento de la respuesta terapéutica. Se puede obtener con facilidad, sin necesidad de personal especializado, y en elevadas cantidades y además por métodos no invasivos. Además, presenta la ventaja de ser estable una vez recogida la muestra, ya que prácticamente todas las degradaciones por proteasas endógenas ya han sucedido cuando estaba en la vejiga. A pesar de todos estos parabienes, la orina es en último término un ultrafiltrado del plasma con lo cual es de esperar que lo que se refleja en orina sea la respuesta a una serie de acciones combinadas que están sucediendo en el cuerpo o el reflejo de diferentes patologías en forma de moléculas alteradas. A esta conclusión se llegó en los primeros estudios que se realizaron cuando se detectaron diferentes tipos de colágenos en orina que podían ser asociados igualmente a enfermedad cardiovascular (1), a diabetes (2), enfermedad renal crónica (3) o al cáncer de próstata (4). El descubrimiento de un potencial marcador o panel de marcadores hasta su aplicación en clínica implica un largo y complicado proceso que pasa por una validación en cohortes perfectamente caracterizadas de miles de individuos y generalmente requiere un desarrollo tecnológico paralelo que haga posible la traslación real al entorno clínico. En otras palabras, convertir un hallazgo molecular en algo fácilmente medible e interpretable, reproducible, robusto y de gran capacidad de muestreo a nivel técnico. En esta tesis doctoral, se aborda la primera de las etapas. El descubrimiento de potenciales nuevos marcadores moleculares en orina que reflejen estadios tempranos y silentes del desarrollo de aterosclerosis.

La orina no se había considerado como posible fluido de estudio hasta hace relativamente poco tiempo, y no está muy extendido su uso para evaluar los cambios producidos en respuesta a las enfermedades cardiovasculares. De entre los escasos ejemplos cabe destacar dos en orina humana y dos en orina de ratón del tipo Apo E(-/-). *Constantin von zur Muhlen et al.* (1) en 2009 evaluaron plasma y orina de 67 sujetos con y sin enfermedad coronaria y encontraron 17 péptidos de orina por CE-MS que permitían diferenciar entre los diferentes grupos pertenecientes a diferentes tipos de colágenos. Esto, por contra, no era posible en las muestras de plasma en las cuales no se observaba diferencia alguna. Un año después y evaluando de nuevo la enfermedad coronaria aguda en este caso en un total de 623 individuos *Delles et al*. (5) encontraron también por CE-MS un panel de 6 proteínas: α-1 antitripsina, colágeno α1 (tipos I y III), péptido precursor tipo granin neuro endocrino, componente 1 del receptor asociado a membrana de progesterona, Nalk transportador de ATPasa cadena γ y la cadena α del fibrinógeno. Los estudios en modelo animal empleando la misma técnica (6, 7) coinciden en la identificación de los colágenos como alterados en la patología a la vez que vuelven a señalar a la α1-antitripsina. A su vez identifican el factor de crecimiento epidérmico (EGF del inglés "epidermal growth factor") y KAP (del inglés "kidney

androgen-regulated protein"). Estos antecedentes ponen de manifiesto la validez de abordar el estudio de la enfermedad cardiovascular mediante aproximación proteómica en la orina. Sin embargo, pocos estudios más se han realizado y ninguno de los presentados ha avanzado más en el camino hacia la clínica. Por otro lado, es lógico pensar que quizás haya una limitación importante en cuanto a la información obtenida teniendo en cuenta el amplio abanico de posibilidades para el estudio de la orina, ya que la técnica utilizada es la misma en todos los estudio. Es por ello que la proteómica de orina es una apuesta en el laboratorio, ya que en nuestra opinión presenta hoy en día infinidad de posibilidades de abordaje de la enfermedad aterosclerótica hasta ahora no aplicados.

Entre las técnicas clásicas de proteómica se encuentra la electroforesis bidimensional por marcaje fluorescente (2D-DIGE). Nuestro laboratorio ha constatado ampliamente que es una técnica muy válida para la búsqueda de marcadores e identificación de dianas en la enfermedad cardiovascular (8-10). En todos estos años de experiencia se ha comprobado que una buena preparación y puesta a punto del protocolo a aplicar es clave para la obtención de buenos resultados, entendiendo por buenos aquellos que son reproducibles y robustos. Por ello los primeros pasos para estudiar la aterosclerosis en orina empleando proteómica clásica se centraron en poner a punto el mejor método posible para evaluar la orina por electroforesis bidimensional. Para ello se compararon 8 métodos diferentes de pre-tratamiento de la orina basados en ultrafiltración, precipitación, desalinización y extracción en fase sólida. La figura 1 representa un resumen de todos ellos. La ultrafiltración se realizó con filtros de corte de 10KDa empleando el dispositivo comercial Amicon (Millipore) resultando en geles bidimensionales pobres en número de manchas proteicas. La limpieza por precipitación se hizo con tres variantes, precipitación con acetona, precipitación por acetona+ácido tricloroacético (TCA) y precipitación empleando el kit comercial denominado "Clean-Up" (GE Healthcare). Cualquiera de estos sistemas mejoraba los resultados previos y de entre ellos destacaban tanto la combinación de acetona con TCA como el empleo del kit comercial siguiendo las indicaciones propias. Para la desalinización se emplearon dos dispositivos comerciales indicados para volúmenes pequeños: PD10 desalting columns (GE Healthcare) y Midi Pur-A-Lyzer (Sigma Aldrich) seguidas de liofilización o precipitación en acetona. De nuevo se apreció una mejora en los perfiles proteicos destacando la desalinización con las columnas pd10 que dan un perfil extremadamente bueno de la parte de alto peso molecular del gel con hasta 1040 puntos proteicos candidatos a estudio. Finalmente se probó una estrategia de extracción en fase sólida con cartuchos comerciales OASIS® (Waters). El cambio en el aspecto de los geles por el pre-tratamiento con esta estrategia es el más destacado, si se compara con el resto, ya que con ningún otro sistema se obtenía un perfil tan "limpio", en el sentido de numerosas manchas proteicas, bien definidas en el gel y sin solapamientos, y con una sorprendente buena definición de las moléculas de bajo peso molecular. La posibilidad de obtener diferentes resultados simplemente variando la limpieza y preparación de la muestra previos a la electroforesis bidimensional, nos da una idea de la gran versatilidad de la técnica. Después de esta exhaustiva comparación nuestro grupo propone dos

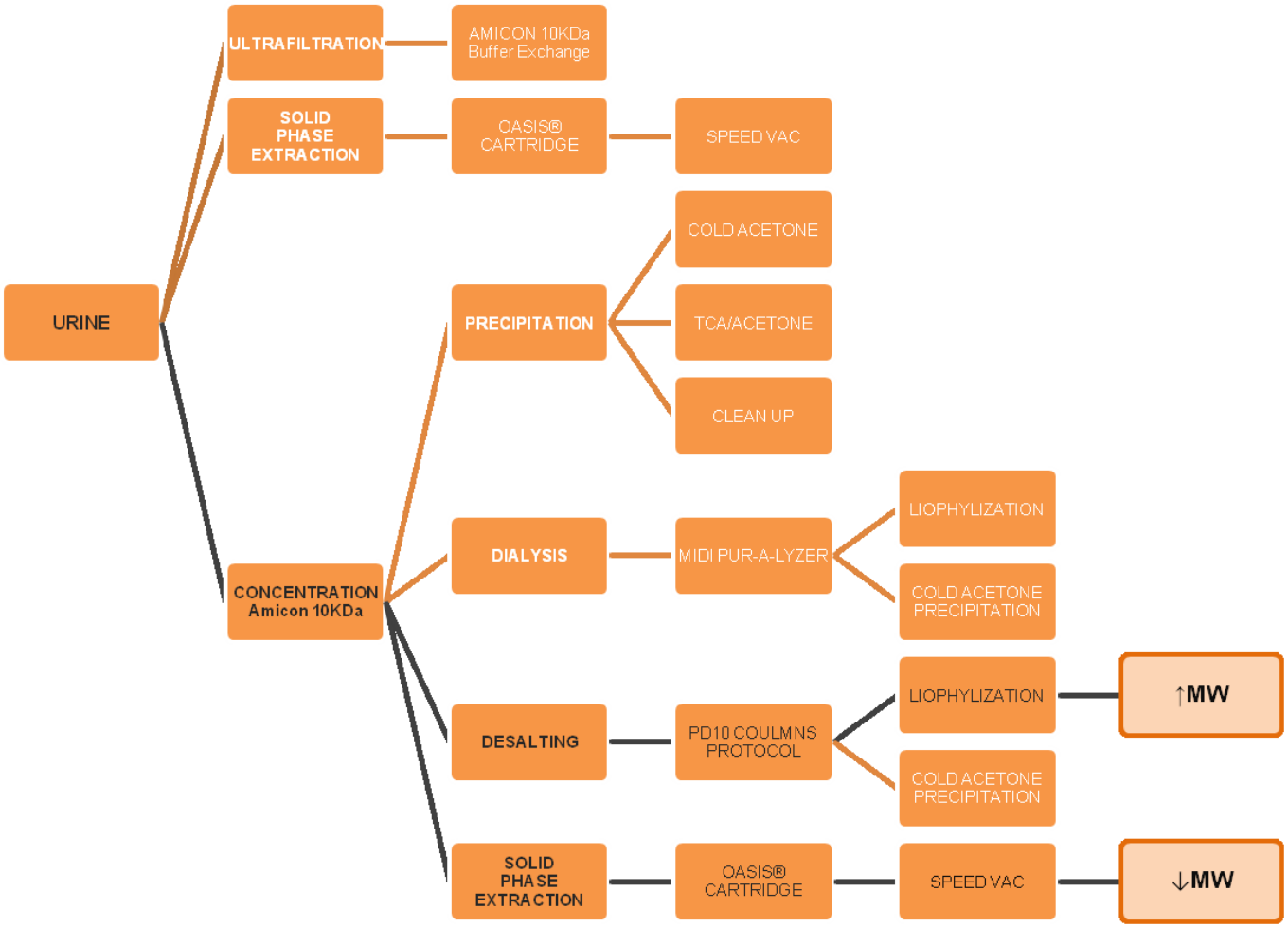

Figura 1. **Esquema de metodología comparada de pre-tratamiento de muestras de orina para posterior análisis por electroforesis bidimensional**. Un total de ocho métodos de limpieza se compararon basados en ultrafiltración: Amicon 10KDa (Millipore), precipitación: acetona fría, tca/acetona, clean up (GE healthcare), desalinización: dialisis con Midi Pur-A-Lyzer (GE healthcare), columnas PD10 (GE healthcare) y extracción en fase sólida: Oasis® (Waters). En negro se destacan los dos protocolos recomendados en ambos casos tras concentración de la orina. Se recomienda el empleo de columnas PD10 seguidas de liofilización para evaluación de proteínas de alto peso molecular y el uso de cartuchos Oasis® en el caso de querer estudiar proteínas de bajo peso molecular.

métodos diferentes para el análisis óptimo de orina en función de si se desea ahondar en proteínas de alto peso molecular (desalinización por uso de columnas comerciales PD10) o por el contrario en proteínas de bajo peso molecular (extracción en fase sólida). Con el fin de asentar esta puesta a punto y demostrar una aplicación real a la investigación clínica como antecedente de estudios posteriores en el contexto cardio-renal se eligió la extracción en fase sólida. En los últimos años el laboratorio ha abierto una línea de trabajo centrada en enfermedades renales además de la ya consolidada línea de cardiovascular. Frecuentemente, pacientes con función renal deteriorada presentan proteinuria, es decir, una concentración anormalmente elevada de la albúmina. Este hecho establece un sesgo en la comparación clínica y dificulta sobremanera la detección de moléculas alteradas que estén en baja concentración. En esta situación clínica particular, el rango dinámico está totalmente alterado y para acceder a las variaciones existentes de las proteínas de menor concentración es necesario incluir un paso de depleción de albúmina como proteína mayoritaria. Se compararon dos de las estrategias más descritas en la literatura basadas ambas en afinidad y que se habían aplicado previamente en el laboratorio con éxito; ProteoPrep inmunoaffinity Albumin IgG (Sigma) (11) y Human 14 multiple affinity removal System (Agilent) (12). Los resultados perfilaron la combinación de Oasis® junto con ProteoPrep como la más adecuada para el análisis proteómico de orina por 2D cuando existe una condición clínica de proteinuria. En particular, es recomendable realizar este paso en situaciones en las que las proteínas superen los 30mg/L. La depleción asegura la evaluación de moléculas presentes en baja concentración a la vez que permite una comparación real, sin sesgo entre condiciones "sana" y "patológica" en diferentes condiciones de proteinuria. Estudios adicionales de robustez, repetitividad y reproducibilidad se realizaron empleando diferentes alícuotas de orina, diferentes sujetos, diferentes analistas en los mismos días y en días diferentes.

Identificación de proteínas marcadoras de respuesta temprana, evento agudo y recuperación.

La aterosclerosis, como ya se ha mencionando en esta tesis doctoral, es una enfermedad de los vasos que se desarrolla durante años de manera silente y asintomática hasta que en muchos de los casos desemboca en un evento sin previo aviso. Es por ello que es de extrema necesidad la detección de marcadores de diagnóstico temprano, sin dejar de ser importantes los de prognosis y recuperación. Sin embargo, dado este perfil asintomático es muy difícil la correcta clasificación de individuos en cuanto a su mayor o menor riesgo cardiovascular en los primeros estadios de la enfermedad así como la obtención de muestras humanas cuando aún no se ha producido un evento que precise de cirugía. Es precisamente por ello que los modelos animales juegan un papel de gran importancia en la investigación cardiovascular básica. Para esta aproximación a la aterosclerosis temprana se empleó un modelo animal en conejo.

El análisis proteómico de la orina de modelo temprano se analizó por electroforesis bidimensional con marcaje fluorescente, en lo que se conoce como 2D-DIGE. Esta técnica de marcaje mejora los límites de detección y debido a que emplea un patrón

interno formado por una combinación de todas las muestras del estudio minimiza el sesgo debido a posibles errores aleatorios relativos al proceso experimental. Del análisis diferencial y posterior validación por SRM LC-MS/MS (del inglés " Selected Reaction Monitoring") se desprenden 4 proteínas alteradas en los estadios tempranos: Catepsina D aumentada en aterosclerosis y Hemopexina , Calicreína 1 (KLK1: del inglés Kallikrein 1) y ZG16B (del inglés: Zymogen granule protein 16b rat homolog) disminuidas en la condición patológica. Se buscó una translación de estas alteraciones a humano como prueba de concepto y aplicabilidad del modelo animal al estudio de la enfermedad cardiovascular en humanos. Para ello se emplearon orinas de controles y de sujetos que habían sufrido un síndrome coronario agudo recogiendo la muestra en el momento del ingreso y al alta médica. Empelando la técnica de SRM LC-MS/MS se confirmó la alteración de KLK1 y ZG16B con similar tendencia a lo observado en el modelo. Esto hace que estas dos proteínas se perfilen tanto como marcadores de diagnóstico temprano como de progresión. Además, ambas presentan recuperación de niveles a valores de control en pacientes al momento del alta, lo que hace que sirvan igualmente de marcadores de recuperación, es decir, presentan características para realizar un seguimiento completo a la aterosclerosis, su posible desenlace en un evento y la recuperación de los pacientes dado el caso tras sufrir el mencionado evento. KLK1 es una proteasa serina que libera bradiquina por activación de quininógeno y se le considera una proteína cardioprotectiva principalmente por acción sobre el endotelio (13) . Además, parece tener efectos inhibitorios en apoptosis, inflamación, hipertrofia y fribrosis (14) por acumulación en el tejido en los puntos de daño. Forma parte del sistema calicreina-cinina, sistema renal menos conocido y que se ha relacionado con el tono de las VSMCs y la regulación de la presión arterial entre otros. Se cree que actúa en sentido contrario al sistema renina-angiotensina en la regulación de la presión arterial y también que ambos participan en el remodelado cardiovascular, aunque la mayor parte de los mecanismos, bien sean cooperativos o contradictorios, comunes de estos sistemas son desconocidos en la actualidad (15). Su implicación en la enfermedad aterosclerótica abre una puerta a nuevos abordajes dirigidos de la enfermedad. Respecto al ZG16B poco se sabe y no hay muchos estudios que estén centrados en esta proteína excepto un dos investigaciones relativas a adenocarcinoma que la implican en la enfermedad (16, 17). Es sabido que ZG16B activa CXCR4 (quimoquina receptora CXR) que es a su vez el receptor de CXCL12 (quimoquina motivo CXC 12) o SDF-1 (factor 1 derivado del estroma). El complejo receptor CXCR4/CXCL12 por su parte sí parece estar relacionado con la aterosclerosis observándose que una disminución en CXCL12 se asocia a una menor infiltración en la capa íntima (18) y que los niveles en plasma están disminuidos en pacientes con una angina inestable con elevado riesgo cardiovascular y que por su parte una disminución de CXCR4 agrava la lesión (19). Considerando que los niveles de ZG16B están disminuidos en orina se podría decir que hay una menor activación o una desregulación de este complejo en la enfermedad y que por lo tanto se está perdiendo el efecto protector que tiene este complejo. Ahondando en estas dos proteínas disminuidas (KLK1 y ZG16B) se hizo un análisis para ver si están relacionadas de alguna manera y se comprobó que efectivamente lo están. La molécula que las une es el receptor tipo tool 2 (TLR2) que interacciona con la KLK1 a través del

kininogen y con el ZG16B a través del receptor CXCR4. Los niveles reducidos de ambos indican una disminución de TLR2. A este receptor se le otorgan papeles contradictorios en la aterosclerosis relacionados con si mantiene la función endotelial o por el contrario favorece una disfunción (20). En este estudio parece indicar que hay menor cantidad de TLR2 por lo que parece que nos encontramos más en la línea de tener un efecto beneficioso. En conclusión se podría decir que la combinación de KLK1 y ZG16B funciona como un parámetro de evaluación de desarrollo de la enfermedad y parece que en parte relacionado con la perdida de la capacidad protectora de las moléculas implicadas. Además, y como un plus, el eje KLK1-ZG16B es capaz de evaluar la recuperación.

Análisis metabólico diferencial. Rutas metabólicas alteradas en respuesta a la progresión, evento agudo y recuperación.

Común a lo relativo a proteínas, la orina no es uno de los fluidos más empleados en el estudio de la aterosclerosis en cuanto al desarrollo de perfiles metabólicos y búsqueda de alteraciones a este nivel, a pesar de todas las ventajas que conlleva asociadas. Los primeros estudios metabolómicos en orina en patología vascular se remontan a 2009 (21, 22) donde se analizaba por resonancia magnética nuclear (NMR) la orina de un modelo de ratón Apo E- y se observaron variaciones relacionadas con el estrés oxidativo en la progresión hacia la formación de la placa. Por cromatografía de líquidos unida a espectrometría de masas UFLC/MS-IT-TOF (del inglés: "ultra fast liquid chromatography coupled with ion trap-time of flight mass spectrometry") la orina de un modelo de aterosclerosis en rata que señala a 8 metabolitos variados (incrementados: 3-OMD "del inglés 3-O-methyl-dopa", N,N-acetilarginato de etilo, leucina-prolina, glucuronato, N6-(N-carboniltreonilo) de adenosina , ácido metil hipúrico y disminuido el ácido hipúrico). En un modelo LDLR knockout (23), se analizó la orina por NMR obteniéndose un perfil metabolómico que mostró alteraciones en el ciclo TCA, el metabolismo de los ácidos grasos y el metabolismo de la colina. En muestras de orina humana, bajo nuestro conocimiento, únicamente se han llevado a cabo dos estudios que emplean NMR. En uno de ellos evaluan y estratifican a diferentes poblaciones en función de su riesgo cardiovascular en China (24), en el otro estudio emplean la espectrometría de masas para establecer diferentes patrones en la orina de sujetos con enfermedad coronaria y/o con disfunción del ventrículo izquierdo tras una operación de isquemia/re-perfusión (25).

Nuestro estudio está centrado en los estadios tempranos de la aterosclerosis empleando orina de conejo y además de comparar los perfiles metabólicos empleando 1H NMR, los metabolitos que potencialmente responden al curso silente de la enfermedad se identificaron por 2D NMR y fueron posteriormente validados por SRM LC-MS/MS. La aplicación pudo ser directa gracias a una puesta a punto previa en el laboratorio que formaba parte de un estudio de orina por NMR de la enfermedad renal crónica (26).

Observamos una perfecta asociación entre la orina de controles frente a la orina de patológicos, y un total de 19 metabolitos se encontraron alterados en los inicios de la

enfermedad. Por similitud al estudio proteómico, se hizo un estudio translacional a humanos que hubieran sufrido un evento recogiendo orina en los momentos de ingreso y alta médica, encontrando 11 metabolitos alterados y destacando 3 de ellos por ser indicadores de recuperación: putrescina, 1-metilhidantoina y ciclohexanol. En la tabla 1 se recogen las alteraciones observadas. Aparentemente, los metabolitos son más susceptibles a los cambios que las proteínas o bien reflejan una respuesta más inmediata frente a un evento agudo, es decir, las proteínas encontradas en el estudio traslacional a humano seguían la misma tendencia que en el modelo y sin embargo entre los metabolitos los hay que sí y los hay que muestran tendencias contrarias en el momento del evento. No hay que olvidar que en el modelo animal no se está evaluando respuesta a un evento agudo como en el estudio llevado a cabo en humanos. Por lo que realmente, los mecanismos subyacentes son el resultado progresivo y en las etapas iniciales de la aterosclerosis. En el estudio en humanos, estos mecanismos operantes durante la formación de la placa confluyen con los que se desencadenan en respuesta a un síndrome coronario agudo. Nuestra hipótesis es que esta situación de evento lleva implícitos una serie de cambios especiales que rápidamente se ven reflejados en el metaboloma y que son en algunos casos más "fuertes" que los propios del desarrollo de la aterosclerosis. Esto hace de los metabolitos un foco de estudio de enorme interés si posteriores estudios confirmasen esa capacidad para un rápido reflejo de mecanismos subyacentes. La 1-metilhidantoina es un producto de la degradación de la creatinina que se encuentra aumentado en el inicio de la aterosclerosis y sin embargo disminuida en el momento del evento con recuperación de niveles al alta. Es sabido que la 1-metilhidantoina se consume produciendo 5-hidroximetilhidantoina en tejidos dañados (27) y esto se relaciona con procesos de inflamación y también como respuesta a niveles elevados de ROS (del inglés " Reactive Oxygen Species") procedentes de plaquetas activadas. Esta última situación se asocia con el evento. La putrescina y la espermidina son poliaminas derivadas de la ornitina. En general la síntesis de poliaminas se asocia a una remodelación arterial y se acumula en los tejidos como respuesta a la proliferación de las VSMCs y el engrosamiento de la capa íntima (28). Esto está de acuerdo con la disminución encontrada en animales patológicos. Sin embargo, en el momento del evento se observa un aumento que en el momento del alta médica revierte a niveles de control. Nuestra hipótesis es que en esta situación concreta se da una o las dos condiciones siguientes; aumenta en orina como resultado de secreción de productos intracelulares al torrente sanguíneo, o como intento de las poliaminas de inhibir la agregación plaquetaria que se ha desencadenado.

Al estudiar en conjunto los metabolitos y sus alteraciones particulares en aterosclerosis y en evento cardiovascular, se vio que una parte importante de los metabolitos alterados forman parte de la ruta metabólica de la arginina-prolina y del metabolismo del glutatión y que además interaccionan entre sí. La degradación de L-arginina puede evolucionar a producción de óxido nítrico, poliaminas, prolina, glutamato, creatinina y agmatina en función de las enzimas que estén mayormente favorecidas, ya que son mecanismos competitivos. En particular existe una competencia entre la arginasa (ARG) hacia la producción de ornitina y poliaminas, y NOS (del inglés "nitric oxide

synthase"), hacia la producción de diferentes tipos de óxido nítrico activándose uno u otro e influyendo así en los diferentes estados de la aterosclerosis (29).

Conclusiones

Las últimas investigaciones apuntan a paneles de marcadores más que a marcadores individuales, ya que es muy difícil que una única molécula aislada sea un buen indicador de enfermedad con la especificidad que ello debe conllevar. Este estudio proteómico y metabolómico combinado en orina ha dado lugar a dos paneles diferenciados que permiten, por un lado, monitorizar la progresión y por otro evaluar la recuperación. El panel de progresión se compone de KLK1, ZG16B, ácido 2-hidroxifenilacético, ácido 3-hidroxibutírico, L-alanina, L-arabitol, ácido N-acetilneuramínico, escilo-inositol. El panel de recuperación se compone de KLK1, ZG16B, 1-metilhidantoina, ácido 3-hidroxibutírico y putrescina. (Figura 2). Se ha puesto de manifiesto el valor del modelo animal de conejo de aterosclerosis temprana en el estudio de la patología y de la misma manera, este estudio confirma el enorme valor de las aproximaciones ómicas y de la orina en el estudio de una patología silente como es la aterosclerosis. Los paneles moleculares aquí propuestos deberán ser evaluados en un futuro en amplias cohortes de sujetos perfectamente caracterizados y podrán contribuir a estratificar los individuos en función de su riesgo cardiovascular, así como monitorizar la recuperación del paciente tras un síndrome coronario agudo.

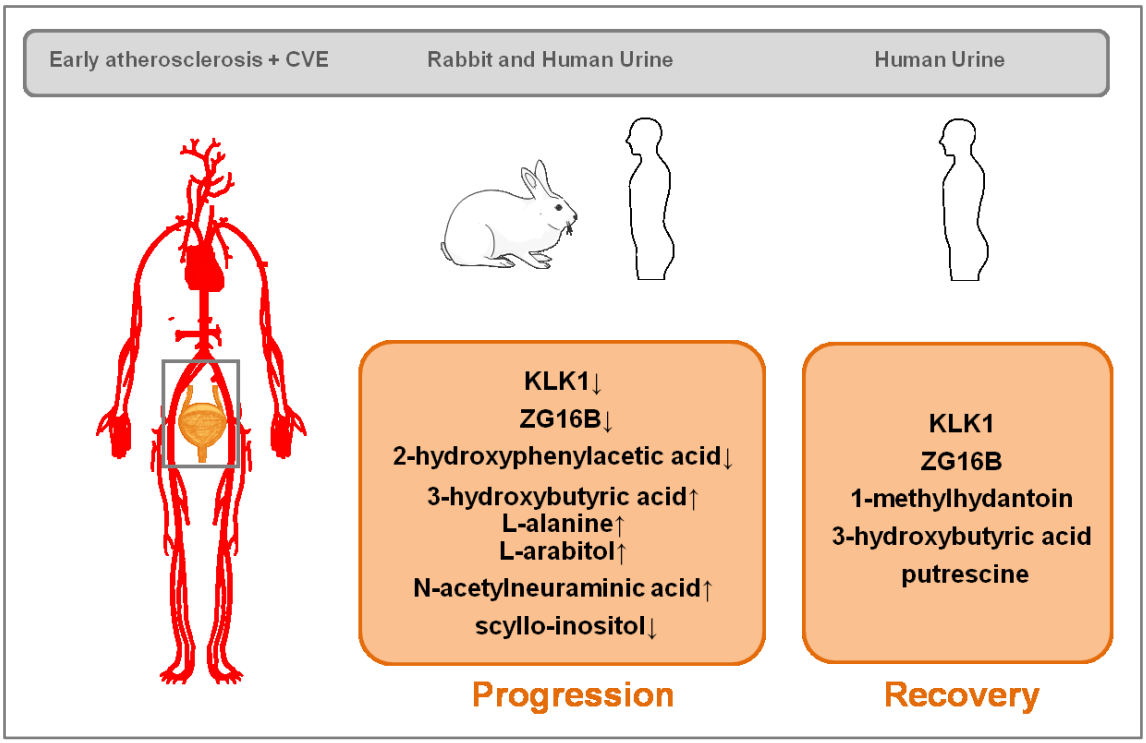

Figura 2. Paneles propuestos en orina para el seguimiento de la aterosclerosis (Progression) y la recuperación tras un evento cardiovascular agudo (Recovery).

ALTERACIONES PROTEÓMICAS Y METABOLÓMICAS A NIVEL ARTERIAL

Identificación de mecanismos subyacentes a la aterosclerosis.

En la actualidad hay un debate abierto entre los especialistas clínicos de si se medica en exceso a las personas mayores sin tener un riesgo real de sufrir un evento y, por contra, se está subestimado el riesgo de personas jóvenes que deberían ser tratadas. La realidad es que las enfermedades cardiovasculares continúan siendo la principal causa de muerte y estos datos ponen de manifiesto que se necesitan unos mejores marcadores de riesgo que clasifiquen correctamente a los individuos tal y como se ha abordado previamente en esta discusión integrada de la tesis doctoral. Un paso de vital importancia en la búsqueda de estos marcadores es entender los mecanismos subyacentes de la enfermedad y, para ello, es fundamental estudiar directamente donde se están produciendo los cambios, en este caso en el tejido arterial. En la aterosclerosis esto es algo fundamental ya que se dan simultáneamente numerosos procesos que además están interconectados entre sí. Es por eso que no son pocos los estudios que tratan de abordar la enfermedad desde esta perspectiva y que han contribuido enormemente al entendimiento de la aterosclerosis, entre ellos varias investigaciones previas de nuestro grupo. Se ha trabajado con extractos del tejido de proteínas y/o de metabolitos (30, 31), con las diferentes capas del tejido (9, 10) o con el secretoma arterial (32). En esta tesis doctoral se ha aplicado una aproximación dual que combina una técnica clásica de proteómica como es la electroforesis bidimensional con marcaje diferencia DIGE junto con una técnica para el análisis de metabolitos que permite el estudio ex vivo del tejido tal cual (técnica no desductriva). La técnica se denomina resonancia magnética de ángulo mágico o resonancia magnética de sólidos (HRMAS, del inglés "high resolution magic angle spectroscopy") y aunque se ha aplicado a investigas alteraciones de la función cardiaca (33-35), en lo que a nuestro conocimiento se refiere, es la primera vez que se aplica en el estudio de la aterosclerosis. Por ello, esta parte de la tesis contribuye a la implantación de una nueva técnica para el estudio de esta patología y que ya ha demostrado ser de interés en diferentes enfermedades como el cancer (36), enfermedad renal e hipertensión (37) o enfermedades inmunes (38).

En general, el estudio simulténeo de las variaciones de las proteínas y los metabolitos en respuesta a la enfeermedad permite evaluar diferentes actores en la cadena de cambios producidos, desde moléculas intermedias, hasta productos finales. En la aterosclerosis temprana hemos observado modificaciones en respuesta al estrés oxidativo, remodelación arterial, y alteraciones en el metabolismo de los aminoácidos junto con el de los glicerofosofolípidos. Todas las alteraciones se encuentran en la Tabla 1.

Es conocido que en el proceso de aterosclerosis se producen cambios en el metabolismo de la energía (39, 40) y que en parte ello se relaciona con la generación de ROS en la aterogenesis y de Ox-LDL (41, 42). El organismo para intentar compensar este estado comienza a utilizar en primera instancia glutatión. El glutatión es un antioxidante natural producido por las células capaz de neutralizar esas especies reactivas y de regular el ciclo de NO (43). Al estudiar su variación directamente en el tejido se ve que

está disminuido en las aortas patológicas, poniendo de manifiesto que se están dando cambios para compensar esos hechos conocidos. Al verse estos niveles disminuidos cabe esperar que traten de compensarse de alguna manera y a eso parecen apuntar los cambios observados en la glicolisis. Se encontraron valores aumentados en las quinasa piruvato y fosfoglicerato a la vez que hay una mayor presencia de piruvato en las arterias ateroscleróticas. El piruvato es un buen antioxidante (44) y esto nos hace pensar que su sobreexpresión es en parte el reflejo de un mecanismo de compensación frente a los niveles reducidos de otros antioxidantes. A nivel de la capa íntima de la arteria, nuestro grupo ya había descrito cambios significativos en el proteoma en respuesta a una desregulación del citoesqueleto (10). En este trabajo, esos cambios también se ponen de manifiesto y, además, diferentes moléculas señalan hacia una remodelación en las paredes arteriales. La disminución en aorta de vinculina (VCL) junto con el aumento de la quinasa ligada a las integrinas (ILK) indica una alteración importante en cuanto a peores uniones adherentes por perdida de funcionalidad y una migración favorecida (45, 46). Lo que concuerda con el cambio de fenotipo contráctil a fenotipo sintetizador y migración de las VSMCs. Además se observa una sobre expresión en dos proteínas íntimamente relacionadas con la actina y su polimerización, parte fundamental del citoesqueleto, la tropomiosina 2 y la proteína reguladora de la actina CAP-G. El gen de la tropomiosina 2 se encuentra sobre expresado en las VSMCs presentes en las placas (marcador de diferenciación) (47) y la sobre expresión de CAP-G se relaciona con una sobreproducción en situaciones de hipoxia (48). Además de existir movimiento celular, también hay un intento del organismo de intentar reparar las zonas dañadas que se refleja de manera importante en este estudio a través del aumento de las encimas glicolíticas que hacen que los macrofágos se polarizen hasta M2 siendo esta la forma favorecida frente a M1 para tratar de reparar el tejido (49). Además se observa una disminución en tejido de valina que puede deberse a su uso descrito en un intento del organismo de minimizar los daños ocasionados por una disfunción endotelial (50). Además de la valina, otros ocho amino ácidos y derivados de amino ácidos se han encontrado variados: guanidoacetato, aspartato y treonina aumentados, y glutamato, glutamina,N-acetil-L-alanina y tiramina disminuidos junto con la valina. De entre todos ellos el aspartato se erige como el punto de unión de estos cambios. Estudios previos ya han relacionado al aspartato con una resuesta de inhibición frente a la formación de la estría grasa y al desarrollo de la aterosclerosis (51) .En global, estas alteraciones parecen enfocar al hecho ya discutido previamente en orina de que en los estadios iniciales de la aterosclerosis se ve favorecida la síntesis de poliaminas en detrimento de NO ya que entre la competición existente entre la arginasa y la sintetizadora de NO la arginasa parece ser la clara ganadora.

Que la aterosclerosis está íntimamente relacionada con el depósito lípidos es algo sabido, de hecho hasta no hace tanto tiempo se consideraba una enfermedad debida únicamente a la acumulación de lípidos en las arterias. En este estudio y gracias a la técnica de resonancia magnética de sólido vemos que hay una variación en el metabolismo de los glicerofosofolípidos y en especial en las especies relacionadas con la colina. La colina, acetilcolina y la fosfocolina están infra expresadas en aterosclerosis

al igual que el producto de la colina TMAO. Por contra la glicerofosfocolina se encuentra sobre expresada. La colina y la acetilcolina participan en la síntesis de la fosfatidilcolina que es un precursor del factor de activación plaquetario (PAF "platelet activation factor"). Este PAF se sintetiza con el fin de remodelar la arteria en condiciones de inflamación y contribuir a los primeros cambios típicos de la aterosclerosis (52), contribuye a la disfunción endotelial y activa la formación de las especies reactivas de oxígeno. Además la baja presencia de colina se relaciona con la acumulación de lípidos (53), la presencia de acetilcolina tiene un efecto vasoconstrictor (54) y por su parte la glicerofosfocolina y su aumento se han relacionado en estudios previos con efectos beneficiosos en isquemia (55).

Monitorización de los cambios moleculares identificados en tejido y su reflejo en plasma.

La sangre está en contacto directo con la arteria y más en concreto con la capa íntima de la arteria. Es por ello que podemos pensar que en muchas ocasiones se pueden monitorizar los cambios que sufre el tejido por su reflejo en el plasma. Si se da este caso, estas moléculas se podrían emplear como potenciales marcadores. En el estudio de tejido recogido en el capítulo 3 de esta tesis doctoral se buscó esta traslación empelando la técnica de SRM LC-MS/MS. De las 29 alteraciones encontradas in situ en el tejido, 12 de ellas tienen su reflejo en plasma. Con la misma tendencia que en el tejido nos encontramos PGK y todos los metabolitos: acetilcolina, colina, glutamato, valina, N-acetil-L-alanina, glucuronato, glutatión y pirtuvato. Con tendencia contraria se encuentra la A1AT y las quinasas PKM e ILK. Por lo tanto, los principales procesos que se ven reflejados en el plasma son la respuesta al estrés oxidativo y los cambios en el metabolismo de los glicerofosfolípidos. Todos estos posibles marcadores se evaluaron estadísticamente por curvas ROC para evaluar la sensibilidad y selectividad de su respuesta. La integración de esos resultados da lugar a un panel conjunto formado por tres amino ácidos: glutamato, N-acetil-L-alanina y valina y tres quinasas: PGK, PKM e ILK. (Figura 3)

Conclusiones

La aplicación de nuevas tecnologías y de diferentes abordajes combinados en el estudio de la aterosclerosis permite la identificación de nuevas y conocidas moléculas y mecanismos que contribuyen al mejor conocimiento del desarrollo de la patología. Además, la inclusión con éxito de nuevas tecnologías en el campo abre la puerta a futuros estudios que enriquezcan aún más dichos conocimientos. En este estudio de tejido se han puesto de manifiesto cambios en mecanismos conocidos que implican a diferentes moléculas y además se ha generado un panel de marcadores en plasma que reflejan dichos cambios tisulares. Aunque este panel deberá ser confirmado en estudios posteriores en una cohorte elevada de individuos, parece un panel robusto para la evaluación individual del riesgo.

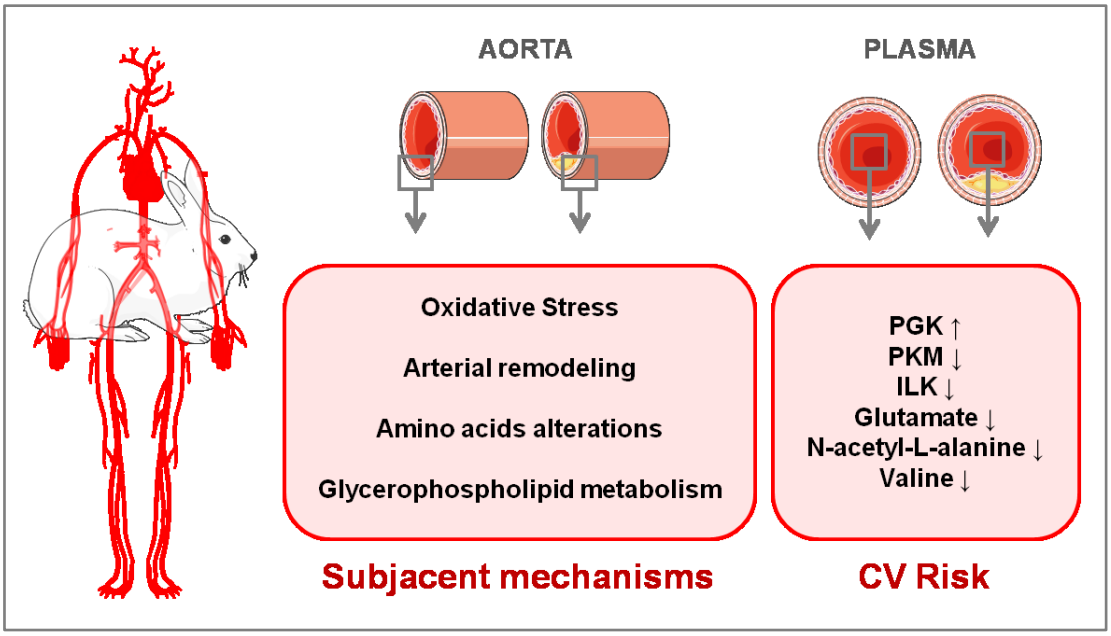

Figura 3. Estudio del desarrollo de la aterosclerosis en tejido y su reflejo en plasma. Mecanismos identificados y panel de marcadores de plasma de riesgo cardiovascular.

IMÁGEN MOLECULAR "*IN-SITU*" DE LOS CAMBIOS MOLECULARES EN RESPUESTA A LA ATEROSCLEROSIS

Obtención de mapas bidimensionales de las arterias por MALDI-Imaging.

Como ya se ha descrito previamente, inrínseco al desarrollo de la aterosclerosis, se produce una remodelación exhaustiva de los vasos incluyendo migraciones celulares de unas capas a otras. Precisamente por ello cobra especial importancia la posiblidad de estudiar las alteraciones moleculares en las distintas capas arteriales, a la vez que se conserva su localización original. Dicho de otro modo, sería de gran valía poder obtener un mapa bidimensional molecular de la arteria en respuesta a la aterosclerosis y ello constituye el objetivo del estudio presentado en lso capítulos cuatro y cinco de esta tesis doctoral.

En el ámbito de la investigación clínica este tipo de abordajes *in situ* llevan unos años viviendo una revolución gracias al desarrollo de la tecnología de espectrometría de masas de imagen y especialmente gracias a la basada en MALDI. A día de hoy son numerosas las contribuciones al avance en el conocimiento de un amplio abanico de enfermedades (56, 57) a nivel de identificación de biomarcadores, de la contribución a la estimación de la prognosis y la supervivencia (58, 59), evaluación y respuesta de fármacos (60, 61) o evaluación de tumores heterogéneos que por otras técnicas serían indistinguibles (62, 63). En el campo de las enfermedades cardiovasculares se han dado los primeros pasos de aplicación de esta técnica evaluando mapas lipídicos en diferentes condiciones experimentales con el fin de encontrar perfiles moleculares (64) y evaluar el comportamiento de fármacos (65). Sin embargo, y en lo que a nuestro conocimiento

confiere, a día de hoy los trabajos presentados en esta tesis doctoral constituyen los dos primeros estudios de proteínas por MALDI-Imaging en aterosclerosis. Como en la mayoría de las técnicas a emplear en cualquier estudio y más cuando son nuevas, la puesta a punto es un paso crucial para la obtención de unos buenos resultados ya que no es posible hacer una transferencia directa de lo encontrado en la bibliografía. Esto es especialmente cierto en el caso de las arterias, ya que son un tejido que a pesar de tener unas dimensiones muy reducidas contiene zonas muy diferentes entre sí como son zonas con alto contenido lipídico o zonas calcificadas, hecho que representa una clara limitación. Los obtención de mapas proteicos por MALDI-Imaging deben conllevar una elevada calidad de imagen, calidad de los espectros y una correcta localización de las proteínas. Para asegurar esto son numerosos los estudios que recomiendan realizar un lavado previo al análisis de las muestra con el fin de eliminar sales, mejorar la fijación del tejido y mejorar la señal de los espectros (66). Para optimizar los mapas obtenidos por MALDI-Imaging del tejido arterial se compararon cinco lavados descritos en la literatura reciente en términos de intensidad media de los espectros, número de picos detectados, ratio señal/ruido, número de espectros excluidos y nivel de deslocalización. Estos lavados consisten en dos de naturaleza orgánica: etanol e isoporpanol; dos que incluyen una disolución acuosa: Carnoy's y solución acuosa acidificada y un último que emplea una solución tampón. La comparación se realizó en carótidas humanas de sujetos sometidos a endarterectomía. Las primeras comparaciones mostraron como los dos lavados orgánicos junto con el lavado de Carnoy's daban lugar a los espectros de imagen de más calidad; buena intensidad media del espectro correspondiente a un elevado número de moléculas detectadas (picos) con alta relación señal/ruido y pocos espectros excluidos . Por ello se realizó una comparación exhaustiva de los diferentes protocolos de lavado en cortes consecutivos de las arterias carótidas ateroscleróticas, y de mamarías humanas como tejido control, evaluando también la calidad de las imágenes y la posible deslocalización de las moléculas debido a los lavados. Al trabajar con estos cortes consecutivos evaluando los mismos parámetros que se han descrito previamente, se observó que los lavados orgánicos daban mejor resultado, probablemente porque ofrecen una mejor fijación del tejido al porta objetos. Para poder discernir entre cual de los dos es más adecuado para el tejido arterial fue necesario evaluar el otro parámetro crucial asociado a la técnica: la obtención de imágenes de calidad sin deslocalización proteica. Para ello se compararon diferentes valores m/z proteicos en función de su localización en las diferentes capas relacionando las imágenes obtenidas con la histología proporcionada por una tinción de hematoxilina-eosina de los mismos cortes sobre los que se había realizado el experimento de MALDI-MSI. Tras evaluar los coeficientes de correlación de Pearson de cada uno de los cortes para los diferentes lavados, se dedujo que la calidad espectral oscilaba de más a menos de la siguiente manera con los lavados: isopropanol>> etanol> Carnoy's. Los lavados con isopropanol eran los únicos que aseguraban una localización de las proteínas en su ubicación inicial. Esta escala se validó en muestras control, dando lugar a la conclusión de que introducir un lavado con isopropanol en los estudios de proteínas por MALDI Imaging en arterias mejora considerablemente los resultados, ya que se mantiene una integridad espacial óptima en las imágenes espectrales además de permitir la obtención

de los mejores perfiles proteicos. Esto es de vital importancia en aterosclerosis ya que los mecanismos subyacentes implican cambios dinámicos de migración entre capas y porque únicamente de esta manera se pueden asociar los cambios moleculares a las diferentes etapas de la enfermedad, progresión, tipo de placa vulnerable o estable, etc. Además, a parte se aumentó la resolución espacial a 30μm para asegurar la obtención de perfiles moleculares especificamente asociados a las distintas capas arteriales y regiones de interés. Este hecho es esencial en muestras de tan reducido calibre de cara a poder realizar un posterior estudio completo de caracterización y comparación de muestras controles y ateroscleróticas tempranas que certifica que, gracias a estos estudios, se ha abierto un amplio campo de investigación mediante la aplicación de esta tecnología ex vivo en el abordaje de las enfermedades cardiovasculares como nueva aproximación.

Localización e identificación por MALDI-MSI de los cambios moleculares en respuesta al desarrollo de la aterosclerosis.

Se analizaron aortas de conejo control y patológicas y se analizaron proteínas y lípidos con el fin de obtener el perfil molecular más amplio posible. Lo primero que se vio es que esta aproximación permitía diferenciar a la perfección entre las diferentes capas media e íntima y que dentro de la íntima era capaz de diferenciar zonas calcificadas y no calcificadas, siempre realizando estas asignaciones en función de la histología del propio corte analizado y la histología de cortes sucesivos. El esqueleto arterial identificado está compuesto por 29 valores de m/z correspondientes a 10 proteínas (7 localizadas en la capa media y 3 en la capa íntima) y 19 lípidos (11 a lo largo de la capa íntima y 8 específicamente localizados en la zona calcificada de la íntima) (Ver Tabla 1). De entre ellos destacan 21 que además de estar localizados presentan una expresión alterada en la patología. En este mapa molecular se encuentra el reflejo de diferentes procesos operantes en el desarrollo de la aterosclerosis. Así, relacionados con una promoción de la disfunción endotelial e inflamación, encontramos ácidos grasos saturados y lisolípidos (29). Además, en este estadio inicial en el que los monocitos son internalizados, aparecen macrófagos y comienza una acumulación de lípidos, se ven localizados en la capa íntima fosfoinositol (PI del inglés "phosphoinositol") (contribuciye a la activación de monocitos y producción de MMP), fosfoglicerol (PG del inglés "phosphoglyceride") (lípidos de carga negativa que se exponen porque favorecen la internalización de macrófagos (67, 68)) y esfingomielina (SM del inglés "sphingomyelin") (se acumula y/o sintetiza in situ siendo un riesgo independiente de riesgo cardiovascular (69-72). A medida que la lesión avanza y como medida de protección se constituye una capsula fibrosa alrededor del núcleo lipídico. Por MALDI Imaging se identificaron triglicéridos (TG del inglés "triglyceriddes"), glycerophospholípidos (que incluyen el ácido lisofosfatídico LPA: "lysophosphatdic acid)) y esfingolípidos (SM and PE-Cer (del inglés "phosphoethanol-ceramides") relacionados con este rproceso. Estos datos parecen indicar que a la vez que los TG se confinan en la zona de placa se están depositando otros lípidos que se están sintetizando ya que, el ácido fosfatídico (PA del inglés "phospatidic acid) es el derivado de una reacción de acetilación de LPA que se describe que se acumula por depósito de los

LDL-ox o proveniente de los PG de los macrófagos y VSMCs (73, 74) y que las PE-Cer son intermediarios en las síntesis de SM. La parte del estudio proteico representa el mayor reto de este estudio y en especial la identificación de los m/z que como bien está descrito en la literatura es en la actualidad el caballo de batalla y cuello de botella para la mayor implantación definitiva del MALDI-Imaging (73-75). En este estudio los esfuerzos se centraron en la identificación de la proteína correspondiente a un m/z de 4762 Da que está localizada en la íntima y presenta la mayor tasa de cambio en la patología, estando aumentada en aterosclerosis. Acudiendo a bases de datos y con una posterior confirmación por IHC y posterior validación/translación a humano la asignación final fue la Timosina β4 (TMBSX4). A la timosina β4 se le asignan numerosos roles relacionados con el proceso aterosclerótico: desregulación del citoesquelto (76); promoción de la expresión de MMP (77) y papel protector en las zonas dañadas gracias a activación selectiva de citoquinas (78). Además estudios en plasma (79) revelan valores disminuidos en infarto agudo de miocardio, lo que lleva a pensar que la timosina β4 o bien se sintetiza in situ o se acumula en tejido con un fin protector y que sirve como posible diana terapéutica pero que además por su reflejo en plasma puede servir para monitorizar la enfermedad.

Conclusiones

Estos estudios constituyen la primera aproximación a obtención de un mapa arterial compuesto por proteínas y lípidos (Figura 4) en arterias sanas y patológicas con el fin de ahondar en los mecanismos subyacentes de la enfermedad, identificar nuevas dianas terapéuticas a nivel tisular que sean potencialmente transferibles a un fluido de fácil acceso para constituir marcadores de enfermedad.

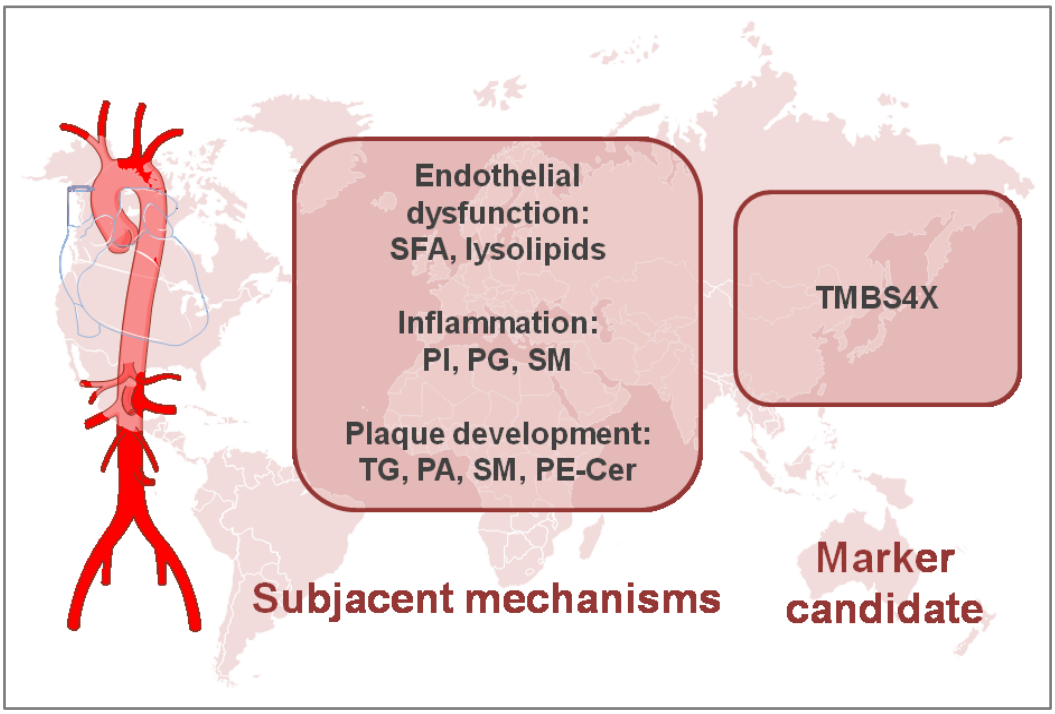

Figure 4. Mecanismos subyacentes y candidato de riesgo cardiovascular identificados en la realización del mapa bidimensional de la aorta ascendente.

REFERENCES

1. von Zur MC, Schiffer E, Zuerbig P, et al. Evaluation of urine proteome pattern analysis for its potential to reflect coronary artery atherosclerosis in symptomatic patients. J Proteome Res 2009; 8:335-45.

2. Maahs DM, Siwy J, Argiles A, et al. Urinary collagen fragments are significantly altered in diabetes: a link to pathophysiology. PLoS One 2010; 5.

3. Good DM, Zurbig P, Argiles A, et al. Naturally occurring human urinary peptides for use in diagnosis of chronic kidney disease. Mol Cell Proteomics 2010; 9:2424-37.

4. Theodorescu D, Schiffer E, Bauer HW, et al. Discovery and validation of urinary biomarkers for prostate cancer. Proteomics Clin Appl 2008; 2:556-70.

5. Delles C, Schiffer E, von Zur MC, et al. Urinary proteomic diagnosis of coronary artery disease: identification and clinical validation in 623 individuals. J Hypertens 2010; 28:2316-22.

6. Adiguzel E, Ahmad PJ, Franco C, Bendeck MP. Collagens in the progression and complications of atherosclerosis. Vasc Med 2009; 14:73-89.

7. von Zur MC, Schiffer E, Sackmann C, et al. Urine proteome analysis reflects atherosclerotic disease in an ApoE-/- mouse model and allows the discovery of new candidate biomarkers in mouse and human atherosclerosis. Mol Cell Proteomics 2012; 11:M111.

8. Alvarez-Llamas G, Zubiri I, Maroto AS, et al. A role for the membrane proteome in human chronic kidney disease erythrocytes. Transl Res 2012; 160:374-83.

9. de la Cuesta F, Alvarez-Llamas G, Maroto AS, et al. A proteomic focus on the alterations occurring at the human atherosclerotic coronary intima. Mol Cell Proteomics 2011; 10:M110.

10. de la Cuesta F, Zubiri I, Maroto AS, et al. Deregulation of smooth muscle cell cytoskeleton within the human atherosclerotic coronary media layer. J Proteomics 2013; 82:155-65.

11. Zubiri I, Posada-Ayala M, Sanz-Maroto A, et al. Diabetic nephropathy induces changes in the proteome of human urinary exosomes as revealed by label-free comparative analysis. J Proteomics 2014; 96:92-102.

12. Darde VM, Barderas MG, Vivanco F. Depletion of high-abundance proteins in plasma by immunoaffinity subtraction for two-dimensional difference gel electrophoresis analysis. Methods Mol Biol 2007; 357:351-64.

13. Dendorfer A, Wolfrum S, Dominiak P. Pharmacology and cardiovascular implications of the kinin-kallikrein system. Jpn J Pharmacol 1999; 79:403-26.

14. Chao J, Shen B, Gao L, Xia CF, Bledsoe G, Chao L. Tissue kallikrein in cardiovascular, cerebrovascular and renal diseases and skin wound healing. Biol Chem 2010; 391:345-55.

15. Moreau ME, Garbacki N, Molinaro G, Brown NJ, Marceau F, Adam A. The kallikrein-kinin system: current and future pharmacological targets. J Pharmacol Sci 2005; 99:6-38.

16. Kim SJ, Lee Y, Kim NY, et al. Pancreatic adenocarcinoma upregulated factor, a novel endothelial activator, promotes angiogenesis and vascular permeability. Oncogene 2013; 32:3638-47.

17. Liu PF, Wu YY, Hu Y, et al. Silencing of pancreatic adenocarcinoma upregulated factor by RNA interference inhibits the malignant phenotypes of human colorectal cancer cells. Oncol Rep 2013; 30:213-20.

18. von HP, Schmitt MM. Platelets and their chemokines in atherosclerosis-clinical applications. Front Physiol 2014; 5:294.

19. Bot I, Daissormont IT, Zernecke A, et al. CXCR4 blockade induces atherosclerosis by affecting neutrophil function. J Mol Cell Cardiol 2014; 74:44-52.

20. Mullick AE, Tobias PS, Curtiss LK. Modulation of atherosclerosis in mice by Toll-like receptor 2. J Clin Invest 2005; 115:3149-56.

21. Leo GC, Darrow AL. NMR-based metabolomics of urine for the atherosclerotic mouse model using apolipoprotein-E deficient mice. Magn Reson Chem 2009; 47 Suppl 1:S20-S25.

22. Zhang F, Jia Z, Gao P, et al. Metabonomics study of atherosclerosis rats by ultra fast liquid chromatography coupled with ion trap-time of flight mass spectrometry. Talanta 2009; 79:836-44.

23. Cheng KK, Benson GM, Grimsditch DC, Reid DG, Connor SC, Griffin JL. Metabolomic study of the LDL receptor null mouse fed a high-fat diet reveals profound perturbations in choline metabolism that are shared with ApoE null mice. Physiol Genomics 2010; 41:224-31.

24. Yap IK, Brown IJ, Chan Q, et al. Metabolome-wide association study identifies multiple biomarkers that discriminate north and south Chinese populations at differing risks of cardiovascular disease: INTERMAP study. J Proteome Res 2010; 9:6647-54.

25. Turer AT, Stevens RD, Bain JR, et al. Metabolomic profiling reveals distinct patterns of myocardial substrate use in humans with coronary artery disease or left ventricular dysfunction during surgical ischemia/reperfusion. Circulation 2009; 119:1736-46.

26. Posada-Ayala M, Zubiri I, Martin-Lorenzo M, et al. Identification of a urine metabolomic signature in patients with advanced-stage chronic kidney disease. Kidney Int 2014; 85:103-11.

27. Ienaga K, Nakamura K, Naka F, Goto T. The metabolism of 1-methylhydantoin via 5-hydroxy-1-methylhydantoin in mammals. Biochim Biophys Acta 1988; 967:441-3.

28. Nishida K, Abiko T, Ishihara M, Tomikawa M. Arterial injury-induced smooth muscle cell proliferation in rats is accompanied by increase in polyamine synthesis and level. Atherosclerosis 1990; 83:119-25.

29. Getz GS, Reardon CA. Arginine/arginase NO NO NO. Arterioscler Thromb Vasc Biol 2006; 26:237-9.

30. Stegemann C, Didangelos A, Barallobre-Barreiro J, et al. Proteomic identification of matrix metalloproteinase substrates in the human vasculature. Circ Cardiovasc Genet 2013; 6:106-17.

31. Mayr M, Yusuf S, Weir G, et al. Combined metabolomic and proteomic analysis of human atrial fibrillation. J Am Coll Cardiol 2008; 51:585-94.

32. de la Cuesta F, Barderas MG, Calvo E, et al. Secretome analysis of atherosclerotic and non-atherosclerotic arteries reveals dynamic extracellular remodeling during pathogenesis. J Proteomics 2012; 75:2960-71.

33. Griffin JL, Williams HJ, Sang E, Nicholson JK. Abnormal lipid profile of dystrophic cardiac tissue as demonstrated by one- and two-dimensional magic-angle spinning (1)H NMR spectroscopy. Magn Reson Med 2001; 46:249-55.

34. Hanana H, Simon G, Kervarec N, Mohammadou BA, Cerantola S. HRMAS NMR as a tool to study metabolic responses in heart clam Ruditapes decussatus exposed to Roundup(R). Talanta 2012; 97:425-31.

35. Costantino L, Gandolfi F, Bossy-Nobs L, et al. Nanoparticulate drug carriers based on hybrid poly(D,L-lactide-co-glycolide)-dendron structures. Biomaterials 2006; 27:4635-45.

36. Tripathi P, Somashekar BS, Ponnusamy M, et al. HR-MAS NMR tissue metabolomic signatures cross-validated by mass spectrometry distinguish bladder cancer from benign disease. J Proteome Res 2013; 12:3519-28.

37. Huhn SD, Szabo CM, Gass JH, Manzi AE. Metabolic profiling of normal and hypertensive rat kidney tissues by hrMAS-NMR spectroscopy. Anal Bioanal Chem 2004; 378:1511-9.

38. Ratai EM, Pilkenton S, Lentz MR, et al. Comparisons of brain metabolites observed by HRMAS 1H NMR of intact tissue and solution 1H NMR of tissue extracts in SIV-infected macaques. NMR Biomed 2005; 18:242-51.

39. Mayr M, Chung YL, Mayr U, et al. Proteomic and metabolomic analyses of atherosclerotic vessels from apolipoprotein E-deficient mice reveal alterations in inflammation, oxidative stress, and energy metabolism. Arterioscler Thromb Vasc Biol 2005; 25:2135-42.

40. Mayr M, Yusuf S, Weir G, et al. Combined metabolomic and proteomic analysis of human atrial fibrillation. J Am Coll Cardiol 2008; 51:585-94.

41. Khatri JJ, Johnson C, Magid R, et al. Vascular oxidant stress enhances progression and angiogenesis of experimental atheroma. Circulation 2004; 109:520-5.

42. Brown DI, Griendling KK. Regulation of signal transduction by reactive oxygen species in the cardiovascular system. Circ Res 2015; 116:531-49.

43. Prasad A, Andrews NP, Padder FA, Husain M, Quyyumi AA. Glutathione reverses endothelial dysfunction and improves nitric oxide bioavailability. J Am Coll Cardiol 1999; 34:507-14.

44. Ojha S, Goyal S, Kumari S, Arya DS. Pyruvate attenuates cardiac dysfunction and oxidative stress in isoproterenol-induced cardiotoxicity. Exp Toxicol Pathol 2012; 64:393-9.

45. Zhang QJ, Goddard M, Shanahan C, Shapiro L, Bennett M. Differential gene expression in vascular smooth muscle cells in primary atherosclerosis and in stent stenosis in humans. Arterioscler Thromb Vasc Biol 2002; 22:2030-6.

46. Zhang R, Zhou L, Li Q, Liu J, Yao W, Wan H. Up-regulation of two actin-associated proteins prompts pulmonary artery smooth muscle cell migration under hypoxia. Am J Respir Cell Mol Biol 2009; 41:467-75.

47. Palsson-McDermott EM, Curtis AM, Goel G, et al. Pyruvate kinase M2 regulates Hif-1alpha activity and IL-1beta induction and is a critical determinant of the warburg effect in LPS-activated macrophages. Cell Metab 2015; 21:65-80.

48. Elena C, Nina F, Carmen U, Cristiana F, Mihai D. Effects of Valine and Leucine on Some Antioxidant Enzymes in Hypercholesterolemic Rats. Health 2014; Vol.06No.17:9.

49. Yanni AE, Agrogiannis G, Nomikos T, et al. Oral supplementation with L-aspartate and L-glutamate inhibits atherogenesis and fatty liver disease in cholesterol-fed rabbit. Amino Acids 2010; 38:1323-31.

50. Brocheriou I, Stengel D, Mattsson-Hulten L, et al. Expression of platelet-activating factor receptor in human carotid atherosclerotic plaques: relevance to progression of atherosclerosis. Circulation 2000; 102:2569-75.

51. Rajaie S, Esmaillzadeh A. Dietary choline and betaine intakes and risk of cardiovascular diseases: review of epidemiological evidence. ARYA Atheroscler 2011; 7:78-86.

52. Ludmer PL, Selwyn AP, Shook TL, et al. Paradoxical vasoconstriction induced by acetylcholine in atherosclerotic coronary arteries. N Engl J Med 1986; 315:1046-51.

53. Barbagallo SG, Barbagallo M, Giordano M, Meli M, Panzarasa R. alpha-Glycerophosphocholine in the mental recovery of cerebral ischemic attacks. An Italian multicenter clinical trial. Ann N Y Acad Sci 1994; 717:253-69.

54. Balluff B, Schone C, Hofler H, Walch A. MALDI imaging mass spectrometry for direct tissue analysis: technological advancements and recent applications. Histochem Cell Biol 2011; 136:227-44.

55. Neubert P, Walch A. Current frontiers in clinical research application of MALDI imaging mass spectrometry. Expert Rev Proteomics 2013; 10:259-73.

56. Balluff B, Rauser S, Meding S, et al. MALDI imaging identifies prognostic seven-protein signature of novel tissue markers in intestinal-type gastric cancer. Am J Pathol 2011; 179:2720-9.

57. Hardesty WM, Kelley MC, Mi D, Low RL, Caprioli RM. Protein signatures for survival and recurrence in metastatic melanoma. J Proteomics 2011; 74:1002-14.

58. Aichler M, Elsner M, Ludyga N, et al. Clinical response to chemotherapy in oesophageal adenocarcinoma patients is linked to defects in mitochondria. J Pathol 2013; 230:410-9.

59. Reyzer ML, Caldwell RL, Dugger TC, et al. Early changes in protein expression detected by mass spectrometry predict tumor response to molecular therapeutics. Cancer Res 2004; 64:9093-100.

60. Jones EA, Schmitz N, Waaijer CJ, et al. Imaging mass spectrometry-based molecular histology differentiates microscopically identical and heterogeneous tumors. J Proteome Res 2013; 12:1847-55.

61. Willems SM, van RA, van ZR, Deelder AM, McDonnell LA, Hogendoorn PC. Imaging mass spectrometry of myxoid sarcomas identifies proteins and lipids specific to tumour type and grade, and reveals biochemical intratumour heterogeneity. J Pathol 2010; 222:400-9.

62. Zaima N, Sasaki T, Tanaka H, et al. Imaging mass spectrometry-based histopathologic examination of atherosclerotic lesions. Atherosclerosis 2011; 217:427-32.

63. Tanaka H, Zaima N, Ito H, et al. Cilostazol inhibits accumulation of triglycerides in a rat model of carotid artery ligation. J Vasc Surg 2013; 58:1366-74.

64. Goodwin RJ. Sample preparation for mass spectrometry imaging: small mistakes can lead to big consequences. J Proteomics 2012; 75:4893-911.

65. Ahsan F, Rivas IP, Khan MA, Torres Suarez AI. Targeting to macrophages: role of physicochemical properties of particulate carriers--liposomes and microspheres--on the phagocytosis by macrophages. J Control Release 2002; 79:29-40.

66. Fidler IJ, Raz A, Fogler WE, Kirsh R, Bugelski P, Poste G. Design of liposomes to improve delivery of macrophage-augmenting agents to alveolar macrophages. Cancer Res 1980; 40:4460-6.

67. Tabas I. Sphingolipids and atherosclerosis: a mechanistic connection? A therapeutic opportunity? Circulation 2004; 110:3400-1.

68. Jiang XC, Paultre F, Pearson TA, et al. Plasma sphingomyelin level as a risk factor for coronary artery disease. Arterioscler Thromb Vasc Biol 2000; 20:2614-8.

69. Nelson JC, Jiang XC, Tabas I, Tall A, Shea S. Plasma sphingomyelin and subclinical atherosclerosis: findings from the multi-ethnic study of atherosclerosis. Am J Epidemiol 2006; 163:903-12.

70. Chatterjee S. Sphingolipids in atherosclerosis and vascular biology. Arterioscler Thromb Vasc Biol 1998; 18:1523-33.

71. Spector AA. Plaque rupture, lysophosphatidic acid, and thrombosis. Circulation 2003; 108:641-3.

72. Pages C, Simon MF, Valet P, Saulnier-Blache JS. Lysophosphatidic acid synthesis and release. Prostaglandins Other Lipid Mediat 2001; 64:1-10.

73. Cillero-Pastor B, Heeren RM. Matrix-assisted laser desorption ionization mass spectrometry imaging for peptide and protein analyses: a critical review of on-tissue digestion. J Proteome Res 2014; 13:325-35.

74. Maier SK, Hahne H, Gholami AM, et al. Comprehensive identification of proteins from MALDI imaging. Mol Cell Proteomics 2013; 12:2901-10.

75. McDonnell LA, Walch A, Stoeckli M, Corthals GL. MSiMass list: a public database of identifications for protein MALDI MS imaging. J Proteome Res 2014; 13:1138-42.

76. Philp D, Huff T, Gho YS, Hannappel E, Kleinman HK. The actin binding site on thymosin beta4 promotes angiogenesis. FASEB J 2003; 17:2103-5.

77. Tung WS, Lee JK, Thompson RW. Simultaneous analysis of 1176 gene products in normal human aorta and abdominal aortic aneurysms using a membrane-based complementary DNA expression array. J Vasc Surg 2001; 34:143-50.

78. Monaco C, Andreakos E, Kiriakidis S, et al. Canonical pathway of nuclear factor kappa B activation selectively regulates proinflammatory and prothrombotic responses in human atherosclerosis. Proc Natl Acad Sci U S A 2004; 101:5634-9.

79. Yesilay AB, Karakurt O, Akdemir R, et al. Thymosin beta4 levels after successful primary percutaneous coronary intervention for acute myocardial infarction. Turk Kardiyol Dern Ars 2011; 39:654-60.

CONCLUSIONS

1. Two different protocols for the study of high and low molecular weight proteins have been proposed for the pre-treatment of urine samples and prior to bidimensional electrophoresis analysis. Additionally, an extra depletion step is indicated in case of analysis of urine samples from proteinuric subjects. Thus, a method of general applicability for urine investigation by bidimensional electrophoresis has been establish.

2. A combined proteomic and metabolomic approach in urine of a rabbit model of early atherosclerosis reveals two panels composed by four proteins and 19 metabolites to be altered in response to disease initial stages. Translational studies to human urine samples from control and patients suffering an acute myocardial infarction showed: a progression marker panel formed by KLK1, ZG16B, 2-hydroxyphenylacetic acid, 3-hydroxybutyric acid, L-alanine, L-arabitol, N-acetylneuraminic acid, scyllo-inositol and a recovery marker panelcomposed by KLK1, ZG16B, 1-methylhydantoin, 3-hydroxybutyric acid and putrescine. Additionally, kallikrein-kinin system has been implicated in atherosclerosis together with alterations in arginine and proline metabolism.

3. A combined proteomic and metabolomic approach in aorta of a rabbit model of early atherosclerosis reveals 12 proteins and 17 metabolites to be involved in underlying mechanism of atherosclerosis development.Oxidative stress, arterial remodeling, amino acid alterations and glycerophospholipids metabolism have been identified to be important changes happening at the early stage of atherosclerosis. Studies in plasma of those cited mechanism lead to a risk marker panel composed by three enzymes: PGK, PKM, ILK, and three amino acids: Glutamate, N-acetyl-L-alanine and L-valine. HRMAS, for the first time applied in this thesis to study atherosclerosis, has proved to be an excellent technique to approach the underlying alterations taking part in aherosclerosis.

4. The molecular anatomy of control and atherosclerotic aortas has been defined by MALDI-Imaging in terms of lipids and proteins. A general protocol for the study of proteins in arterial tissue by MALDI-MSI has been here developed for the first time assuring tissue integrity, good image and spectra quality and high spatial resolution (30μm) as small arterial dimensions demand. As result, MALDI-MSI has been applied here for the first time to study in situ the proteins involved in cardiovascular diseases.

5. Different lipid classes are increased in early atherosclerosis: localized in the intima, SFA, lysolipids, PI, PG and SM, and in calcified regions TG, glycerophospholipids (PA) and sphingolipids (SM and PE-Cer).Immunohistochemistry studies confirmed Thymosin β4 localization in intima layer and also its up-regulation in atherosclerosis. These findings have been translated to human aortic tissue, Thymosin β4 is here proposed as a cardiovascular risk marker candidate.

Anexo

PUBLICACIONES DERIVADAS DE LA PRESENTE TESIS DOCTORAL

KLK1 and ZG16B proteins and arginine-proline metabolism identified as novel targets to monitor atherosclerosis, acute coronary syndrome and recovery.

Marta Martin-Lorenzo, Irene Zubiri, Aroa S. Maroto, Laura Gonzalez-Calero, Maria Posada-Ayala, Fernando de la Cuesta, Laura Mourino-Alvarez, Luis F Lopez-Almodovar, Eva Calvo-Bonacho, Luis M. Ruilope, Luis R Padial, Maria G Barderas, Fernando Vivanco, Gloria Alvarez-Llamas.
Metabolomics. Dec. 2014, doi: 10.1007/s11306-014-0761-8.

Urine 2-DE proteome analysis in healthy condition and kidney disease.

Marta Martin-Lorenzo*, Laura Gonzalez-Calero*, Irene Zubiri, Pedro J Diaz-Payno, Aroa Sanz-Maroto, Maria Posada-Ayala, Fernando Vivanco, Gloria Alvarez-Llamas.
Electrophoresis. 2014 Sep;35(18):2634-41

30µm spatial resolution protein MALDI MSI: In-depth comparison of five sample preparation protocols applied to human healthy and atherosclerotic arteries.

Marta Martin-Lorenzo, Benjamin Balluff, Aroa Sanz-Maroto, René J.M. van Zeijl, Fernando Vivanco, Gloria Alvarez-Llamas*, Liam A. McDonnell*
J Proteomics. 2014 Aug 28;108:465-8.

Molecular anatomy of ascending aorta in atherosclerosis by MS Imaging: specific lipid and protein patterns reflect pathology.
Running Title: New *ex vivo* imaging applied to atherosclerosis.

Marta Martin-Lorenzo, Benjamin Balluff, Aroa S. Maroto, Ricardo J. Carreira, Rene J.M. van Zeijl, Laura Gonzalez-Calero, Fernando de la Cuesta, Maria G Barderas, Luis F Lopez-Almodovar, Luis R Padial, Liam A. McDonnell, Fernando Vivanco, Gloria Alvarez-Llamas.
Under Review. Journal of Proteomics Ref: JPROT-D-15-00238.

Cytoskeleton deregulation and impairment in amino acids and energy metabolism in subjacent early atherosclerosis at aortic tissue with reflection in plasma.

Marta Martin-Lorenzo, Laura Gonzalez-Calero, Aroa S. Maroto, Irene Zubiri, Fernando de la Cuesta, Laura Mourino-Alvarez, Luis F. Lopez-Almodovar, Luis R. Padial, Maria G. Barderas, Fernando Vivanco, Gloria Alvarez-Llamas.
Manuscript in Preparation.

PARTICIPACIÓN EN PUBLICACIONES DURANTE EL DESARROLLO DE ESTE TRABAJO

Exosomes: a potential key target in cardio-renal syndrome.

Laura Gonzalez-Calero, **Marta Martin-Lorenzo**, Gloria Alvarez-Llamas.
Front Immunol. 2014 Oct 8;5:465.

Diabetic nephropathy induces changes in the proteome of human urinary exosomes as revealed by label-free comparative analysis.

Zubiri I, Posada-Ayala M, Sanz-Maroto A, Calvo E, **Martin-Lorenzo M**, Gonzalez-Calero L, de la Cuesta F, Lopez JA, Fernandez-Fernandez B, Ortiz A, Vivanco F, Alvarez-Llamas G.
J Proteomics. 2014 Jan 16;96:92-102.

Identification of a urine metabolomic signature in patients with advanced-stage chronic kidney disease.

Posada-Ayala M, Zubiri I, **Martin-Lorenzo M**, Sanz-Maroto A, Molero D, Gonzalez-Calero L, Fernandez-Fernandez B, de la Cuesta F, Laborde CM, Barderas MG, Ortiz A, Vivanco F, Alvarez-Llamas G.
Kidney Int. 2014 Jan;85(1):103-11.

Application of Metabolomics to Cardiovascular and Renal Disease Biomarker Discovery.

Gloria Alvarez-Llamas, Maria G. Barderas, Maria Posada-Ayala, **Marta Martin-Lorenzo**, Fernando Vivanco.
Book chapter. Application of advanced omics technologies: from genes to metabolites. 2014. Elservier

A role for the membrane proteome in human chronic kidney disease erythrocytes.

Alvarez-Llamas G, Zubiri I, Maroto AS, de la Cuesta F, Posada-Ayala M, **Martin-Lorenzo M**, Barderas MG, Fernandez-Fernandez B, Ramos A, Ortiz A, Vivanco F.
Transl Res. 2012 Nov;160(5):374-83

Urinary CD59 glycoprotein and alpha-1 antitrypsin are identified as novel predictors of progression of cardiovascular and renal disease in hypertensive patients chronically RAAS suppressed.

Laura Gonzalez-Calero, **Marta Martin-Lorenzo**, Fernando de la Cuesta, Aroa S Maroto, Montserrat Baldan-Martin, Gema Ruiz-Hurtado, Helena Pulido-Olmo, Julian Segura, Maria G Barderas, Luis M Ruilope, Fernando Vivanco, Gloria Alvarez-Llamas.
Submitted to American Journal of Kidney Diseases.

Decreased Kininogen-1 and increased Retinol binding protein-4 in urine in response to Acute Kidney Injury. Novel markers of early diagnosis and patient recovery.

Laura Gonzalez-Calero; **Marta Martin-Lorenzo**; Jorge Ruiz-Criado; Angeles Ramon-Barron; Aroa S Maroto; Alberto Ortiz; Carlos Gomez-Alamillo; Manuel Arias; Fernando Vivanco; Gloria Alvarez-Llamas.
Submitted to Critical Care.